AN EXPERIMENTAL AND THEORETICAL INVESTIGATION OF A WICK-TYPE SOLAR STILL FOR WATER DESALINATION

Thesis submitted for the degree of

doctor of philosophy

by

JASSIM TALIB MAHDI

BSc,MSc

Department of Mechanical Engineering

Brunel University

December 1992

I dedicate this work to :

- The memory of my late parents
- My wife, Sumaya
- My children, Hiba, Mohammed, Aimen, Ammar.

ACKNOWLEDGMENTS

I would like to express my sincere gratitude to my supervisor Dr. B. E. Smith for his many constructive comments and invaluable suggestions and for his encouragement in the progress of this investigation.

I wish to acknowledge the encouragement and support of the Department of Mechanical Engineering and the Head of the Department Professor A. J. Reynolds.

I would like to take this opportunity to thank Dr. J. J. Freeman for useful information in relation to use of the charcoal cloth.

Thanks are due to Professor A. L. Yettram, for his assistance in using the digitizer, to Dr. A.J. Ward-Smith and Dr. M.R. Mokhtarzadeh for useful discussions regarding the use of the solar still.

I am grateful to Professor H. P. Garg and Professor O. Headley for their valuable discussions, on many aspects of solar desalination during ISES Conference in Reading.

Thanks are due to Mr. C. Barrett for his assistance with the modification of the data logger and to other technician staff in the department, G. Reading, J. Langdon, G. Morvay, T. Gates, B. Dear, L. Soanes, L. Smith, D. Headley and J. Richardson for their cooperation.

The assistance of the staff of ETC for their help with the scanning electron microscopy and electron probe microanalysis is acknowledged with thanks.

The help of the Brunel librarians and the computer centre together with Mr. R. S. Lee and Mr. L. A. Jones in Techni Chem Laboratories Ltd. in the analysis of some water samples is greatly appreciated.

Not the least, I thank each and every member of my patient family for their forbearance during the lengthy process of this work and in particular my wife for assistance with typing parts of the thesis.

NOMENCLATURE

A	Area of absorber cloth or glass cover (m^2)
C	Concentration of salt in the input water by weight (%)
C_p	Specific heat (J/kg.K)
$C_{p,a}$	Specific heat of air (J/kg.K)
$C_{p,w}$	Specific heat of water (J/kg.K)
d	Distillate mass production rate ($kg/m^2.s$)
D	Distillate mass production rate ($kg/m^2.h$)
g	Gravitational constant (m/s^2)
H	Spacing between absorber cloth and glass cover (m)
h_b	Heat transfer coefficient from the absorber cloth to the ambient air through absorber insulation materials ($W/m^2.K$)
h_c	Convective heat transfer coefficient from the absorber cloth to the glass cover ($W/m^2.K$)
h_{ca}	Convective heat transfer coefficient from the glass cover to the ambient air ($W/m^2.K$)
h_e	Evaporative heat transfer coefficient from the absorber cloth to the glass cover ($W/m^2.K$)
h_{fg}	Latent heat of vaporization of water (J/kg)
h_i	Convective heat transfer coefficient from bottom of the insulation to surroundings ($W/m^2.K$)
h_r	Radiative heat transfer coefficient from the absorber cloth to the glass cover ($W/m^2.K$)
h_{ra}	Radiative heat transfer coefficient from the glass cover to surroundings ($W/m^2.K$)
I	Hourly radiant energy incident on the glass cover per unit area (Insolation) ($J/m^2.h$)

k_a	Thermal conductivity of the air (W/m.K)
k_{i1}	Thermal conductivity of the masterclad (W/m.K)
k_{i2}	Thermal conductivity of the polystyrene (W/m.K)
k_{i3}	Thermal conductivity of the styrofoam (W/m.K)
L_{i1}	Thickness of the masterclad (m)
L_{i2}	Thickness of the polystyrene (m)
L_{i3}	Thickness of the styrofoam (m)
m	Mass of the absorber support or the glass cover (kg)
m'	Mass flow rate of input water ($kg/m^2.h$)
Nu_H	Nusselt number
P_{abs}	Partial pressure of water vapour at absorber temperature (N/m^2)
P_{cov}	Partial pressure of water vapour at cover temperature (N/m^2)
q_c	Convective heat transfer rate from the absorber cloth to the glass cover (W/m^2)
q_{ca}	Convective heat transfer rate from the glass cover to the ambient air (W/m^2)
q_D	Heat transfer rate of produced distillate (W/m^2)
q_e	Evaporative heat transfer rate from the absorber cloth to the glass cover (W/m^2)
q_k	Heat transfer rate from the absorber cloth to the ambient air through bottom insulation material (W/m^2)
q_r	Radiative heat transfer rate from the absorber cloth to the glass cover (W/m^2)
q_{ra}	Radiative heat transfer rate from the glass cover to surroundings (W/m^2)
$q_{w,in}$	Heat transfer rate of the input saline water (W/m^2)
$q_{w,out}$	Heat transfer rate of the output brine (W/m^2)
Ra_H	Rayleigh number
S	Incident solar irradiance (W/m^2)
t	Time (s or h)

T_{abs} Temperature of the absorber cloth (°C or K)
T_{amb} Temperature of ambient air (°C or K)
T_{cov} Temperature of the glass cover (°C or K)
T_{sky} Temperature of the sky (°C or K)
$T_{w,in}$ Temperature of input water (°C or K)
$T_{w,out}$ Temperature of output brine (°C or K)
V Wind speed (m/s)

Greek Letters

$\alpha_a = \frac{k_a}{\rho_a C_{p,a}}$ Thermal diffusivity (m^2/s)

α_{cov} Absorptance of glass cover
α_w Absorptance of absorber wick
α_λ Spectral absorptance
β_a Volumetric thermal expansion coefficient (1/K)
ε_{abs} Emittance of absorber cloth
ε_{cov} Emittance of cover glass
η Instantaneous still efficiency
θ Angle of inclination to horizontal (degree)
μ_a Viscosity of air ($N\ s/m^2$)
$\nu_a = \frac{\mu_a}{\rho_a}$ Kinematic viscosity of air (m^2/s)
ρ Solar reflectance
ρ_a Density of air (kg/m^3)
ρ_λ Spectral reflectance
σ Stefan-Boltzmann constant (W/m^2K^4)
τ Transmittance of glass cover
τ_λ Spectral transmittance

ABSTRACT

Solar distillation using a wick-type solar still was investigated theoretically and experimentally. A tilted flat plate wick-type solar still was designed and constructed. Charcoal cloth was used as an absorber/evaporator material and for saline water transport.

A theoretical model for the performance of the wick-type solar still has been developed and analysed. It investigates the effect of various factors on the still productivity. A Fortran computer program has been developed and a finite difference technique was used to solve the main equations and to determine related parameters.

Indoor experimental testing was carried out to investigate the effect of input water flow rate and salinity on the still productivity together with the variation of the solar still efficiency with absorber temperature. The tests were conducted using the irradiance from a lamp array.

Outdoor testing was carried out with and without a V-trough solar concentrator on clear days in summer and winter. Representative daily efficiencies of the still with and without the solar concentrator were about 60% and 50% respectively on clear days in summer.

The solar absorptances of samples of charcoal cloth and blackened hessian cloth were determined before and after environmental exposure. The solar reflectances of samples of 3M Scotchcal Films and aluminised plastic (as potential reflecting materials for the concentrator mirrors) were investigated before and after environmental exposure and also exposure to elevated temperatures and humidities.

It has been concluded that: charcoal cloth is a good material for use as an absorber/evaporator and also as a water transport medium. Increase of the input water mass flow rate leads to a reduction in the efficiency of the wick-type solar still. The still efficiency decreased linearly with increase of salinity of the input saline water. The productivity of the still increases linearly with absorber temperature. The best absorber-cover separation is found to be in the range 20-25 mm. Wind speed has no significant effect (up to about 10 m/s) on the performance of a well sealed still. The transmittance of the glass cover has a strong influence on the still efficiency. Use of the solar concentrator with the inclined wick-type solar still leads to a greater fractional increase in still productivity on clear days in winter than on clear days in summer.

CONTENTS

LIST OF TABLES

LIST OF FIGURES

Chapter Four

CHAPTER ONE

INTRODUCTION

1.1 DISTILLATION

1.1.1 The sun and water desalination

The sun is a renewable source of energy. Its surface temperature is approximately 5700 K and it emits radiant energy at the rate of 380 X 10^5 GW. The solar constant i.e. the solar irradiance normal to the solar rays at the average Sun-Earth distance of 149.6 X 10^6 km is 1353 ± 1.5% W/m^2, Simonson (1984). Solar energy is an effectively inexhaustible form of energy that can be used indirectly and directly. Indirect forms of solar energy include biomass, ocean thermal and wind energies, Sayigh (1977). Direct use of solar energy includes heating of buildings and water and desalination of water.

Water is essential to sustain human life. It is abundant, but not infinite in quantity. Man is dependent on rivers, lakes, and underground water to get fresh water, but these sources are not always clean. Salts and organisms will be present. The ocean covers some 70.8 percent of the earth's surface

containing about 1350 million cubic kilometers of saline water with 35000 ppm impurities. However the maximum salt level in fresh water for human consumption is only 550 ppm, Garg (1991). With the present rise of world population, intensified agriculture, possible climate change and industrial growth in certain parts of the world, the available annual water supply will probably be insufficient on a world basis. The growth of the world's population may require expansion into relatively isolated and arid zones which are characterised by shortage of fresh water. Unfortunately a major portion of the fresh water supply is not available where it is needed. The problem can be partially solved by transporting potable water to some of these communities, but the costs involved are of such magnitude that this proposition is not feasible. Some other way of obtaining potable water will have to be found.

One of the promising options to solve this problem of water shortage appears to be desalination. Desalination methods are already mitigating water shortages in parts of the world adjacent to the sea or saline bodies of water by desalination plants. These plants use fossil fuels which have finite reserve and contribute to environmental pollution. Therefore, it is natural to look at some other methods of desalination using renewable sources of energy like solar, wind and biomass. Solar desalination can be used to purify either seawater or brackish water in areas which lack potable water and have abundant solar radiation such as some of those located in the Middle East, Sayigh (1977).

1.1.2 Solar distillation

Solar distillation has been long known and the earliest documented work is that of the Arab alchemists in 1551, Malik *et al.* (1982). It has been investigated since the nineteenth century, but, used on a limited scale. Normally, two approaches have been taken in using solar energy. One is the direct absorption of energy in saline water and the other is indirect heating of water followed by evaporation in a centralised facility.

The first approach is more suitable for small capacities, (less than 50 m^3/day) while the second approach is economically unfeasible for plants with a capacity of less than 200 m^3/day, because of the capital costs Howe and Tleimat (1977).

Solar distillation has similarities to the natural hydrologic cycle, which consists of: (i) absorption of solar energy by the top layers of water in oceans, lakes and rivers, (ii) heating up these layers, (iii) evaporation of the water, (iv) transport of the resulting vapour to cooler regions and (v) condensation of the vapour leading to precipitation as e.g. rain or snow.

Accordingly, since very early ages engineers have considered this process for supplying fresh water from saline water in the following conditions:

1) Places lacking natural fresh water but where brackish water is abundant e.g. coasts, ships and deserts.

(2) Transport of water is expensive.

(3) High levels of solar radiation are available.

(4) Potable water is needed on a small scale.

(5) The land is available.

Water distillation is accomplished by exposing layers of saline water (usually in black trays or a basin) to solar radiation, and condensing the water vapour produced under a transparent sloping cover. The condensate runs down the sloping cover and is collected in a trough along the lower end of the cover and flows out of the enclosure to provide pure water. There are many solar stills which use the distillation process. All are aimed at optimising the efficiency and lowering the construction cost. They may differ from one another in shape and materials used, but all use the same principles and serve the same functions.

The most commonly used type of solar still (i.e. the basin still) is sometimes called the greenhouse, roof, conventional or simple still. This type of solar still was designed and fabricated in 1872 near Las Salinas in Northern Chile by Carlos Wilson, a Swedish engineer. Since then until the present day numerous examples have been constructed and deployed both on large and small scales, as shown in Table 1.1.1, Garg (1991).

Solar distillation has been combined with salt production in various investigations by many authors Kettani and Abdel-Aal (1973), Comkal and Datta (1973) and Abdel-Aal (1978). In this process the combined production of water, chlorine and magnesium from sea water by using the solar stills is the aim.

The concept is dependent on the development of solar energy systems for the segregated precipitation of ocean salts Kettani (1979).

1.2 SOLAR STILLS

In this work, the tilted wick-type solar still has been investigated and its literature is mentioned in subsections (1.2.2 and 1.2.3). Literature relating to the basin-type solar still is briefly reviewed in the next subsection and in Appendix A1.

1.2.1 Basin-type solar still

This is the most commonly investigated type of solar still. As shown in Fig. 1.2.1, it contains a shallow layer of brine. It is sometimes constructed from galvanised steel sheet with a rectangular plan area (supplied either continuously or intermittently with brackish or saline water). Above the brine is a sloping transparent cover of glass or plastic sheet. The generated water vapour can condense on the lower surface of the cover. The cover is sloped to allow the distillate to trickle into troughs from where it is collected in an external reservoir.

The incident solar radiation which penetrates the transparent cover is partially absorbed by the saline water, the major portion being absorbed in the basin bottom which is usually blackened by a high solar absorption material or lined with a black material. The base of the still radiates energy in the infra-red region which is partially absorbed and re-radiated

back into the still by the cover. Heat, from the still base, is then transferred into the water, thereby increasing its temperature and evaporation of the heated upper layers of the water is enhanced. This process increases the temperature of the air adjacent to the upper layers of the water. Convection currents inside the still carry this warm vapour-air mixture to the cooler transparent cover. Moisture condenses on the underside of this cover, the heat of condensation being conducted through it to the surrounding atmosphere and the partially dehumidified air drifts back to the water surface for further addition of moisture. The water film of condensate on the inner side of the cover flows down the surface into the collecting trough and is collected as distilled water. The output of the still varies with various atmospheric conditions e.g. insolation, wind speed, ambient temperature, and design parameters e.g. blackness of basin liner, transmittance of cover materials etc.

A very comprehensive review of the history, theory, applications and economics of solar stills has been prepared by Talbert *et al.* (1970). It describes the work done in various countries from 1872 to 1970. Large installations and small laboratory scale models are described. Malik *et al.* (1982) have reviewed, thoroughly, the work on solar distillation. They have described the design and performance of a wide range of solar stills. They also summarised several studies by various engineers of the effect of climatic and design parameters on the performance of a conventional type solar still. Many other reports and historical reviews of solar distillation are

available in the literature such as Telkes (1953); Kettani (1979) and Tiwari and Malik (1982).

Dunkle (1961) analysed the basin-type still and the multiple effect diffusion still. He proposed and discussed the heat and mass transfer relationships and indicated the effect of temperature and pressure on the performance.

Experimentally, Sayigh and El-Salam (1977) tested several single sloped concrete basin-type solar stills in Ryadh, Saudi Arabia. The stills had various thicknesses and slopes of glass cover and their water trays were covered with different solar absorbent materials e.g. black and red sand, black stones, straw and charcoal. Various adhesive materials for sealing the glass cover to the stills were used. They found the optimum thickness and slope of the glass cover were 3 mm and 20° respectively, and the best adhesive was the silicon rubber, produced by the Dow Corning Corporation. The average efficiency in April was 58%. Rai *et al.* (1990) studied, experimentally, the effect of salinity of the input water on the performance of a single basin-type solar still connected with a solar collector. They also studied the still performance with blackened jute cloth floating over the water in the basin of the still. They observed that the rate of daily distillate decreases with salt concentration, as shown in Fig. 1.2.2, and increases with the use of jute cloth up to a maximum of 35 percent.

Several attempts have been made to improve the efficiency of the basin-type solar still (some of them are mentioned in Appendix A1) e.g. using air flow through the still,

forced bubbling of ambient air inside a solar still, using the latent heat of evaporation and dyes dissolved in the brine.

The recommended design of the solar still has the following characteristics:

(1) The cover should be thin and have excellent transparency to the solar wavelengths.

(2) Salt crystals should not be allowed to form at the surface of the water.

(3) The brackish layer should be as thin as possible.

(4) The distance between the cover and the water surface should be as small as possible.

(5) The basin floor should be insulated and its surface blackened.

(6) It should be economic and weatherproof.

1.2.2 Tilted solar still

Except in the tropics, a horizontal surface intercepts less solar radiation than one which is tilted toward the equator. The more nearly perpendicular a receiving surface to the sun's rays, the greater is the radiation intercept by a unit area , Lof (1980). Using an inclined solar still is a way to achieve this. However, a greater gain of solar radiation can be achieved with a high transmittance still cover and a high absorptance absorber/evaporator surface. These enhance a higher absorber temperature which, in turn, is a strong factor affecting the evaporation rate in inclined solar stills. Consequently, the production rate of the distillate is enhanced.

The tilted wick-type solar still is one among other sorts of inclined solar stills e.g. inclined plate, multiple-ledge and tilted tray solar stills. Tilted stills have been suggested to increase the incident solar energy on the absorber surface. An improvement to the inclined plate solar still can be made by using porous black wicks of cotton cloth (fabric) to make what is now called the Wick-Type solar still which is the still type of this research.

For basin-type solar stills there have been many studies of the effects of climatic, design and operating parameters e.g. solar insolation, wind speed, presence of dye, insulation thickness. But, relatively, there is a lack of attention to the inclined wick solar still, although it has been recommended by many authors as a low cost, easily constructed still and has higher operating temperatures and higher efficiencies than those of basin still. The reason for the lack of attention is due to some disadvantages of this type of solar still. For example, when blackened jute is used the colour is subjected to fade, dry spots are created due to insufficient flow rate, and consequently salts accumulate on the absorber surface and block the pores of the wick. Such problems, although they are inherent, could be overcome by giving a flow rate of input water 3 - 4 times higher than the expected productivity, Moustafa *et al.* (1979), and by keeping the input water always flowing on and through the absorber cloth prevents salt accumulation and keeps the absorber always wet.

Low heat capacity of the evaporating water (thin layer flowing through the cloth) and the solar still makes a faster

response to the solar flux intensity than occurs in basin solar stills (of a layer of certain depth).

In the last two decades, the tilted wick-type solar still has gained the interest of many solar engineers in solar distillation research and is being developed to enhance its efficiency and reduce its cost, which are the most important aims.

1.2.3 Wick-type solar still

A schematic cross section of a tilted wick-type solar still is shown in Fig. 1.2.3. It consists of a porous black material, either supported by a tray or stretched on a frame, covered by a sheet of transparent material to make an airtight enclosure. The still can be inclined to be perpendicular to the direction of the beam solar radiation at a given time of day and to avoid dripping back the distillate into the wick. It can either be insulated or uninsulated, Jundi (1982). The saline water feed is distributed along the upper edge of the porous material which is usually a blackened cloth. This cloth serves as the absorption and evaporation surface. The transparent cover acts as a condenser. On its inside surface the condensate flows down to be collected in a trough at the lower edge of the cover. A drain for the excess saline water can be fixed along the lower edge of the cloth.

The blackened cloth used in this type of solar still has some advantages:

(1) It increases the evaporating surface area of the brine.

(2) It provides the still with a low thermal capacity and consequently faster response to incident solar radiation

(compared with basin-type stills) and higher evaporator (brine) temperatures are achieved, which, in turn, yield higher evaporation rates.

(3) The still can be oriented to intercept the maximum solar radiation.

(4) The glass cover is parallel to the water surface to minimise reflection losses.

(5) The brine-cover distance can be reduced to a few millimetres to make the still a diffusion-type still, Elsayed (1983), and to eliminate shadowing of the bottom due to the side walls.

(6) The tilted-wick stills have relatively high productivity during the winter months, in comparison with basin solar stills, Lof (1980).

These are all advantages of wick-type stills but they also have some problems e.g. development of dry spots, difficulties in precise control of brine flow, deterioration of the wick material and clogging of its pores with salt when jute is used as the wick.

Hirschmann (1975) presented a product comparison between different designs of wick-type and basin-type solar stills. He suggested a linear relation between daily production rate for each design and daily solar radiation over the horizontal surface. In addition he concluded that wick-type solar stills have higher production rates than basin stills. Moustafa *et al.* (1979) have demonstrated experimentally the enhanced performance of the wick-type solar still, in comparison with the basin-type still. They used a black synthetic wettable

mat of 2.5 cm thickness and area 0.182 m^2. The flow of water in the wick was controlled using a flow regulator and shut-off valve operated with a photocell. They observed that it had a faster response to incident solar radiation, higher operating temperatures and higher efficiency than a basin-type solar still.

Frick and Sommerfeld (1973) suggested the use of jute cloth along the width of the still dipped in saline water trays. The aim was that the jute cloth should remain wet due to capillary action therefore avoiding the use of a water distribution system. Efficiencies as high as 40 to 50 percent were reported. However, the wick-type solar still developed by Frick and Sommerfeld (1973), suffered from the limitation of having part of the inclined evaporating cloth dry at times. Sodha *et al.* (1981) have presented a design, analysis and performance investigation of a multiple-wick solar still, in which the wet surface is created by a series of jute cloth pieces of increasing length separated by thin black polythene sheets. Their results were based on Dunkle's (1961) relation. They claimed that the cost of their wick-type still was less than half that of a basin-type still of same area. Tanaka *et al.* (1981) compared experimentally the hourly and daily productivity of a tilted wick-type solar still with that of a conventional single roofed basin-type solar still, under the same insolation (Fig. 1.2.4) and indoor simulated conditions. The measured performance was then compared with the results obtained by the theoretical analysis of the wick solar still. Their results have proved the

superiority of the tilted wick-type solar still to the basin-type and a productivity increase of (20 - 50) percent has been confirmed. Yeh and Chen (1986) investigated experimentally the effects of climate, design and operating conditions on the performance of wick-type solar stills using blackened jute cloth and an artificial radiation source. Their results show an insignificant effect of the wind speed and a minor effect of the ambient temperature on the productivity of the still as shown in Figs. 1.2.5 and 1.2.6 respectively. They also show that the productivity decreases with increase of the input water flow rate as shown in Fig. 1.2.7. However their results are limited.

Dual purposes of the wick-type solar stills have been studied theoretically by Gandhidasan (1983). They are to be applied for solar distillation and as a regenerator for liquid desiccants.

In 1984, Tiwari *et al.* published a paper dealing with a double condensing multiple-wick solar still. This kind of still has been proposed to overcome the high temperature of the glass cover during hot days, by introducing an additional galvanised iron sheet just below the blackened wet jute cloth with a slight spacing around the absorbing surface. Tiwari (1984), Tiwari and Yadav (1985) have studied the galvanised iron sheet multiwick solar distillation plant economically and by a performance analysis. They proposed fibre reinforced plastic instead of the galvanised sheet for a longer lifetime of (15 - 20) years. Tiwari and Rao (1985) have also discussed in detail the design and performance of fibre reinforced plastic multiwick solar distillation plant.

Recently an analytical model of a multiwick solar still with water flowing over the glass cover has been presented by Dhiman and Tiwari (1990). Different expressions for various still parameters have been obtained. They found a slight improvement in the output of the still and an increase with the water flow rate over the glass cover. Very recently double effect distillation in a multiwick solar still has been developed by Singh and Tiwari (1992). They showed a higher efficiency can be obtained by reuse of the latent heat of evaporation. The efficiency increases as the flow rate in the still decreases.

1.2.3.1 Analysis of heat transfer modes of a tilted wick-type solar still

A brief analysis of the wick-type solar still is given below. A more detailed analysis is presented in Ch.4.

The modes of heat transfer inside and outside a tilted wick-type solar still are shown in Fig. 1.2.8. They can be classified as follows:

1) Modes inside the still

a) From the absorber/evaporator surface to the glass cover the evaporative heat transfer (q_e) is the most effective mode. It should be as large as possible compared with the other heat transfer modes. That is because theoretically the distillate output of any solar still is linearly proportional to it. The other internal heat transfer rates are convection (q_c) and radiation (q_r).

b) From the absorber/evaporator to the back of the still

conductive heat transfer rate (q_b) occurs and to the exterior the brine heat content($q_{w,out}$).

2) Modes outside the still

a) From the glass cover to the ambient are the convective (q_{ca}) and radiative (q_{ra}) heat transfer modes, and that with the distillate (q_D).

b) From the back of the solar still to the ambient air through the insulation material is the heat flow rate (q_k).

Assuming the wick surface behaves as a very thin layer of water the energy balance on the absorber/evaporator surface is written as:

$$q_{w,in} + \alpha_w \tau S = q_e + q_c + q_r + q_k + q_{w,out} + \left(\frac{mC_p}{A}\right)_{abs} \frac{dT_{abs}}{dt} \quad (1.2.1)$$

Where A, C_p, m are area, specific heat and mass of the absorber support board respectively.

On the assumption of a negligible heat capacity of the distillate on the glass cover the energy balance of the glass cover is expressed as:

$$\alpha_{cov} S + q_e + q_c + q_r = q_{ca} + q_{ra} + q_D + \left(\frac{mC_p}{A}\right)_{cov} \frac{dT_{cov}}{dt} \quad (1.2.2)$$

Here A, C_p, m are the area, specific heat and mass of the glass cover respectively. For the whole still, energy balance equations are given as:

are given as:

$$(\alpha_{cov}+\alpha_w\tau)S + q_{w,in} = q_{ca} + q_{ra} + q_D + q_k + q_{w,out}$$

$$+ \left(\frac{mC_p}{A}\right)_{cov} \frac{dT_{cov}}{dt} + \left(\frac{mC_p}{A}\right)_{abs} \frac{dT_{abs}}{dt} \qquad (1.2.3)$$

Where

α_w is the absorptance of the absorber wick,

α_{cov} is the absorptance of the glass cover,

τ is the transmittance of the glass cover

Under the assumption of steady state conditions, the last two terms in eq. (1.2.3) go to zero. Hence

$$(\alpha_{cov}+\alpha_w\tau)S + q_{w,in} = q_{ca} + q_{ra} + q_D + q_k + q_{w,out} \qquad (1.2.4)$$

The instantaneous distillate rate (d) is:

$$d = \frac{q_e}{h_{fg}} \qquad (1.2.5)$$

and the instantaneous still efficiency (η) is expressed as:

$$\eta = \frac{q_e}{S} = \frac{dh_{fg}}{S} \qquad (1.2.6)$$

where h_{fg} is the latent heat of vaporization of water and S is the incident solar irradiance.

1.2.3.2 Other types of wick solar still

Use of vertical wick solar stills may minimise the cost of land which is very expensive in cities. In 1987 Kiatsiriroat *et al.* analysed the transient performance of the vertical-type solar still, and the mass transfer in it has been estimated. Earlier Coffey (1975) suggested, briefly in a technical note, different designs of vertical wick solar stills e.g. floating vertical still, ground suction vertical solar still and vertical solar still with basin of feed water at its base.

An inclined stepped solar still has been developed by Akhtamov *et al.* (1978). It has a housing with double glazing with inclined blackened trays divided by baffles. Water passes through the double glazing gap from its bottom to the top to feed the still. The latent heat of evaporation released by condensation passes through the glass to the water. Its average efficiency was around 65 percent

A diffusion-type solar still has been suggested by Dunkle (1961). He pointed out the advantages of a multiple effect diffusion still and indicated the effect of different parameters on the still performance. Elsayed (1983) compared the predicted transient performance of a solar operated diffusion-type still with a roof-type still. He concluded that the diffusion still is superior to the roof-type still in both production rate and operating efficiency.

1.3 USE OF SOLAR CONCENTRATORS TO ENHANCE SOLAR DISTILLATION

Solar concentrators have a wide variety of applications. They are used to improve the overall collector efficiency, to enhance the aperture-to-cost ratio for a flat collector Broman (1984). They increase the incident solar energy on smaller absorber surfaces where a relatively high temperature is required.

A V-trough reflector (flat booster mirrors) has been used with different designs of solar collectors such as vacuum tube collector Selcuk (1979) and in improving solar cell performance by an east-west groove alignment which has been proposed by Hollands (1971). The optical and thermal analyses of this type of concentrator has been studied by Meyer *et al.* (1982) and Dang *et al.* (1983). Various geometries and designs of the booster mirrors have been studied by several authors e.g. Rabl (1976), Bannerot and Howell (1977), Mannan and Bannerot (1978), Chiam (1982) and Broman (1984).

Mousa *et al.* (1978) described a double exposure solar still. The water basin evaporator was exposed to the solar radiation at both its upper and lower surfaces using inner reflectors on the left and right side walls of the still as well as underneath the tray. Experimentally they obtained a yield improvement of 26 percent due to the presence of the reflectors with a solar intensity difference of 7 percent. Their main

conclusions were that the effect of double exposure is more effective in the first half of the day and the idea of double exposure is a successful technique. Its disadvantage is the rapid spoiling (degradation) of the mirrors. Tamimi (1987) confirmed that the installation of reflectors on the inside walls of a basin-type solar still enhances the still production of distilled water. A comparison of results using the reflectors and black dye has been shown, from which it is indicated the yield increase due to the reflectors is more than that due to the black dye. Recently, Zabeltitz (1990) has investigated four different distillation systems, in a basin still, black parallel cloths hang vertically in the water of the basin with their upper parts above the water surface. Its north inner vertical wall was covered with a reflecting aluminium film. In another basin still, black irrigation pad is hanging at the vertical north wall. Salt water is pumped up to the upper end of the wetted pad. The productivity of the former still was less than that of the latter. However, the paper is short and gives little information, being only a limited experimental investigation.

In this work, the effect of intensification of the solar radiation incident on the wick-type solar still is investigated. A V-trough concentrator-solar still combination was used. The concentrator has an apex angle of 30° with flat mirrors and fixed on the glass cover of a flat wick solar still.

1.4 OBJECTIVES OF THE PRESENT WORK

The objectives of the present work are as follows:

(1) Investigation of the suitability of charcoal cloth for use as a standard solar absorber and water transport medium in wick-type solar stills.

(2) Investigation of the effect of a V-trough solar concentrator (with 30° apex angle) fixed on the glass cover of the still in relation to the performance of the solar still, and still material durabilities under enhanced solar insolation.

(3) Investigation of the performance of the wick-type solar still using the charcoal cloth and the V-trough solar concentrator with various saline water flow rates and water with various salinities. Some of these investigations have been carried out indoors after construction of an experimental lamp array.

(4) Investigation of the durability of the charcoal cloth including maintenance of solar absorptance after environmental treatment and solar still conditions for different periods of time.

(5) Investigation of the durability of reflective materials in relation to use as mirrors on the walls of the solar concentrator. This objective has been carried out through the following tests:

(i) Environmental exposure for various times.

(ii) Ageing in air at various temperatures and times.

(iii) Temperature and humidity cycling at various temperatures, relative humidities and periods of time.

Table 1.1.1. Major solar stills of the world. (After Garg (1991)).

Country	Place	WaterYield m^3/day	Area m^2	Year	Feed Water	Remarks
Australia	Muresk I	0.83	372	1963	Brackish	Rebuilt
	Muresk II	0.83	372	1966	Brackish	Operating
	Coober Pedy	6.35	3160	1966	Brackish	Operating
	Caiguna	0.78	372	1966	Brackish	Operating
	Hamelin Pool	1.21	557	1966	Brackish	Operating
	Griffith	0.91	413	1967	Brackish	Operating
Cape Verde Islands	Santa Maria	2.12	743	1965	Seawater	Abandoned
Chile	Las Salinas	14.76	4460	1872	Brackish	Operating
	Quillaqua	0.4	100	1968	Seawater	Operating
	Quallaqua	0.4	103	1969	Seawater	Operating
China	Wuzhi	-	385	1976	-	-
	Zhungjian	-	50	1979	-	-
Greece	Symi I	7.56	2685	1964	Seawater	Rebuilt
	Symi II	-	2600	1968	Seawater	Dismantled
	Aegina I	4.24	1490	1965	Seawater	Rebuilt
	Aegina II	-	1486	1968	Seawater	Abandoned
	Salamis	1.1	388	1965	Seawater	Abandoned
	Patmos	26.11	8600	1967	Seawater	Operating
	Kimolos	7.57	2508	1968	Seawater	Operating
	Nisyros	6.06	2005	1979	Seawater	Operating
	Fiskardo	-	2200	1971	Seawater	Operating
	Kionion	-	2400	1971	Seawater	Operating
	Megisti	-	2528	1973	Seawater	Operating
India	Bhavnagar	0.83	377	1965	Seawater	Operating
	Awania	-	1866	1978	Brackish	Operating
	Bitra	2	-	1980	Brackish	Operating
	Kulmis	3	-	1980	Brackish	Operating
Pakistan	Gwadar I	-	306	1969	Seawater	Operating
	Gwadar II	7	9072	1972	Seawater	Operating
Spain	Las Marinas	2.57	868	1966	Seawater	Operating
Tunisia	Chakmou	0.53	440	1967	Brackish	Operating
	Mahdia	4.16	1300	1968	Brackish	Operating
U. S. A.	Daytona Beach	0.53	228	1959	Seawater	Rebuilt
	Daytona Beach	0.57	246	1961	Seawater	Dismantled
	Daytona Beach	0.38	216	1961	Seawater	Dismantled
	Daytona Beach	0.61	148	1963	Seawater	Dismantled
	Balcharden	1.62	600	1969	Brackish	Operating
W. Indies	Petit St.Vincent	4.92	1710	1967	Seawater	Operating
	Haiti	0.76	223	1969	Seawater	Operating

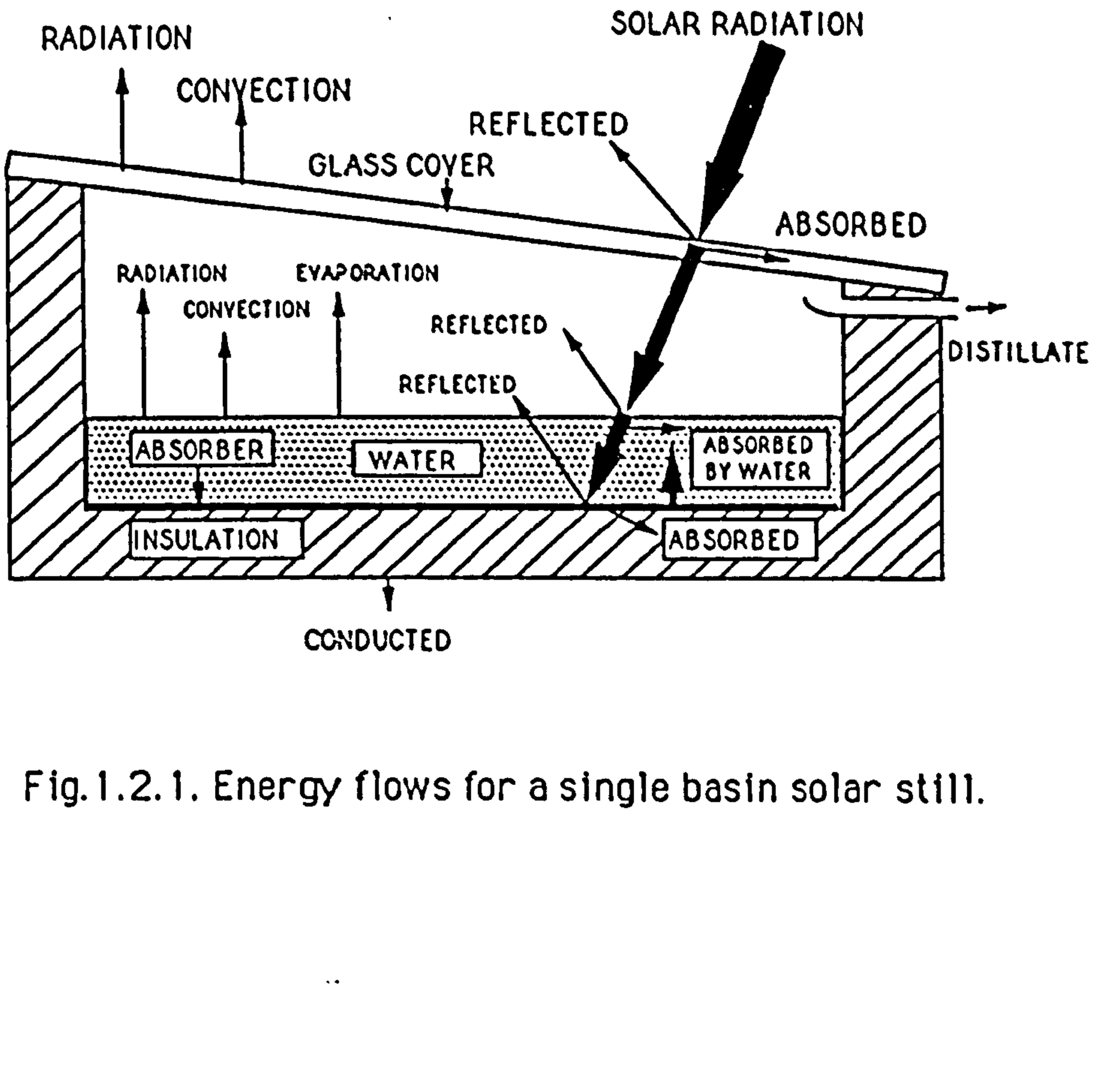

Fig. 1.2.1. Energy flows for a single basin solar still.

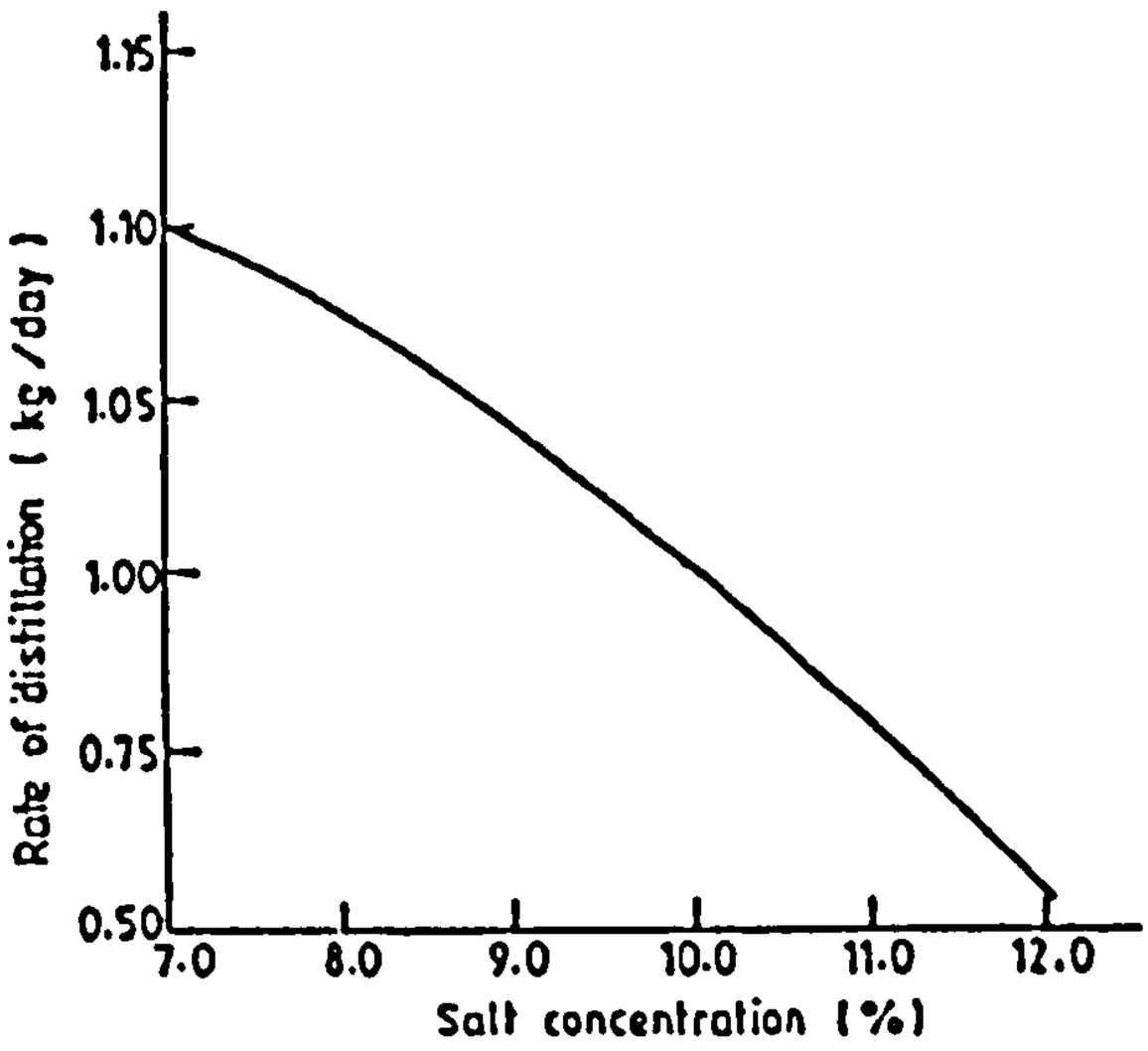

Fig. 1.2.2. Variation of rate of distillation with concentration of salt, in a basin-type solar still, (After Rai *et al.* (1990)).

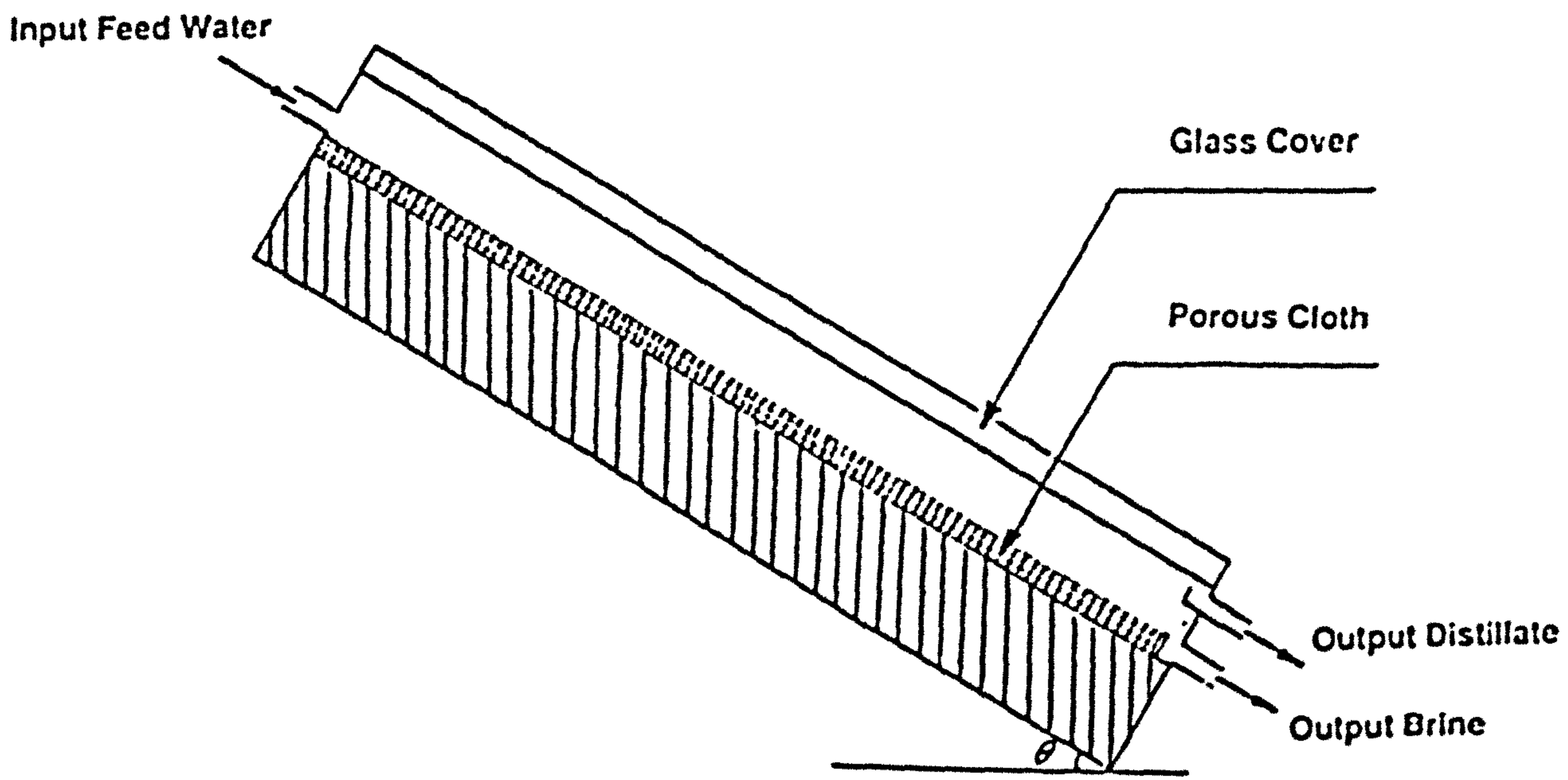

Fig. 1.2.3. Schematic cross section of a tilted wick solar still.

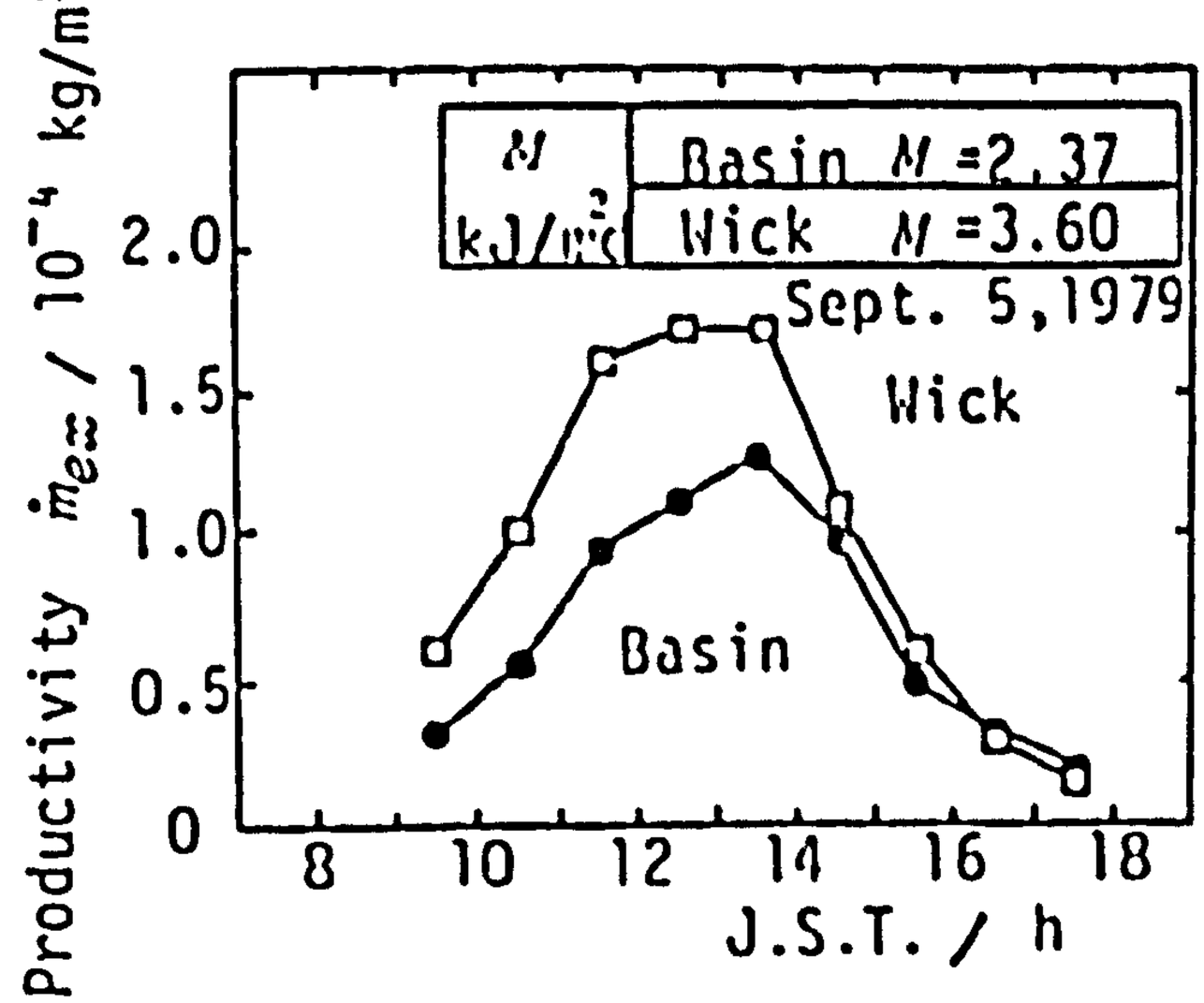

Fig. 1.2.4. Comparison of typical daily and hourly performances of experimental wick-type solar still with basin-type solar still. (After Tanaka *et al.* (1981)). J.S.T.: Japan Standard Time, M: Daily productivity of distillate.

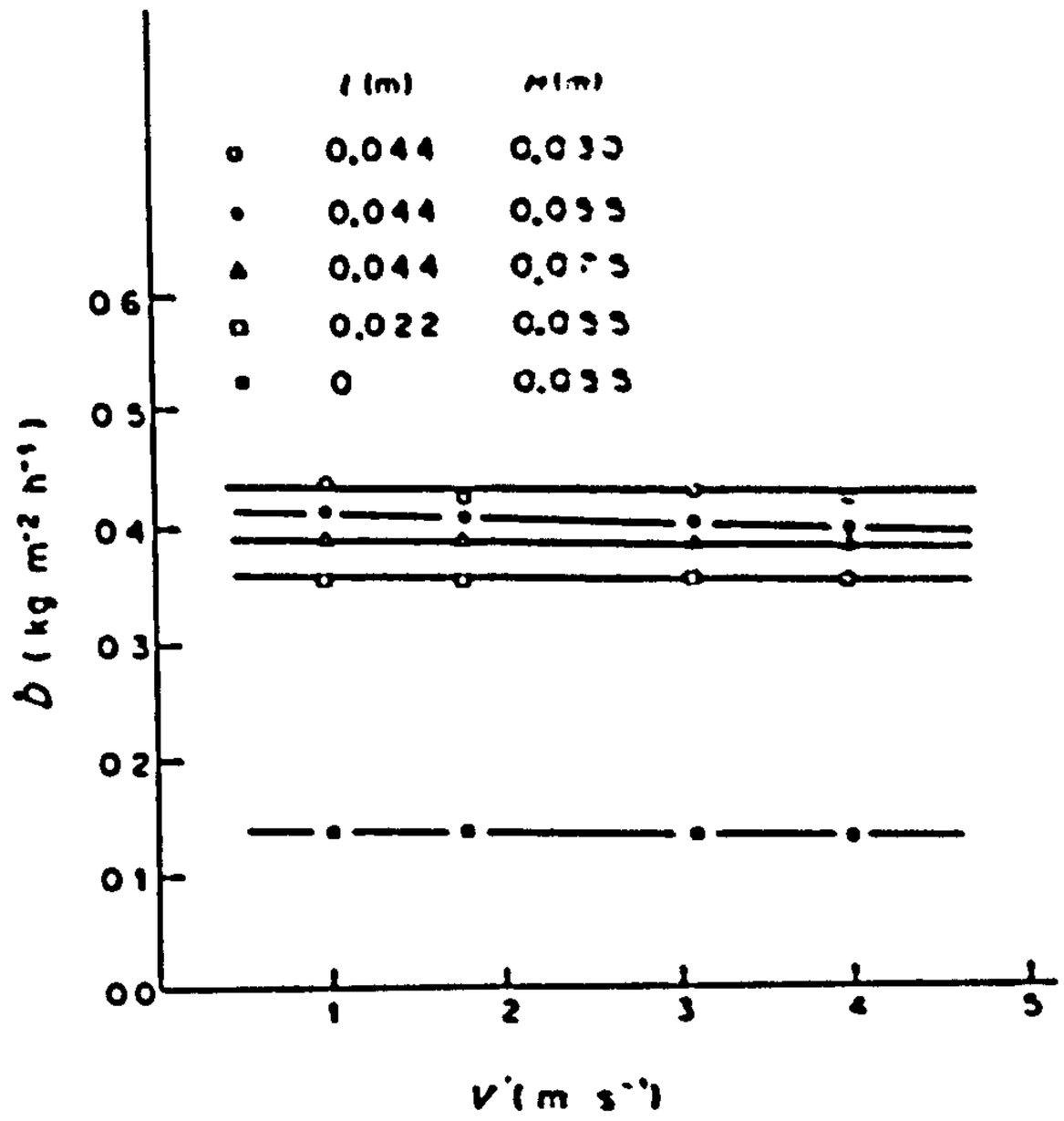

Fig. 1.2.5. Variation of wick-type solar still productivity with wind speed (After Yeh and Chen, (1986)). *l*: Insulation thickness, H Cover-absorber separation.

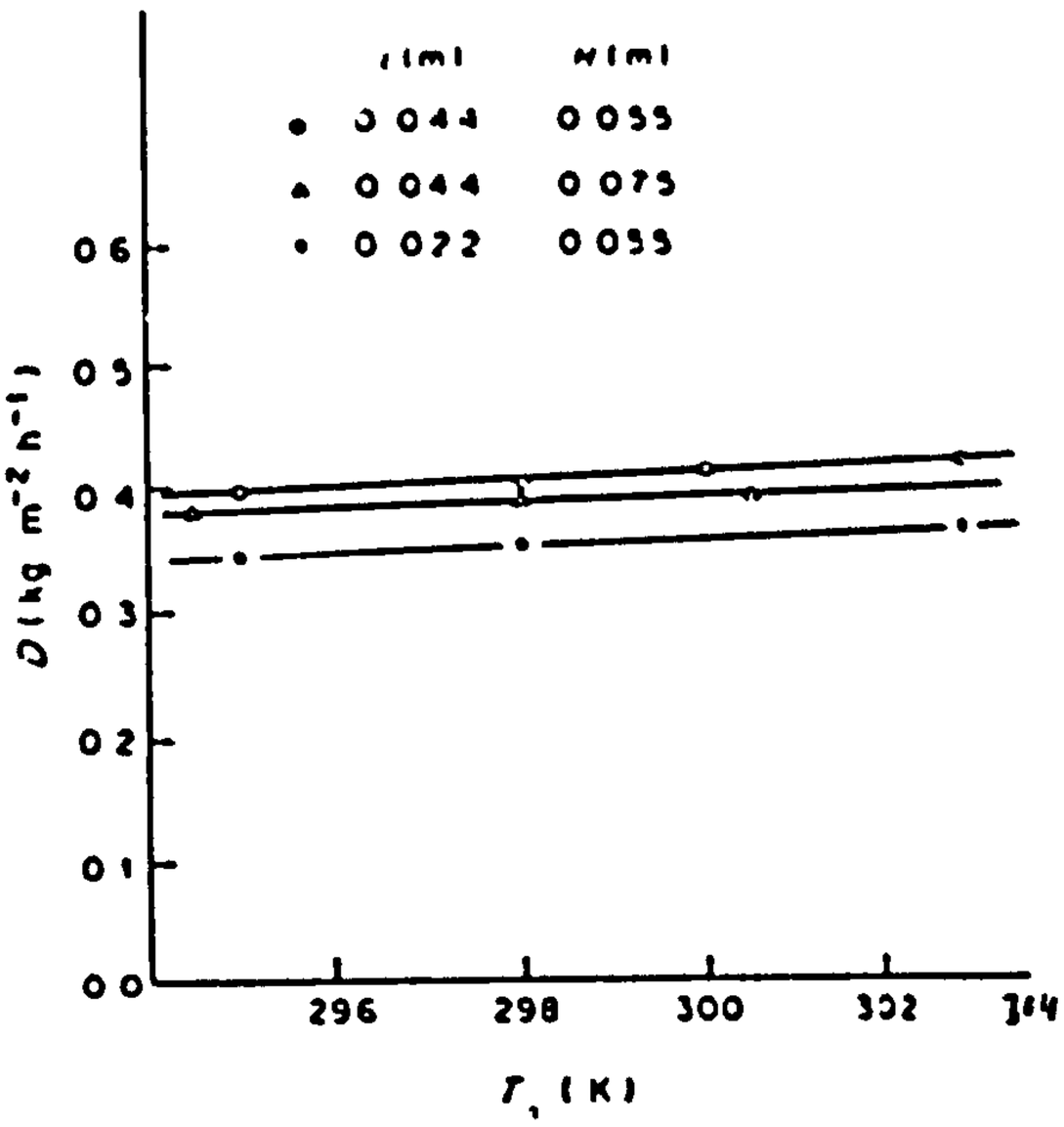

The effect of T_a on D ($I_o = 550$, $V = 1$ s. $\dot{m} = 0.826$).

Fig. 1.2.6. Variation of a wick-type solar still productivity with ambient temperature. (After Yeh and Chen, (1986)). *l*: Insulation thickness, H: cover-absorber separation. V: Wind speed, I_o: Irradiance, $\dot{m}$: Input water flow rate (kg/m^2.h).

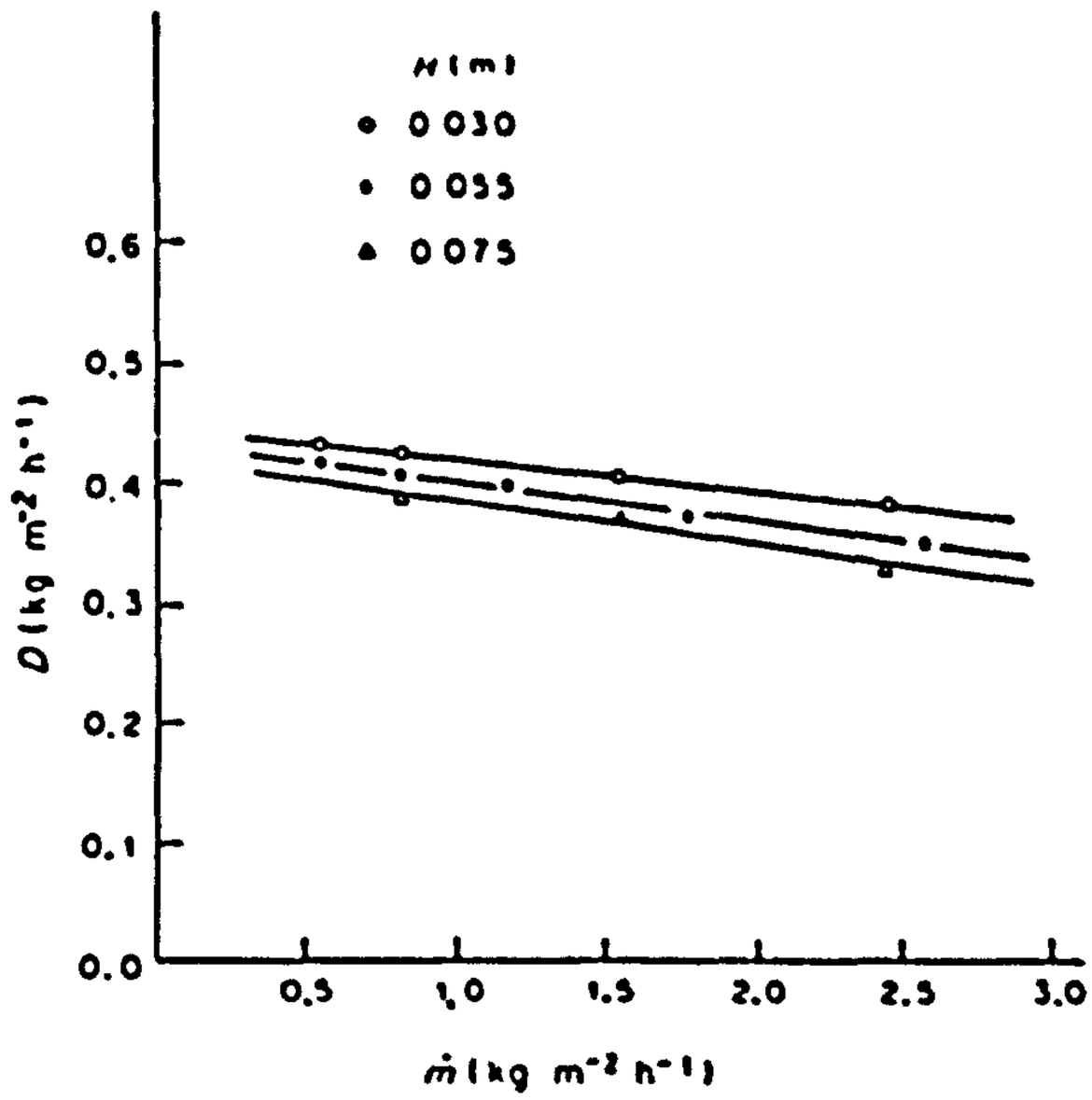

The effect of $\dot{m}$ on D ($I_o = 550$, $V' = 1.8$, $T_a = 298$, $l = 0.044$).

Fig. 1.2.7. Variation of a wick-type solar still productivity (D) with input water flow rate ($\dot{m}$) of saline water (After Yeh and Chen, (1986)). I_o: Irradiance, V': Wind speed, T_a: Ambient temperature, l: Insulation thickness.

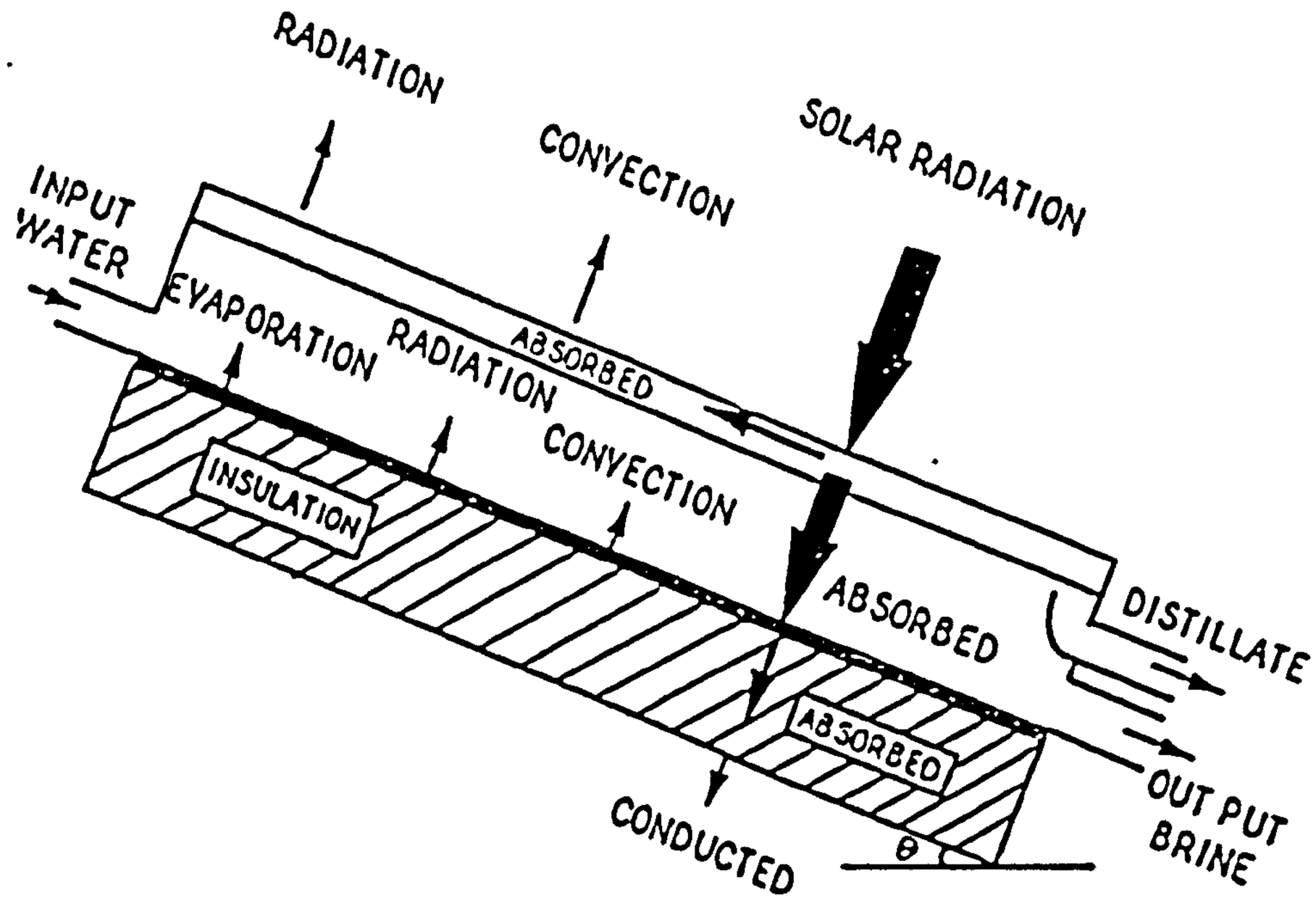

Fig. 1.2.8. Energy flows for a tilted wick solar still.

CHAPTER TWO

EXPERIMENTAL EQUIPMENT AND PROCEDURES

This chapter is concerned with the construction and operation of an experimental wick-type solar still, together with the ageing treatment of absorbing and reflecting materials and instrumentation adopted for this work.

2.1 SOLAR DISTILLATION SYSTEM

The distillation system consists of five main parts as shown in Fig. 2.1.1 and Plate No. 1. The still (1) is fed by saline water from the main reservoir (2) through the constant head device (3) which controls the input flow rate. The distillate is collected in a distillate bottle (4) below the still. The excess brine drains away to a brine reservoir (5) which is also below the still. The instrumentation system is described in section (2.2).

2.1.1 Wick-type still: construction and materials

The wick-type solar still is as shown in Fig. 2.1.2. A sheet of galvanized steel with rectangular dimensions 1000 mm × 700 mm was folded to make a 52 mm deep rectangular tray (1) with a U-shape section at the top of the lower edge and a right-angled section at the top of the upper one. The cover glass sheet (2) was fitted between these two sections. The sides of the tray are wooden battens of 25 mm thickness. One layer of 9 mm thickness moisture (and fire) resistant board (Masterclad, Cape Insulation) (3) is fixed inside the tray to support the absorber cloth. A sheet of 12.5 mm thickness polystyrene (4) is positioned underneath the support board to insulate the bottom of the tray. The absorber wick (5) is made of charcoal cloth, Freeman *et al.* (1986), which is commercially available (Charcoal Cloth Limited). Its upper edge is immersed in the brine in a rectangular cross section aluminium channel (6) in which a constant water level can be maintained by a constant head device arrangement. The upper part of the charcoal cloth goes over the lower edge of the aluminium channel. The tray is covered by a sheet of 4 mm thickness glass with a rubber gasket (7). A sponge rubber gasket between the glass and the tray helps to ensure there are no gaps between the glass pane and the tray walls. The glass cover is pressed on the inner walls of the still to make the enclosure airtight. The upper edge of the cover is pressed by a steel strip (8) of 5 mm thickness and 25 mm width having the same length as the cover by means of two steel clamps, and the lower edge is inserted in the U-shape section at the lower edge of the tray.

The tray is insulated from the ambient conditions by boards of styrofoam (9) of thickness 35 mm. It is fixed on a dexion frame by which the system can be oriented towards the south. The inclination of the still can be adjusted according to the solar altitude angle at noon. A drain (10) for the excess saline water has been fixed along the lower edge of the support board. It is an aluminium gutter, commercially available with rectangular cross section 15 mm x 20 mm. Another shorter aluminium channel (11) with rectangular cross section 10 mm x 12 mm is fixed on the inner surface of the glass cover to collect the distillate. The glass cover width exceeds the length of this aluminium channel by about 60 mm so that distillate can pass to a second channel (12) with square cross section 15 mm side. This is connected to the distillate reservoir. The geometrical drawing of the still is shown in Fig. 2.1.3.

2.1.2 Flow rate system

Obtaining a uniform and controllable saline water flow rate through the absorber cloth of the still is an important requirement of the present work. The flow rate is small and in the range of (2 - 6) kg/m^2.h. A flow rate control system has been developed and consisting of four main parts as shown in Fig. 2.1.4.

(a) A plastic tank of 15 liters maximum capacity with water surface area 400 mm x 400 mm. This is the saline water main reservoir connected to the constant head device. The outlet flow rate is always more than that to the solar still and is controlled by means of a stop-cock valve. This replaced a (previously used) 4 litre plastic bag reservoir which is

commercially available for horticultural drip feeding of plants Mahdi *et al.* (1990). This arrangement was not adequate for long runs.

(b) A constant head device (CHD) as shown in Fig. 2.1.4. maintains the water level constant in the aluminium channel. A flexible connection tube, 12 mm inner diameter, connects the CHD and the aluminium channel.

(c) An adjustable platform controls the level of the CHD and consequently the saline water level in the aluminium channel.

(d) A dial gauge device by which one can monitor the vertical level of the CHD relative to a fixed level.

2.1.3 Controlling the saline water flow rate

The plastic main reservoir is fixed on a frame at a level higher than the CHD by a distance of about one meter. The saline water is fed from the main reservoir through a 12 mm inner diameter flexible tube into the CHD. The stop-cock valve is fixed at the outlet of this tube and clamped at a constant level relative to the main reservoir to keep the head difference constant.

The overflow saline water goes via pipe (1) in Fig. 2.1.4 to a bottle from which it is sent back to the reservoir using a peristaltic pump. The water is fed to the still through pipe (2) by a 12 mm inner diameter tube to the aluminum channel. The water level in this channel is the same as in the CHD. The charcoal cloth, with its upper edge, is immersed in the saline water in the channel. The water rises upwards to pass over the edge of the channel by capillary action of the charcoal cloth (Fig. 2.1.2). The water passes down the cloth on the inclined surface.

The flow rate of the saline water can be controlled by moving the adjustable platform up and down and monitoring the dial gauge. This action affects the water level in the CHD and consequently in the aluminium channel inside the still. So, the upward distance, which the water has to be raised by suction due to the capillary property of the charcoal cloth, is variable. The flow rate of the saline water is highly dependent on the water level in the aluminum channel.

2.1.4 Solar concentrator

The solar concentrator used in this work is of the V-trough type. Its sides are made of two flat boards of Dow Corning Styrofoam (i.e. extruded polystyrene) of 1000 mm x 610 mm x 35 mm dimensions. These are lined with a self adhesive 3M Scotchcal Film 530 to form the mirrors of the concentrator. The boards are fixed at their ends by a truncated V-shape area, of the same styrofoam material, with a fixed apex angle of 30°. The cross section of the trough is shown in Fig. 2.1.5. The height of the concentrator is 542 mm. It can be fixed on the still glass cover using four wires, one from each top corner to the frame of the solar still.

2.1.5 Lamp array

A radiant energy source has been constructed. It has two rows of three lamps and one row of four lamps with 25 cm separation distance between adjacent lamp centres. The rows are separated by a distance of 21.6 cm. Eight Osram 120 watt PAR

(Parabolic Aluminised Reflector) lamps with 30° beam width are used. These are positioned around two 275 watt infrared lamps (Thorn EMI) as shown in Fig. 2.1.6. No attempt was made to obtain parallel radiation. The aim was to achieve a reasonable uniform irradiance.

The lamp spectrum will have about 70% infrared radiation while solar radiation has about 47.3%. The radiant energy source can produce an average radiant energy flux of about 420 W/m^2 on a surface area of 50 cm x 100 cm located 125 cm from the front plane of the lamps. The lamps are fixed on wooden battens. These are connected to each other and to a dexion frame to allow for tilting, parallel to the plane of the solar still as shown in Fig. 2.1.7.

2.2 INSTRUMENTATION

Various parameters have to be measured simultaneously and periodically in order to investigate the performance of a wick-type solar still e.g. absorber and cover temperatures, solar insolation and wind speed.

In this work the emphasis has been on temperature and solar insolation measurements. These were collected and stored by a Delta-T Devices data logger in nineteen individually configured channels. Temperatures were measured in various positions of the still using thermocouples. The solar insolation was measured by Kipp and Zonen solarimeters.

2.2.1 Temperature measurements

In order to measure the temperature of the wetted charcoal cloth, four metal sheathed thermocouples from Comark Electronics Limited are fixed underneath the cloth and distributed in a suitable arrangement. Five self-adhesive patch thermocouples supplied by TC Ltd. are attached at different locations on the outer surface of the glass cover to measure the cover temperatures. Another two patch thermocouples are fixed on the back surface of the galvanized steel tray to monitor the temperature at the interface of the styrofoam with the tray. These patch thermocouples are standard, type K, suitable for operating up to 250 °C. They were supplied with a lead length of two meters. Also, another metal sheathed thermocouple is inserted between the support board and the polystyrene sheet. This is used as an indicator of the thermal insulation of the support board and to monitor the temperature there. The inlet and the outlet saline water temperatures were also measured by means of sheathed thermocouples. One patch thermocouple was attached in a shaded point somewhere underneath the inclined support board of the solarimeters to measure the ambient temperature. All these thermocouples are connected to the data logger which records the temperatures each minute and stores the average values of the temperature over five minutes. These thermocouples were calibrated, together with the temperature measurement data logger, against a mercury thermometer at temperatures between the ice point and the water boiling point. The accuracy of their measurement was in the range of ± 0.2 °C.

2.2.2 Insolation measurements

The solar insolation data were measured by two Kipp and Zonen dome solarimeters of serial Nos. 774038 (called Kipp and Zonen No.1) and 752429 (called Kipp and Zonen No.2) and one tube solarimeter supplied by Delta-T Devices serial No. T6M 6640. Kipp and Zonen No. 2 is shaded by 6 cm width semicircular ring to measure the diffuse irradiance. The tube solarimeter was used on different occasions when the solar concentrator was in use and it was centred on the base of the solar concentrator parallel to the long edge. The specifications of these solarimeters are in Appendix A2. The two dome solarimeters were calibrated on 22/3/1989 by the U.K. Meteorological Office. The certificates are shown in Appendix A2. The dome solarimeters were fixed on an inclined board in the same plane of the solar still. They were connected to the data logger which measured the solar irradiance every 10 seconds. The five minute average irradiance was stored by the data logger during the experiment running time.

2.2.3 Wind speed measurement

The wind speed passing over the still was measured by a propeller type anemometer (battery operated) supplied by Air Flow Developments. The propeller is fixed 50 cm above the mean level of the solar still. The anemometer measurement was calibrated against an electronic TSI model 1650 air velocity meter using the wind tunnel in the aerodynamic laboratory at the department. Wind speed was recorded manually every 30 minutes during the course of the experimental test.

2.2.4 Data logger

This is a Delta-T Devices data logger with a serial No. DL6902. It is a battery operated electronic device for taking and storing readings from sensors. Up to 62 input channels, using four input/output cards, are available and the logger can accept input in the form of voltages, resistances, counts, frequencies or digital levels. In this work nineteen channels were used and their input was in the form of voltages from the solarimeters and the thermocouples. Their labels, sensors type and functions are shown in Table 2.2.1.

Recording of the data by the logger is completely automatic. Recorded data are stored in the logger's memory and can be displayed by a printer or transferred to a computer for storage on a disc. Instructions are given to the data logger via a BBC computer by using computer software. Seven software files are used to deal with the logger. These are as follows: (1) EDITLIB, (2) EDITLOG, (3) COMMS, (4) COLLECT, (5) UTILITY, (6) LOGDAT3, (7) SENSORS. The main stages and more detailed instructions are shown in the flow charts in Figs. 2.2.2 and 2.2.3 respectively. A sample of the printout of the logger is shown in Fig. 2.2.4.

. Standard sensor information is contained in the SENSORS file, e.g. thermocouples types available are J, K, and T. The temperatures are measured by thermocouples relative to a cold junction channel usually channel No. 1. This is a two kΩ cold junction thermistor. Its maximum error is 0.18 °C when the

logger works in an ambient temperature range of -20 to +80 °C, Delta-T Devices Manual (1987).

2.2.5 Other instruments

(a) Spirit level to fix the horizontal level of the still.

(b) Inclinometer to fix the still inclination angle relative to the horizontal.

(c) Stop watch to measure the amount of the saline water flow rate with the help of a measuring cylinder.

(d) Electronic balance to weigh the distilled water produced every 30 minutes.

2.3 EXPERIMENTAL PROCEDURE

Outdoor and indoor tests of the solar distillation system were carried out with various variables. There were some similar and other different steps achieved for the both tests. Those steps have been classified according to their time relative to the data collection i.e. before, during and after data collection by the data logger.

2.3.1 Outdoor tests

Tests of the solar still were conducted with and without the V-trough solar concentrator on various sunny days by varying the saline water salt concentration and the input water flow rate. The following steps were needed for each experiment.

2.3.1.1 Before data collection

(i) The data logger was configured and its start logging time was set then connected to the various sensors.

(ii) The top and lower edges of the still were set horizontally using the adjustable platform and spirit level.

(iii) The inclination angle of the still was set in relation to the solar altitude at noon with the aid of the inclinometer.

(iv) Sufficient of the feed water of a certain salt concentration was prepared.

(v) The absorber was rinsed with tap or distilled water by letting a high flow pass through the charcoal cloth for (10-15) minutes.

(vi) The required flow rate of the feed water was adjusted by measuring the over-flow rate and the total flow rate leaving the main reservoir, with the aid of a stop watch, measuring cylinder and the adjustable platform.

2.3.1.2 During data collection

(i) The data logger recorded the temperatures and solar insolation.

(ii) The weight of distillate produced each 30 minutes was determined.

(iii) The wind speed was determined using the propeller connected to the digital meter, every 30 minutes.

(iv) The over-flow feed water was periodically returned to the main reservoir by using the peristaltic pump.

(v) Step (vi) of the above subsection (2.3.1.1) was repeated once per hour.

(vi) The volume of the excess brine was measured every 30 minutes.

2.3.1.3 After the data collection

(i) The data logger was disconnected from the sensors and connected to a BBC computer.

(ii) The data was converted to a readable form using the computer and then printed.

2.3.2 Indoor tests

Tests were carried out by using the lamp array as a source of energy. The parameters which have been studied indoor are input water flow rate and its salinity. The steps required in these tests are mostly the same as mentioned in section (2.3.1) with some exceptions.

2.3.2.1 Before the data collection

(i) The lamp array was switched on and left about 30 minutes to reach a steady state by checking the lamps surface temperature.

(ii) Steps (i), (ii) and (iv-vi) as in subsection (2.3.1.1).

(iii) The inclination angle required of the solar still and the lamp array was fixed.

2.3.2.2 During the data collection

(i) As in subsection (2.3.1.2).

(ii) To vary the input water flow rate the CHD level was varied by means of the adjustable platform relative to a fixed level by monitoring the dial gauge.

2.3.2.3 After the data collection

As in subsection (2.3.1.3).

2.4 INVESTIGATION OF MATERIALS

2.4.1 Introduction

The absorber of a solar still is one of the most important components influencing the performance of a solar still because of its direct effect on the fraction of incident solar energy which is absorbed. Therefore the absorber material should have high absorptance and good durability. Reflecting materials for solar concentrators should have high spectral reflectance and durability to withstand the environmental conditions.

Charcoal cloth has been selected as the absorber material and the self adhesive 3M Scotchcal Film 530 as the reflecting material in the present work. The durability and optical properties of these and some other materials have been investigated by determination of solar reflectance of the samples using an integrating sphere reflectance spectrometer and an infrared spectrometer.

2.4.2 Charcoal cloth as a solar still absorber and capillary wick water transport material

In the construction of a wick-type solar still, the absorber should be a porous black material which serves as the solar radiation absorber and brine transport medium. Many investigators, e.g. Sodha *et al.* (1981) and Tiwari *et al.* (1984, 1985), Yeh and Chen (1986) and Tiwari and Yadav (1987) have used blackened jute as an absorber material. This suffers from blockage of pores and fading. It needs frequent replacement and/or black dye injections. Charcoal cloth has been used in this work instead of the jute, since it is inherently black, no dye is required and exhibits no contraction after being soaked by water.

Charcoal cloth is a textile form of activated carbon. It is a highly porous adsorbent used for a wide variety of purposes including air purification, pollution control and medical applications. It is produced in the U.K. by Charcoal Cloth Limited from viscose rayon cloth (regenerated cellulose) in a knitted or woven form. It is therefore more costly than conventional powdered or granular activated carbons, Hitchcock *et al.* (1983). The rayon is first pre-treated with a mixture of inorganic chlorides in aqueous solution and dried. The impregnated cloth is then carbonized in an inert atmosphere and activated in carbon dioxide gas in a furnace at temperatures up to 880 °C, Freeman *et al.* (1986). The material currently produced on a commercial basis in the U. K. is highly microporous (pore widths < 2 nm) with 0.55 mm thickness. Fig. 2.4.1 shows a scanning electron

micrograph of a specimen of charcoal cloth which has been used at this work at two magnifications using a Cambridge Stereoscan 250 MK-2 scanning electron microscope.

The solar absorptance of the charcoal cloth has been measured as received and after environmental treatment using a Lambda-9 Perkin-Elmer spectrometer, for the visible (VIS) and near infrared (NIR) radiation, and 683 Perkin-Elmer infrared (IR) spectrometer for the IR radiation.

Samples of charcoal cloth were compared with others of blackened hessian supplied by B. Brown (Holborn) Ltd. They had been exposed to the outdoor conditions for different periods of time. They were fixed in a shallow box covered by a transparent thin plastic sheet to prevent direct rainfall, dust accumulation etc. This box was tilted facing the south. A monthly adjustment of angle was made in relation to the average solar altitude at noon. The solar reflectance of the samples was measured before and after such treatment.

2.4.3 Reflecting materials for the solar concentrator

Self adhesive 3M Scotchcal Film 530 has been used in the V-trough concentrator, (subsection 2.1.4). This material (together with others) has been investigated before and after various treatments. The selection of the reflecting material is based on relatively high spectral reflectance, low cost and good durability. Different samples were tested in high humidity and/or heated enclosures at various temperatures and periods of time. Outdoor exposure tests were conducted on different samples for different times with varying weathering conditions.

The heat treatment was done in an oven (Medical Electronics Ltd., Type M. P. C.) of size 0.3 x 0.3 x 0.3 m^3 with adjustable temperature for periods up to hundreds of hours at temperatures between 80 °C and 180 °C.

The cycling heat and humidity treatment was done in a humidity chamber (Kelvinator, Model HCVH14, serial No. S04145) of size 0.72 x 0.72 x 0.68 m^3 with monitoring relative humidity (R.H.) and temperature which were 5, 7 and 10 cycles 24 hours each cycle.

Samples of reflecting materials were also fixed inside a shallow box covered with transparent plastic sheet and then exposed to the outdoor environmental conditions. Some of the samples were exposed for up to one year. Analyses of the surface microstructures and composition of the reflecting samples were carried out using a Cambridge Stereoscan 250 MK-2 scanning electron microscope equipped with a solid state detector.

2.4.4 Reflectance measurements using the Perkin-Elmer integrating sphere

In this study the spectral reflectance ρ_λ (for wavelengths throughout the solar spectrum) of every sample was measured using a 60 mm Perkin-Elmer integrating sphere serial no. 6125, connected to Lambda-9 Perkin-Elmer Spectrometer. This gives the spectral reflectance of a sample in the region (0.3 - 2.5) μm. This region of the spectrum has been divided into twenty equal increments of energy, (Appendix A3); each has a mean wavelength that divides the increment into two equal parts, Duffie and

Beckman (1980). According to selected ordinates for air mass 2 and 23 km visibility, the spectral reflectance has been measured on a chart in each midpoint wavelength using a cursor key, by which the spectrum can be traced, connected to a digitizer which is connected to a main computer terminal. A sample of a traced spectrum and the corresponding numerical data after conversion by the digitizer are shown in Fig. 2.4.2. The average of the reflectances of the twenty midpoints were calculated using a simple program developed especially for this purpose, (Appendix A3). The calculated average represents the reflectance of the sample in the solar region. A sample of a calculated spectrum is shown in Fig. 2.4.3.

The Perkin-Elmer spectrometer is a double beam instrument and, in reflectance measurements, one beam falls on a reference plate of $BaSO_4$ powder, while the other strikes the sample. The instrument measures the ratio of the radiation reflected from the sample to that reflected from the reference, and it would appear that the instrument measures the reflectance of the sample relative to the reference. However, before recording the sample measurement, another reference sample needs to be put in the sample position so that the recorded sample reflectance on the chart would be on a (0 - 100)% scale in the wavelength region (0.3 - 2.5) μm. This calibration is memorized in the instrument's computer for all other samples while the instrument is in the ON condition.

Table 2.2.1. Channels of the data logger, their labels, sensor types and functions.

CHANNEL NUMBER	SENSOR TYPE	CHANNEL LABEL	SENSOR FUNCTION
1	TM1	COJ	COLD JUNCTION
2	DOME SOLARIMETER	KIP1	GLOBAL INSOLATION
3	DOME SOLARIMETER	KIP2	DIFFUSE INSOLATION
4	TUBE SOLARIMETER	TSA	CONCENTRATED INSOLATION
5	PATCH TC.	TC1	AMBIENT TEMPERATURE
6	SHEATHED TC.	TC2	INPUT BRINE TEMPERATURE
7	SHEATHED TC.	TC3	OUTPUT BRINE TEMPERATURE
8	PATCH TC.	TC4	COVER TEMPERATURE
9	PATCH TC.	TC5	TRAY TEMPERATURE
10	PATCH TC.	TC6	TRAY TEMPERATURE
11	PATCH TC.	TC7	COVER TEMPERATURE
12	PATCH TC.	TC8	COVER TEMPERATURE
13	PATCH TC.	TC9	COVER TEMPERATURE
14	PATCH TC.	TC10	COVER TEMPERATURE
15	PATCH TC.	TC11	COVER TEMPERATURE
16	SHEATHED TC.	TC12	ABSORBER TEMPERATURE
17	SHEATHED TC.	TC13	ABSORBER TEMPERATURE
18	SHEATHED TC.	TC14	ABSORBER TEMPERATURE
19	SHEATHED TC.	TC15	ABSORBER TEMPERATURE

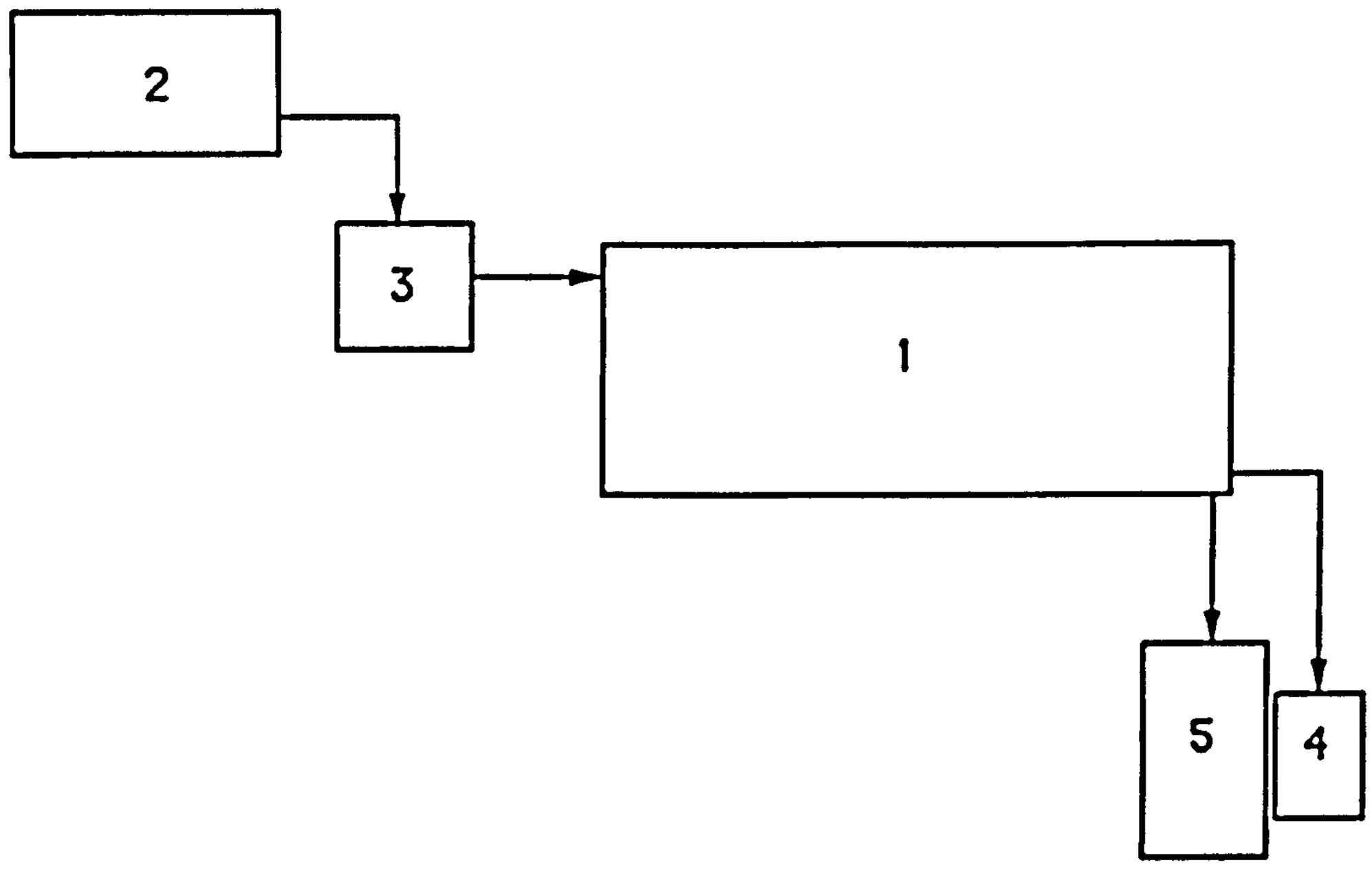

Fig. 2.1.1. Block diagram of the solar distillation system.(1) The still, (2) main reservoir of saline water, (3) constant head device, (4) distillate bottle and (5) brine reservoir.

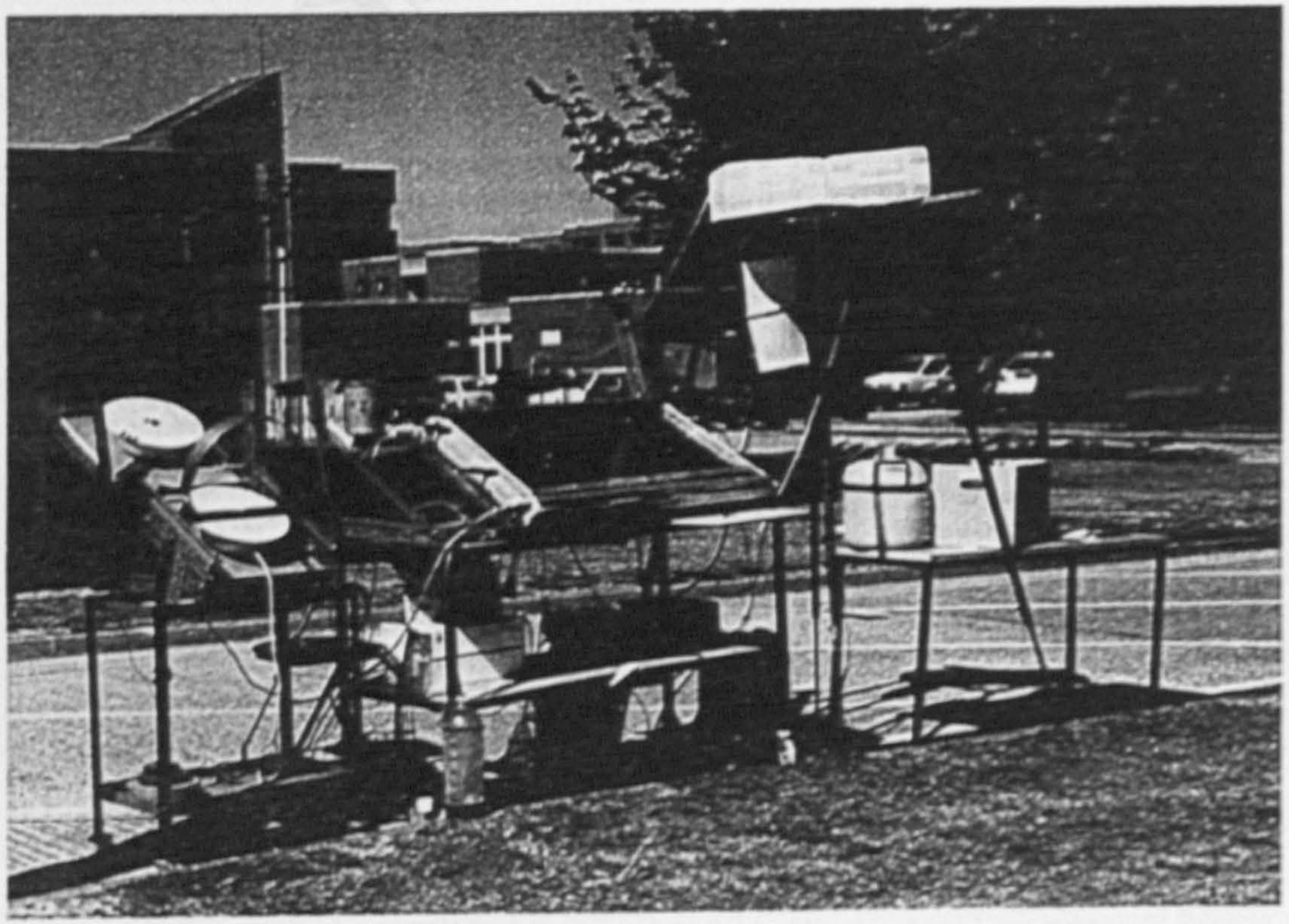

Plate No. 1

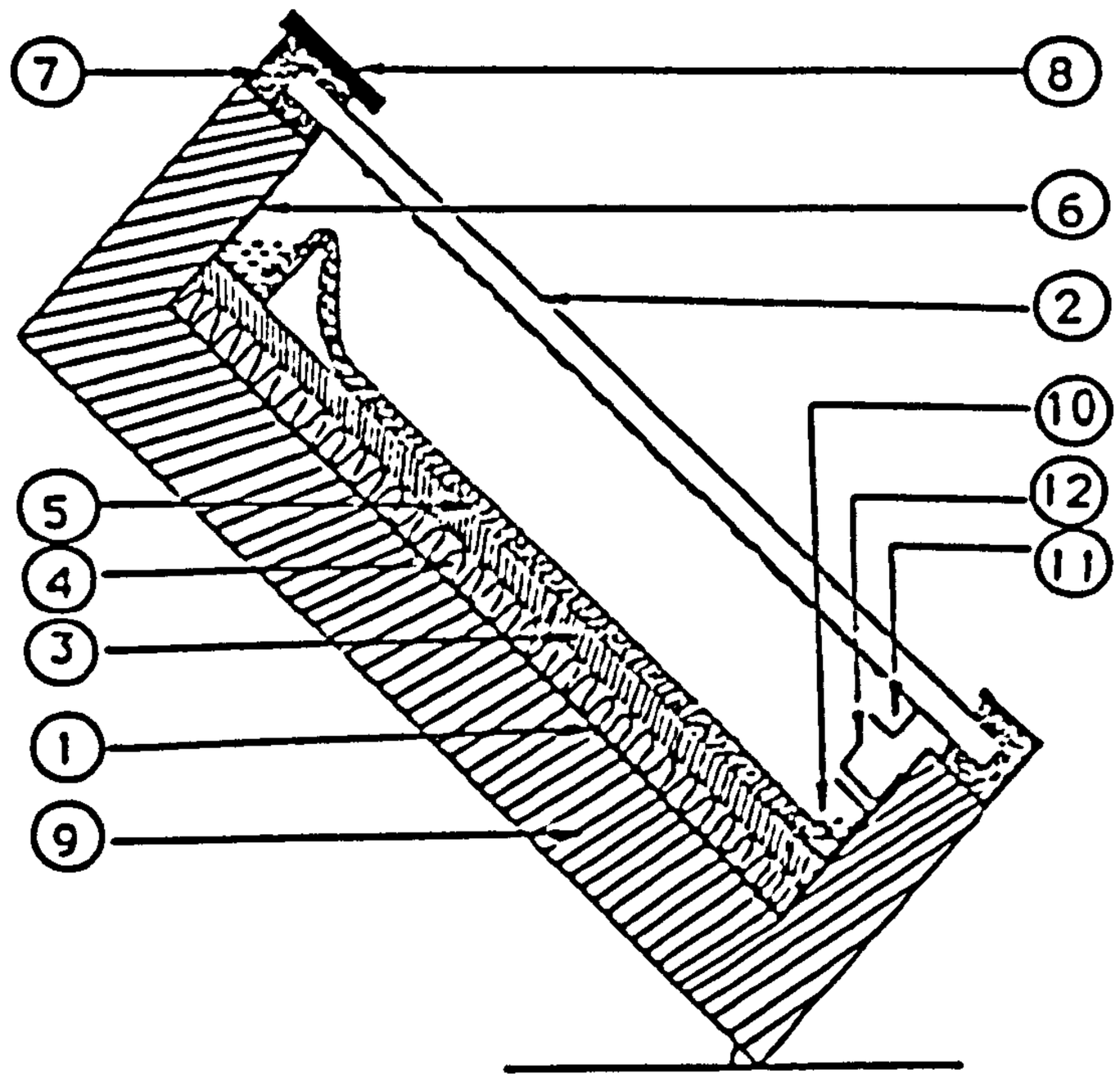

Fig. 2.1.2. Cross-sectional view of the solar still.

(1) Galvanised steel tray, (2) glass cover, (3) support board, (4) polystyrene, (5) charcoal cloth, (6) aluminium channel, (7) rubber gasket, (8) steel strip, (9) styrofoam, (10) brine gutter, (11) distillate gutter and (12) distillate outlet channel.

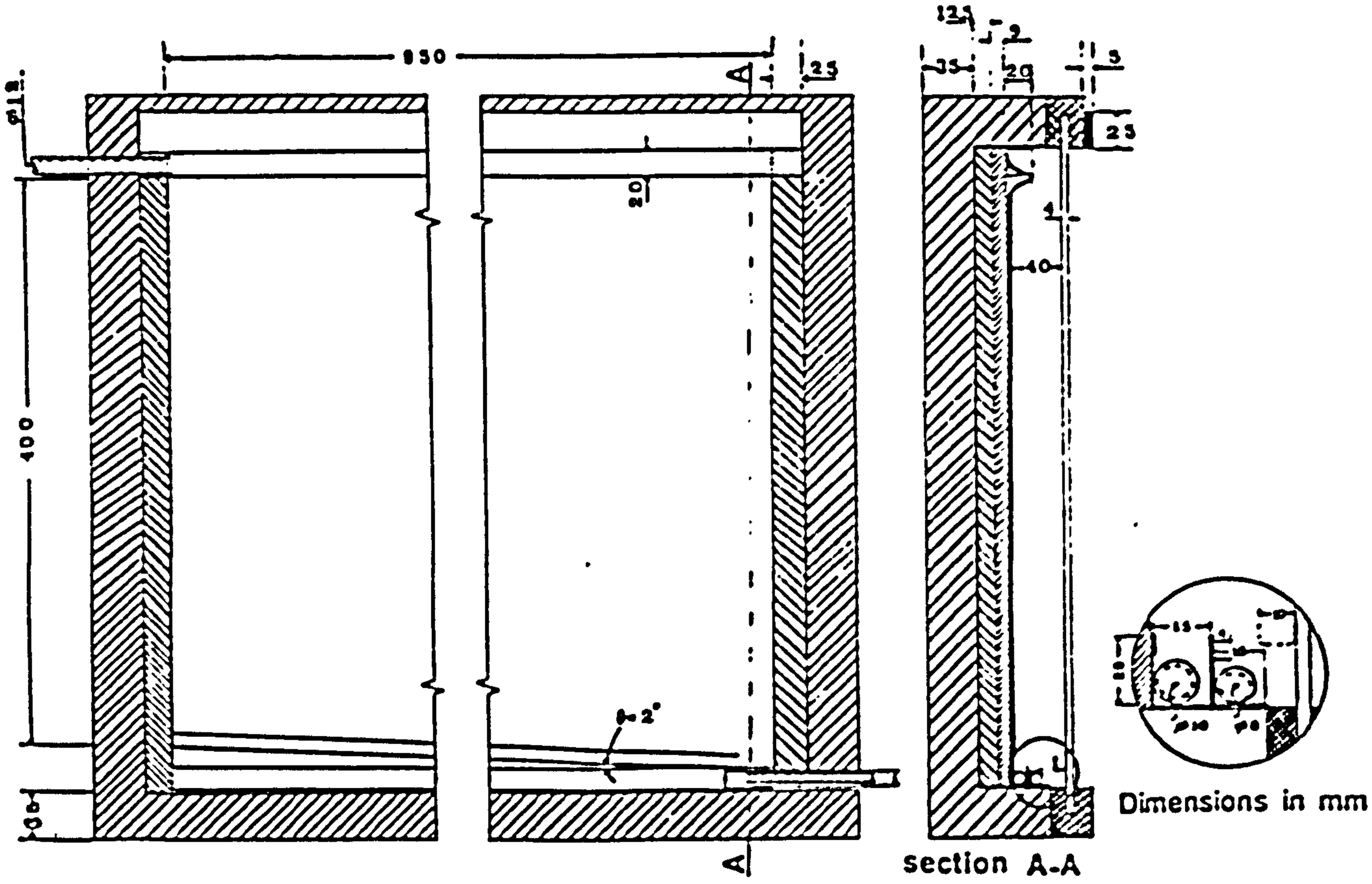

Fig. 2.1.3. Scale drawing of the solar still.

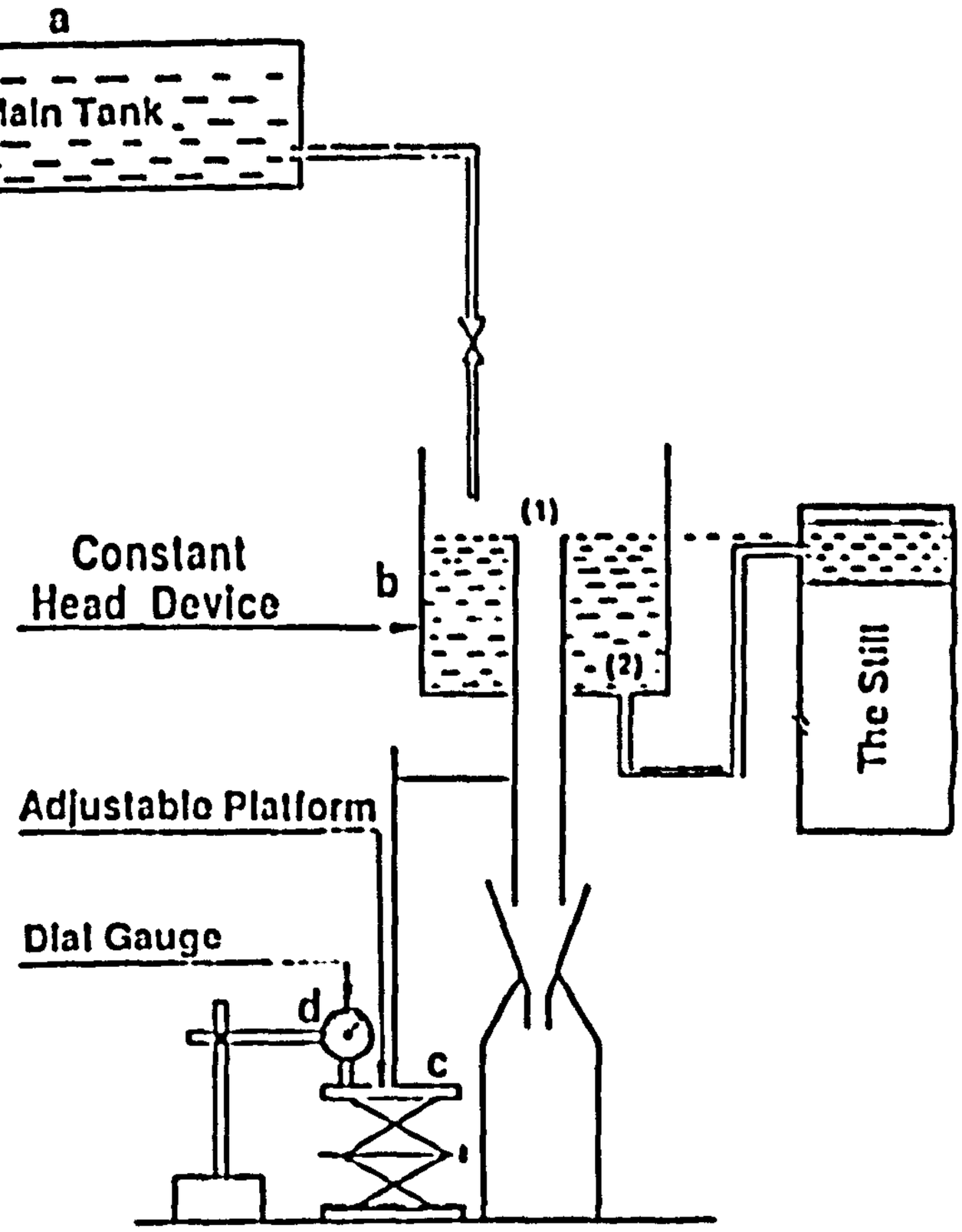

Fig. 2.1.4. Schematic diagram of the flow rate system. (1) Over flow pipe. (2) Still feeding water pipe.

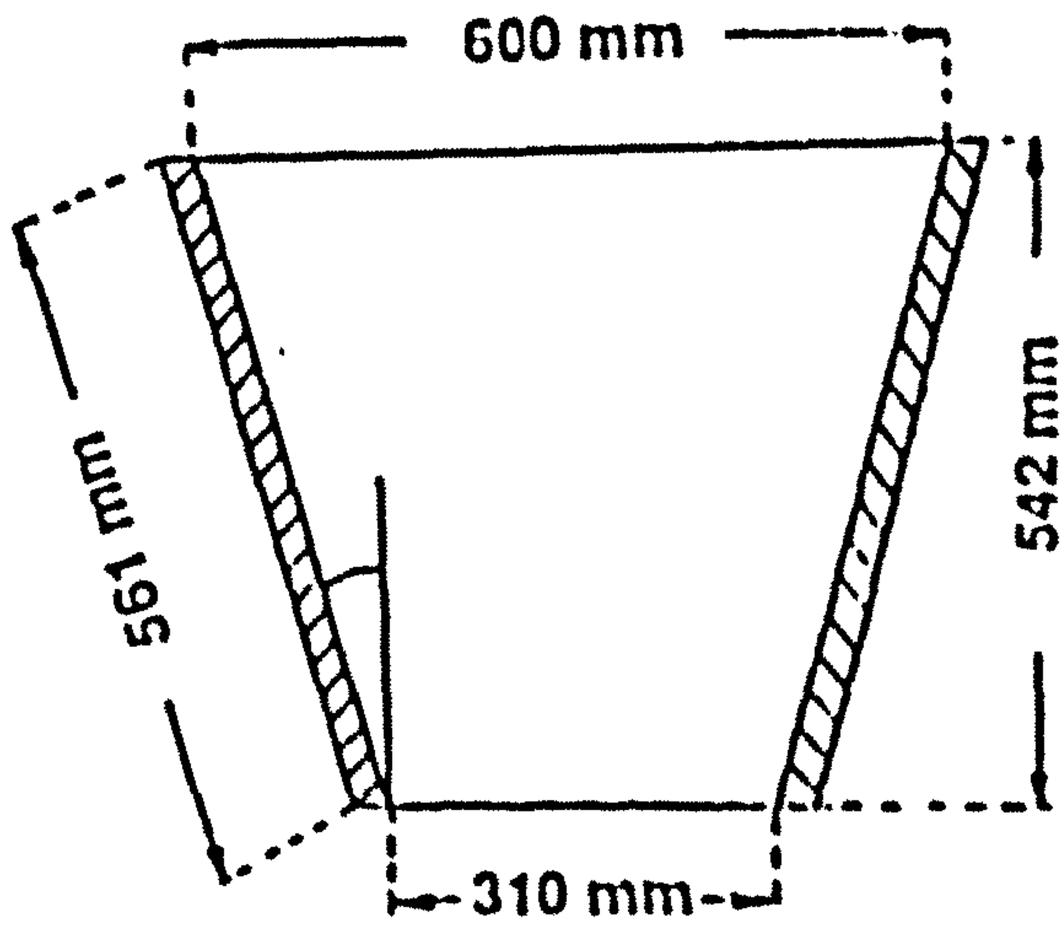

Fig. 2.1.5. V-trough solar concentrator geometry.

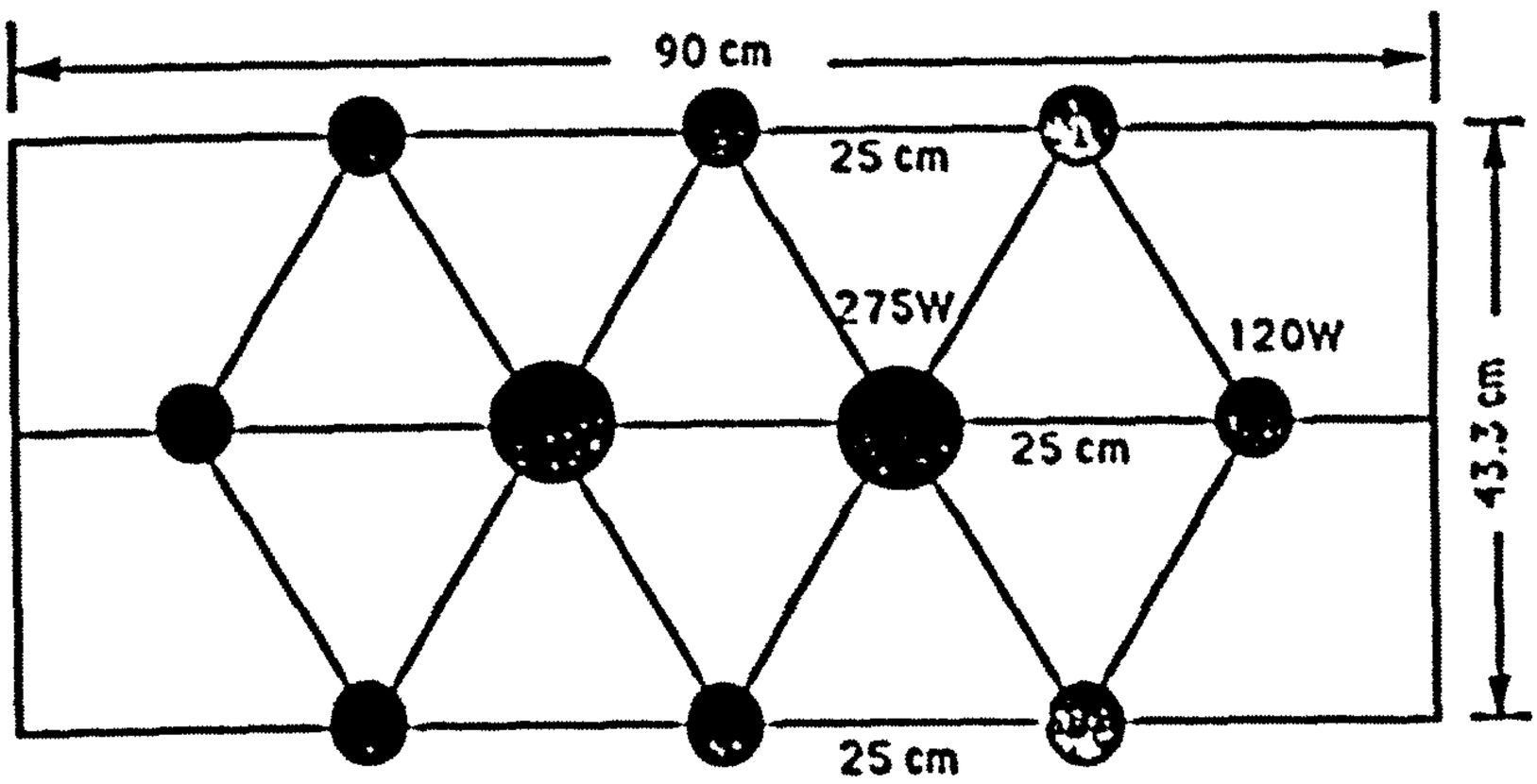

Fig. 2.1.6. Relative positions of the lamps in the lamp array.

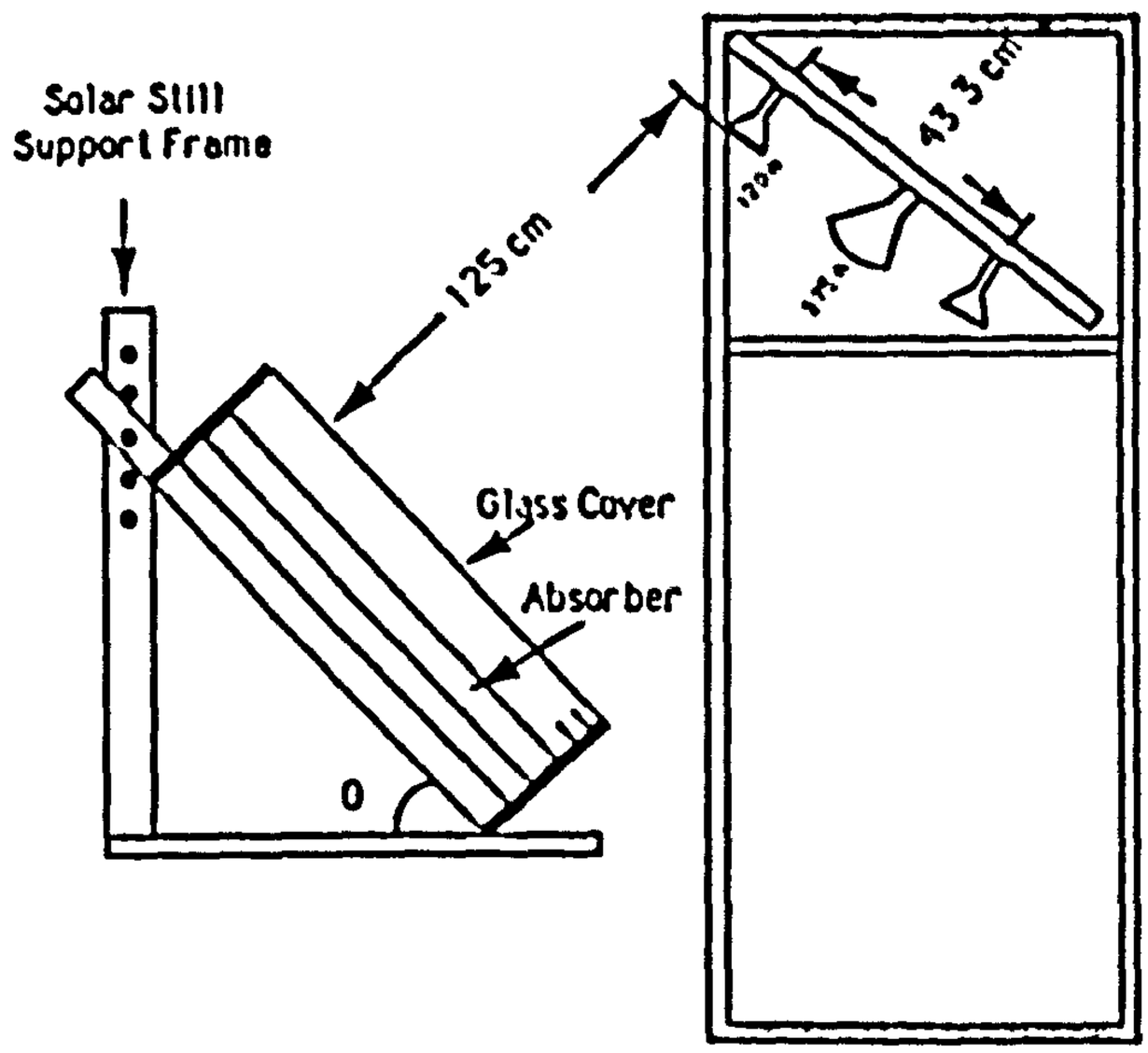

Fig. 2.1.7. Schematic side view of the still and the lamp array.

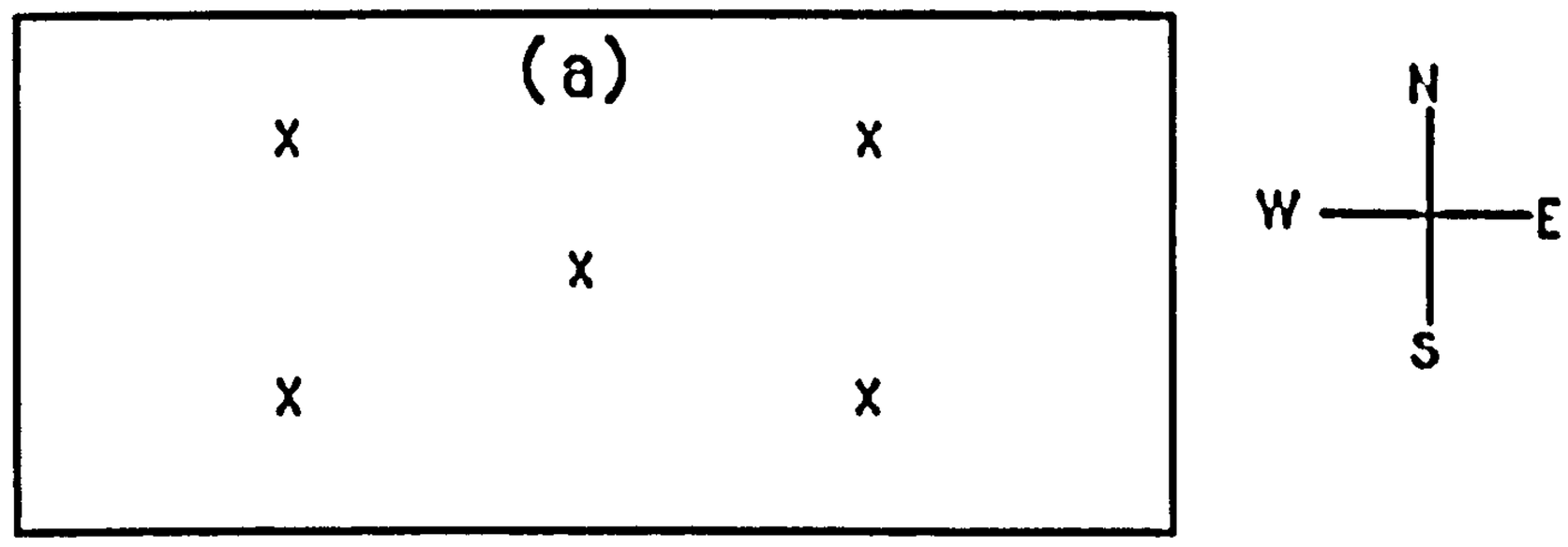

Fig. 2.2.1. Distribution of thermocouples (a) on the glass cover and (b) beneath the absorber cloth.

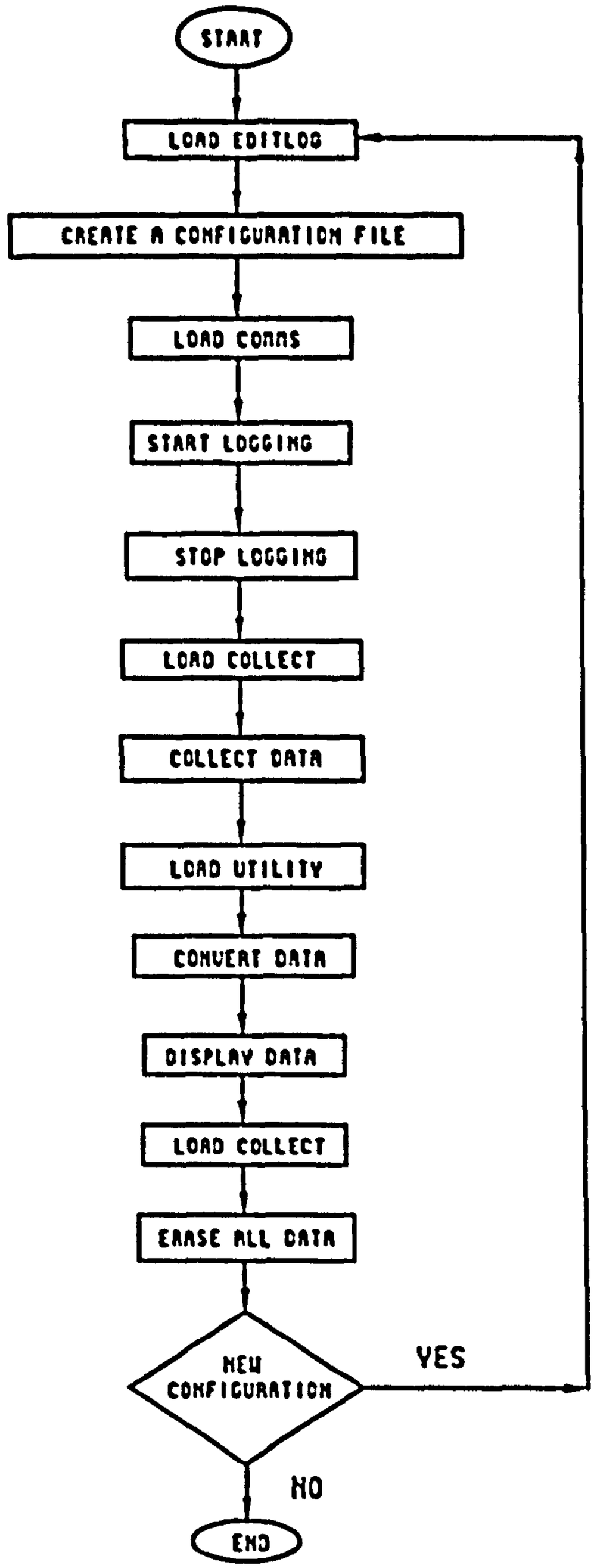

Fig. 2.2.2. Flow-chart of the main stages of use of the data logger.

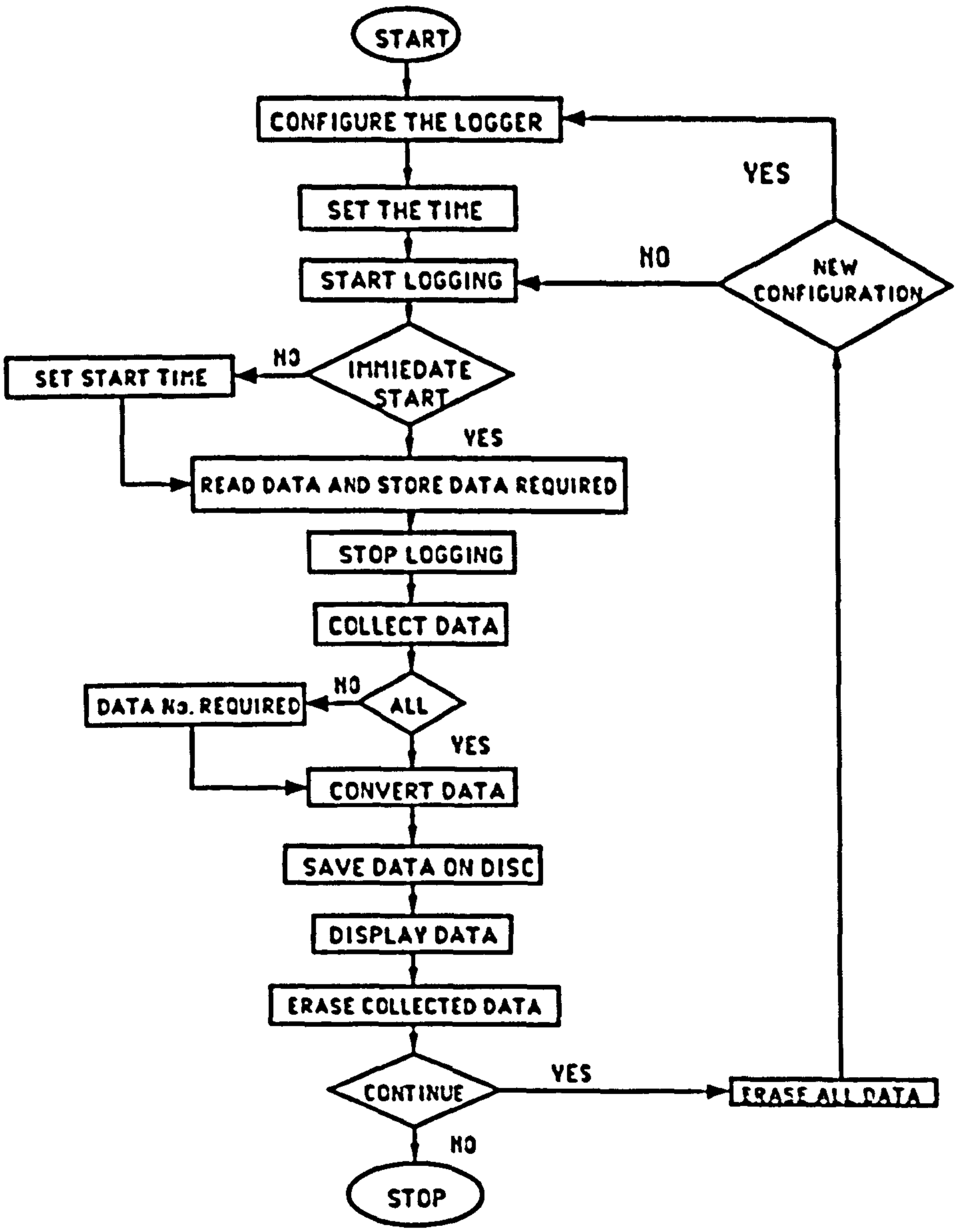

Fig. 2.2.3. Flow-chart for data logger instructions.

DELTA-LOGGER Data-Typing Utility
Typing Data File: DVI.DAT

E - over-run error
$ - noisy reading
% - o/s limits reading
& - over-range reading

Serial Number: DL 6902
Experiment: OCT
Started Logging: 26/11 11:15:00
Data Collected: 26/11 17:30:59
Data Type: TIMED

Channel Number	1	2	3	4	5	6	7	8	9	10
	11	12	13	14	15	16	17	18	19	20
Sensor Type	TMI	VLT	VLT	TSA	TCK	TCK	TCK	TCK	TCK	TCK
	TCK	TCK	TCK	TCT	TCK	TCK	TCK	TCT	TCT	TCT
Label	CO2	KIP1	KIP2	TSA	TC0	TC1	TC2	TC3	TC4	TC5
	TC6	TC7	TC8	TC9	TC10	TC11	TC12	TC13	TC14	TC15
Unit	deg C	Wm-2	Wm-2	Wm-2	deg C	deg C	deg C	deg C	deg C	deg C
	deg C	deg C	deg C	deg C	deg C	deg C	deg C	deg C	deg C	deg C
Minimum Value	18	7.8832E-5	.765412E-3	12.6	17.5	18.3	15.2	16.1	15.5	15.8
	21.4	20.7	22.1	21	16.9	17.7	16.7	16.9	17.7	16.8
Maximum Value	22	42.9	51.2	19.9	24	60.9	21.6	23.2	22.7	22.8
	26.3	25.9	27	26.6	80.6	24.4	23.9	24.1	24.8	60.6
26/11 11:15:00	3.956	.677113E-4	1.032495E-3	1.185072	3.756	3.036	3.396	3.516	3.396	3.436
	40%	40%	40%	40%	40%	40%	40%	40%	40%	40%
26/11 11:20:00	19.4	.374388E-2	2.81525E-2	20.52	18.1	20	16	16.8	16.2	16.3
	200%	200%	200%	200%	200%	200%	200%	200%	200%	200%
26/11 11:25:00	19	.901688E-2	.076998E-2	19.32	17.7	19.3	15.4	16.2	15.7	15.9
	92%	92.3%	93.3%	92.6%	91.7%	91%	90.7%	90.7%	91%	20%
26/11 11:30:00	18.7	.856428E-2	.929788E-2	19.32	17.5	18.8	15.2	16.2	15.7	15.8
	21.6	20.9	22.3	21.2	19.3	17.9	17	17.1	17.9	91.9%
26/11 11:35:00	18.5	.514558E-2	1.60635E-2	19.72	17.6	18.5	15.3	16.3	15.8	16
	21.7	20.9	22.4	21.4	19.1	17.7	16.7	16.9	17.2	18.9
26/11 11:40:00	18.4	.400125E-2	.466518E-2	19.92	17.7	18.4	15.4	16.5	16	16.2
	21.8	21.1	22.5	21.6	17	17.8	16.8	17	17.9	18.7
26/11 11:45:00	18.2	.317358E-2	.374756E-2	20.12	17.7	18.2	15.5	16.7	16.2	16.3
	21.9	21.2	22.6	21.7	18.9	18	17	17.2	18	18.6
26/11 11:50:00	18.1	.072818E-2	.101368E-2	20.52	17.7	18.1	15.6	16.9	16.4	16.5
	22	21.3	22.7	21.8	19.7	18.1	17.2	17.4	18.2	18.4
26/11 11:55:00	18	.781478E-3	.607758E-2	20.52	17.8	18	15.8	17.1	16.6	16.7
	22.1	21.3	22.8	21.9	16.6	18.3	17.4	17.5	18.4	18.3
26/11 12:00:00	18	.025158E-2	.082568E-2	20.42	17.9	25.2	16	17.3	16.8	17
	22.2	21.5	22.9	22	26.9	19.4	17.5	17.7	19.6	24.4
26/11 12:05:00	18	.781498E-3	.026668E-2	20.42	18	30	16.1	17.5	17	17.2
	22.2	21.6	23	22.2	32.2	18.7	17.7	17.9	18.8	29.9
26/11 12:10:00	18	.465968E-3	.290758E-3	20.72	18	30.8	16.3	17.7	17.2	17.4
	22.4	21.7	23.1	22.3	31.8	18.9	18	18.1	19	31.4
26/11 12:15:00	18	.112258E-2	.210358E-2	20.52	18.1	19.9	16.5	18	17.4	17.6
	22.5	21.9	23.2	22.5	23.6	19.1	18.2	18.4	19.3	21.4

Fig. 2.2.4. Sample of the data logger printout.

(a)

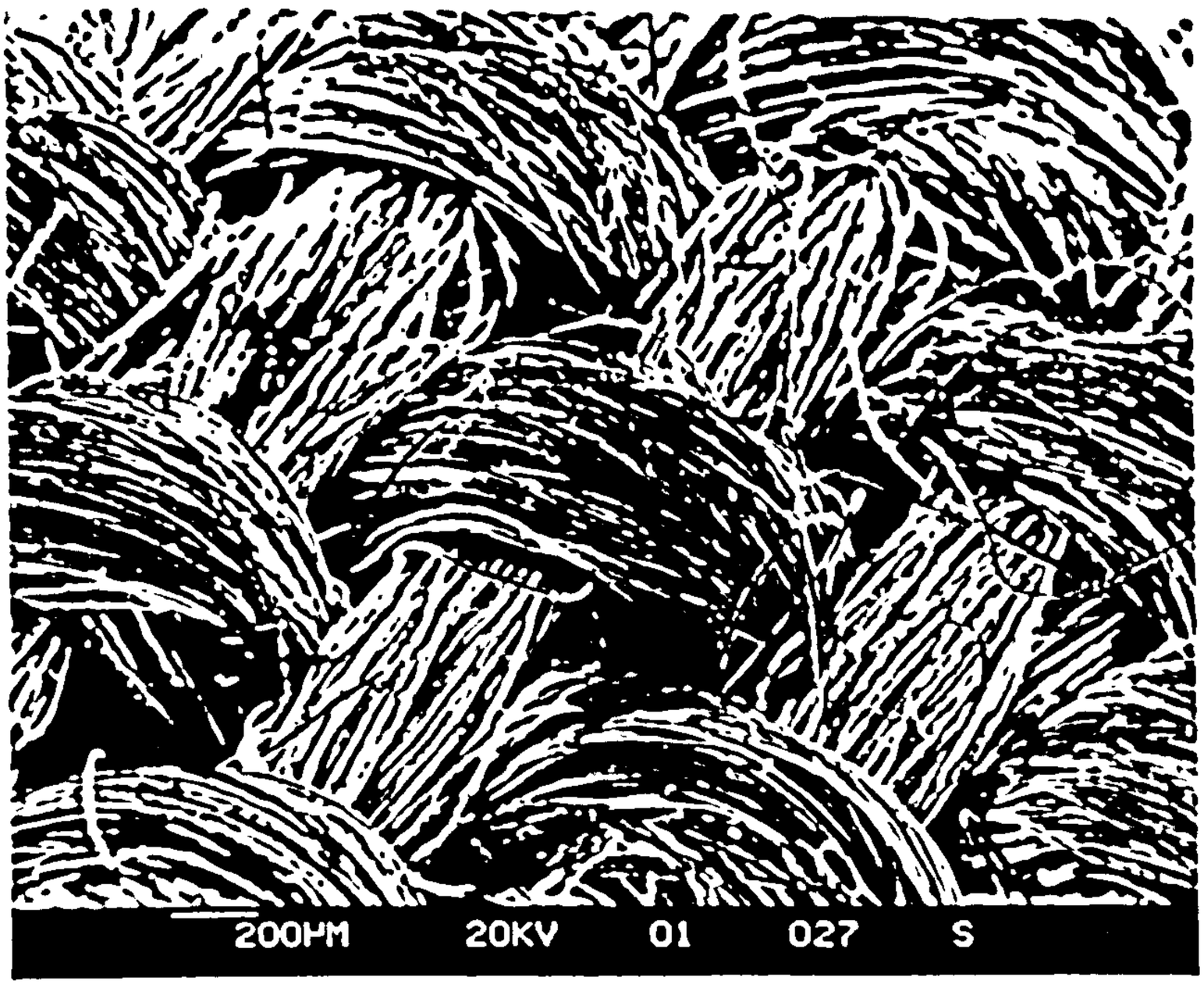

(b)

Fig. 2.4.1. Scanning electron micrograph of an as-received sample of charcoal cloth, (a) low and (b) high magnifications.

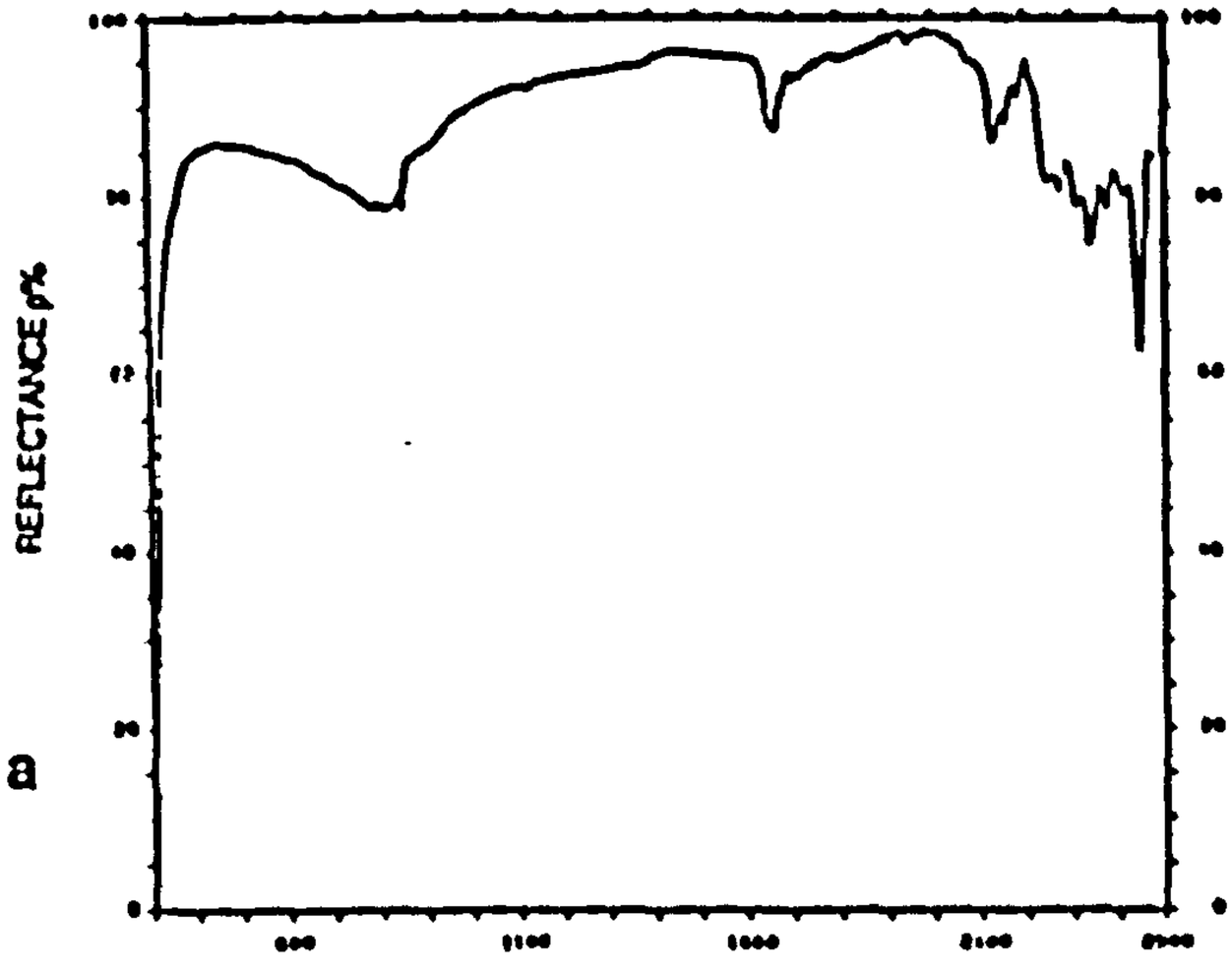

a

b

```
SAMPLE : 3M SCOTCHCAL FILM 530
01+0010.1,+0166.8/        01+0052.2,+0151.5/
01+0015.0,+0169.4/        01+0056.9,+0163.5/
01+0020.1,+0169.2/        01+0062.3,+0170.5/
01+0023.5,+0168.6/        01+0070.0,+0179.0/
01+0027.7,+0167.2/        01+0076.5,+0182.5/
01+0031.2,+0166.0/        01+0086.5,+0185.8/
01+0034.9,+0164.4/        01+0095.6,+0187.8/
01+0039.3,+0161.7/        01+0122.8,+0191.9/
01+0043.1,+0159.1/        01+0138.2,+0184.5/
01+0046.6,+0155.1/        01+0198.6,+0167.3/
```

Fig. 2.4.2. Spectral reflectance of a sample, (a) before and (b) after tracing by a cursor and conversion by a digitizer.

SAMPLE : 3M SCOTCHCAL FILM 530, AS RECEIVED.

X/mm	Y/mm	LAMDA/MICRON	ρ/%
10.1	169.9	401	84.9
15.0	172.0	450	86.0
20.0	171.5	500	85.8
23.5	171.1	535	85.6
27.5	169.5	575	84.8
31.5	168.3	615	84.2
34.7	166.6	647	83.3
39.2	163.8	692	81.9
43.0	161.4	730	80.7
46.7	158.0	767	79.0
52.0	155.0	820	77.5
56.6	165.0	866	82.5
62.3	172.6	923	86.3
70.0	180.6	1000	90.3
76.4	183.8	1064	91.9
86.7	186.8	1167	93.4
95.7	188.7	1257	94.3
122.7	192.5	1527	96.3
138.4	186.2	1684	93.1
198.4	165.5	2284	82.8

SOLAR REFLECTANCE

86.2

Fig. 2.4.3. Sample of calculated solar reflectance of an as-received sample of 3M Scotchcal Film (530) measured by Lambda-9-Perkin Elmer Spectrometer.

CHAPTER THREE

EXPERIMENTAL RESULTS

3.1 SOLAR STILL PERFORMANCE

The performance of solar stills is usually expressed in terms of the operating efficiency (η) which is defined as follows:

$$\eta = \frac{\text{(mass of distillate produced per unit area per unit time)}}{\text{(energy incident on the still cover per unit area per unit time)}} \times \text{(latent heat of evaporation)} \qquad (3.1)$$

$$\eta = \frac{D h_{fg}}{I} \qquad (3.2)$$

This definition of efficiency has been used throughout the present work. Other definitions are sometimes used, e.g. Lof (1980), in Principles of Desalination edited by Spiegler and Laird, defined it as the condensed water actually produced divided by the water which could theoretically be evaporated by all the solar energy reaching the outer cover.

This investigation has compared the still performance with and without a V-trough solar concentrator (of apex angle 30°) attached to the still. The combination of the still with the concentrator can be used to investigate the performance of the still under a greater range of irradiance than is possible without the concentrator. The still was of the flat wick-type. It was located at Brunel University at Uxbridge 51° 33' north latitude, 0° 29' west longitude and 35 meter elevation above sea level, Ordnance Survey (1988).

During the experimental tests of the solar still, the absorber and cover temperatures at selected positions were recorded every five minutes by means of thermocouples. The distribution of these thermocouples on the glass cover and beneath the absorber cloth is shown in Fig. 2.2.1. The arithmetic means of these recorded values over longer periods of time were used in calculating the efficiency of the solar still. A sample of a detailed manual calculation of the still efficiency is shown in Appendix A4.

3.2 INDOOR RESULTS

In order to maintain steady climatic conditions many investigators have used indoor solar simulators, with basin-type solar stills Clark (1982,1990) and Clark *et al.* (1983) and with wick-type solar stills Yeh and Chen (1986).

In this work indoor experiments were carried out to investigate the performance of the wick-type still. Lamps were

used as the radiant energy source. The still performances when using charcoal cloth and blackened jute as absorbers were compared. The insolation and the temperatures were recorded by the data logger. The input water flow rate and the distillate produced were measured frequently and manually.

3.2.1 Lamp array insolation data

Before the commencement of the experimental tests two Kipp and Zonen dome solarimeters were calibrated by the U.K. Meteorological Office. The certificates are shown in Appendix A2. The calibration factor of dome solarimeter No.1 is 12.677 ± 1.5 % $mV/kW.m^{-2}$ and that of No. 2 is 10.623 ± 1.5 % $mV/kW.m^{-2}$. The tube solarimeter was calibrated, outdoors, versus dome solarimeter No.1. Its calibration plot is shown in Fig. 3.2.1 together with the appropriate calibration linear relation between irradiances determined using the two types of solarimeters. A digital irradiance meter (Gossen Mavolux-Digital) was used for some measurements where use of the other meters is very difficult practically. It has also been calibrated, outdoors, using the dome solarimeter No.1. Its calibration curve is shown in Fig. 3.2.2.

Under various irradiances of the lamp array, the Delta-T-Devices data logger and Solartron 7055 Microprocessor Voltmeter (serial No. 202134) were used simultaneously to compare their readings of the output voltage of each of the two dome solarimeters No. 1 and No. 2 separately. Figs. 3.2.3 and 3.2.4

represent readings of the two solarimeters respectively and show their voltage outputs as functions of irradiance determined by the data logger. They show calibration factors of 12.702 and 10.626 $mV/kW.m^{-2}$ compared with those given by the U.K. Meteorological Office of 12.677 and 10.623 $mV/kW.m^{-2}$ respectively.

The lamp array insolation was measured on the solar still glass cover which was kept parallel to and located 1.25 m from the front plane of the lamps for indoor still testing. The average radiation flux on the glass cover of the still was about 420 W/m^2. The flux measurements was carried out by dividing the cover area into 36 identical squares of area 10 x 10 cm^2 each. The irradiance distribution on each of these squares was measured using the digital irradiance meter. A typical irradiance falling on the still glazing is shown in Fig. 3.2.5.

3.2.2 Variation of input saline water flow rate

The saline water feed flow rate was controlled manually by means of a stop-cock valve, constant head device (CHD), adjustable platform and a dial gauge as explained in subsections (2.1.2) and (2.1.3). Measurements of the saline water flow rate during the experiments were taken once per hour after the chosen flow rate was achieved. The flow rate could be adjusted by the vertical movement of the adjustable platform relative to a particular level which could be monitored using the dial gauge. Fig. 3.2.6 shows variations of flow rates of distilled water, 2.5% and 5% by weight of NaCl solution through the charcoal cloth as functions of their levels in the CHD. It shows that when the CHD

level increases from 1 mm to 3 mm, with respect to a fixed reference or arbitrarily chosen level, the flow rate of the distilled water increases from 8.5 ml/min to 81 ml/min while that of the 5% NaCl solution increases from 26.5 ml/min to 57.5 ml/min. However, more investigations need to be done in the future in relation to the effect of salinity as water uptake rate by charcoal cloth.

From Fig. 3.2.7 it can be seen that, when the flow rate in the wick-type solar still increases, the solar still efficiency decreases and, also, the absorber and the cover temperatures decrease as shown in Table 3.2.1. As the absorber temperature increases the productivity of the still increases (Fig. 3.2.8). These results were obtained indoors under simulated condition by using the electric lamp array and a small fan. The still inclination angle was 45°, the average incident irradiance on the glass cover was 420 W/m^2, the wind speed was 0.7 m/s and the average ambient temperature was 22.3°C.

3.2.3 Variation of salt concentration in saline water

The performance of the solar still was studied with various salt concentrations of the input saline water. Sodium chloride (NaCl) as a standard salt was dissolved in distilled water in weight concentration ratios (salinities) of 2.5%, 5.0% and 10.0 %. The salinity (C) is defined as:

$$C\% = \left(\frac{\text{weight of NaCl}}{\text{weight of NaCl} + \text{weight of water}}\right) \times 100 \qquad (3.3)$$

The still was tested indoors under the lamp array radiation. The inclination angle was 45° and the irradiance was about 420 W/m². At each of these water salinities, the water was feeding the still for 3 - 4 hours at a mass flow rate of about 2.5 kg/m².h. The distillate was collected every 30 minutes. The efficiency was calculated as :

$$\eta = \frac{\sum_{i=1}^{n} D_i h_{fg,i}}{nS \times 3600} \qquad (3.4)$$

where:

D_i is the mass of distillate collected per 30 minutes (kg/m².h).

n is number of the 30 minutes intervals, for which the distillate was collected.

$h_{fg,i}$ is the latent heat of evaporation (J/kg).

S is the irradiance (W/m²).

The variation of the still efficiency with the salt concentration is plotted in Fig. 3.2.9. From this figure it is clear that increasing the salt concentration results in a decrease in the efficiency of the solar still.

3.2.4 Determination of the still time constant

The still time constant is defined as the time required for the absorber temperature to drop to a factor of 1/e of the total possible temperature drop to lowest possible absorber temperature while the input water flow rate and temperature are kept constant.

An ASHRAE (American Society of Heating, Refrigerating and Air-Conditioning Engineers, Inc.) standard test outlines a procedure for estimating the time constant of a collector, Duffie and Beckman (1980). The wick solar still was kept running for 2 - 3 hours, indoors, under the lamp array insolation (420 W/m^2) and the still at 45° inclination angle. Then the lamps were switched off, while the temperature measurements were continued and the input water flow rate (2.5 kg/m^2.h) and temperature (22.3 °C) were kept constant. Fig. 3.2.10 shows the cooling curve of the still. From this figure the still time constant has been determined and it is equal to 55 minutes.

3.3 OUTDOOR RESULTS

Outdoor testing of the still was carried out with and without the V-trough solar concentrator. The still angle to the horizontal of the cover was set so as to be perpendicular to the direction of beam radiation at noon. The still was tested with various salt concentrations, also, with various input water flow rates. The distilled water production was measured every 30 minutes. The temperatures were measured each minute and the solar irradiance was measured every 10 seconds. The five minute averages of these quantities were stored by the data logger. The wind speed was measured every 30 minutes.

3.3.1 V-trough concentrator and wick-type solar still combination

A V-trough solar concentrator (of apex angle 30°) has been combined with the flat wick solar still. It was used to investigate the enhancement of the outdoor performance of the wick-type solar still by the solar concentrator. This was attached to the outer surface of the glass cover of the flat still. An internal concentrator exposed to the evaporating water was also investigated but was found to be ineffective (Appendix A5).

Prior to testing, some measurements were carried out to obtain an instantaneous localised concentration factor over seven hours at 15 minute intervals. These measurements were done by locating the tube solarimeter (TSA) centrally on the long axis of the base of the concentrator as shown in Fig. 3.3.1 and the dome solarimeter No.1 at its aperture plane. The data obtained from these measurements are shown in Fig. 3.3.2 on both a very sunny day (25/7/1990) and a very cloudy day (27/7/1990).

In order to measure the average local concentration factor (ALCF, Mazumder and Hussain (1991)), the base area of the trough was divided into 108 squares each of 5 x 5 cm^2. With the aid of the digital irradiance meter, the concentrated irradiance at each of those squares was measured in addition to that at the aperture. This was done at times of 8.00, 10.00, 12.00, 15.00, and 18.00 GMT on a sunny day (11/7/1990). The (ALCF), has been determined by calculating the average concentrated irradiance at the base divided by the aperture irradiance. The variation of ALCF

with time of the day is shown in Fig. 3.3.3. This shows the effect of the shadow created by the end walls of the concentrator. An actual distribution of irradiance in the base of the trough concentrator is shown in Appendix A6. The maximum value of ALCF determined was 1.62 at 12.00 GMT while this was 0.24 at 18.00 GMT.

3.3.2 Solar still performance dependence on input water flow rate

Solar still testing with and without the solar concentrator was carried out using input distilled water with various flow rates. Table 3.3.1 shows the still efficiency variation with input water flow rate and irradiance range. These data were obtained from outdoor testing of the solar still with and without the solar concentrator. The efficiency decreases as the flow rate increases under nearly similar conditions. When the still is combined with the concentrator the efficiencies are higher but the trend in results is as before, i.e. still efficiency decreases as the flow rate increases.

In outdoor experiments, where the irradiance varies with time, it is difficult to vary the flow rate according to the outdoor conditions, particularly in unsettled weather. Hence, in the present work, the flow rate was in the range (3.0 - 5.5) $kg/m^2.h$. This was sufficient to keep the absorber surface wet during the clear days. This was decreased, in winter, to (1.0 - 2.0) $kg/m^2.h$. The inclination angle was in the range 60° - 65° in winter and in the range 29° - 45 • in summer.

3.3.3 Solar still performance with salinity variation of the input water

The input water flow rate was set at an average of 3.8 kg/m².h in summer and 2.0 kg/m².h in winter. NaCl solutions of concentrations of 2.5 % and 5.0 % by weight in addition to the distilled water (0.0 %) were used, as feed water. The performance of the still with and without the concentrator at these salinities was investigated. These salinities have been chosen to be in the normal range that would be encountered in solar distillation operation. Common sea water salinities are in the range (3.0 % - 4.3 %) and the standard is 3.5%, Howe and Dekker (1974). Table 3.3.2 shows the daily efficiency of the still with and without the concentrator and when the concentrator was used from 11.00 am to 13.00 pm in GMT. The efficiency decreases when higher salinity water is used whether or not the concentrator is used. It decreased from 63.6 percent to 35.3 percent when the concentrator was used, and from 53.4 percent to 33.7 percent when the concentrator was not used. These decreases occurred when the input water was changed from distilled water to 5 % NaCl solution.

3.3.4 Comparison of the solar still performance with and without the concentrator

It has been shown experimentally that using the solar concentrator under clear condition and during the middle part of the day, the incident solar energy on the absorber surface

increased significantly (subsection 3.3.1). This increased the absorber temperature as shown in Fig. 3.3.4.

Various outdoor runs for the solar still were carried out on clear days. The V-trough solar concentrator was used to investigate the enhancing of the performance of the wick solar still. Some of the runs were carried out in winter (late November 1989) and others in summer (July/August 1990). In winter runs, the conditions were : ambient temperature (7 - 13) °C input water flow rate (1.0 - 2.0) kg/m^2.h at temperature (8 - 15) °C and still inclination angle in the range 62° - 63°. The summer conditions were ambient temperature (20 - 35)°C, input water flow rate (3.0 - 5.5) kg/m^2.h, at temperature (25 - 38)°C and inclination angle in the range 29° - 45° according to CIBSE guide.

The V-trough concentrator was fixed on the glass cover during some of these days e.g. 23/11/1989, 1/8/1990. The distillate was collected every thirty minutes. The still inclination was chosen according to the solar altitude angle at noon, to receive maximum solar radiation.

Figs. 3.3.5 - 3.3.7 show the variations of the ambient, absorber and cover temperatures together with the solar insolation and the productivity of the still with time. These results relate to clear days in summer. Some other runs were carried out on clear days in winter, when 2.5% NaCl solution was used. These days were on 23/11/1989 (using the concentrator) and on 29/11/1989 (without concentrator). Variation of the still performance for these days is shown in Figs. 3.3.8 and 3.3.9.

From these figures can be shown the response of the wick solar still to the solar insolation in terms of the productivity, and operating temperatures. Figs. 3.3.10 and 3.3.11 show variation of the ratio of the still productivity to the corresponding solar insolation when the concentrator was used and not used at various times of day. They are for the total and beam incident radiation. These figures are in summer and winter respectively. It can be seen that use of the concentrator appears to be more beneficial on winter clear days than on summer clear days. In winter, the input water was 2.5% NaCl solution (in summer run on 25/7/1990 and 1/8/1990 distilled water was used) with a flow rate in range (1.0 - 2.0) $kg/m^2.h$. In summer the flow rate was (3.0 - 3.5) $kg/m^2.h$.

Tables 3.3.3 and 3.3.4 show the hourly (11.00 - 13.00) and daily performance of the solar still with and without solar concentrator in summer and in winter. It is clear that the efficiency of the still was higher when the concentrator was used.

3.4 MATERIAL INVESTIGATION RESULTS

As is mentioned in chapter two, the spectral reflectance of the absorbing and reflecting materials were measured by the available instrumentation. According to the law of conservation of energy, for any surface, the sum of spectral absorptance (α_λ), spectral transmittance (τ_λ) and spectral reflectance (ρ_λ) at a

given wavelength (λ) must be unity. Thus for an opaque material,

$$\alpha_\lambda + \rho_\lambda = 1 \quad (\text{as } \tau_\lambda = 0) \tag{3.5}$$

Hence by using this equation the solar absorptance (α_s) of the absorbing materials was calculated.

3.4.1 As received materials

3.4.1.1 Water transport and solar absorber capillary wick materials

The charcoal cloth used in the present work is an expensive material (about £20 per a square meter). It might become available at a lower price if it could be produced commercially from natural cheaper sources e.g. coir, Hitchcock *et al.* (1983). No reference has been found to its previous use for solar still testing. Its solar absorptance has been measured in the present work. The spectral reflectance of the charcoal cloth for the visible VIS and near infrared NIR radiation is shown in Fig. 3.4.1 and for infrared IR radiation is shown in Fig. 3.4.2. These typical spectra show an average solar absorptance of about 98.0 ± 0.2 percent for VIS and NIR and 99.0 ± 0.2 percent for IR; i.e. a very large portion of the incident solar energy is absorbed by the charcoal cloth.

Blackened hessian cloth (supplied by Brown, B. (Holborn) Ltd.) is studied in this research to compare some of its properties with those of the charcoal cloth. Hessian samples show spectral reflectance for IR radiation with no significant difference from that of the charcoal cloth samples. Typical spectral reflectance

spectra for VIS and NIR and IR radiation of hessian cloth samples are shown in Figs. 3.4.3 and 3.4.4 respectively. The average solar absorptance of the hessian cloth is about 64.8 percent in a dry condition. It is about 13.8 percent larger when the hessian is wetted by distilled water and 11.2 percent, when wetted by a 15 percent by weight concentration of NaCl solution.

3.4.1.2 Reflecting materials

Reflecting materials are used as mirrors to redirect incident solar energy in solar concentrators construction. They are exposed to the atmosphere and subjected to degradation mechanisms such as deposition of dust, corrosion by water vapour and chemicals in the atmosphere. Cost reduction is an essential element of the solar energy programs, so, in order to reduce the construction cost, in addition to damage risks and significant absorptance of internal sides of solar concentrators, self adhesive mirrors have been suggested. This is as an alternative to relatively expensive glass mirrors or high polished metal sheets with a high probability of corrosion of most metals. Some self adhesive reflecting materials have been investigated. They are flexible, inexpensive materials and commercially available.

Because of the daily variation of solar insolation and because of short term fluctuations resulting from cloud passage, reflective materials need to be tested with a cyclic treatment. Thus five different materials, namely, 3M Scotchcal Films 530, 680, 3658 and 5400, in addition to an aluminised plastic mirror have been investigated for use as mirrors of the solar

concentrator. Their response to various humidity and/or heat treatments has been studied. Their degradation in the outdoor environment and exposure has also been investigated. Scanning electron microscopy (SEM) of samples of the mirrors was carried out. Their surface topographies are shown in Figs. 3.4.5 - 3.4.9 as received from suppliers. A sample of 3M Scotchcal 680 shows cracks in its surface, (Fig. 3.4.6) and low average solar reflectance, about 52 percent. This discouraged further investigation of this material. Surface composition of as received 3M Scotchcal Films has been carried out, after specimen preparation.

The electron probe microanalysis (EPMA) of samples of 3M Scotchcal 530, 3658 and 5400 is shown in Figs. 3.4.10 - 3.4.12. No elemental composition of their surfaces can be detected (apart from the gold coating applied to avoid charging of the films) except for 3M Scotchcal 3658 film which shows a high presence of chlorine and a lower proportion of aluminium. This indicates a high thickness of an organic coating layer used in these materials (e.g. to reduce corrosion and degradation effects). The spectral reflectance of five to eight samples of each of the reflecting materials, from different parts of the supplied quantities, have been measured. No significant difference in their spectra has been observed for a given material. Their reflectance spectra are shown in Figs. 3.4.13 - 3.4.17. Calculation of averages of their solar reflectances shows that 3M Scotchcal Film 5400 has the highest reflectance while 3M Scotchcal Film 680 has the lowest reflectance.

3.4.2 After treatment materials

3.4.2.1 Heat treatment

Various samples of the reflecting materials have been heat treated in the air inside the oven for different periods of time and at different temperatures. Before any treatment, the average solar reflectance of each sample has been determined as shown in Table 3.4.1.

Heat treated samples were put in the oven at temperatures between 80 °C and 180 °C with an accuracy of ± 5 °C for continuous periods of 50, 100, 150, 200, 250 and 300 hours. Aluminised plastic and 3M Scotchcal 5400 were excluded from temperatures higher than 120 °C. These materials showed sample shrinkage and bending at the higher temperatures. After each period, at a certain temperature, the average reflectance was determined as shown in Tables 3.4.2-3.4.5. The tables show the heat is affecting aluminised plastic and 3M Scotchcal Film 5400 and the lowest effect is on 3M Scotchcal Film 530. The degradation of the heat treated samples in air at elevated temperatures for various periods of ageing are shown in Figs. 3.4.18 - 3.4.21. From these figures can be seen the effect of heating time and temperatures on solar reflectance of the materials.

3.4.2.2 Humidity and thermal cycling treatment

Samples of four reflecting materials namely 3M Scotchcal Films 530, 3658 and 5400 and aluminised plastic were put in the humidity chamber for various cycle numbers (each

cycle of 24 hours) at average relative humidities (R.H.) in the range (68 - 95) % and at temperatures (23.5 - 77) °C with accuracies of ± 5% and ± 3 °C respectively. Figs. 3.4.22 - 3.4.24 show SEM of samples after the ten cycles of the heat and humidity treatment.

Another set of samples were put in a humid atmosphere above a shallow tray containing saline water inside a sealed semitransparent enclosure for two months. The temperature range was about (15 - 35)°C. Table 3.4.6 shows the solar reflectances of the heat and humidity-cycle-treated materials. There were minor changes to the reflectance of the exposed sample except samples of 3M Scotchcal Film 5400. These samples suffered shrinkage and large reduction in their reflectance when they exposed to humidity and thermal cycling in the ranges (75 - 95) R.H. and (30 - 77)°C temperature.

3.4.2.3 Environmental treatment

Samples of reflecting and absorbing materials were fixed in a very shallow wooden box with a concave transparent plastic cover, outdoors. The reflecting materials exposure time was along 3, 6, 9, and 12 months starting from April 1988 for samples of 3M Scotchcal 530 and 3568 and aluminised plastic and April 1989 for samples of 3M Scotchcal 5400. The absorbing materials exposure time was 1, 2, 3, 6, 9, 12 and 18 months for the hessian samples and up to 24 months for the charcoal cloth samples starting from September 1988. The effect of this

exposure on the reflectance of the reflective materials is marginal as shown in Table 3.4.7. In the case of the hessian samples, the blackness almost faded within the first three months and faded completely within the second period of three months. That decreased the solar absorptance of the treated hessian samples by 6.0% as shown in Table 3.4.8. The charcoal cloth did not fade even after twenty four months and the reflectance showed no significant change due to outdoor exposure. (Table 3.4.8)

Table 3.2.1. Variation of absorber and cover temperatures with input water flow rate, obtained indoors with average irradiance = 420 W/m², wind speed = 0.7 m/s and inclination angle = 45°, using distilled water.

Flow Rate kg/m^2.h	Temperature / °C	
	Absorber	Cover
11.70	35.2 ± 0.5	32.1 ± 0.5
9.00	39.0	34.8
8.70	40.9	36.1
7.20	39.1	33.7
6.10	43.4	36.0
5.30	45.0	37.6
5.10	46.3	37.8
3.00	49.3	39.9
2.00	53.0	41.7

Table 3.3.1. Variation of the still efficiency with input distilled water flow rate obtained from outdoor testing in summer (Inclination angle 30° - 40°).

Without Solar Concentrator

Flow Rate kg/m^2.h	Irradiance Range kW/m^2	Efficiency %
14.10	0.7 - 0.8	30.90
11.00	0.3 - 0.5	35.00
9.10	0.7 - 0.9	41.40
8.30	0.4 - 0.7	38.80
5.00	0.8 - 0.9	43.10
4.30	0.4 - 0.7	43.90
3.30	0.7 - 0.9	55.10

With Solar Concentrator

Flow Rate kg/m^2.h	Irradiance Range kW/m^2	Efficiency %
9.20	0.5 - 0.8	45.70
5.50	0.8 - 0.9	68.90
4.20	0.7 - 0.8	63.70

Table 3.3.2. Experimental efficiency of the still with and without the solar concentrator, in summer, using input NaCl solutions with different salinities, (Hourly efficiencies refer to the period (11.00 - 13.00) GMT. when the concentrator was used).

NaCl Salinity %wt	Without Concentrator %	With Concentrator	
		Daily %	Hourly %
0.00	53.40	63.6	68.9
2.50	39.00	48.5	59.4
5.00	33.70	35.3	48.9

Table 3.3.3. Comparison of the hourly performance (11.00 - 13.00) GMT. of the solar still with and without the solar concentrator, (a) in summer using distilled water (b) in winter using 2.5% NaCl solution.

(a)

	Units	With Concentrator on 1/8/1990	Without Concentrator on 25/7/1990
Mean Solar Intensity	W/m^2	870	931
Mean Absorber Temp	°C	78.9	69.4
Mean Cover Temp.	°C	69.6	57.5
Mean Distillate Productivity	kg/m^2.h	0.933	0.773
Efficiency	%	68.9	53.8

(b)

	Units	With Concentrator on 23/11/1989	Without Concentrator on 29/11/1989
Mean Solar Intensity	W/m^2	738	767
Mean Absorber Temp.	°C	59.9	44.9
Mean Cover Temp.	°C	48.3	28.3
Mean Distillate Prod.	kg/m^2.h	0.622	0.304
Efficiency	%	55.2	36.3

Table 3.3.4. Comparison of the daily performance of the wick-type solar still with and without the solar concentrator, (a) in summer using distilled water (b) in winter using 2.5% NaCl solution.

(a)

	Units	With Concentrator on 1/8/1990	Without Concentrator on 25/7/1990
Solar Insolation	kJ/m^2.day	17090	19723
Distillate Prod.	kg/m^2.day	4.679	4.515
Efficiency	%	63.6	53.4

(b)

	Units	With Concentrator on 23/11/1989	Without Concentrator on 29/11/1989
Solar Insolation	kJ/m^2.day	10242	8622
Distillate Prod.	kg/m^2.day	2.333	1.313
Efficiency	%	52.1	36.5

Table 3.4.1. Solar reflectance of as-received samples of the investigated materials.

Material	Reflectance ρ %
3M Scotchcal 530	86.3 ± 0.08
3M Scotchcal 680	51.5 ± 0.09
3M Scotchcal 3658	60.6 ± 0.02
3M Scotchcal 5400	86.8 ± 0.13
Aluminised plastic	85.0 ± 0.05
Hessian cloth	35.4 ± 0.06
Charcoal cloth	2.0 ± 0.2

Table 3.4.2. Solar reflectance of samples of 3M Scotchcal Film 530, after various periods of ageing in air at elevated temperatures.

Ageing Temperature (°C)	Ageing Time Hours	Reflectance ρ %
As-received	——	86.3 ± 0.08
100	100	85.8
	150	86.1
	200	85.5
	300	85.9
140	100	84.9
	150	84.4
	200	83.9
	300	84.4
160	100	81.9
	150	81.0
	200	81.3
	300	80.6
180	100	81.7
	200	81.0
	250	80.6
	300	80.5

Table 3.4.3. Solar reflectance of samples of 3M Scotchcal Film 3658, after various periods of ageing in air at elevated temperatures.

Ageing Temperature (°C)	Ageing Time Hours	Reflectance ρ %
As-received	———	60.6 ± 0.02
100	50	61.7
	100	61.4
	150	60.3
	200	59.7
	300	59.3
140	100	60.4
	150	59.5
	200	59.1
	300	59.0
160	100	53.4
	150	51.3
	200	50.4
	300	47.8
180	100	52.0
	200	50.6
	250	48.5
	300	48.2

Table 3.4.4. Solar reflectance of samples of 3M Scotchcal Film 5400, after various periods of ageing in air at elevated temperatures.

Ageing Temperature (°C)	Ageing Time Hours	Reflectance ρ %
As-received	———	86.8 ± 0.13
80	100 150 200 300	86.0 86.7 86.1 86.6
100	100 150 200	82.5 80.1 76.3
120	2 5 50 100 200	47.6 41.6 34.9 34.3 35.0
140	50 100	33.3 32.8

Table 3.4.5. Solar reflectance of samples of Aluminised plastic, after various periods of ageing in air at elevated temperatures.

Ageing Temperature (°C)	Ageing Time Hours	Reflectance p %
As-received	———	85.0 ± 0.05
100	50 100 150 200	84.3 84.1 83.8 83.0
120	50 100 200	83.9 83.1 81.2
140	50 100	38.1 34.2

Table 3.4.6. Solar reflectance (ρ) of 3M Scotchcal films and aluminised plastic after temperature and humidity cycling.

Temperature Range (°C)	Relative Humidity Range (%)	Number of Cycles	3M Scotchcal Films			Aluminised Plastic Sheet
			530	3658	5400	
As-received	-----	-----	86.3 ± 0.08	60.6 ± 0.02	86.8 ± 0.13	85.0 ± 0.05
15 - 37	-----	60	85.7	59.5	85.7	83.5
23.5 - 60	68 - 80	7	85.3	62.3	85.7	83.7
30 - 77	75 - 95	5	87.1	61.4	48.6 *	80.0
30 - 77	75 - 95	10	87.0	61.2	33.7 *	76.2

* Samples Suffered Shrinkage

Table 3.4.7. Solar reflectance (ρ) of samples of reflecting materials after various time in sheltered outdoor environment.

Treatment Period month	3M Scotchcal Films			Aluminised Plastic Sheet
	530	3658	5400	
As-received	86.3 ± 0.08	60.6 ± 0.02	86.8 ± 0.13	85.0 ± 0.05
3	85.4	59.5	85.0	83.4
6	85.8	59.4	83.6	82.9
9	85.6	58.8	82.5	82.9
12	84.8	58.7	81.1	82.0

Table 3.4.8. Solar absorptance (α) of samples of absorbing materials after various time in sheltered outdoor environment.

Material	As-Received	Exposure Period / month							
		1	2	3	6	9	12	18	24
Charcoal Cloth	98.0 ± 0.2	97.8	97.8	97.6	97.1	----	97.9	----	98.1
Blackened hessian	64.6 ± 0.06	64.0	63.2	60.9	60.7	59.8	58.3	58.7	---

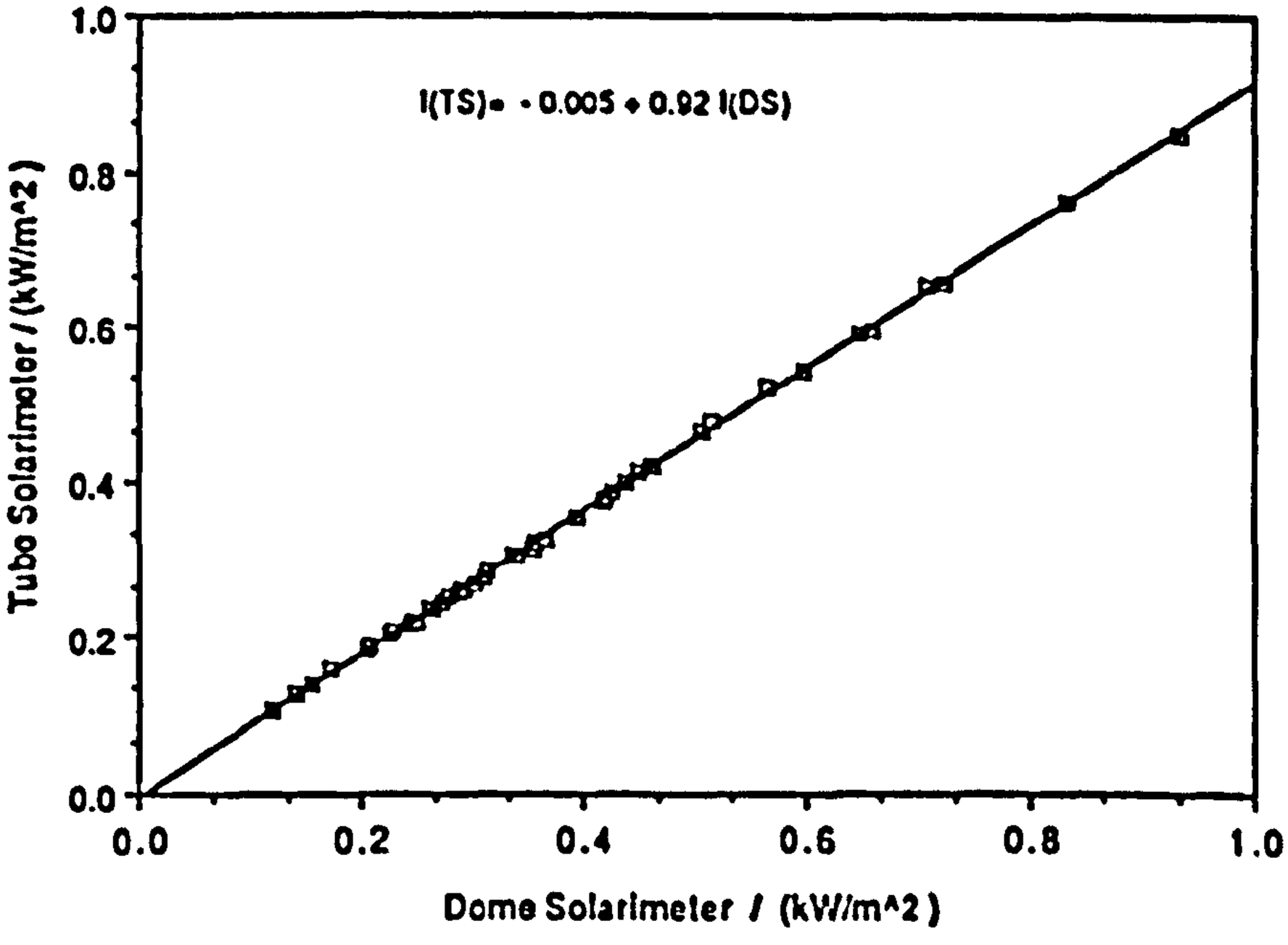

Fig. 3.2.1. Calibration curve of Delta-T-Devices tube solarimeter versus Kipp and Zonen dome solarimeter No. 1, (outdoors).

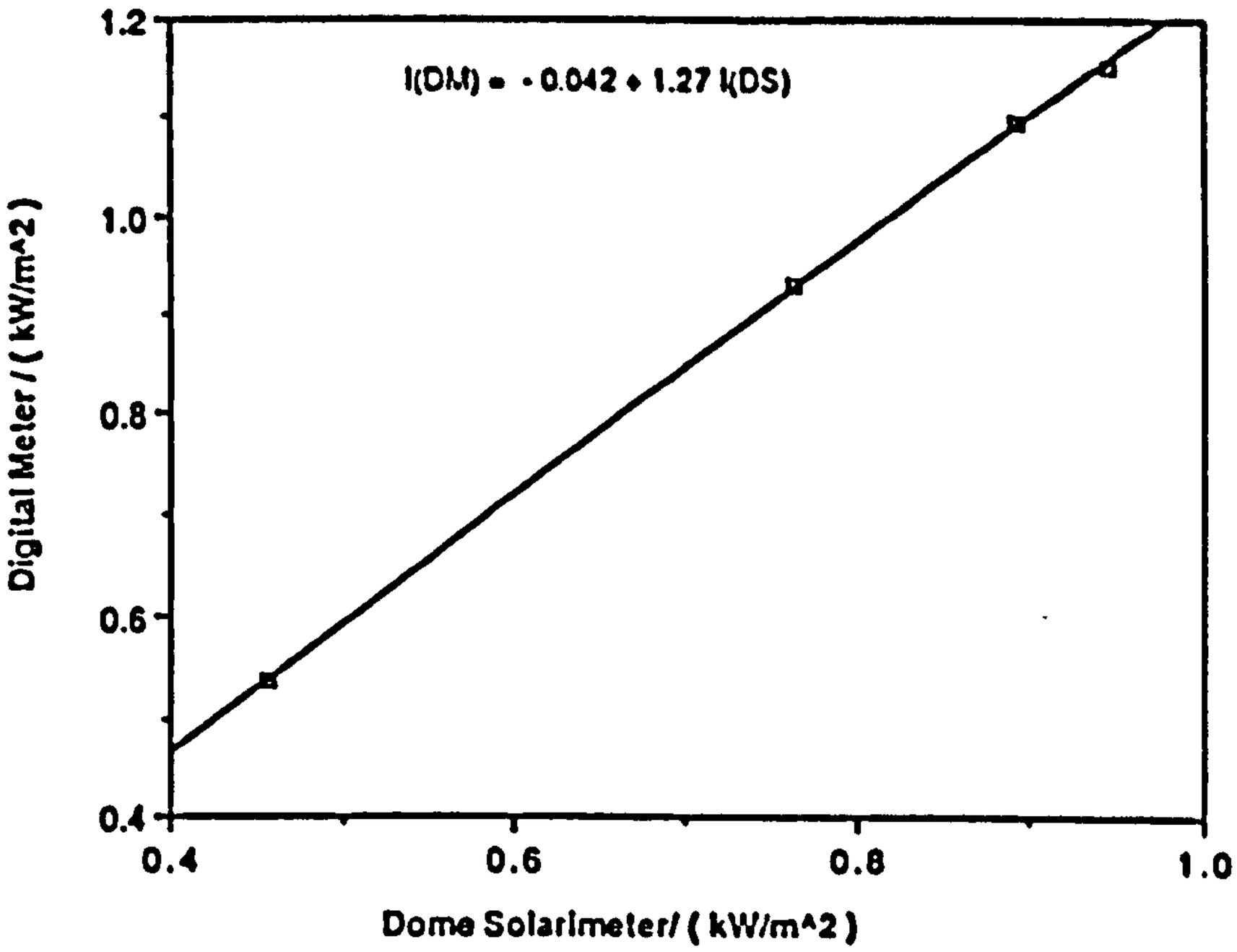

Fig. 3.2.2. Calibration curve of Gossen Mavolux-Digital Irradiance meter versus Kipp and Zonen dome solarimeter No. 1 (outdoors).

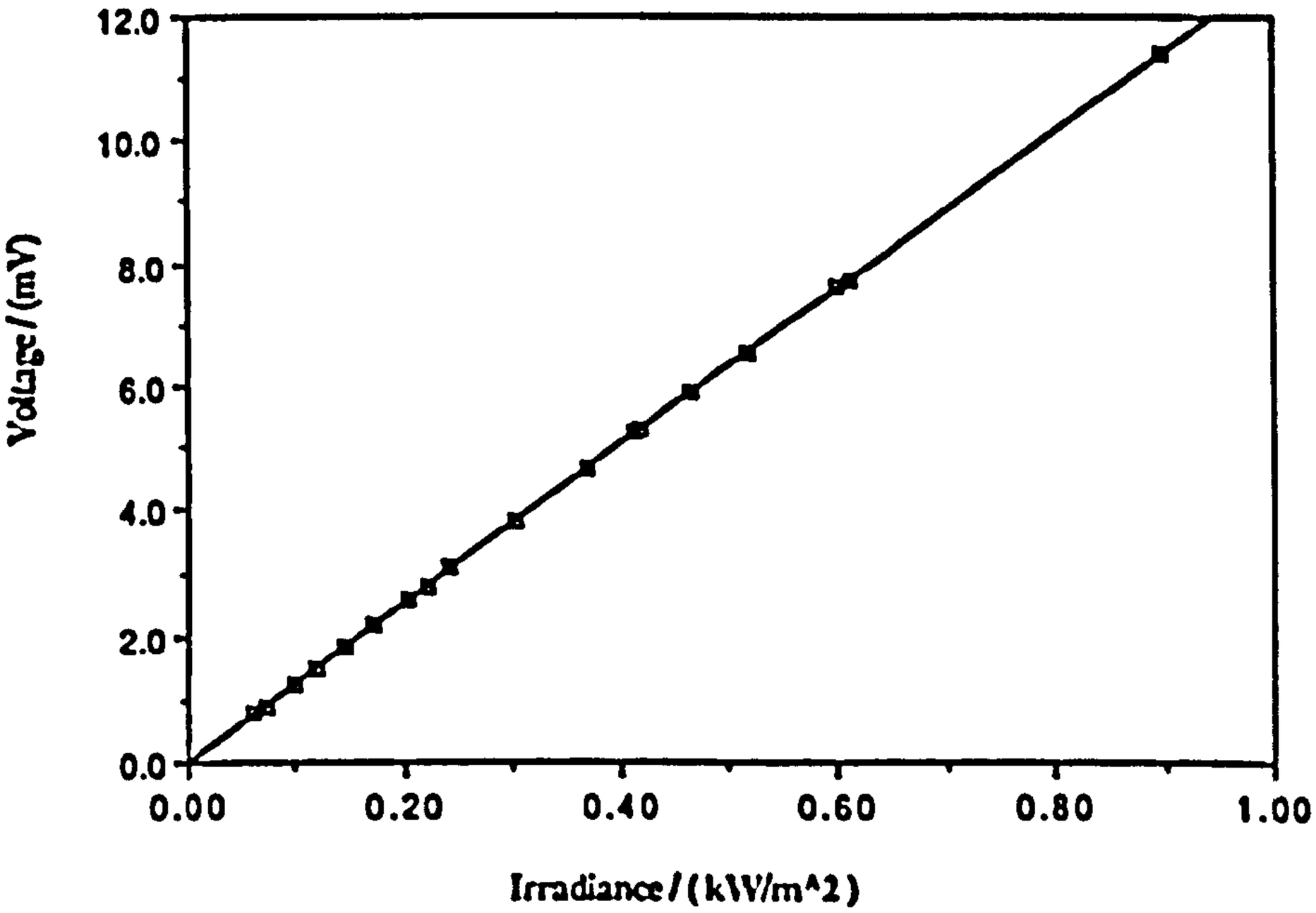

Fig. 3.2.3. Voltage output of Kipp and Zonen dome solarimeter No.1 as a function of irradiance value obtained using the Delta-T-Devices data logger with the solarimeter.

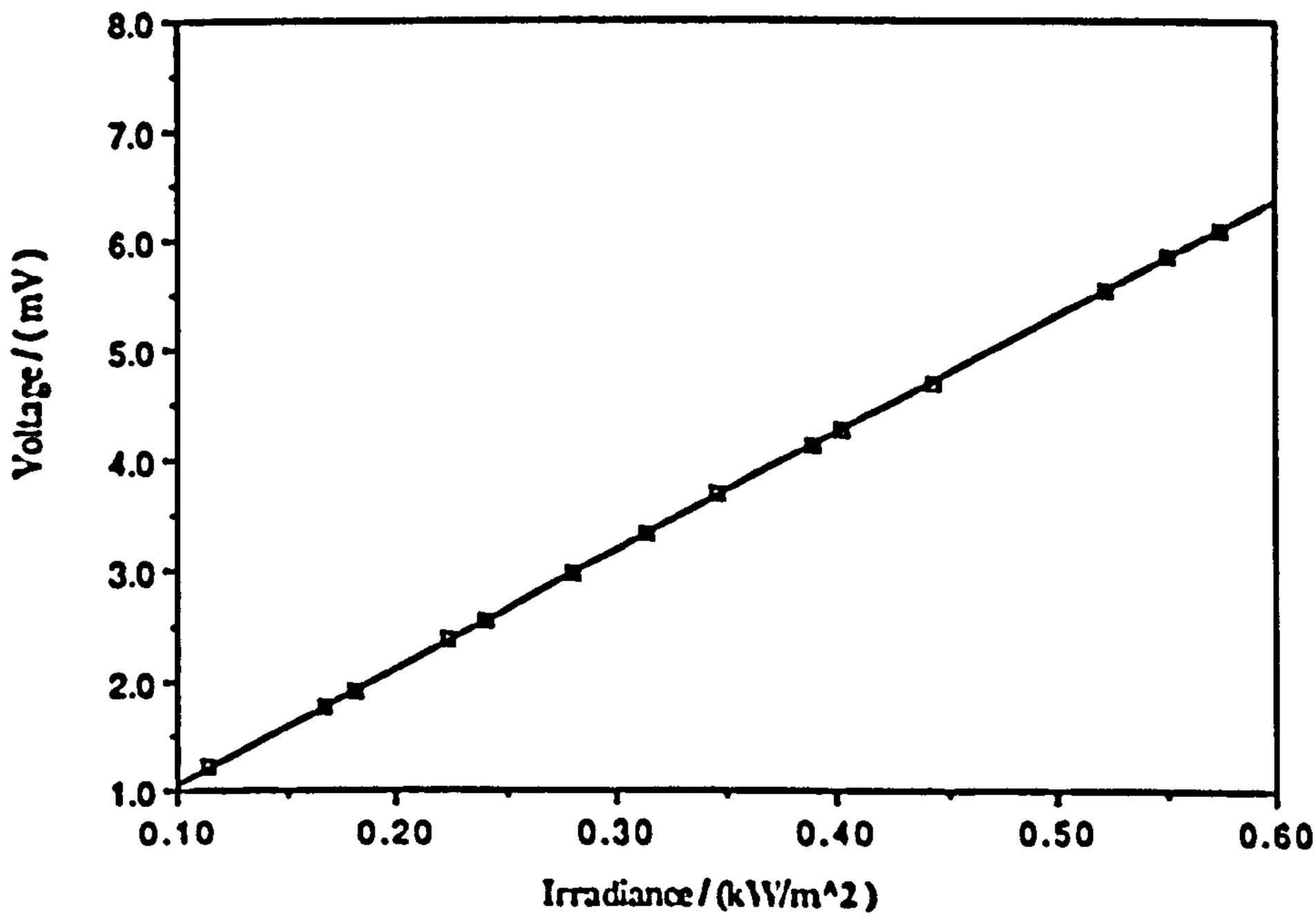

Fig. 3.2.4. Voltage output of Kipp and Zonen dome solarimeter No.2 as a function of irradiance value obtained using the Delta-T-Devices data logger with the solarimeter.

392	401	424	436	441	435	417	406	390
399	410	421	457	446	431	420	409	393
389	416	426	448	438	428	416	397	385
380	396	419	435	426	401	404	386	381

Fig. 3.2.5. Irradiance (W/m^2) distribution of the lamp array on the glass cover for the present lamps configuration.

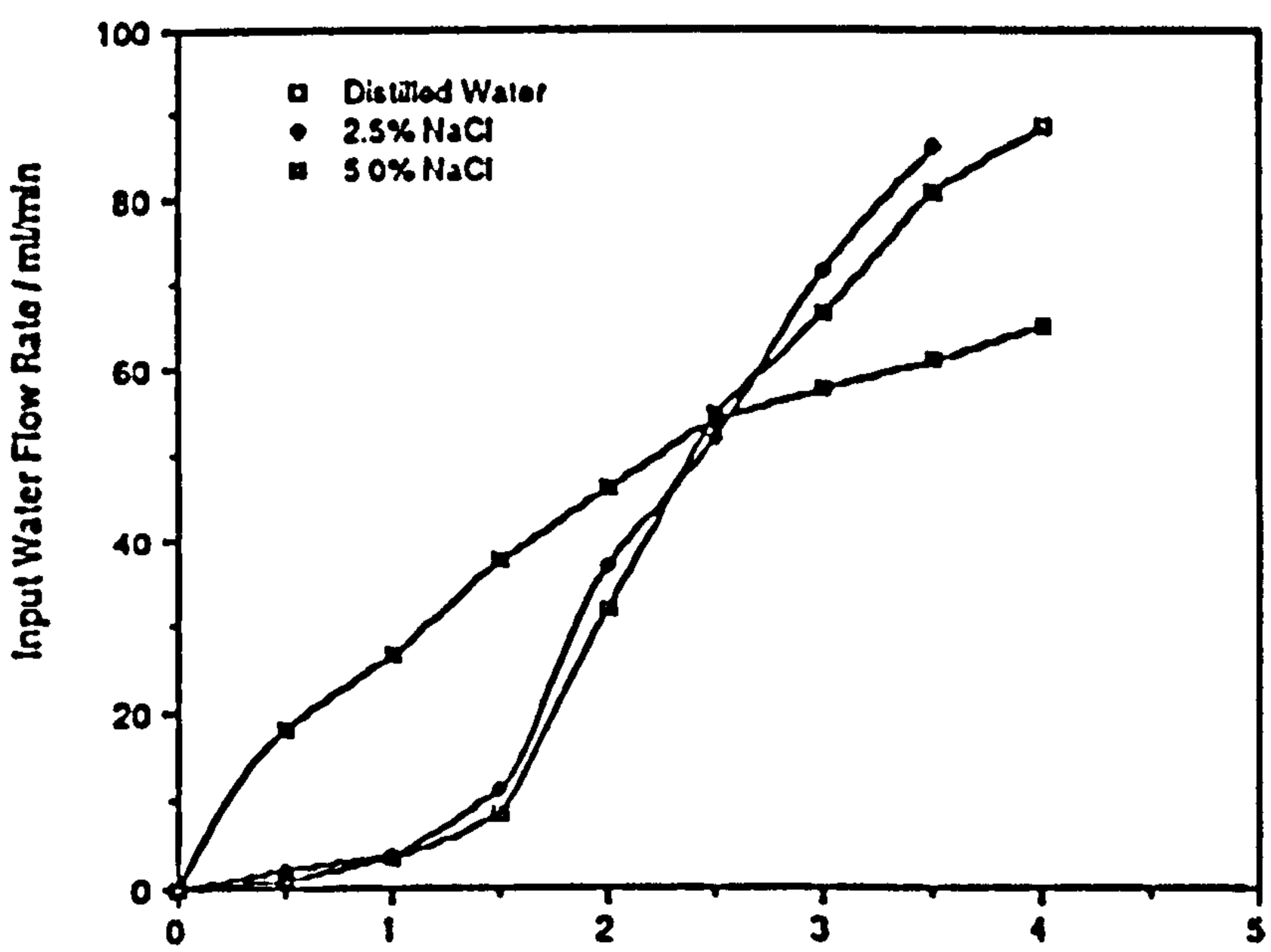

Fig. 3.2.6. Variation of input water flow rate with the level of the constant head device (CHD).

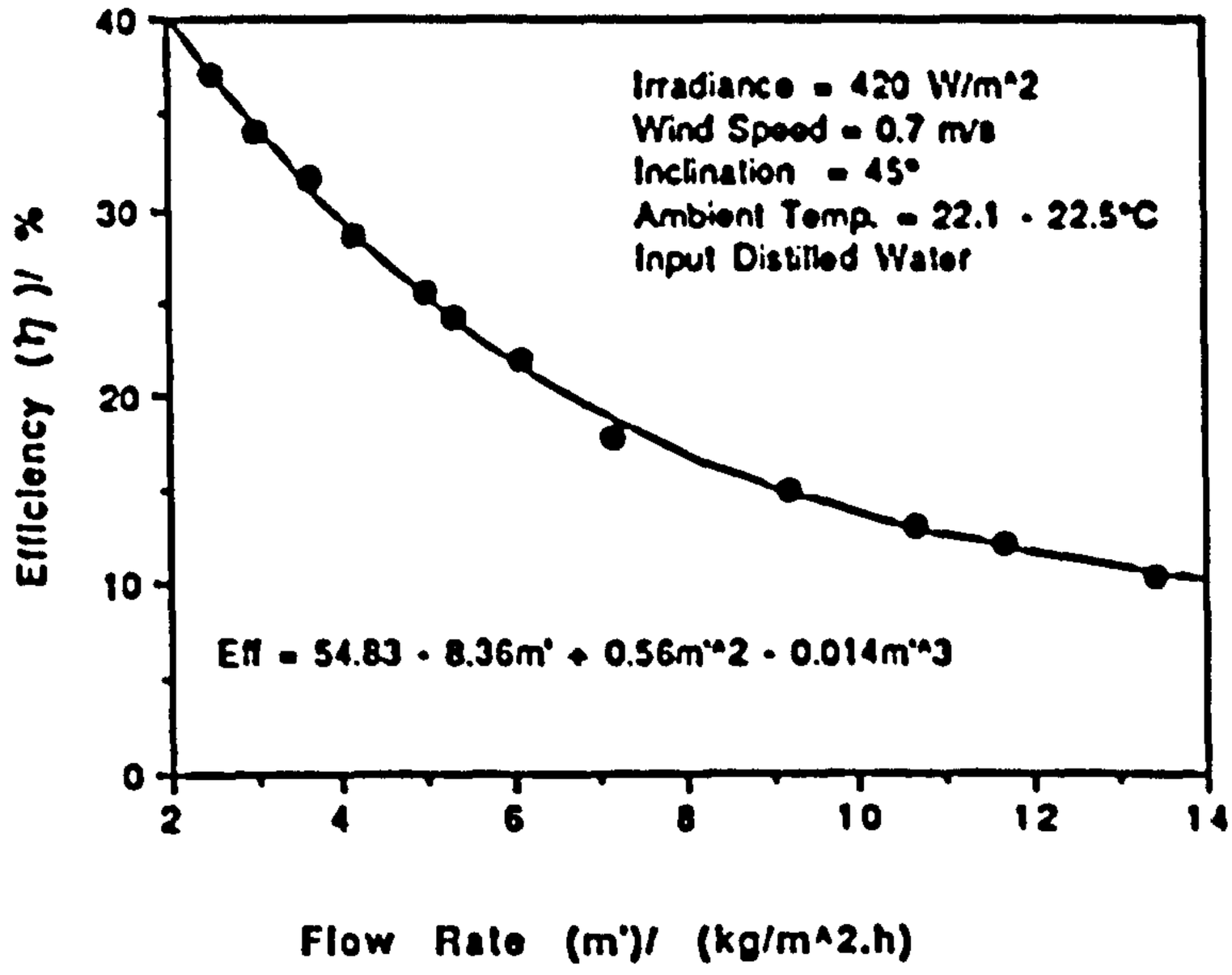

Fig. 3.2.7. Variation of the still efficiency (η) with input water flow rate (m'), (determined by indoor testing).

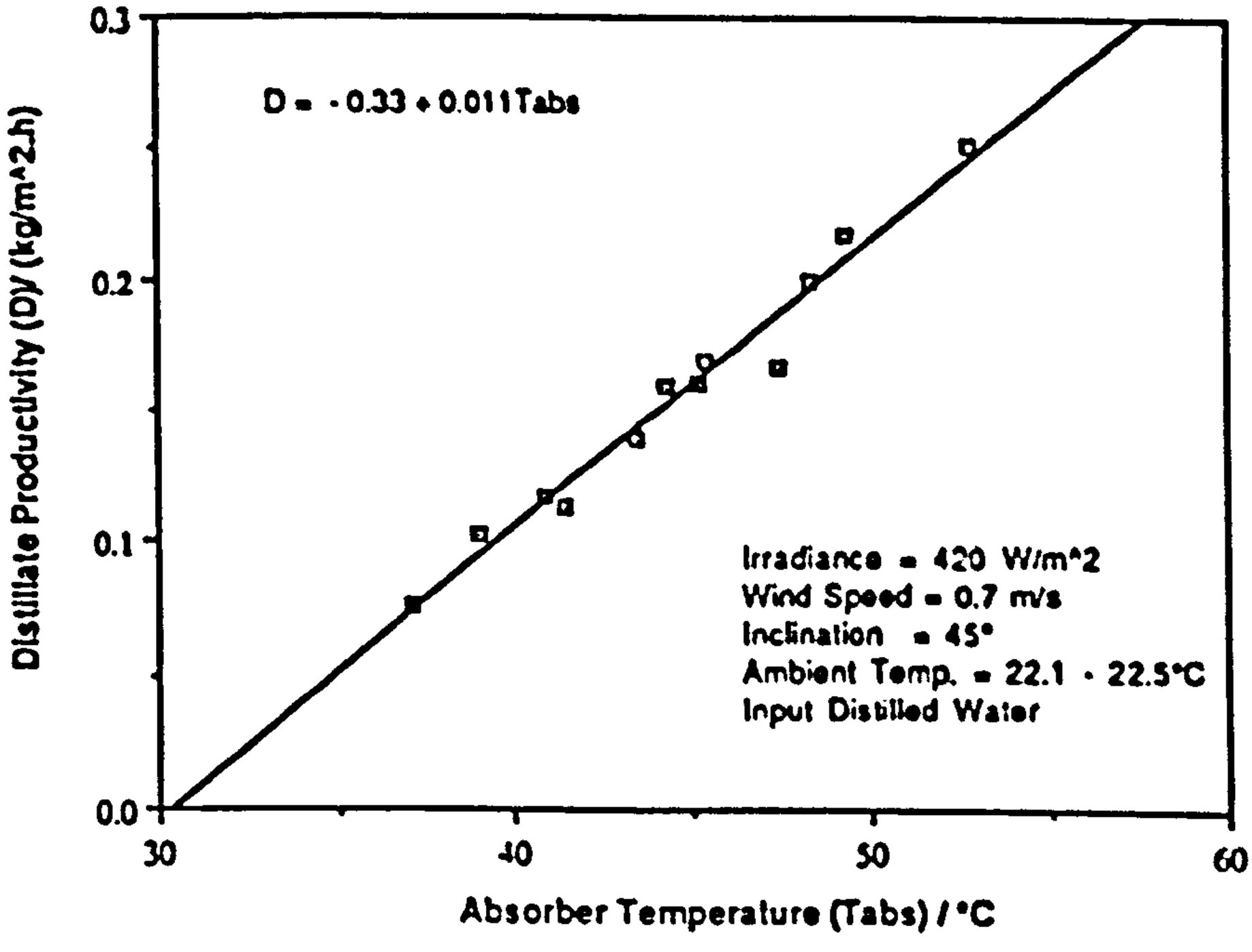

Fig. 3.2.8. Variation of distillate productivity with absorber temperature, (determined by indoor testing) by varying the flow rate.

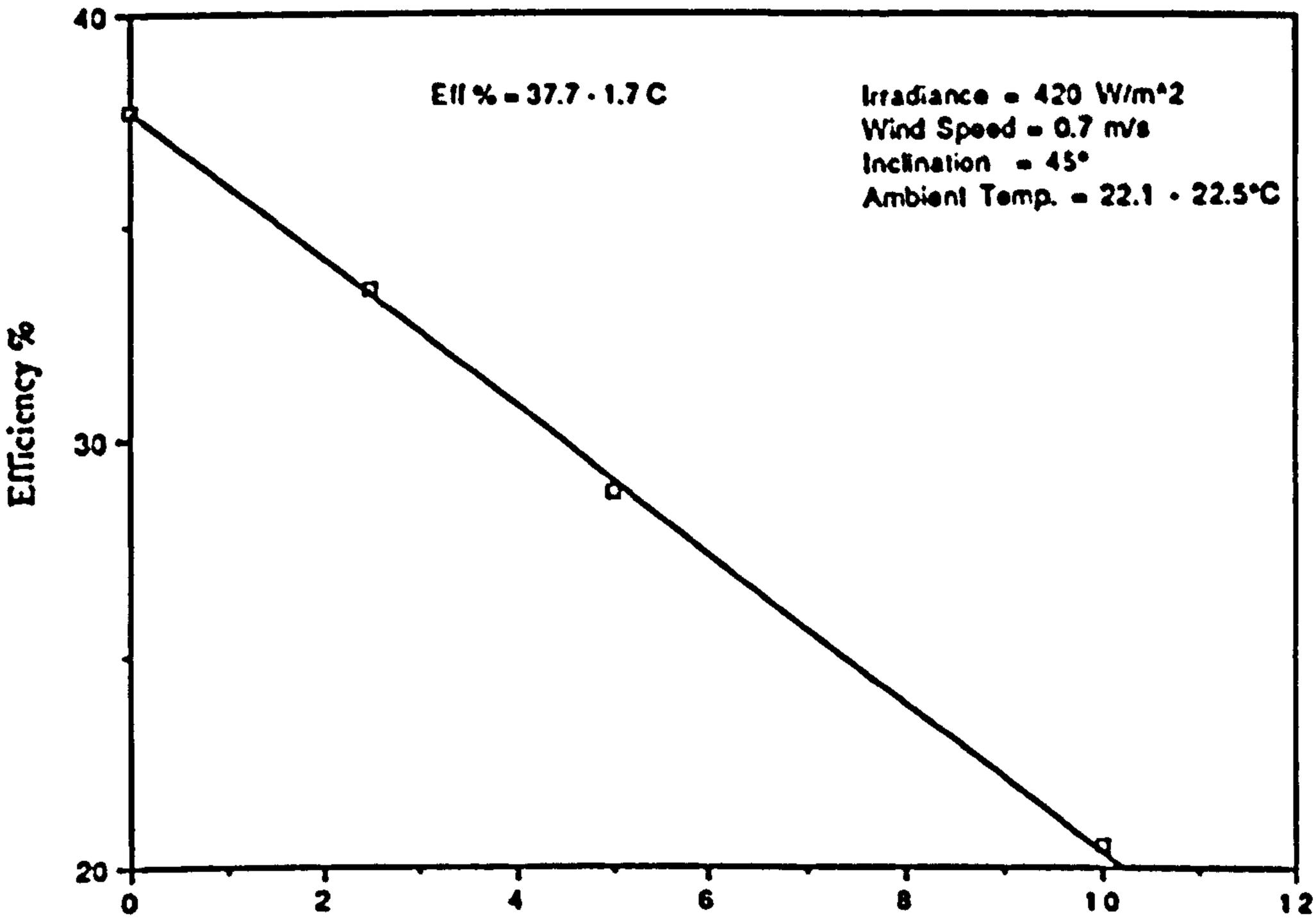

Fig. 3.2.9. Experimental variation of the still efficiency with salt concentration in the input saline water, (determined by indoor testing).

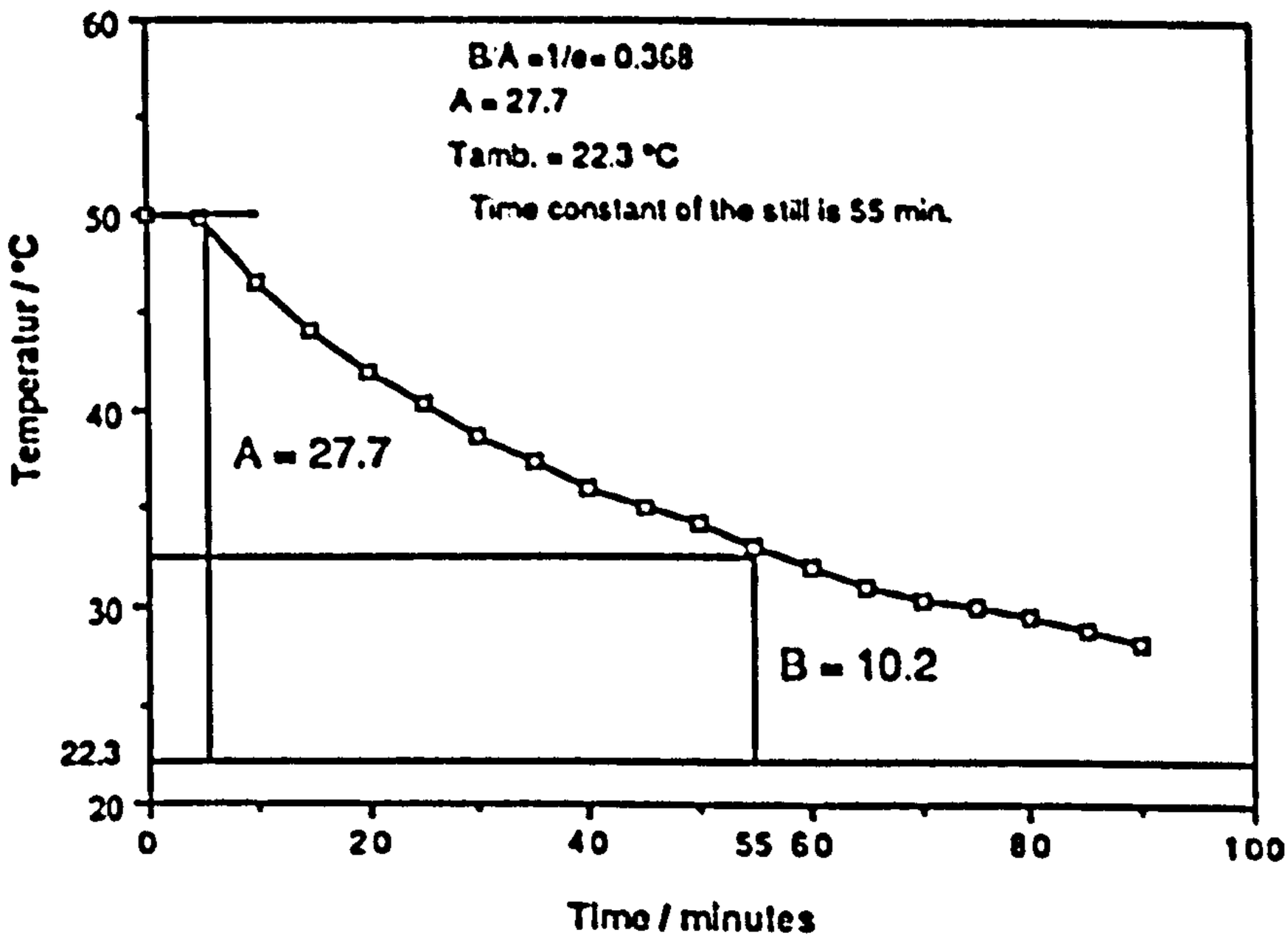

Fig. 3.2.10. Cooling curve of the absorber of the still after switching off of lamps.

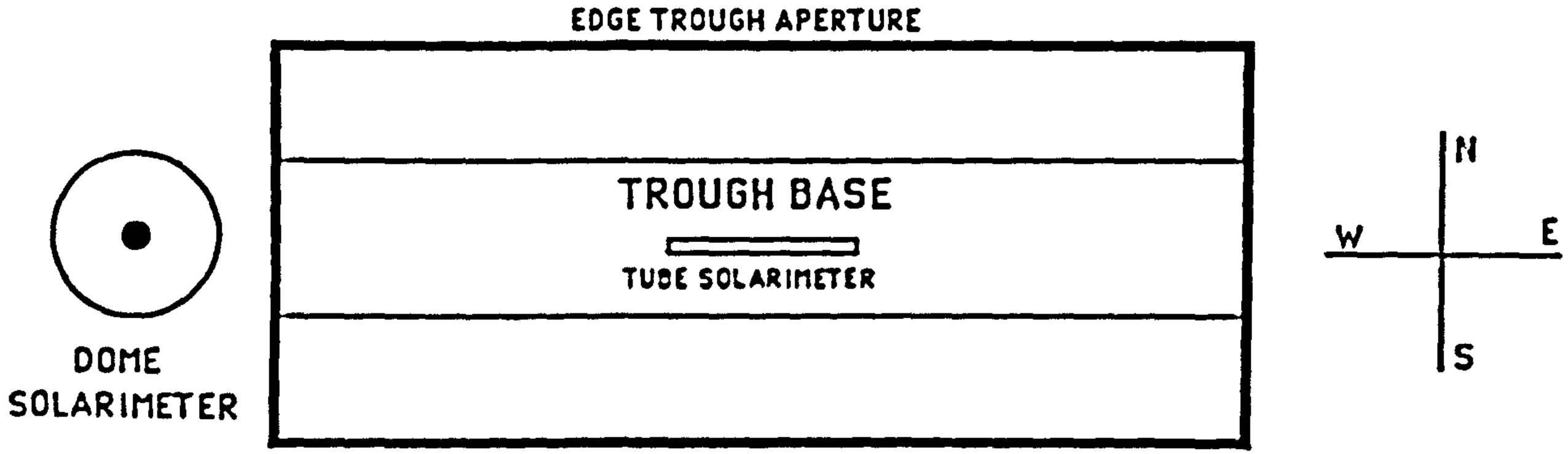

Fig. 3.3.1. Schematic diagram showing positions of the tube solarimeter and the dome solarimeter, during the measurement of the instantaneous concentration factor for the central part of the receiving surface.

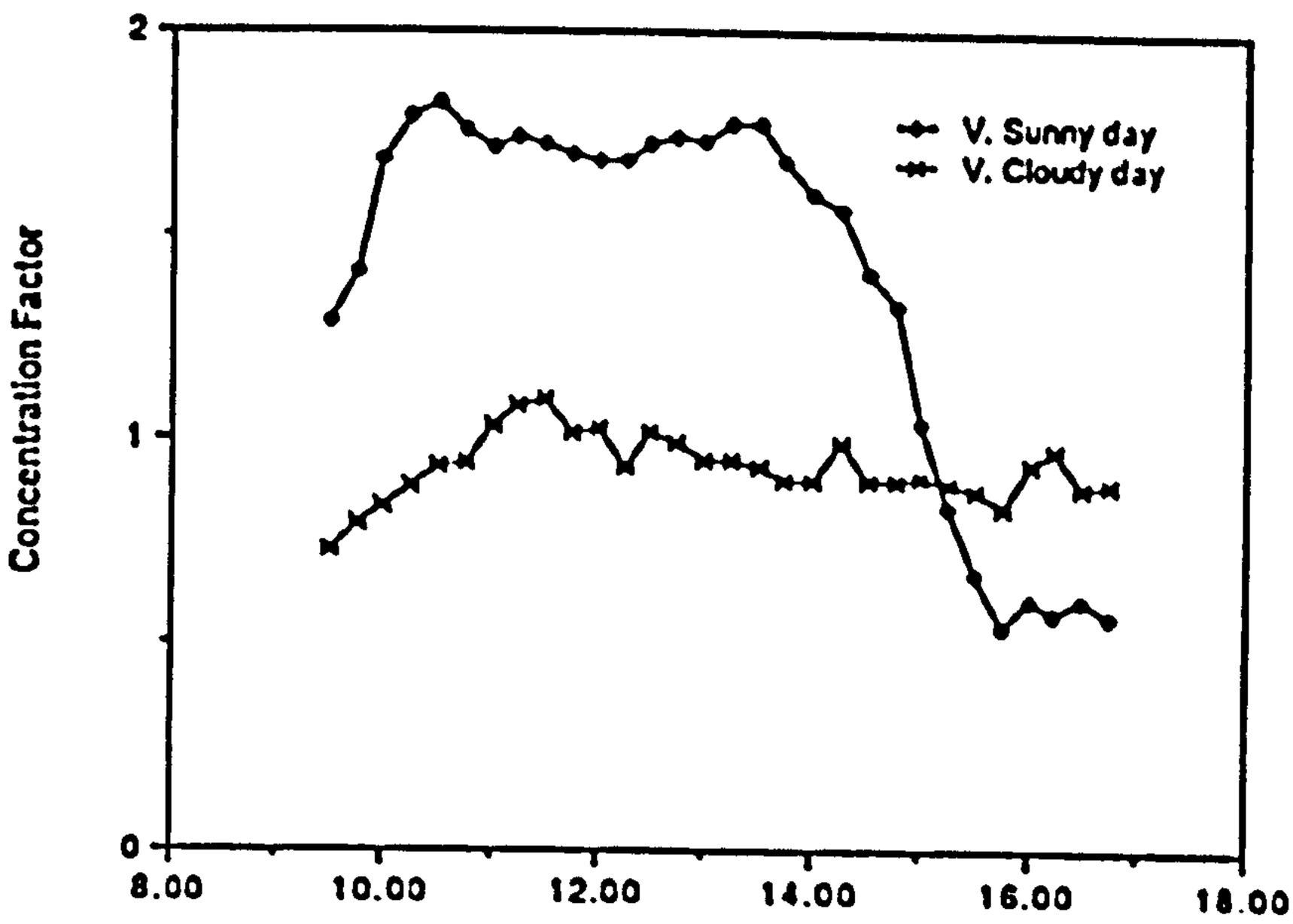

Fig. 3.3.2. Experimental time variation of an approximate instantaneous concentration factor (determined using tube solarimeter) for the central part of the receiving surface using V-trough solar concentrator.

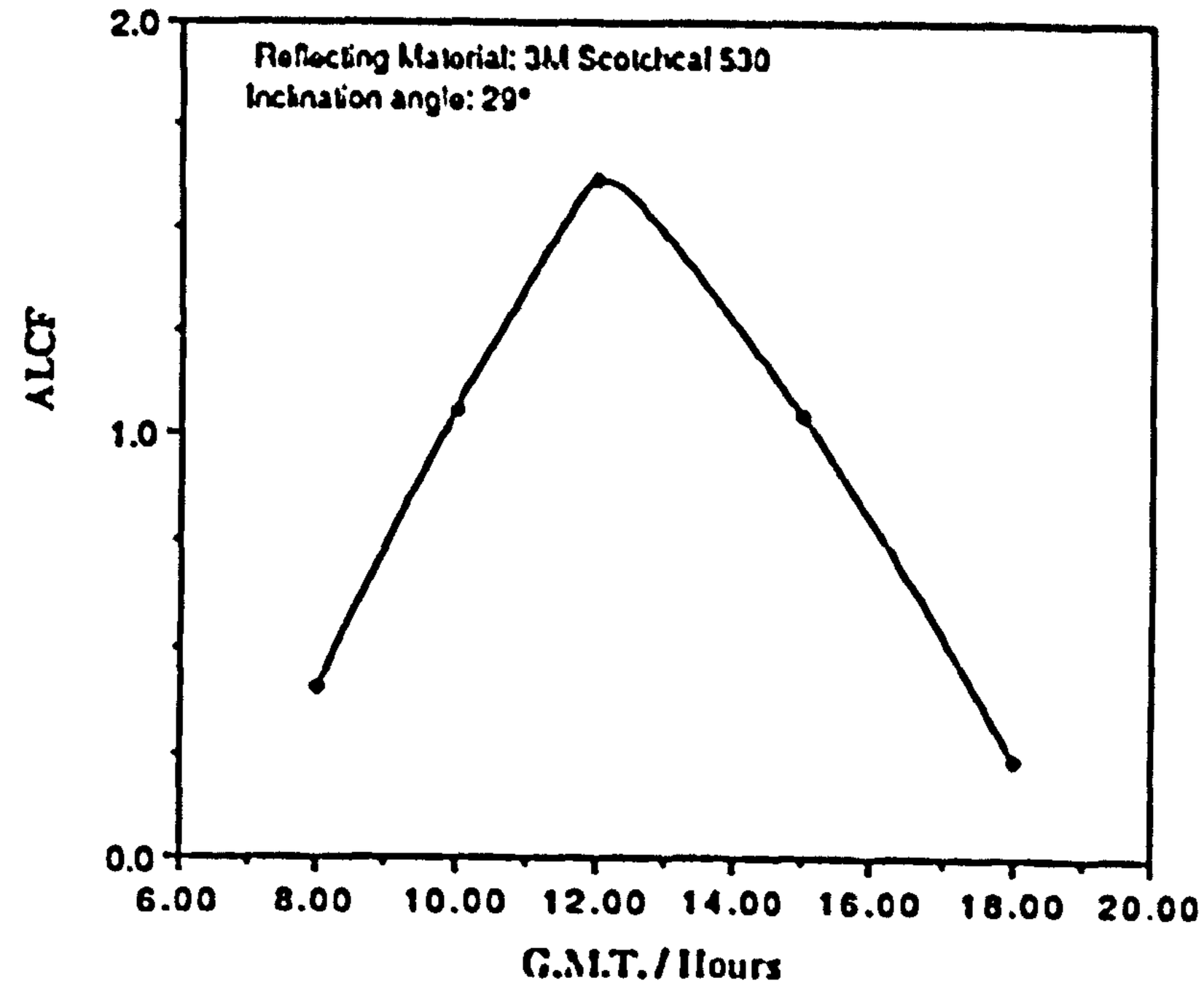

Fig. 3.3.3. Variation of averaged local concentration factor (ALCF) of the concentrator with time on 11/7/1990.

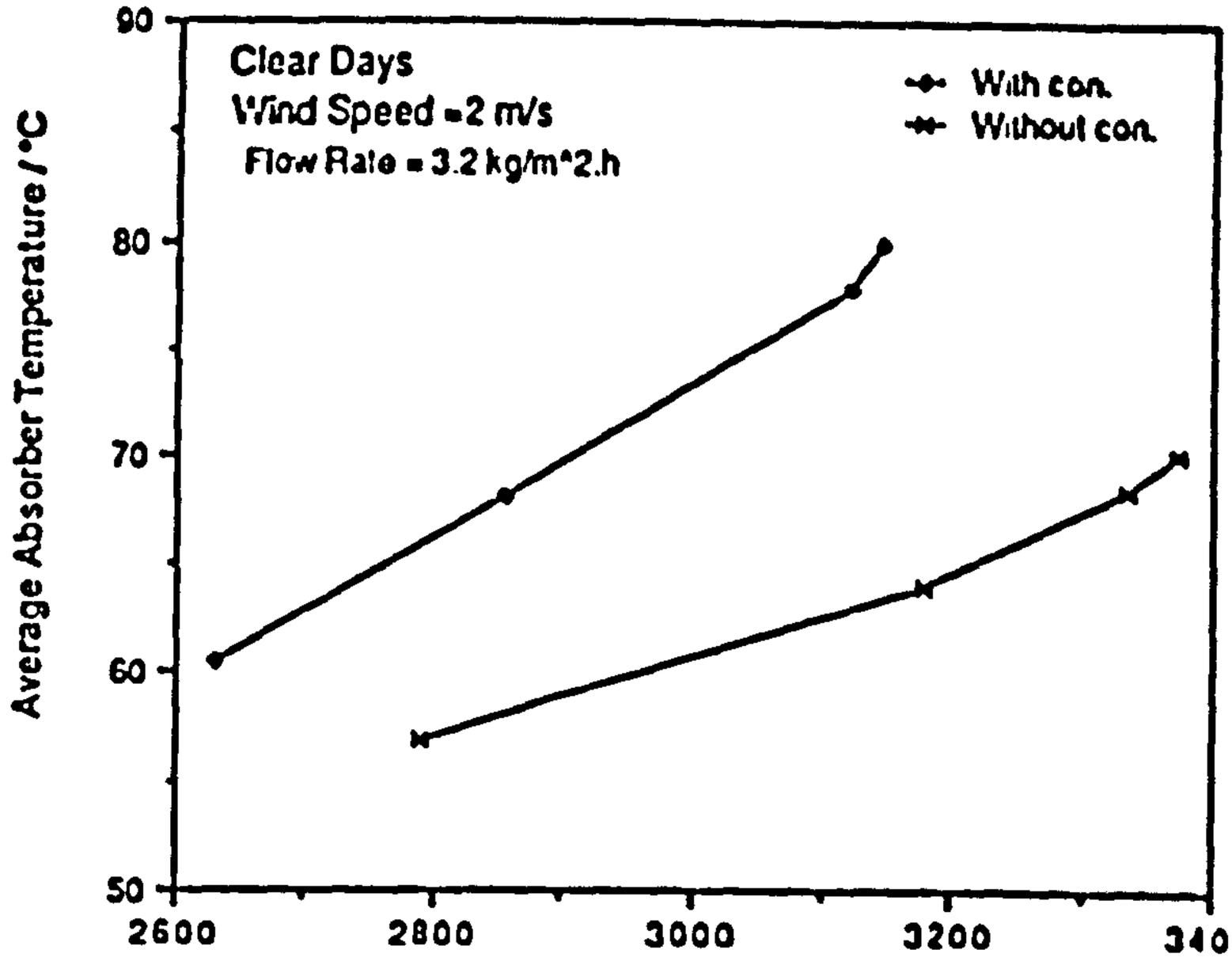

Fig. 3.3.4. Variation of hourly average still absorber temperature with solar insolation (with and without the concentrator).

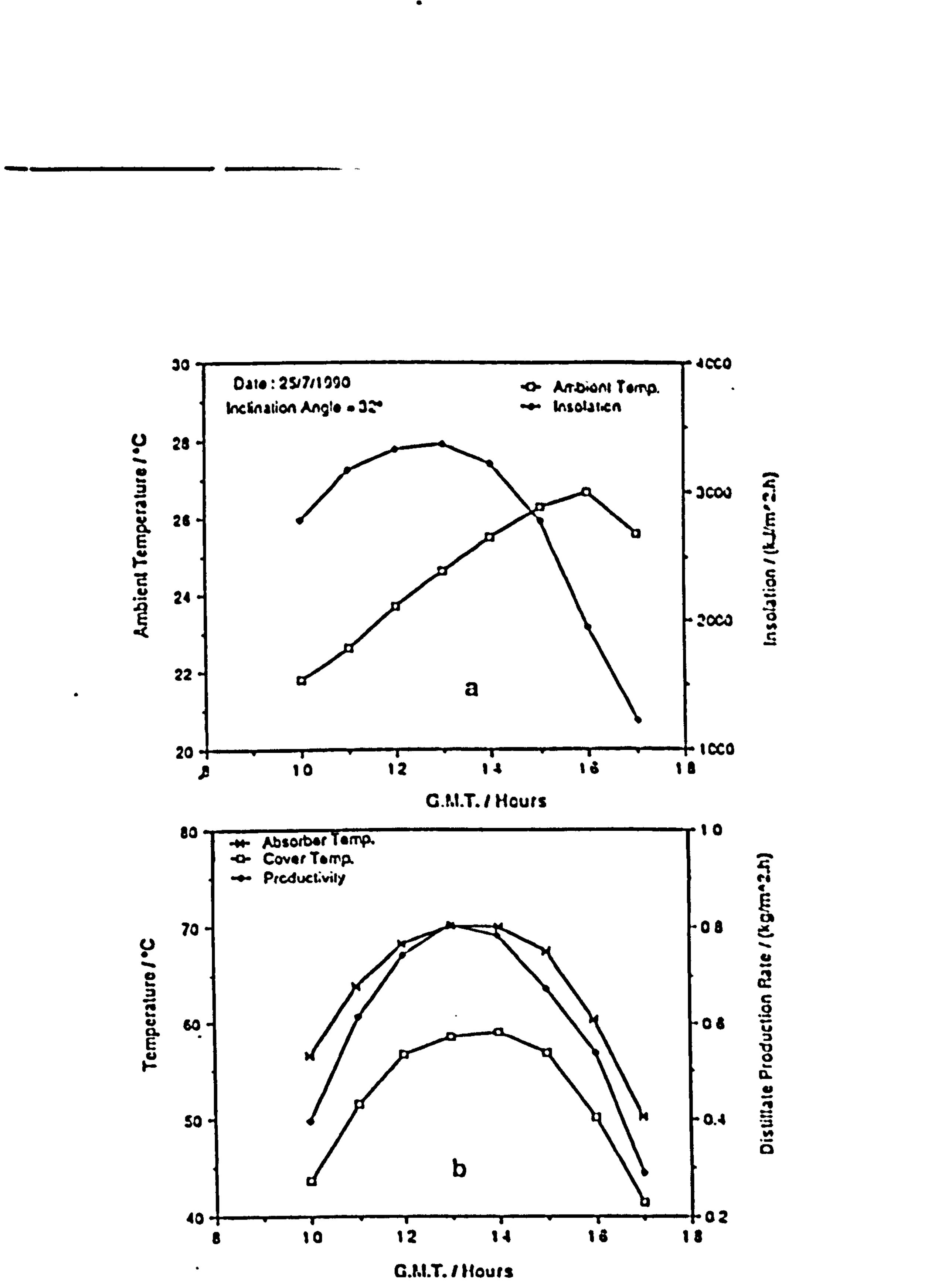

Fig. 3.3.5. Variation of (a) solar insolation and ambient temperature (b) absorber and cover temperatures and distillate production rate of the wick-type solar still with time on 25/7/1990 (distilled input water was used).

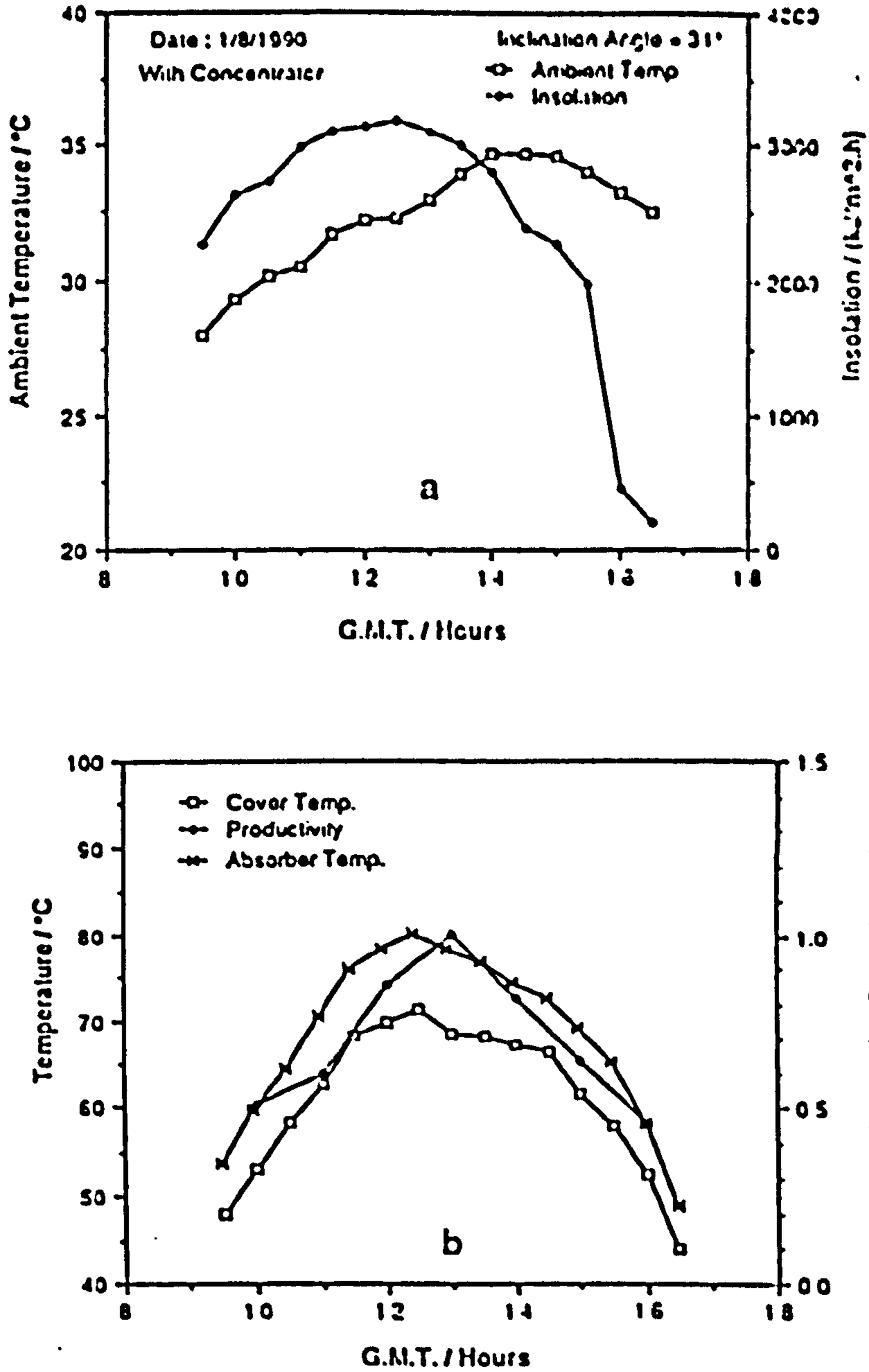

Fig. 3.3.6. Variation of (a) solar insolation and ambient temperature (b) absorber and cover temperatures and distillate production rate of the solar still, with concentrator, with time on 1/8/1990 (distilled input water was used).

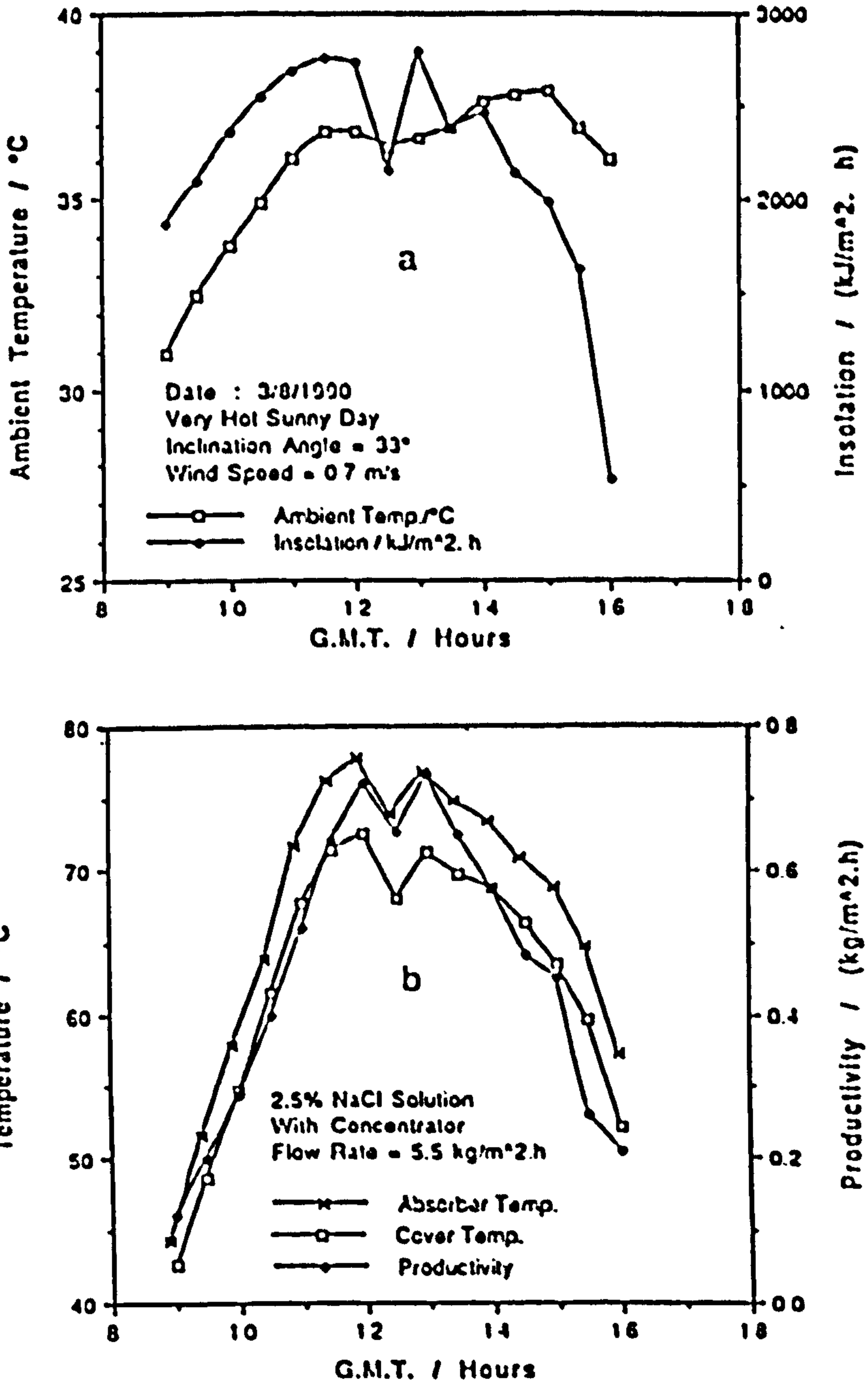

Fig. 3.3.7. Variation of (a) solar insolation and ambient temperature (b) absorber and cover temperatures and distillate production rate of the solar still with concentrator with time on 3/8/1990 (2.5% NaCl solution was used).

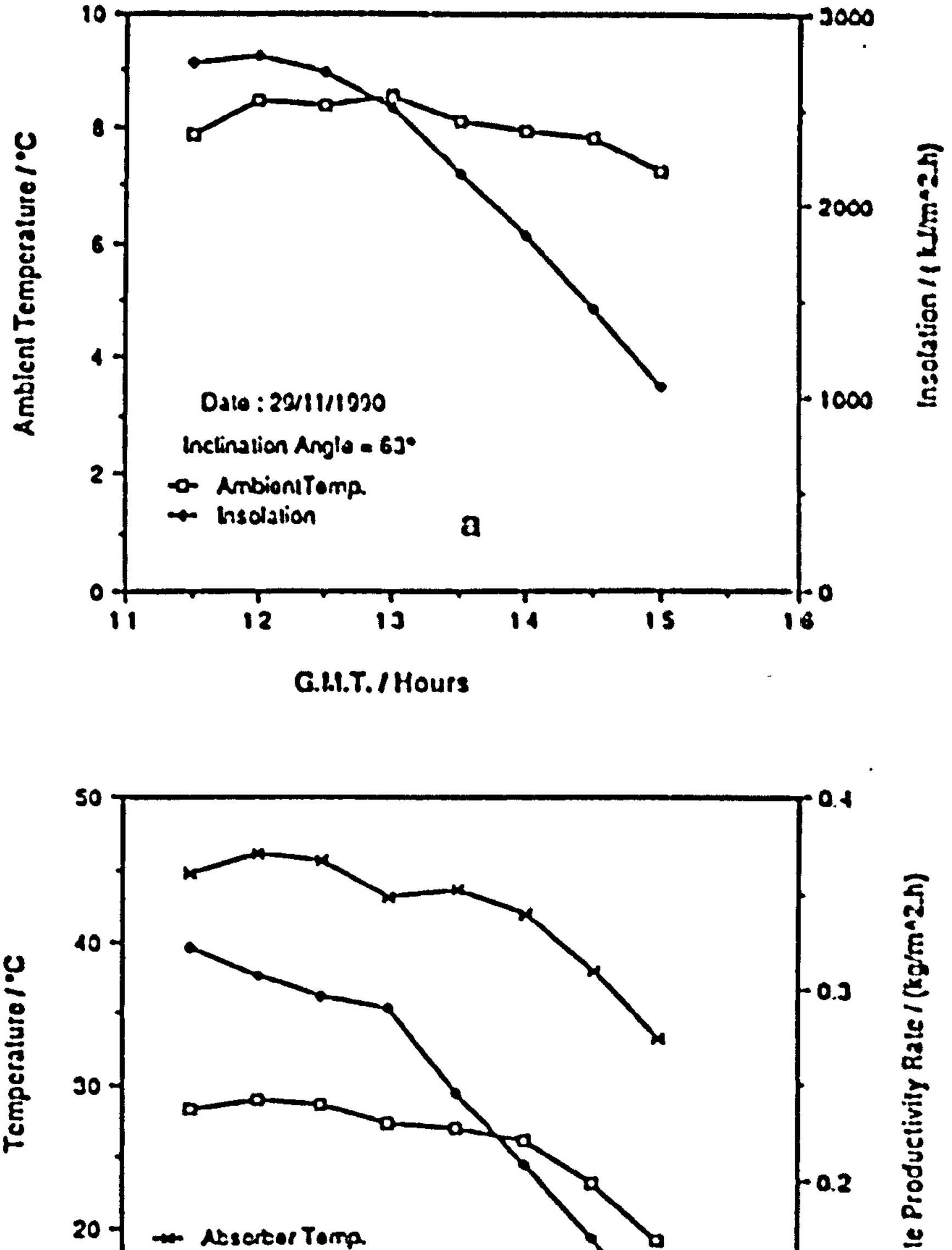

Fig. 3.3.8. Variation of (a) solar insolation and ambient temperature (b) absorber and cover temperatures and distillate production rate of the solar still with time on 29/11/1990 (2.5% NaCl solution was used).

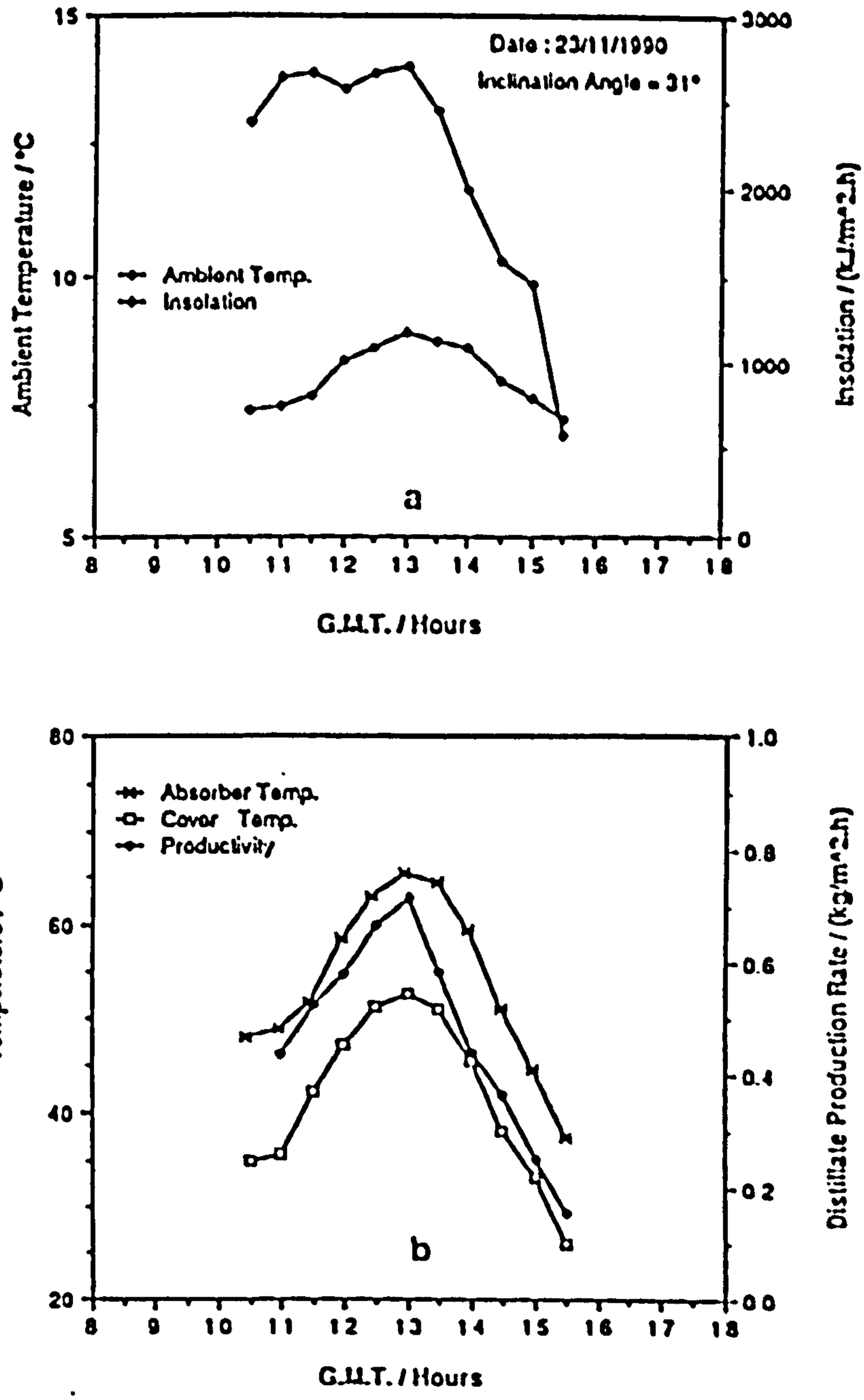

Fig. 3.3.9. Variation of (a) solar insolation and ambient temperature (b) absorber and cover temperatures and distillate production rate of the solar still with concentrator with time on 23/11/1990 (2.5% NaCl solution was used).

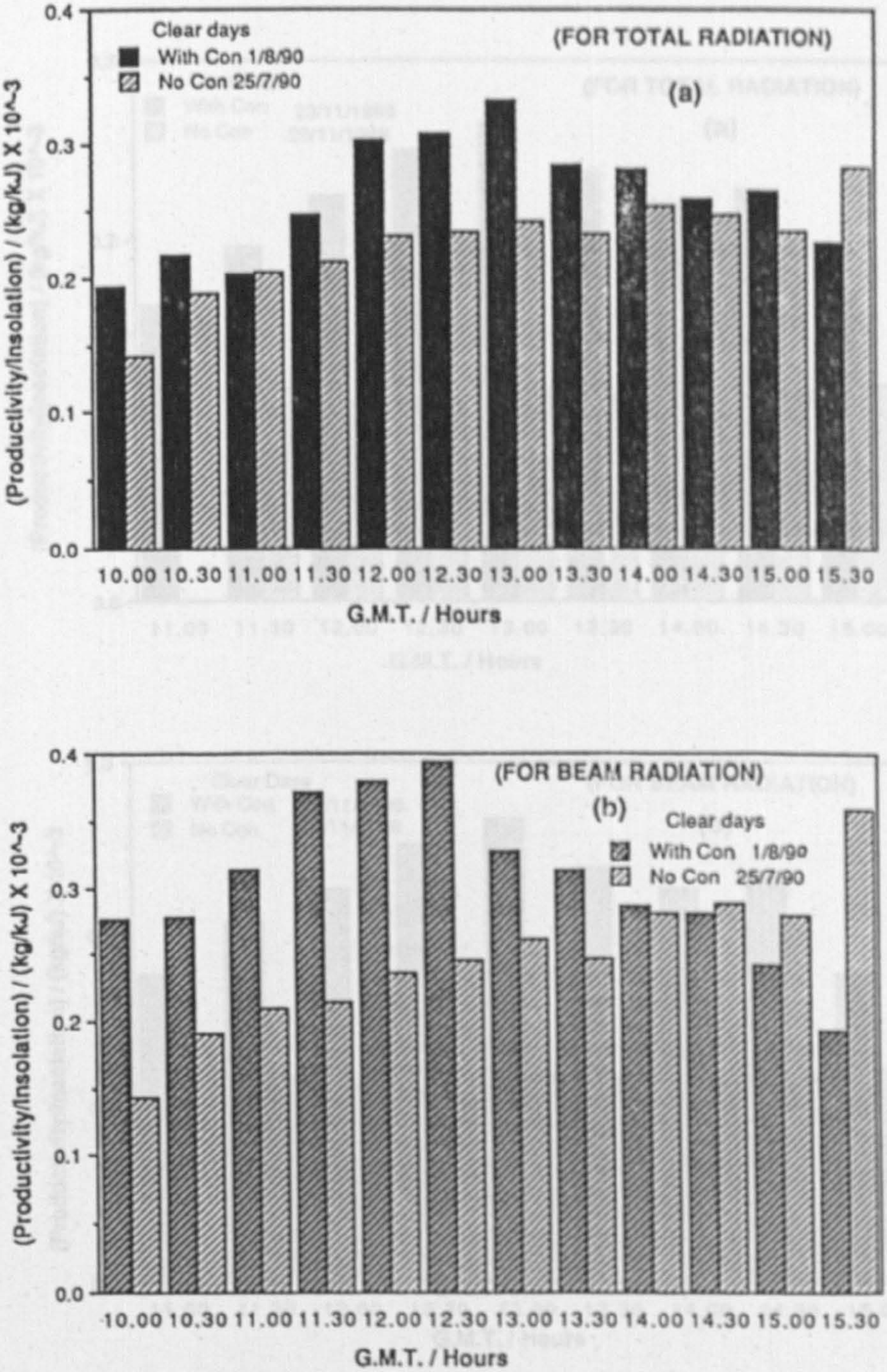

Fig. 3.3.10. Variation of (productivity/insolation) using the still with and without the concentrator, (a) for total (b) for beam radiation in summer (distilled water was used).

Fig. 3.3.11. Variation of (productivity/insolation) using the still with and without the concentrator, (a) for total (b) for beam radiation in winter (2.5% NaCl solution was used).

Fig. 3.4.1. Spectral reflectance of an as-received sample of charcoal cloth for VIS and NIR radiation, $\rho = 2.0 \pm 0.2$.

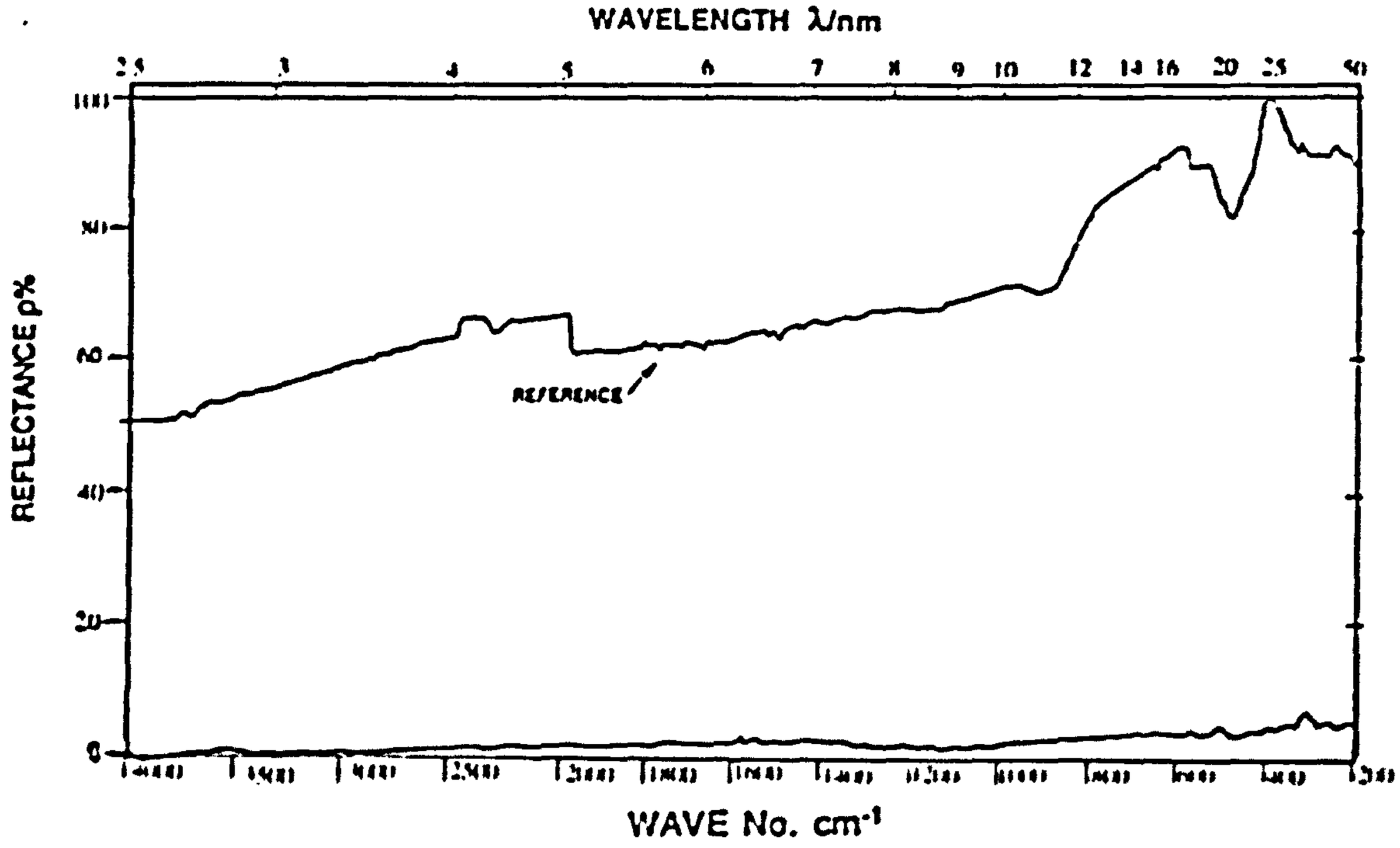

Fig. 3.4.2. Spectral reflectance of an as-received sample of charcoal cloth for IR radiation, $\rho = 1.0 \pm 0.2$.

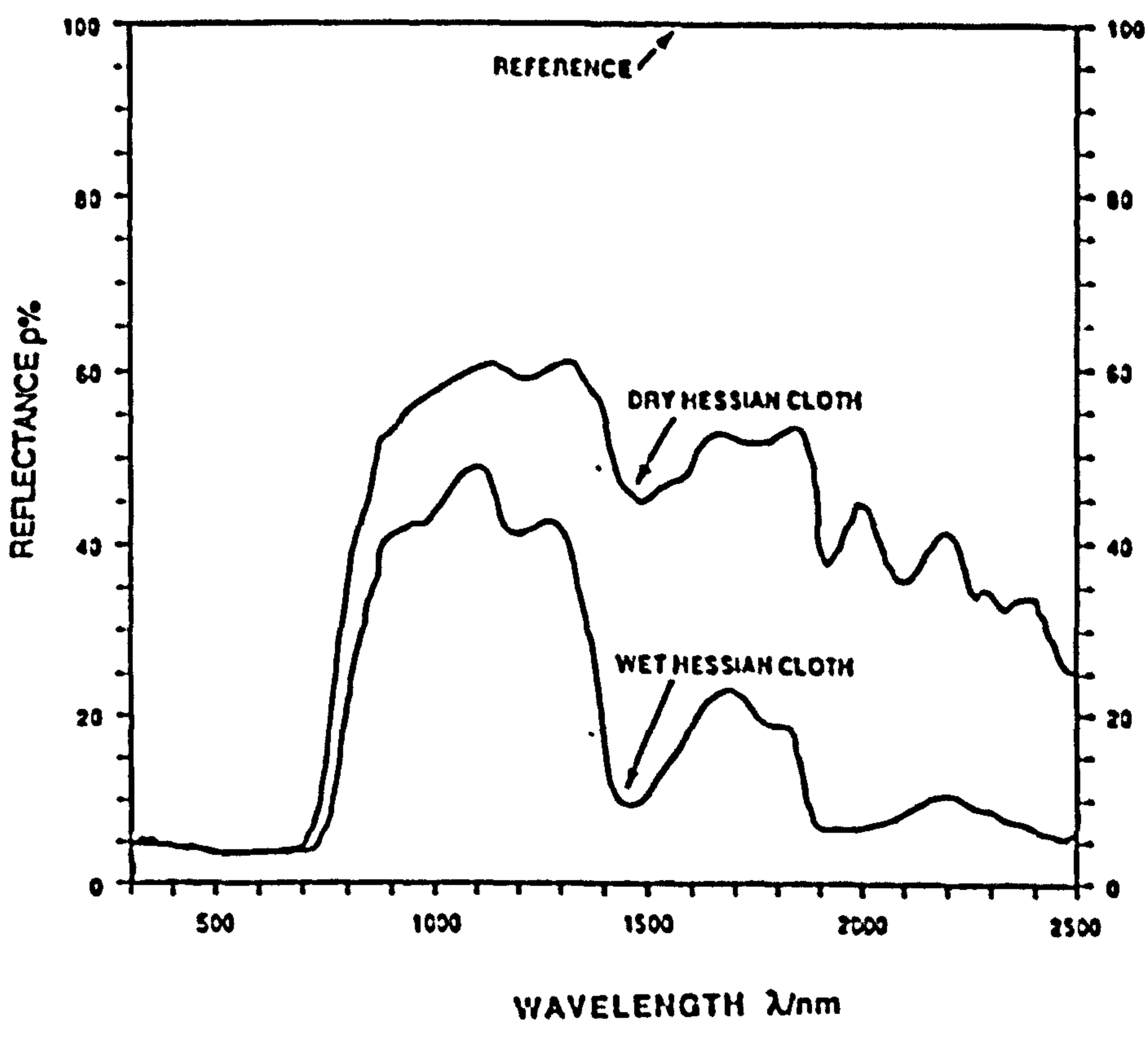

Fig. 3.4.3. Spectral reflectance of an as-received sample of hessian cloth for VIS and NIR radiation, $\rho = 35.4 \pm 0.06$.

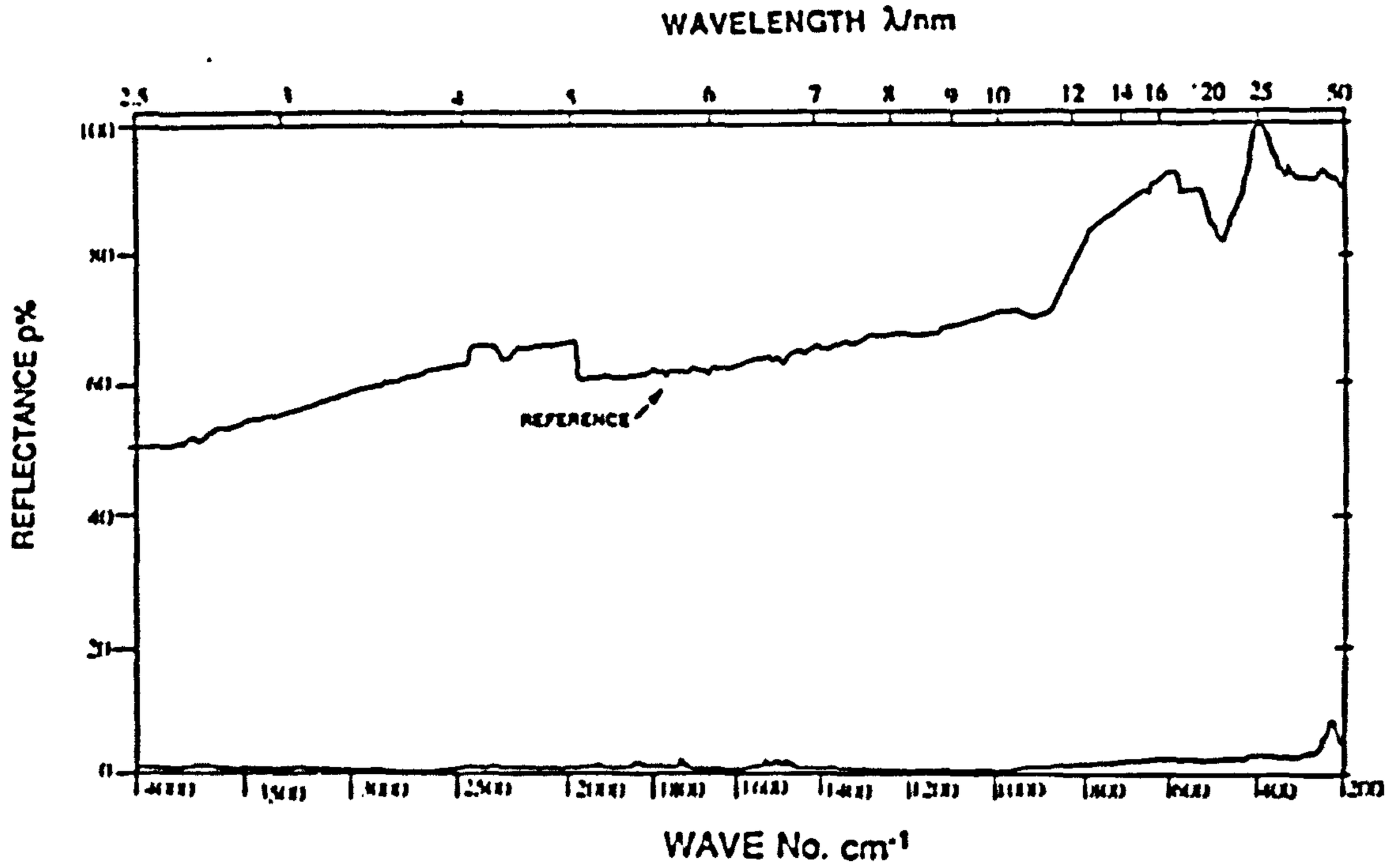

Fig. 3.4.4. Spectral reflectance of an as-received sample of hessian cloth for IR radiation.

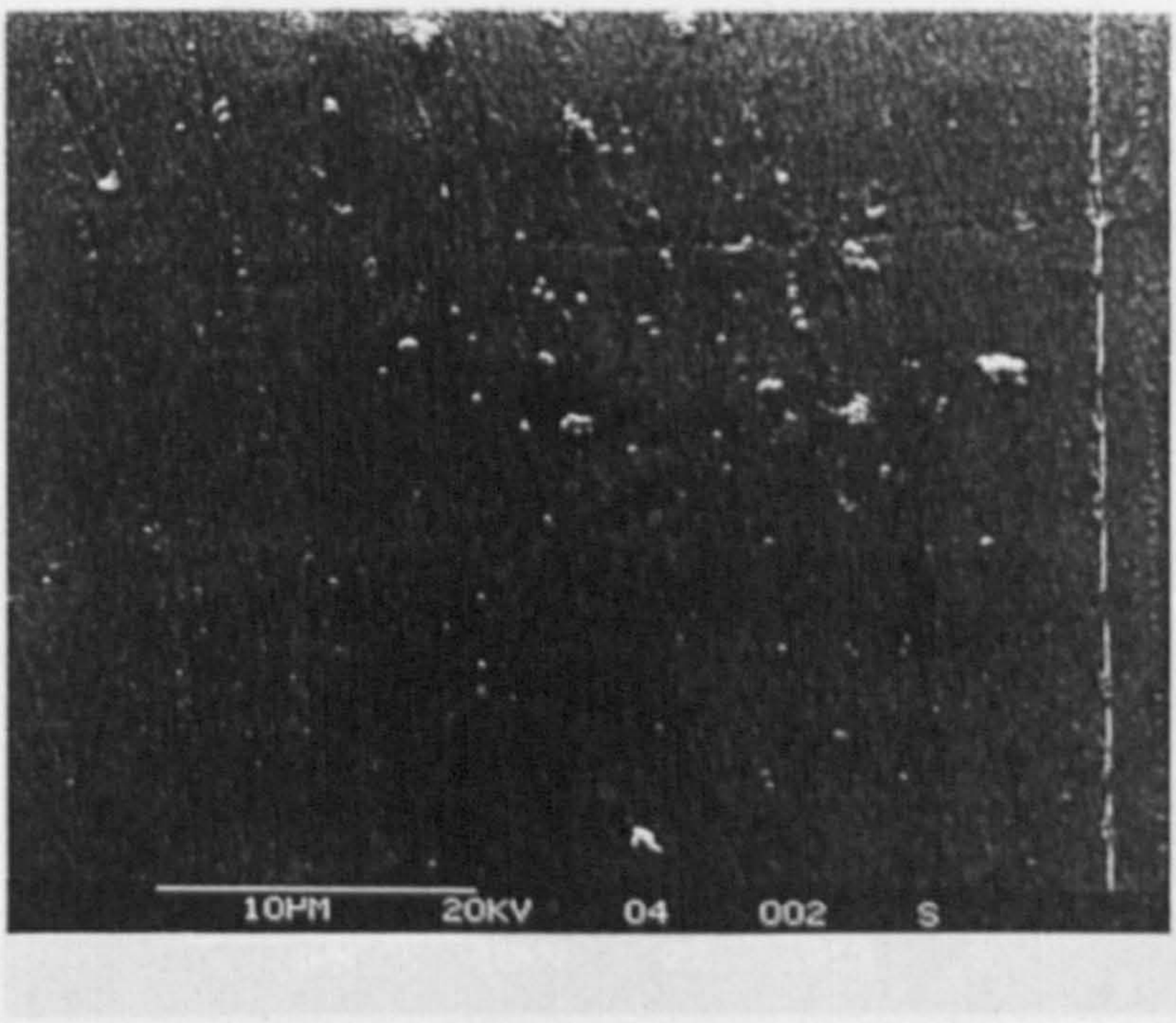

Fig. 3.4.5. Scanning electron micrograph of an as-received sample of 3M Scotchcal Film 530.

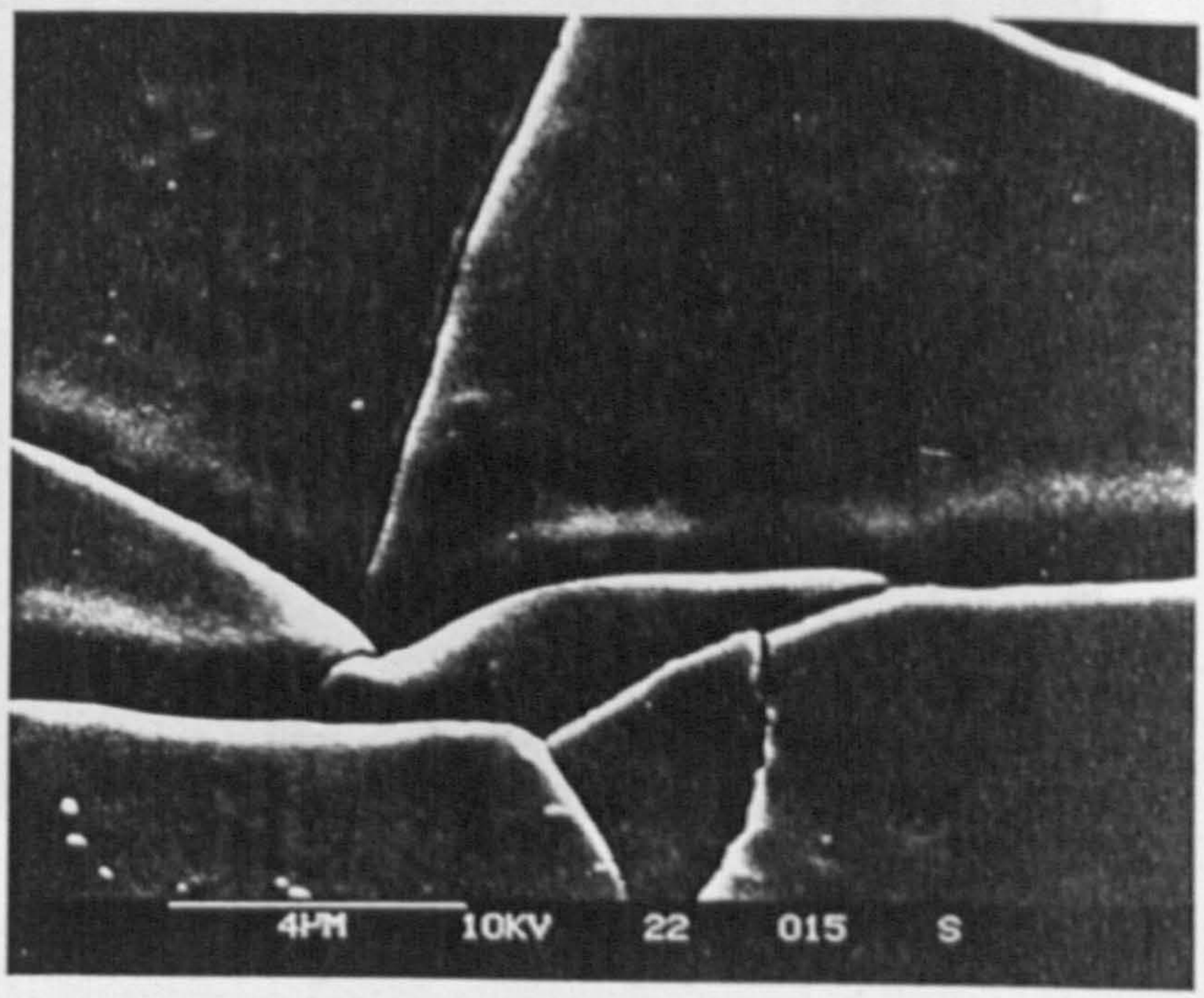

Fig. 3.4.6. Scanning electron micrograph of an as-received sample of 3M Scotchcal Film 680.

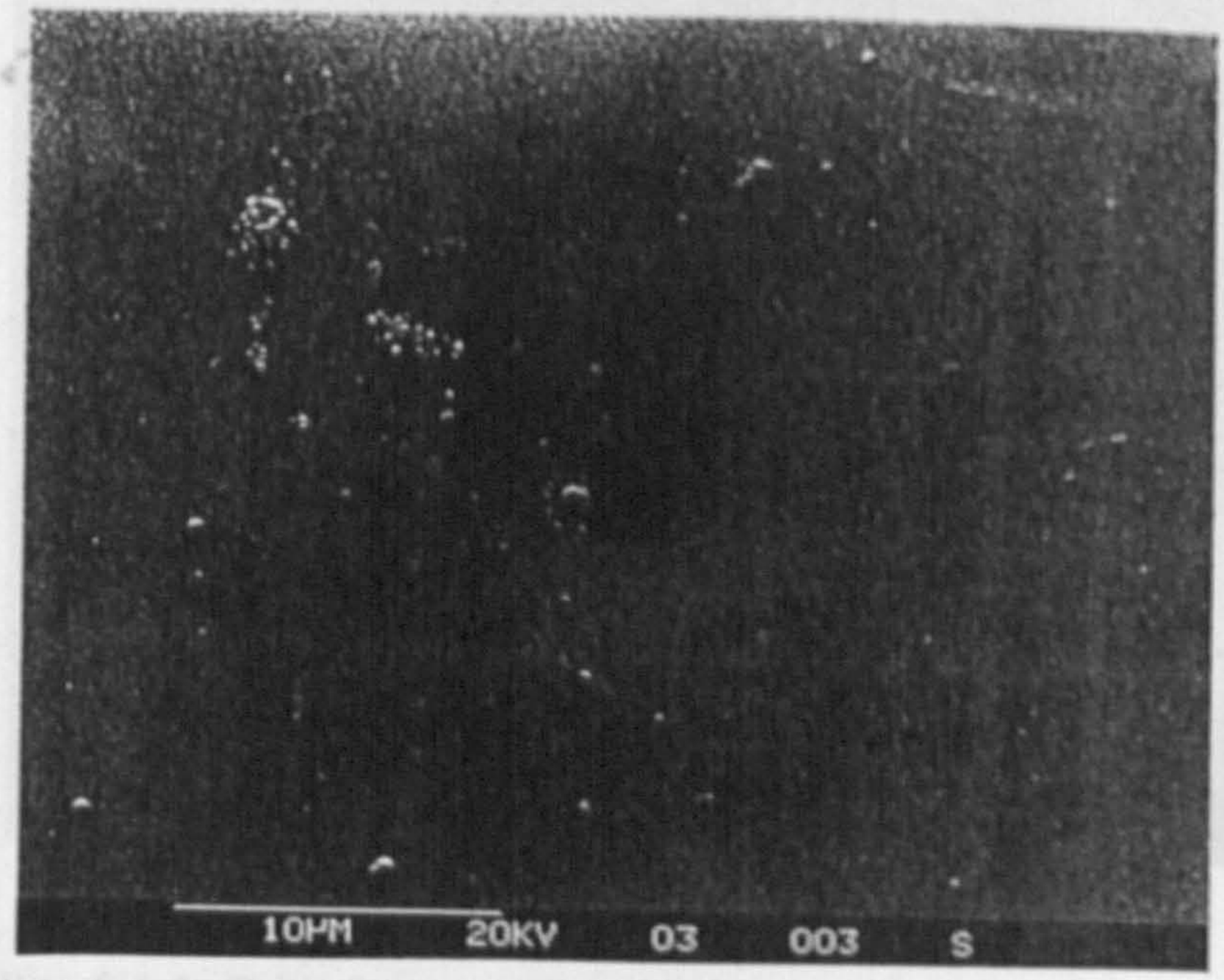

Fig. 3.4.7. Scanning electron micrograph of an as-received sample of 3M Scotchcal Film 3658.

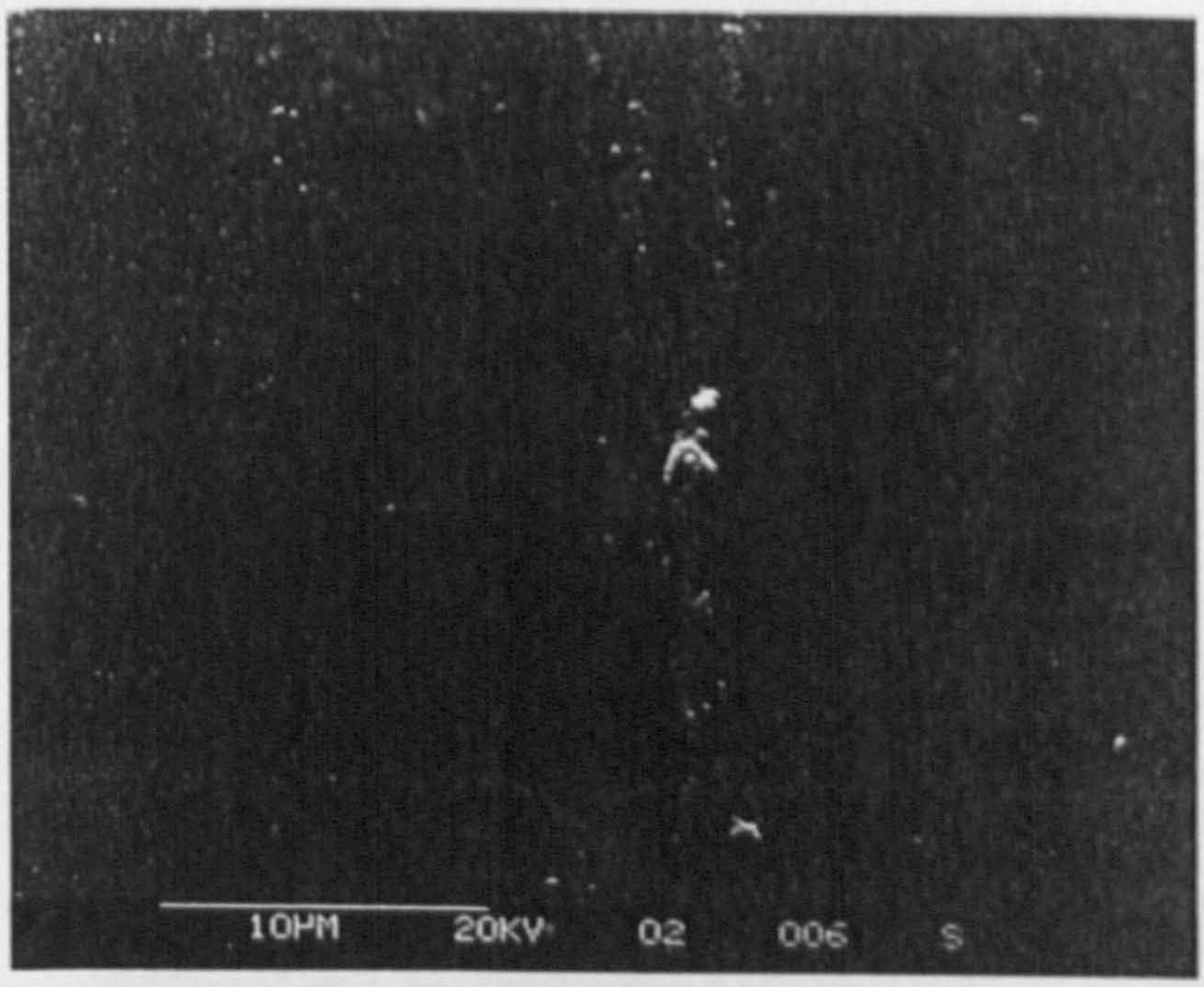

Fig. 3.4.8. Scanning electron micrograph of an as-received sample of 3M Scotchcal Film 5400.

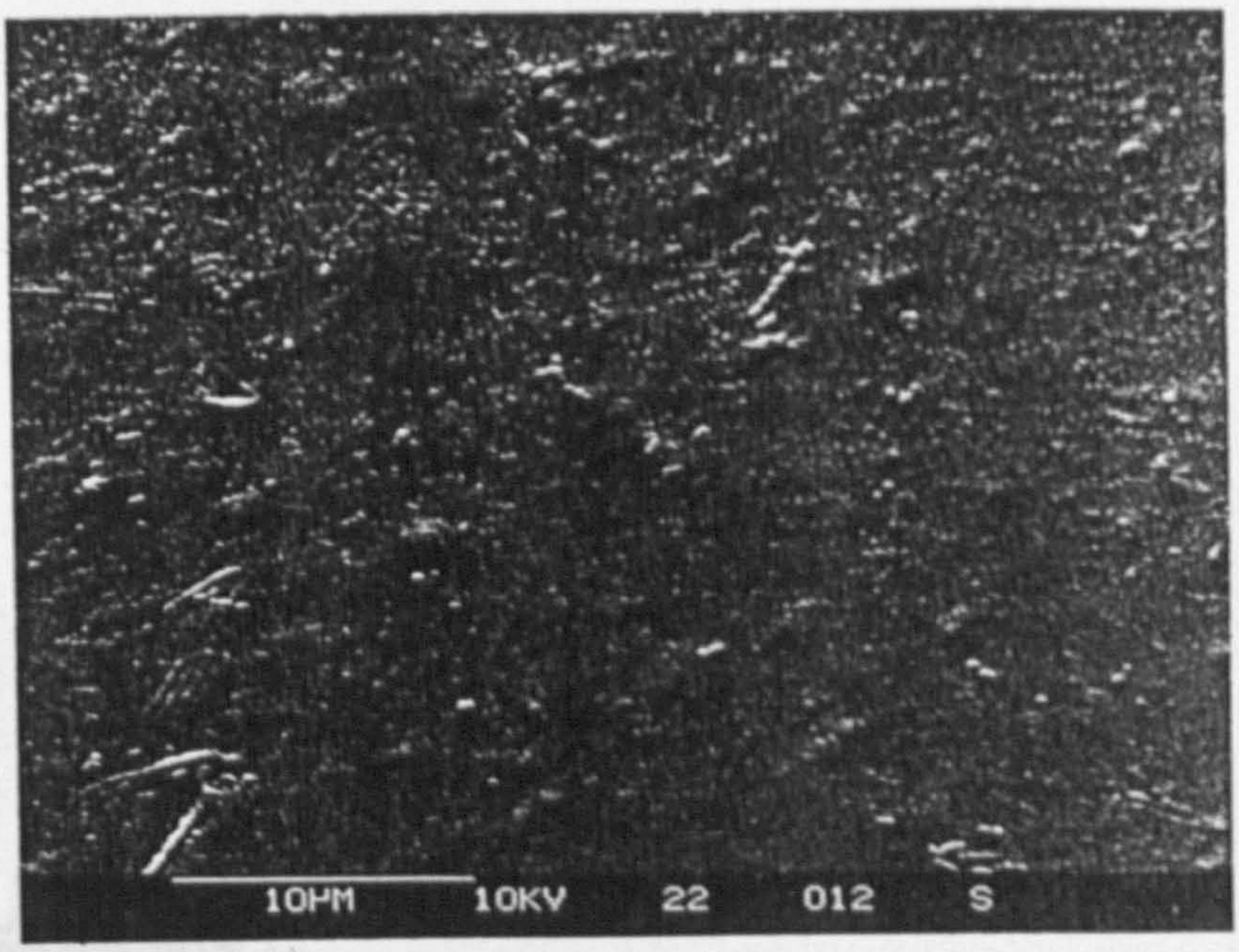

Fig. 3.4.9. Scanning electron micrograph of an as-received sample of aluminised plastic.

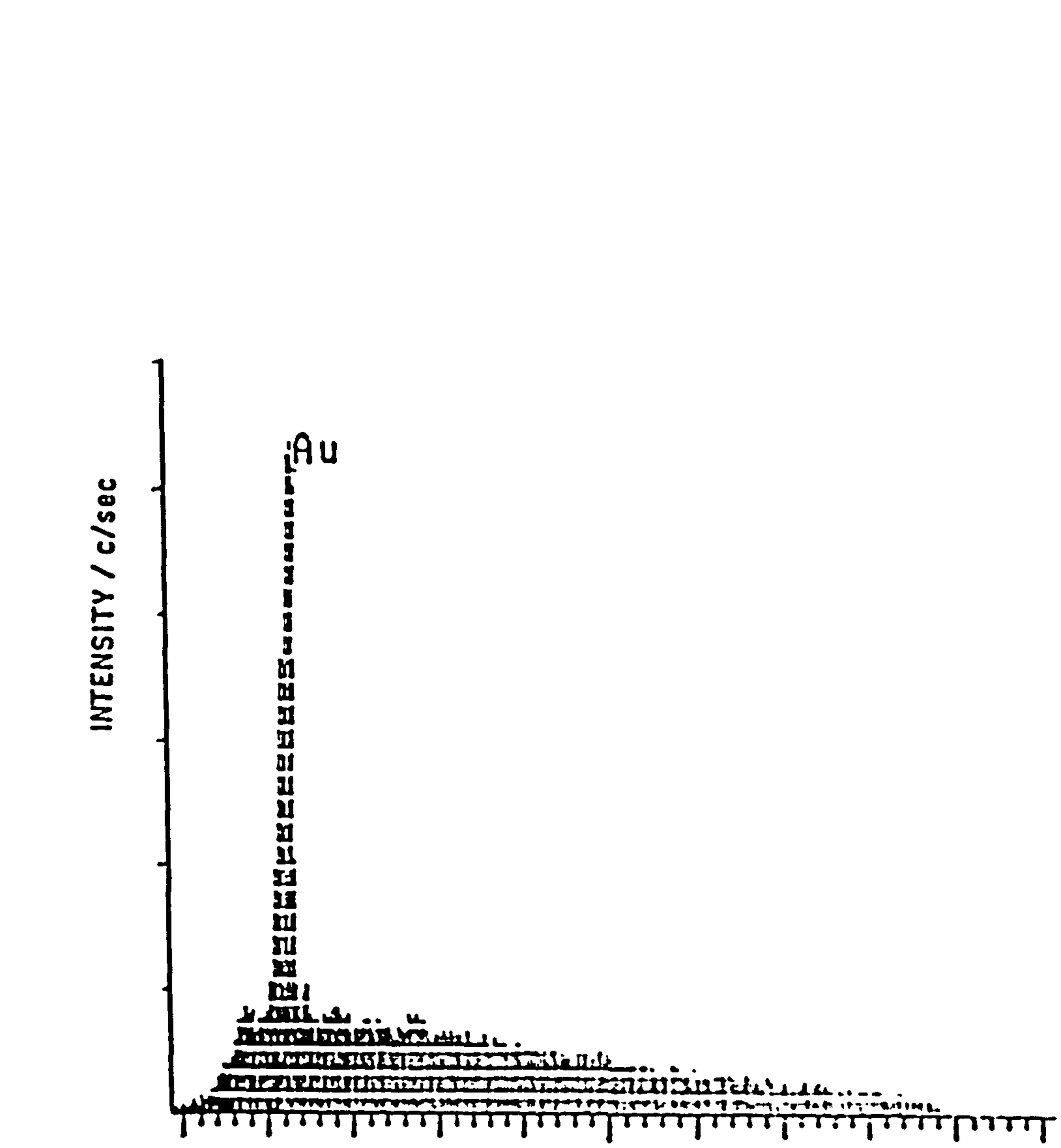

Fig. 3.4.10. Electron probe microanalysis of an as-received sample of 3M Scotchcal Film 530.

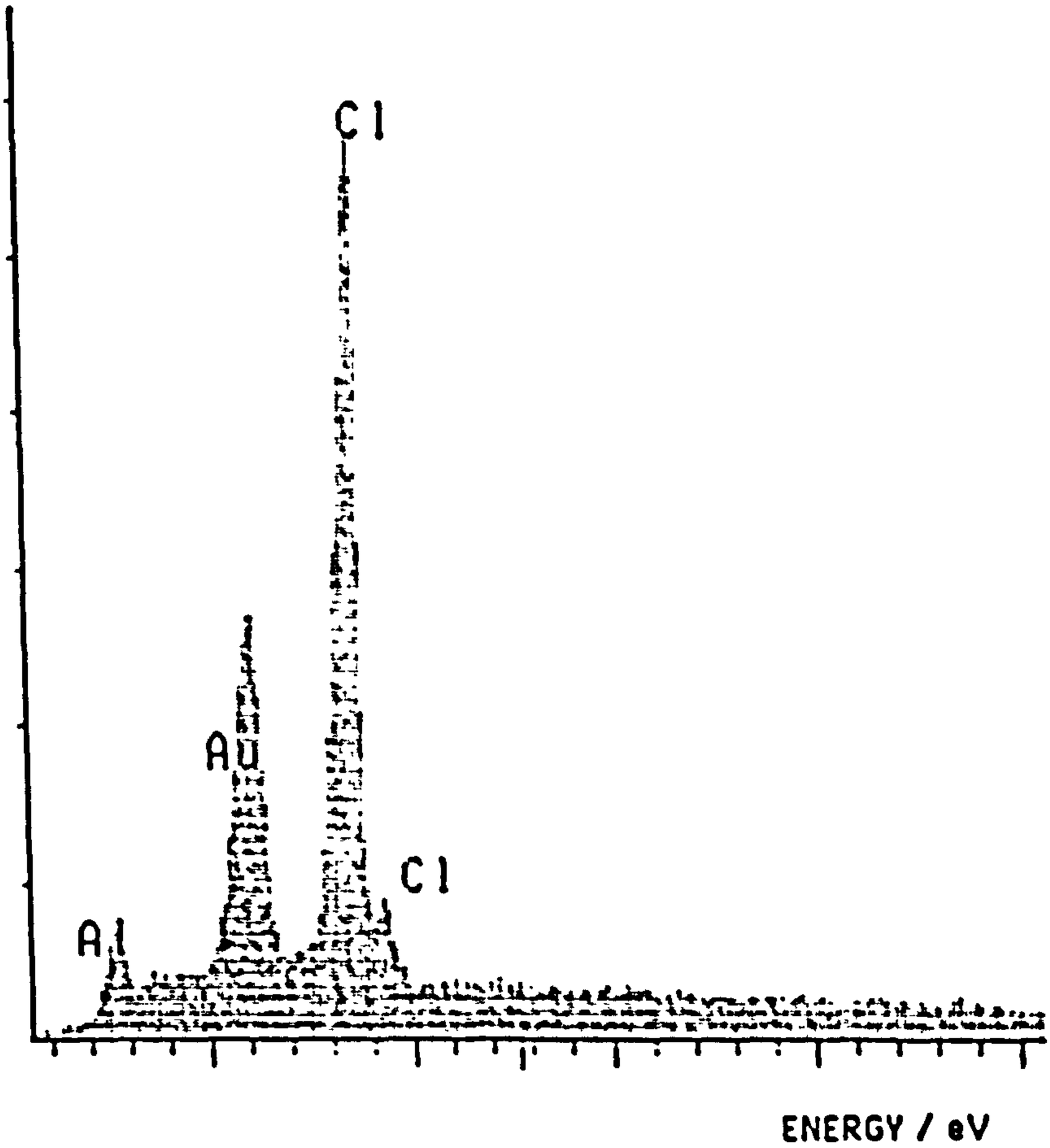

Fig. 3.4.11. Electron probe microanalysis of an as-received sample of 3M Scotchcal Film 3658.

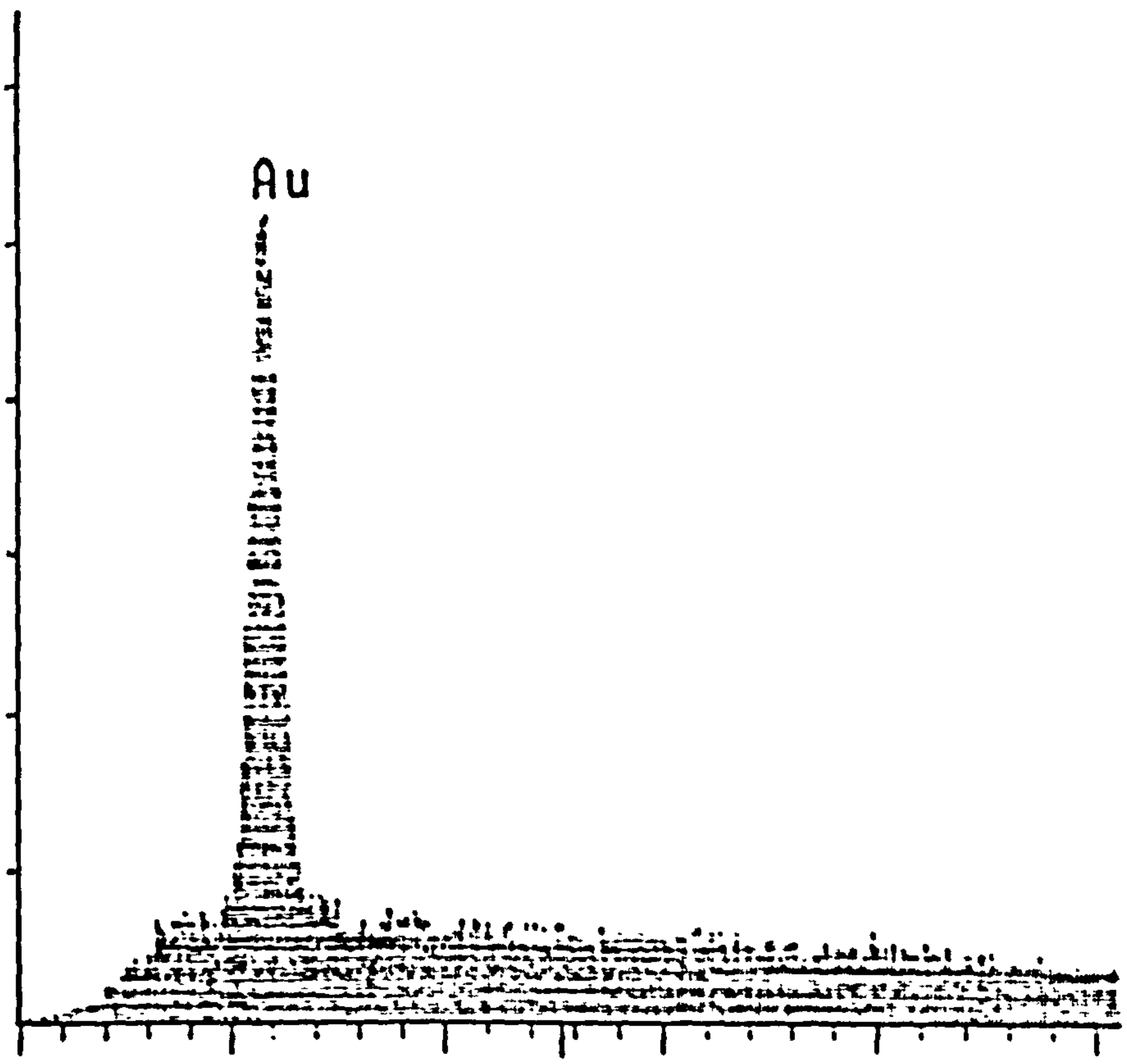

Fig. 3.4.12. Electron probe microanalysis of an as-received sample of 3M Scotchcal Film 5400.

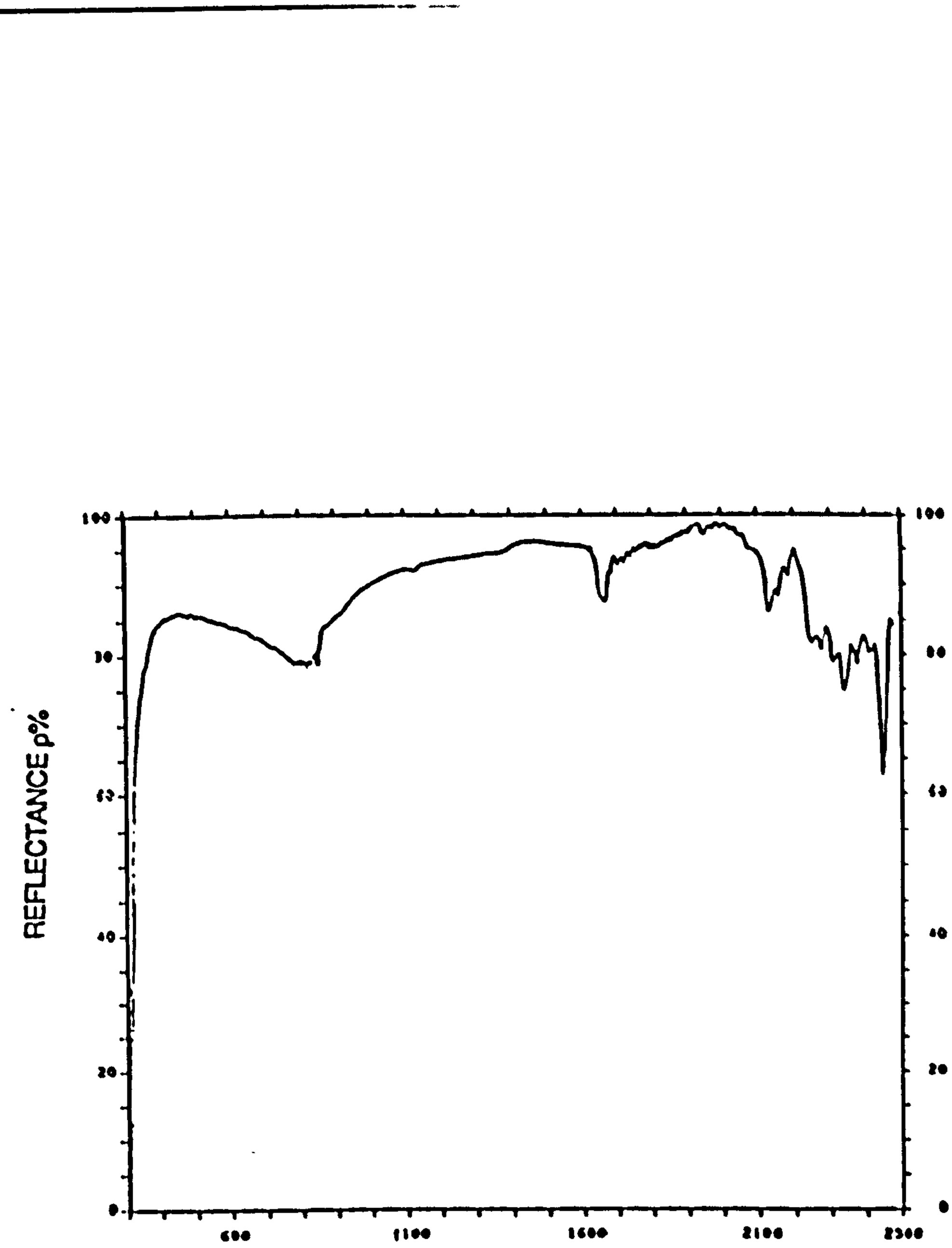

Fig. 3.4.13. Spectral reflectance of an as-received sample of 3M Scotchcal Film 530 for VIS and NIR radiation, $\rho = 86.3 \pm 0.08$.

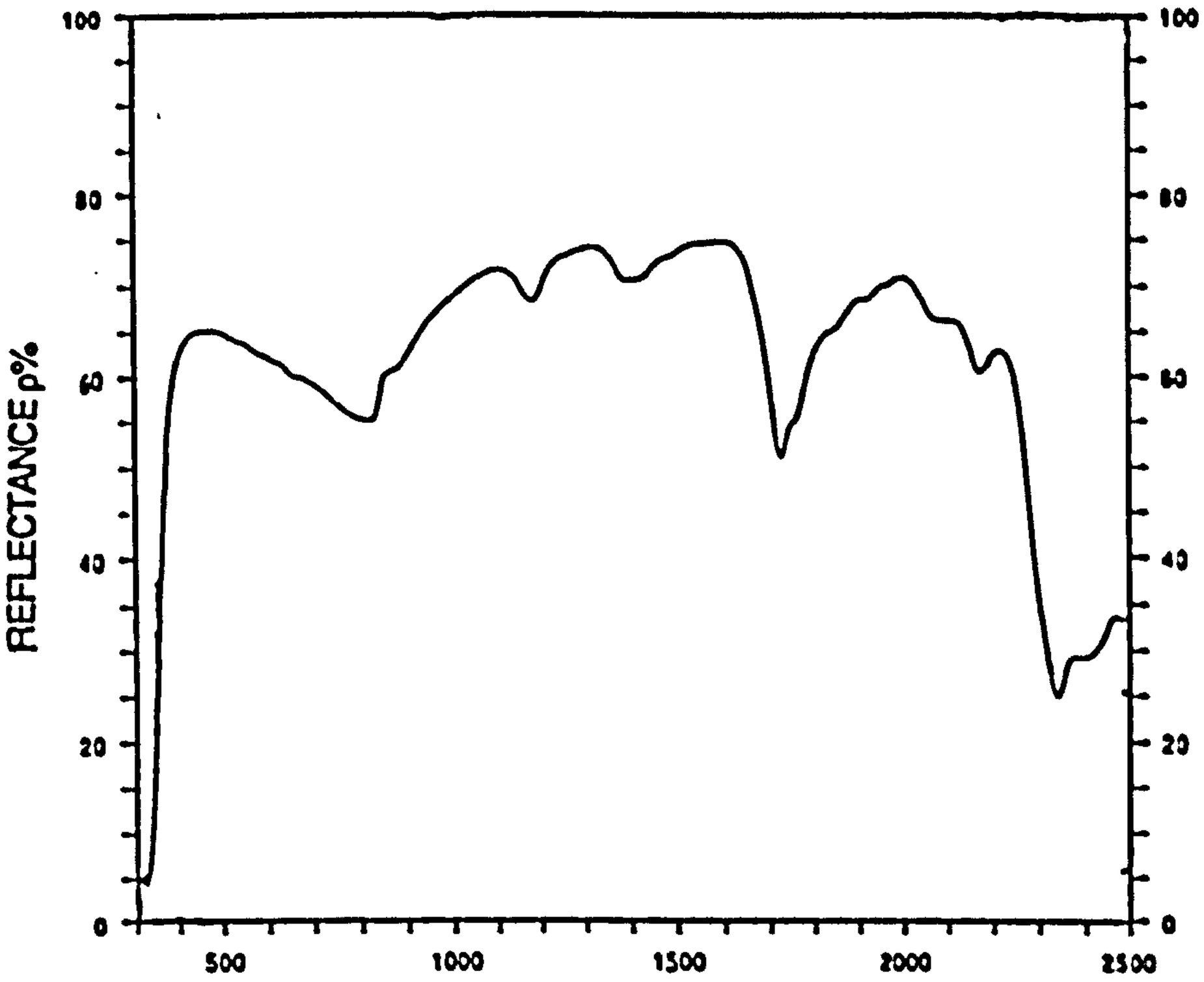

Fig. 3.4.14. Spectral reflectance of an as-received sample of 3M Scotchcal Film 680 for VIS and NIR radiation, $\rho = 51.5 \pm 0.09$.

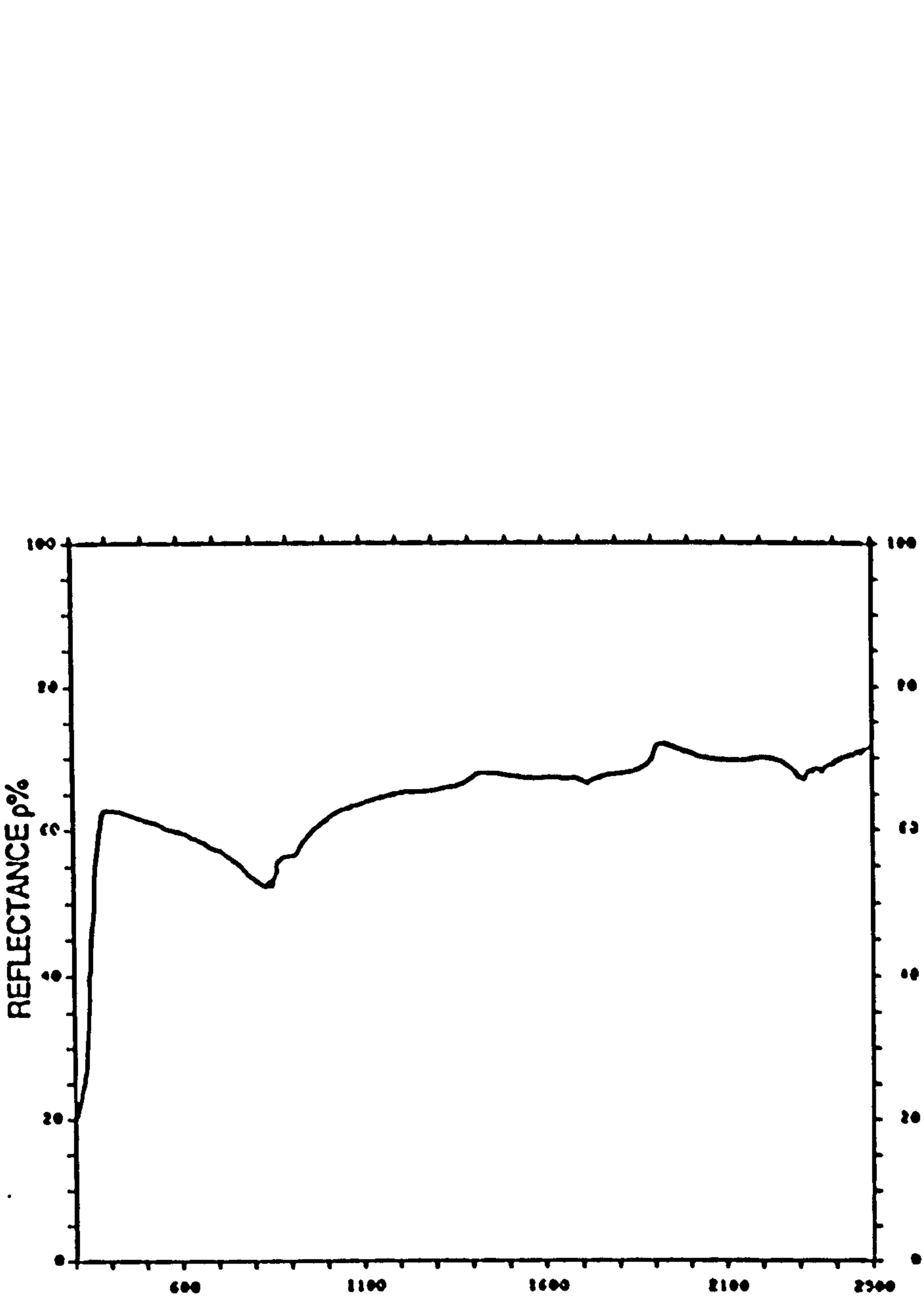

Fig. 3.4.15. Spectral reflectance of an as-received sample of 3M Scotchcal Film 3658 for VIS and NIR radiation, p = 60.6 ± 0.02.

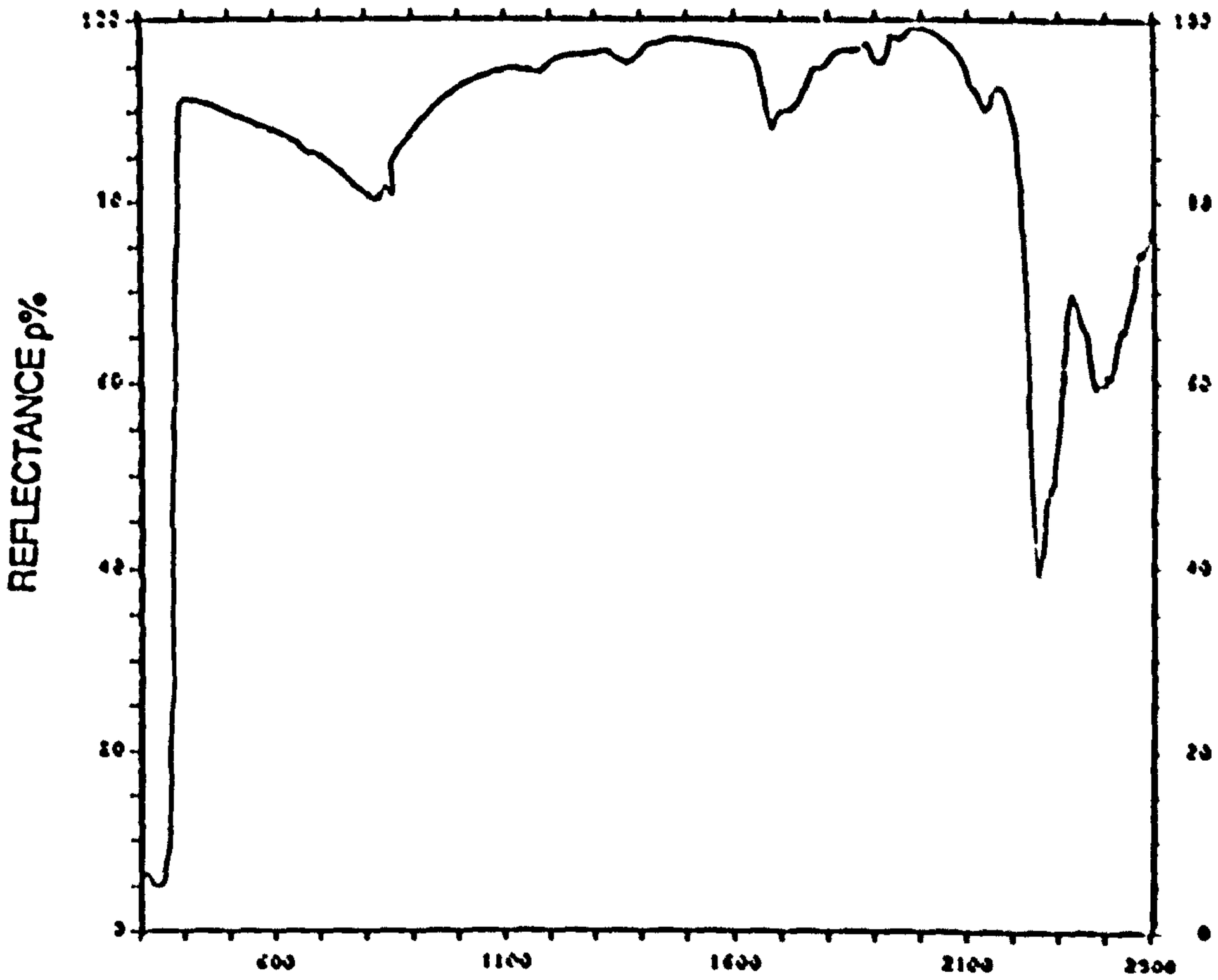

Fig. 3.4.16. Spectral reflectance of an as-received sample of 3M Scotchcal Film 5400 for VIS and NIR radiation, ρ = 86.8 ± 0.13.

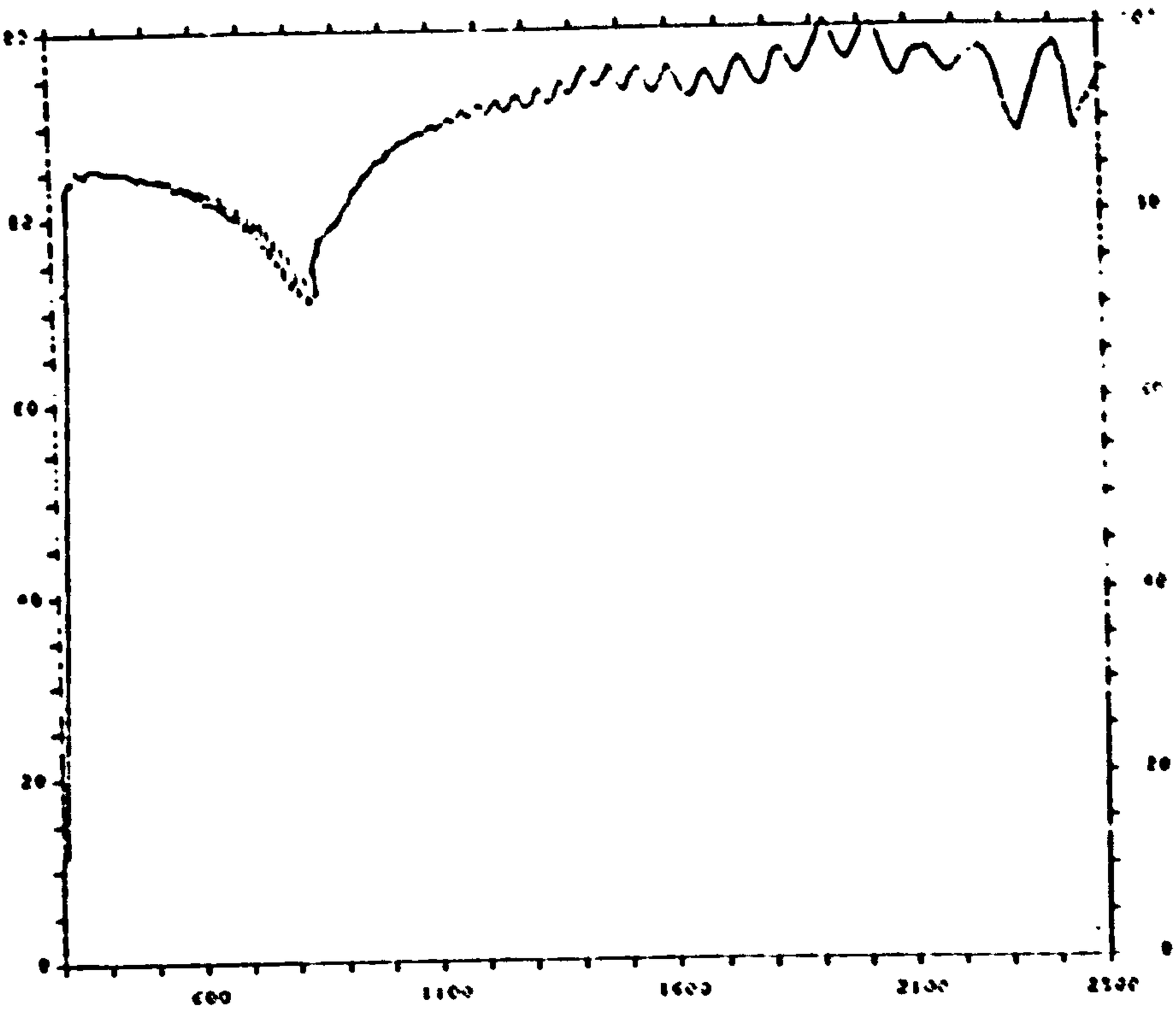

Fig. 3.4.17. Spectral reflectance of an as-received sample of aluminised plastic for VIS and NIR radiation, ρ = 85.0 ± 0.05.

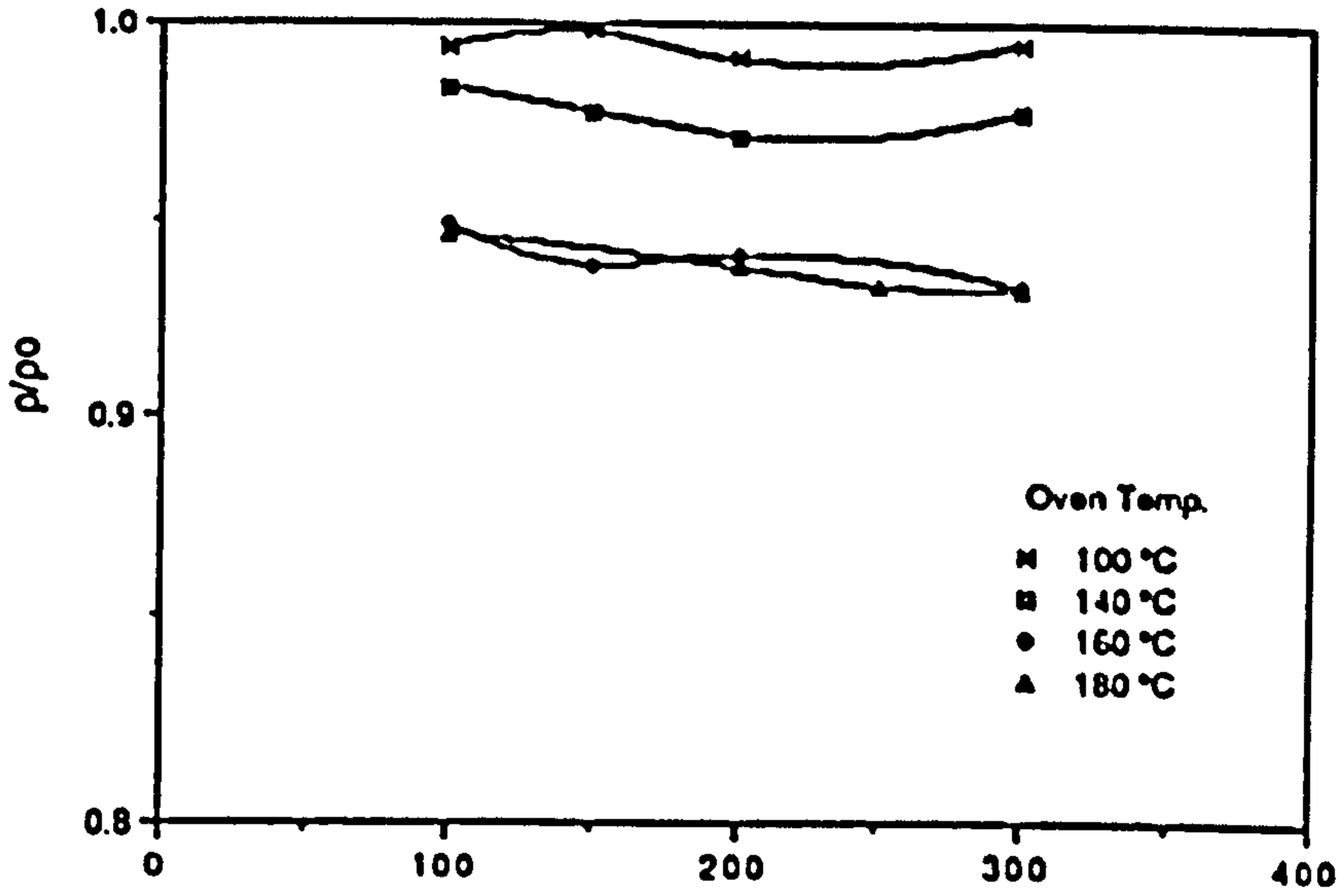

Fig. 3.4.18 Ratio of solar reflectance of aged samples (ρ) to solar reflectance of an as-received sample (ρ_o) of 3M Scotchcal Film 530, after various periods of ageing in air at elevated temperatures.

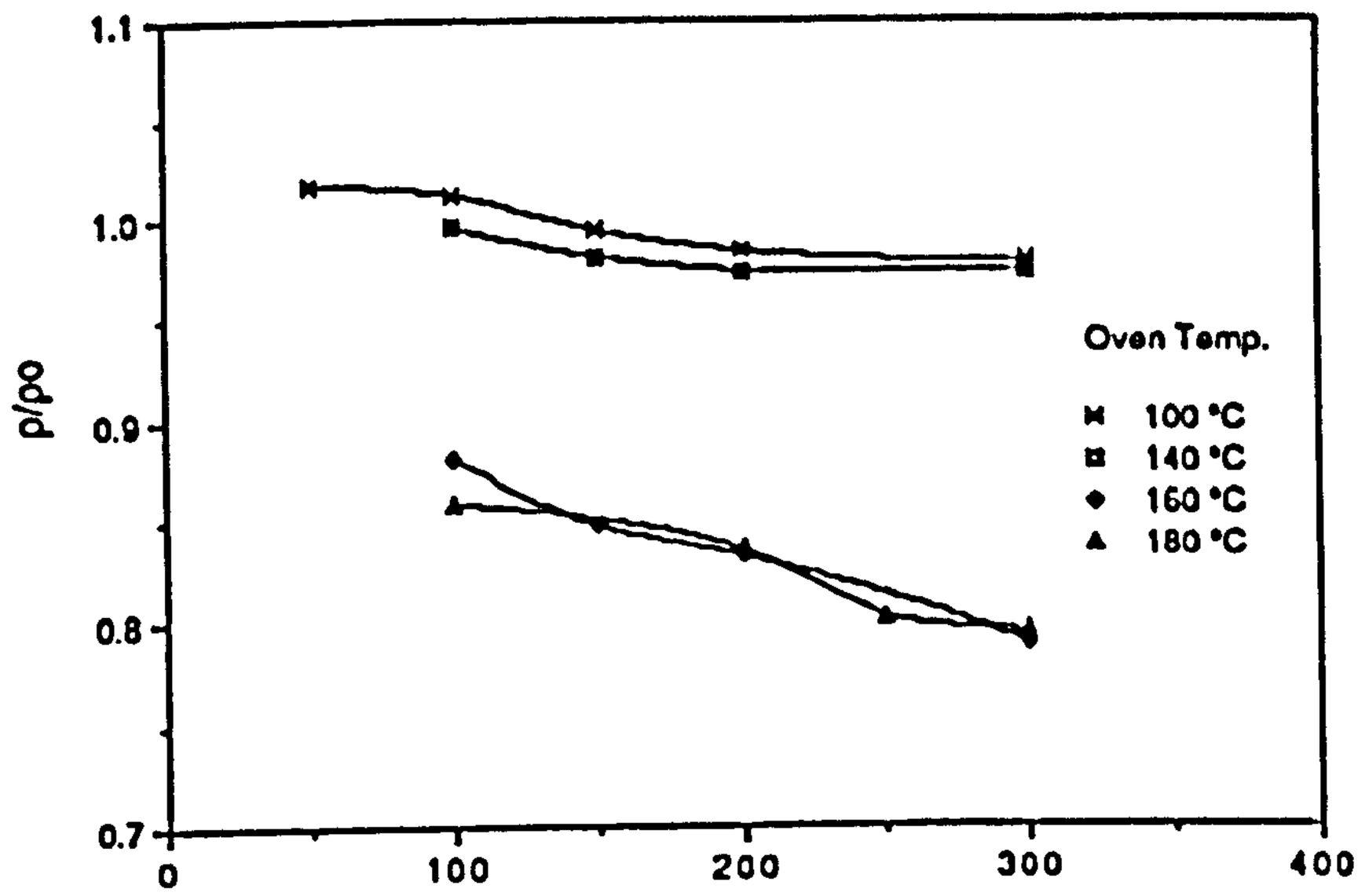

Fig. 3.4.19 Ratio of solar reflectance of aged samples (ρ) to solar reflectance of an as-received sample (ρ_o) of 3M Scotchcal Film 3658 after various periods of ageing in air at elevated temperatures.

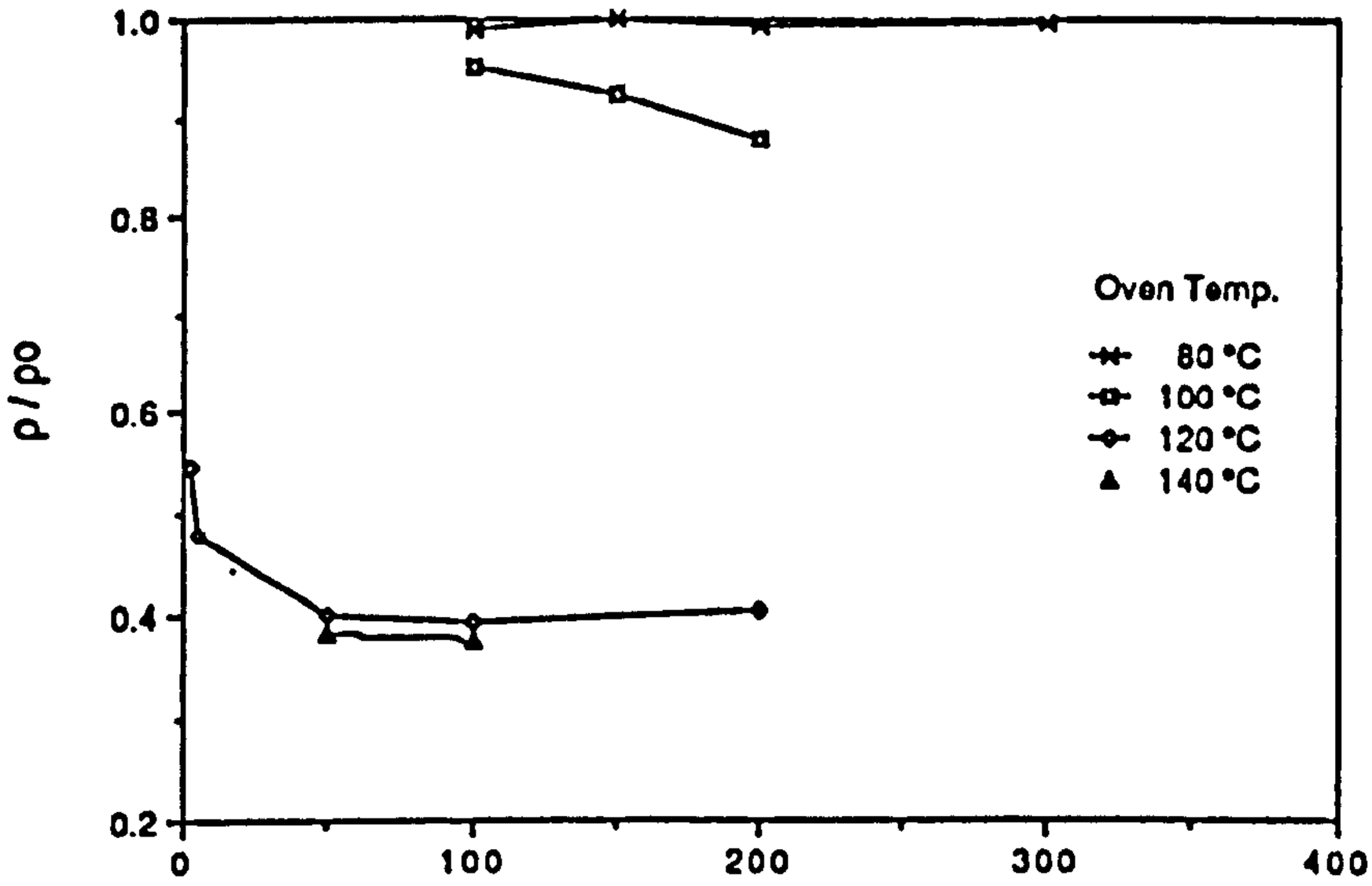

Fig. 3.4.20 Ratio of solar reflectance of aged samples (ρ) to solar reflectance of an as-received sample (ρ_o) of 3M Scotchcal Film 5400 after various periods of ageing in air at elevated temperatures.

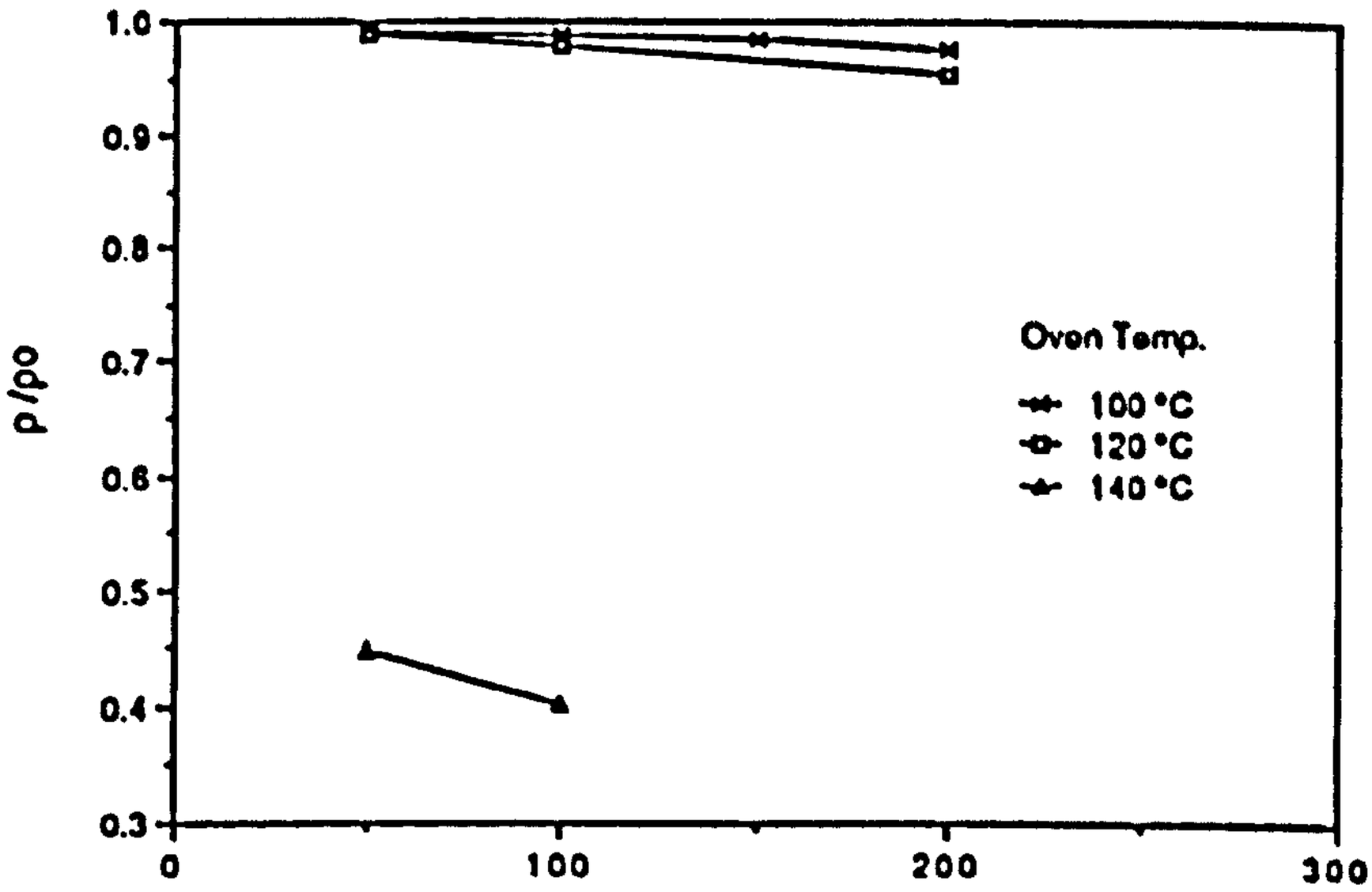

Fig. 3.4.21 Ratio of solar reflectance of aged samples (ρ) to solar reflectance of an as-received sample (ρ_o) of aluminised plastic after various periods of ageing in air at elevated temperatures.

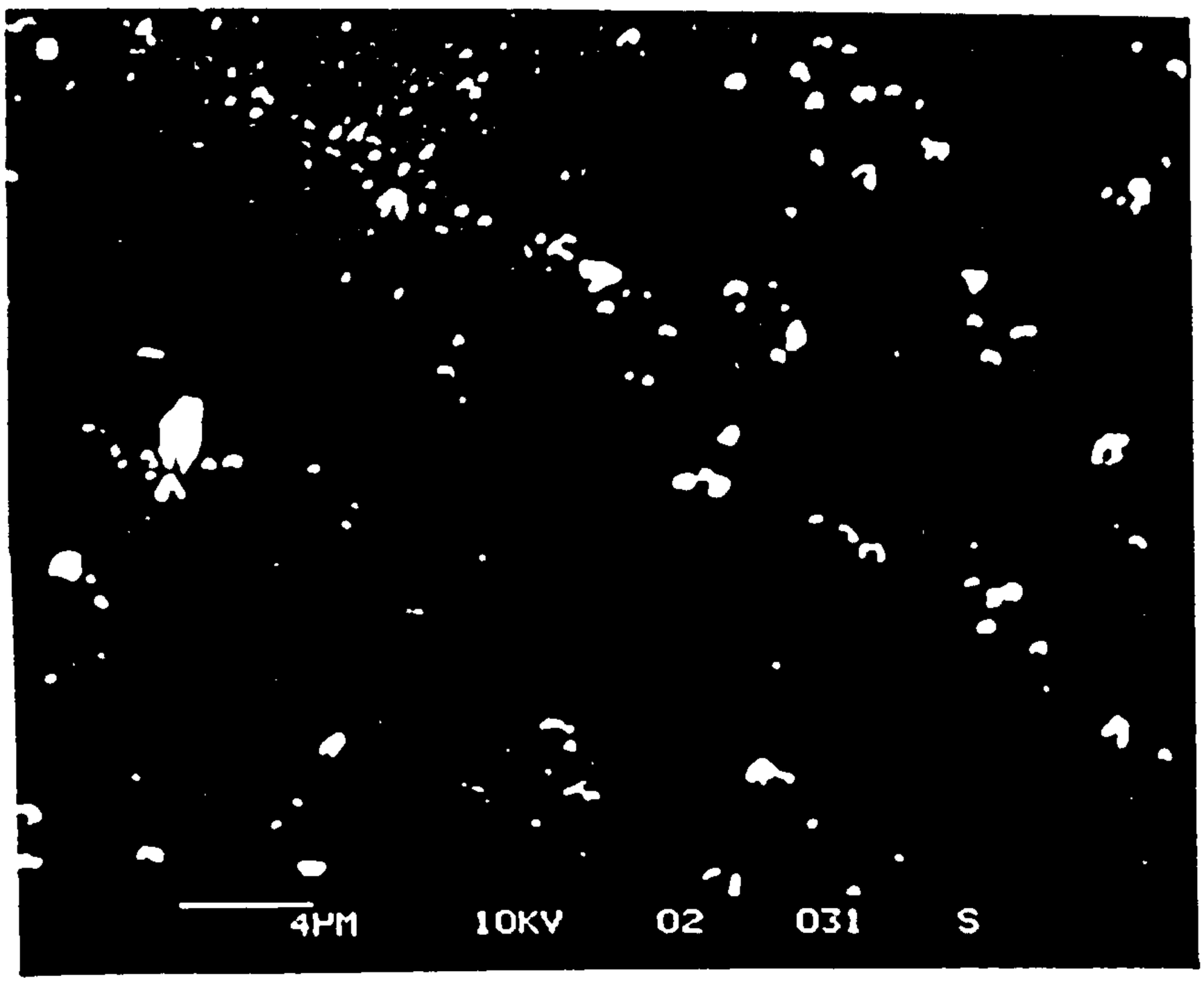

Fig. 3.4.22. Scanning electron micrograph of a sample of 3M Scotchcal Film 530 after 10 days of temperature and humidity cycling.

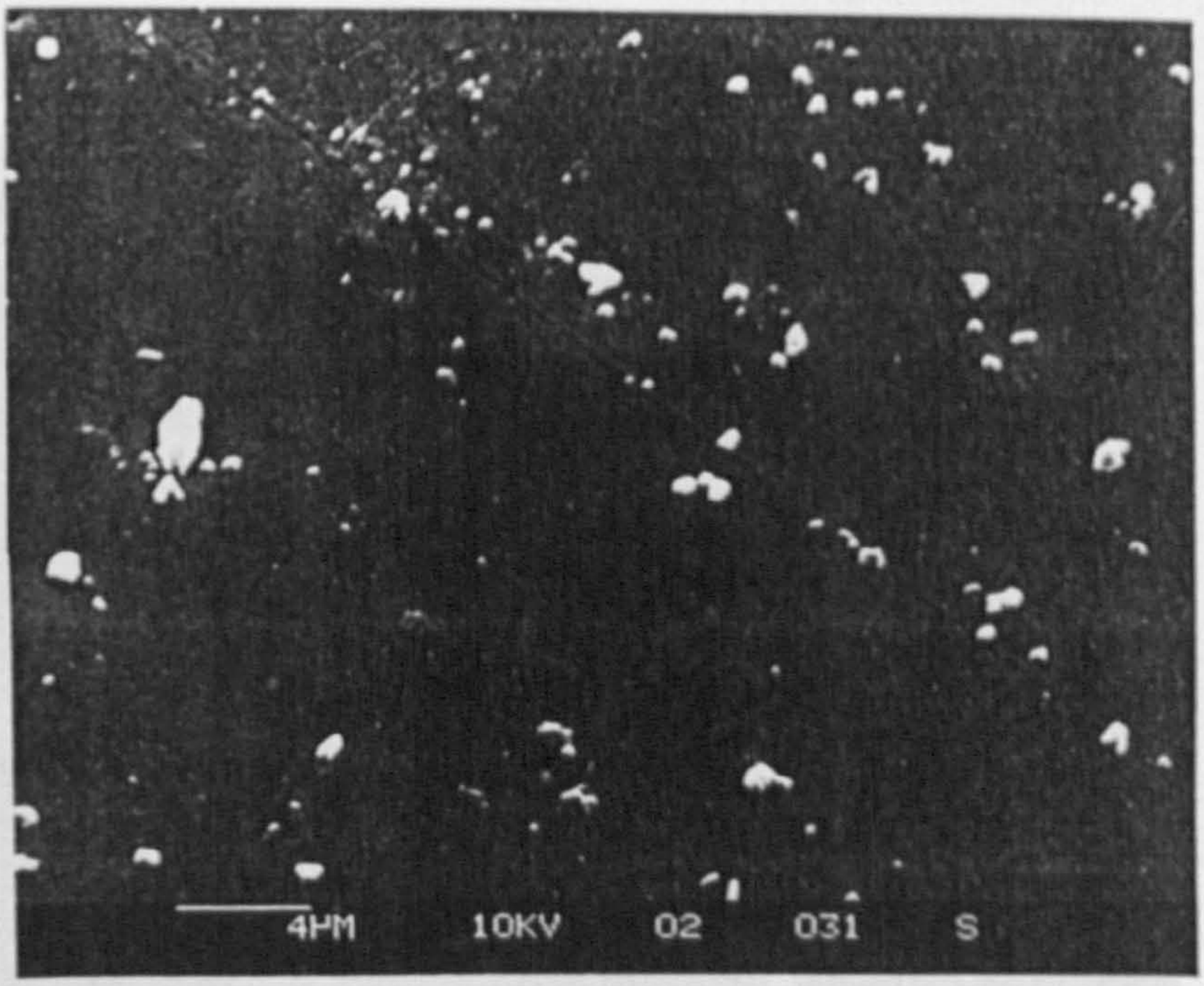

Fig. 3.4.22. Scanning electron micrograph of a sample of 3M Scotchcal Film 530 after 10 days of temperature and humidity cycling.

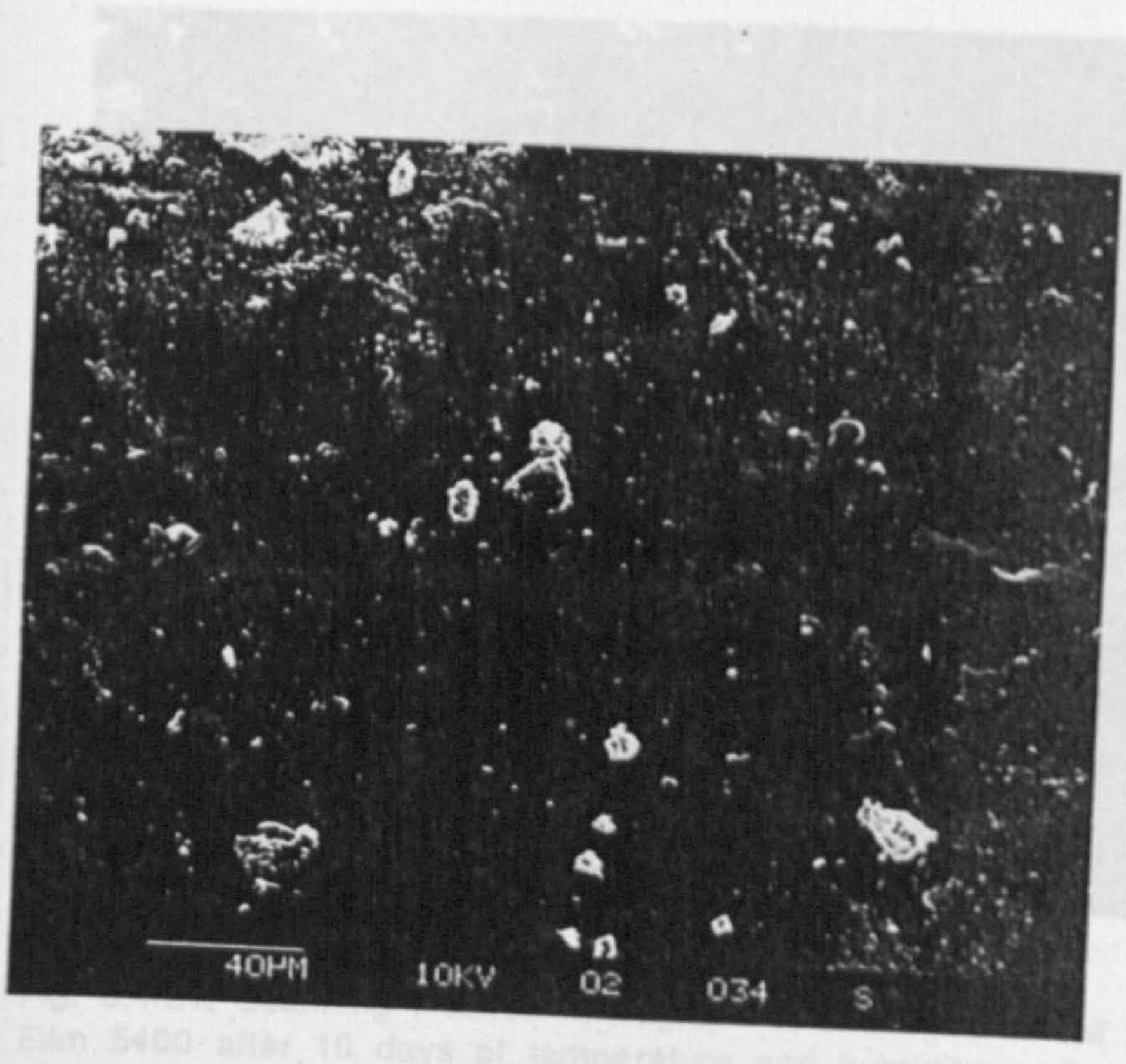

Fig. 3.4.23. Scanning electron micrograph of a sample of 3M Scotchcal Film 3658 after 10 days of temperature and humidity cycling.

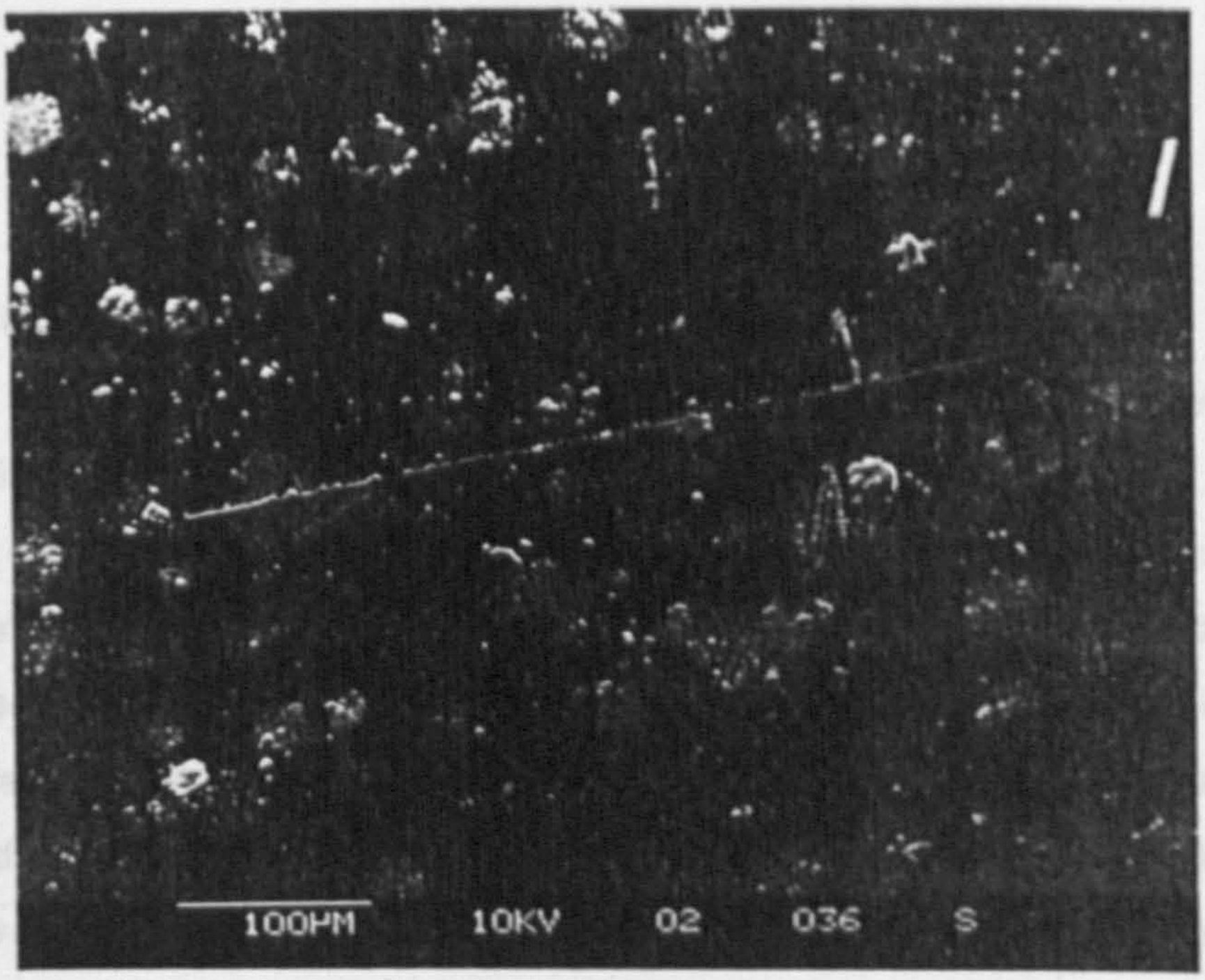

Fig. 3.4.24. Scanning electron micrograph of a sample of 3M Scotchcal Film 5400 after 10 days of temperature and humidity cycling.

CHAPTER FOUR

THEORETICAL ANALYSIS

4.1 INTRODUCTION

In this chapter a theoretical analysis for a tilted wick-type solar still is presented.

The basic principles of operation of solar stills have been stated and developed by many authors; e.g. Dunkle (1961) analysed and discussed the heat and mass transfer relationships in a conventional roof type solar still. He suggested the use of a reflector to increase the irradiation and hence the operating temperature of the still. That work was slightly modified by Morse and Read (1968), who considered the heat and mass transfer relationships in the unsteady state and expressed the various heat fluxes as functions of the cover temperature by obtaining a graphical solution and constructing a characteristic chart. Cooper (1973) examined the simultaneous energy transfer modes within a solar still envelope from a theoretical and experimental point-of-view over a wide range of operating conditions.

The above analyses are for basin type solar stills. They are independent of the inclination of the glass cover and spacing between the evaporative and condensing surfaces (cavity volume). Tiwari and Lawrence (1991) made an attempt to derive a new formula for the convective heat transfer coefficient in basin-type solar stills from the evaporating surface to the condensing surface including the influence of the inclination of the glass cover and the cavity volume. Some authors, have studied the performance relationships of wick-type solar stills, e.g. Yeh and Chen (1986) for a single-effect wick solar still and Tiwari *et al.* (1989) for the multi-effect solar still. (The multi-effect solar still is that in which the latent heat of evaporation of condensed water on a condensing surface can be used to increase the input heat of the next evaporating surface). Kiatsiriroat *et al.* (1987) studied the vertical wick-type solar still. They expressed the transient energy balance for the absorber and both covers in finite difference form to obtain the new temperature at the end of a specified time period.

Previous work on the inclined wick-type solar still does not appear to have included an analysis which takes into account the inclination angle of the still. This has been presented in this work. In addition, the transient analysis of the wick-type still considers (i) the absorber-cover spacing, (ii) input feed water and output brine energies, (iii) mass flow rate of the input water, (iv) heat capacity of the absorber support board and the glass cover and (v) the latent heat variation of water with the absorber temperature.

4.2 PRINCIPLES OF ENERGY FLOW IN A WICK-TYPE SOLAR STILL

The wick-type solar still used in this work is, briefly, an inclined, shallow box with a tray covered by a sheet of glass and insulated on the back and sides. A thin film of water flows through an absorber/evaporator cloth parallel to the cover where a film of condensation is created. This flows down the lower side of the cover to be collected. The still energy flow diagram is shown schematically in Fig. 4.2.1. From this figure, it can be seen that solar irradiance (S) is incident on the glass cover. Some of this is absorbed by the glass ($\alpha_{cov}S$) but the major portion (τS) passes through it and strikes the absorber/evaporator (charcoal) cloth. The amount of the incident radiation absorbed by the cloth, is equal to ($\alpha\tau S$). A portion of this energy is conducted away through the insulation (q_k). Some is carried away by the brine ($q_{w,out}$) and the rest is carried away from absorber/evaporator surface to the inner surface of the glass cover by three modes of heat transfer i.e. convection (q_c), evaporation (q_e) and radiation (q_r).

The glass cover conducts the energy from the inner surface to the outer one. This is then carried away to the surroundings by convection (q_{ca}) and radiation (q_{ra}). The thermal network of this system is shown in Fig. 4.2.2.

4.3 TRANSFER MODES INSIDE AND OUTSIDE A TILTED WICK-TYPE SOLAR STILL

In the analysis of the modes of the wick-type solar still operation the following assumptions have been made:

(1) The average absorber temperature is equal to the temperature of the water film flowing through the charcoal cloth.

(2) The temperature gradient perpendicular to and along the surface of the glass cover is negligible, i.e. it has a uniform temperature.

(3) There is no vapour leakage from the still.

(4) The condensation film on the glass cover is uniform and has small heat capacity which can be neglected

(5) The surface area of the evaporator/absorber surface and the glass cover are identical.

(6) All the distilled water is collected without leakage.

(7) Enhanced reflection of solar radiation due to dropwise condensation is negligible.

(8) The mass flow rate of the water is uniform through the charcoal cloth.

(9) The temperature of the absorber/evaporator surface is uniform.

4.3.1 Heat and mass transfer modes inside the still

The modes of heat exchange inside the still between the absorber/evaporator and the cover surfaces are heat radiation and convection accompanied by evaporative heat and mass transfer (in the form of water vapour) Kiatsiriroat *et al.* (1987).

4.3.1.1 Convective heat transfer mode inside the tilted wick-type solar still

This mode of heat exchange occurs between the absorber/evaporator and cover surfaces. It is entirely dependent on the temperature difference and the value of h_c. This is a function of the air vapour mixture properties. It must be obtained from empirical data, which is usually correlated using dimensionless equations of the Nusselt-Grashof type, (Howe and Tleimat (1977)).

An appropriate relationship for estimating h_c for the tilted wick-type solar still (as a rectangular inclined cavity) is the Nusselt number correlation as a function of Rayleigh number (Ra_H) and inclination angle (θ) which is reported by Hollands *et al.* (1976). It is expressed as:

$$Nu_H = 1 + 1.44\left[1 - \frac{1708}{Ra_H \cos\theta}\right]\left[1 - \frac{1708(\sin 1.8\theta)^{1.6}}{Ra_H \cos\theta}\right] + \left[\left(\frac{Ra_H \cos\theta}{5830}\right)^{1/3} - 1\right] \quad (0 < Ra_H < 10^5 \text{ and } \theta < 60^\circ) \qquad (4.3.1)$$

Nu_H has a maximum error (with respect to practical values) of about ±5% for $\theta \leq 60°$ and up to ±10% for θ in the range 60° to 75°. Also, the convection heat transfer coefficient between two parallel plates separated by a distance H, is related to the Nusselt number which is defined in the usual form as:

$$Nu_H = \frac{h_c H}{k_a} \qquad \text{Kamaraj } et\ al. \text{ (1980)} \qquad (4.3.2)$$

Where, the Rayleigh number is expressed as:

$$Ra_H = \frac{g\beta H^3 \Delta T}{\alpha_a \nu_a} \qquad (4.3.3)$$

and the diffusivity (α_a) is expressed as

$$\alpha_a = \frac{k_a}{\rho_a C_{p,a}} \qquad (4.3.4)$$

Here,

θ is the inclination angle (degree),

ρ_a is the air density (kg/m^3),

ν_a is the air kinematic viscosity (m^2/s),

$C_{p,a}$ is the air specific heat (J/kg.K),

and

k_a is the air thermal conductivity (W/m.K).

The notation $[\ ]^{\cdot}$ implies that, if the quantity in brackets is negative, it must be set equal to zero, Incropera and De Witt (1985).

In solar stills (ΔT) is the effective temperature difference between the evaporation and condensation surfaces. This has been expressed as:

$$\Delta T = T_{abs} - T_{cov} + \frac{(P_{abs} - P_{cov})(T_{abs} + 273.15)}{268900 - P_{abs}} \qquad (4.3.5)$$

Dunkle (1961) and Tiwari and Lawrence (1991).

Where the water vapour pressure at the absorber temperature is

$$P_{abs} = 10^{\left[0.622 + 7.5\,(T_{abs} - 273.15)/(T_{abs} - 35.0)\right]}, \text{ (here in mm Hg)} \qquad (4.3.6)$$

while at the cover temperature it is

$$P_{cov} = 10^{\left[0.622 + 7.5\,(T_{cov} - 273.15)/(T_{cov} - 35.0)\right]}, \text{ (here in mm Hg)} \qquad (4.3.7)$$

Yeh and Chen (1986).

Therefore, the convection heat transfer rate from the absorber cloth to the inner surface of the glass cover can be expressed as:

$$q_c = h_c (T_{abs} - T_{cov}) \qquad (4.3.8)$$

4.3.1.2. Evaporative mass transfer mode inside the tilted wick-type solar still

Evaporative mass transfer accompanies the heat convection in the form of water vapour. The amount of water transferred from the water surface to the condensate film on the cover can be estimated in terms of the analogy between heat and mass transfer. Accordingly, the mass flow rate is proportional to the heat transfer coefficient and the driving potential. The latter is the difference in

partial pressures of the material being transferred Howe and Tleimat in Sayigh (1977). The algebraic formulation of the corresponding rate of heat flux is:

$$q_e = 0.016\, h_c (P_{abs} - P_{cov}) \qquad (4.3.9)$$

Where

$$q_e = h_e (T_{abs} - T_{cov}) \qquad (4.3.10)$$

and

$$h_e = 0.016\, h_c \frac{P_{abs} - P_{cov}}{T_{abs} - T_{cov}}, \qquad (4.3.11)$$

Tiwari *et al.* (1988) and Tiwari *et al.* (1989)

This is related to the amount of the condensation on the inner surface of the glass cover by the expression:

$$q_e = \frac{D h_{fg}}{3600} \qquad (4.3.12)$$

where h_{fg} is the latent heat of evaporation of the water and D is the distillate production rate. h_{fg} is expressed as a function of water temperature as :

$$h_{fg} = 10^3 (2501.67 - 2.389\, T_{abs}) \qquad (4.3.13)$$

where T_{abs} is in °C and h_{fg} is in (J//kg), Elsayed (1983)

4.3.1.3 Radiative heat transfer mode

Radiative heat transfer inside the wick-type solar still, between the glass cover and the absorber/evaporator surfaces is considered as that between two infinite parallel plates. With

assumptions of diffuse and gray surfaces and that the aspect ratio is sufficiently large to neglect edge effects, it is given per unit area as:

$$q_r = \frac{\sigma(T_{abs}^4 - T_{cov}^4)}{\frac{1}{\varepsilon_{cov}} + \frac{1}{\varepsilon_{abs}} - 1} \qquad (4.3.14)$$

(Charters, in Sayigh (1977)), where σ is Stefan-Boltzmann's constant (5.6697×10^{-8} W/m^{2}K^4). The measured value of ε_{abs} of the charcoal cloth is equal to 0.98. For simplicity it can be approximated to unity. Hence equation (4.3.14) becomes:

$$q_r = \varepsilon_{cov}\sigma(T_{abs}^4 - T_{cov}^4) \qquad (4.3.15)$$

and hence the radiative heat transfer coefficient from the absorber/evaporator to the glass cover can be expressed as:

$$h_r = \varepsilon_{cov}\sigma(T_{abs}^2 + T_{cov}^2)(T_{abs} + T_{cov}) \qquad (4.3.16)$$

4.3.2 Heat transfer modes outside the still

Outside flat tilted solar stills, the heat is transferred to the surroundings by radiation and convection from the glass cover and the back and sides of the solar still (neglecting conduction through the still support structure). The convection heat transfer coefficient is assumed to be a function of wind speed only and is expressed as :

$$h_{ca} = 5.7 + 3.8V \qquad (4.3.17)$$

Duffie and Beckman (1980), where V is the wind speed in (m/s). Hence, the convective heat losses can be expressed as:

$$q_{ca} = h_{ca}(T_{cov} - T_{amb}) \qquad (4.3.18)$$

where T_{amb} is equal to the air temperature.

The radiative heat transfer is a function of the cover temperature and sky temperature. The sky temperature is assumed to be a function of ambient temperature, Duffie and Beckman (1980), and expressed as:

$$T_{sky} = 0.0552 T_{amb}^{1.5} \text{ ; (Temperatures are in degrees Kelvin)} \qquad (4.3.19)$$

Therefore, the radiative heat losses can be expressed as:

$$q_{ra} = \varepsilon_{cov}\sigma (T_{cov}^4 - T_{sky}^4) \qquad (4.3.20)$$

and hence the radiative heat transfer coefficient from the glass cover to the surroundings in a form of long wave radiation can be express as:

$$h_{ra} = \frac{\varepsilon_{cov}\sigma (T_{cov}^4 - T_{sky}^4)}{T_{cov} - T_{amb}} \qquad (4.3.21)$$

4.4 ENERGY BALANCE EQUATIONS

4.4.1 Energy balance on the absorber/evaporator surface

At the absorber/evaporator surface, the energy is transferred to the glass cover by convection, evaporation and radiation. Thus, the energy input into and output from the surface in a given time can be written as:

energy input = solar energy absorbed by the absorber + energy of the input water (4.4.1)

energy output = energy of evaporation of water from the evaporating surface + radiant energy loss to the glass cover + convection energy loss to the glass cover + conduction energy loss to the back of the still + energy of output brine (4.4.2)

Hence, the energy balance expressions can be written as:

energy in - energy out = increase of energy of the absorber/evaporator (4.4.3)

i.e. for a unit time interval and unit absorber area

$$\alpha\tau S + q_{w,in} - (q_c + q_e + q_r + q_k + q_{w,out}) = \left(\frac{mC_p}{A}\right)_{abs} \frac{dT_{abs}}{dt} \qquad (4.4.4)$$

where

$$q_{w,in} = m'C_{p,w}(T_{w,in} - T_{cov}) \qquad (4.4.5)$$

$$q_k = h_b(T_{abs} - T_{amb}) \qquad (4.4.6)$$

and

$$q_{w,out} = (m' - D)\, C_{p,w}(T_{abs} - T_{cov}) \qquad (4.4.7)$$

Here, T_{cov} is considered as a reference temperature in which $q_{w,in}$, $q_{w,out}$ and q_D are expressed. This gives:

$$q_D = DC_{p,w}(T_{cov} - T_{cow}) = 0 \text{ , Yeh and Chen (1986)} \qquad (4.4.8)$$

h_b is considered as the resistance of heat flow through the absorber wick support (masterclad) and the two layers of insulation (polystyrene and styrofoam)

i.e.

$$\frac{1}{h_b} = \frac{L_{i1}}{k_{i1}} + \frac{L_{i2}}{k_{i2}} + \frac{L_{i3}}{k_{i3}} + \frac{1}{h_i} \qquad (4.4.9)$$

where

L_{i1}, k_{i1} are the thickness and thermal conductivity of the masterclad respectively.

L_{i2}, k_{i2} are the thickness and thermal conductivity of the polystyrene respectively.

L_{i3}, k_{i3} are the thickness and thermal conductivity of the styrofoam respectively.

4.4.2 Energy balance on the glass cover

The energy incident on and leaving the glass cover can be written as :

energy input = solar radiation absorbed by the glass cover + energy input by (convection + evaporation + radiation) from the absorber/evaporator surface (4.4.10)

energy output = energy loss from the glass cover by convection and radiation to the environment + energy loss of distillate. (4.4.11)

Therefore,

energy input - energy output = increase of energy stored in the glass cover (4.4.12)

i.e.

$$(q_c + q_e + q_r) + \alpha_{cov} S - (q_{ca} + q_{ra}) - q_D = \left(\frac{mC_p}{A}\right)_{cov} \frac{dT_{cov}}{dt} \quad (4.4.13)$$

4.5 SOLVING OF THE TRANSIENT ENERGY EQUATIONS

The transient energy balance equations (4.4.4) and (4.4.13) for the absorbing/evaporating cloth and the transparent cover can be respectively, rewritten as:

$$\frac{dT_{abs}}{dt} = \left(\frac{A}{mC_p}\right)_{abs}\left[\alpha\tau S + q_{w,in} - (q_c + q_e + q_r + q_k + q_{w,out})\right] \quad (4.5.1)$$

$$\frac{dT_{cov}}{dt} = \left(\frac{A}{mC_p}\right)_{cov}\left[\alpha_{cov}S + (q_c + q_e + q_r) - (q_{ca} + q_{ra})\right] \quad (4.5.2)$$

These equations can be rewritten in finite difference form to obtain the new temperatures $\dot{T}_{abs}$ and $\dot{T}_{cov}$ at the end of a specified increment of time Δt, as:

$$\frac{dT_{abs}}{dt} = \frac{(\dot{T}_{abs} - T_{abs})}{\Delta t} \quad (4.5.3)$$

similarly,

$$\frac{dT_{cov}}{dt} = \frac{(\dot{T}_{cov} - T_{cov})}{\Delta t} \quad (4.5.4)$$

Therefore, the new expressions become:

$$\dot{T}_{abs} = T_{abs} + \Delta t\left(\frac{A}{mC_p}\right)_{abs}\left[\alpha\tau S + m'C_{p,w}(T_{w,in} - T_{cov}) - h_1(T_{abs} - T_{cov}) - h_b(T_{abs} - T_{amb}) - (m'-D)C_{p,w}(T_{abs} - T_{cov})\right] \quad (4.5.5)$$

$$\dot{T}_{cov} = T_{cov} + \Delta t\left(\frac{A}{mC_p}\right)_{cov}\left[\alpha_{cov}S + h_1(T_{abs} - T_{cov}) - h_2(T_{cov} - T_{amb})\right] \quad (4.5.6)$$

where,

$$h_1 = h_c + h_e + h_r \quad (4.5.7)$$

and

$$h_2 = h_{ca} + h_{ra} \quad (4.5.8)$$

4.6 NUMERICAL ANALYSIS

4.6.1 Computer simulation of the tilted wick-type solar still

In order to use the analytical model of the previous sections, a computer program (Appendix A7) was developed to solve equations (4.5.5) and (4.5.6) to calculate the absorber and cover temperatures and then the other related parameters after time interval Δt. The time interval Δt was chosen to be 0.01 hour to avoid unstable solutions. The sequence steps of the computer program are illustrated in a flow-chart which is shown in Fig. 4.6.1. It indicates, briefly, the operations and their functions.

Hence, from the measured initial values of the absorber and cover temperatures, and by giving the hourly averages of solar irradiance, in the plane of the glass cover, and ambient temperature for each hour of the day, the performance factors of the wick-type solar still can be predicted.

The calculations were started after giving the initial conditions, by obtaining the partial vapour pressures at the given absorber and cover temperatures according to equations (4.3.6) and (4.3.7) respectively. From these the effective temperature difference was calculated as in equation (4.3.5). Having calculated this factor Rayleigh and Nusselt numbers can be calculated, from which the

internal coefficients of convective heat transfer, and hence, the evaporative one can be determined with the other heat coefficients and parameters.

The new absorber and cover temperatures, after the increment of time, can be calculated. These would be considered as initial values for the next increment.

From the calculation of the instantaneous distillate production rate the hourly and daily averages of the productivity and the efficiency can be determined.

4.6.2 Predicted results and their discussion

By applying the transient model and a finite difference technique, numerical calculations were carried out for various still performance parameters based on realistic data of solar insolation incident on the glass cover and ambient temperature of a typical summer day (25/7/1990) at the experimental site. These calculations show variations of the still performance and the heat transfer coefficients with time of the day, input water flow rate, wind speed and still cover transmittance in addition to the absorber-cover distance.

To carry out the calculations various relevant material properties have been used. They are shown in Table 4.6.1. The thermodynamic properties for thermal diffusivity (α_a), kinematic viscosity (ν_a) and density (ρ_a) of humid air have been given absolute values. Their variations with temperature (in the range 50°C - 70°C) did not significantly influence the predicted performance of the solar

still (less than 0.02%). Therefore, absolute values have been considered with an average temperature of 60°C as shown in Table 4.6.1.

Figures (4.6.2) and (4.6.3) show the predicted variations of the daily and hourly (11.00 - 12.00) still efficiencies with wind speed. It can be seen that the wind speed up to (4 m/s) only marginally affects the efficiency, particularly, when the input water flow rate is within the range (3 - 4) kg/m^2.h. This is in agreement with Lof (1980) and the experimental paper by Yeh and Chen (1986). This range of flow rates has been adopted and applied experimentally in this work. Therefore, to predict other variations of other parameters (2 m/s) the average wind speed has been chosen as shown in Figs. 4.6.4 - 4.6.14.

The flow rate of the input saline water into a wick-type solar still has been seen as an important parameter in the performance of inclined solar stills, as shown in Figs. 4.6.3 - 4.6.6 and Table 4.6.2. This was validated by the experimental part of this work as in Table 3.3.1. It has to be sufficient to keep the evaporator wet and to avoid creating dry spots and salts accumulation. In Fig. 4.6.4 the daily efficiency of the wick-type solar still is related to the input water mass flow rate according to the following equations:

$$\eta\% = 68.06 \times 10^{-0.0355m'} \quad \text{when } \tau = 0.90 \qquad (4.6.1)$$

$$\eta\% = 64.29 \times 10^{-0.0360m'} \quad \text{when } \tau = 0.86 \qquad (4.6.2)$$

$$\eta\% = 58.70 \times 10^{-0.0367m'} \quad \text{when } \tau = 0.80 \qquad (4.6.3)$$

$$\eta\% = 49.59 \times 10^{-0.0378m'} \quad \text{when } \tau = 0.70 \qquad (4.6.4)$$

Unfortunately, there is a lack of literature in which the input water flow rate has been taken into account. In Tiwari *et al.* (1989) and Yeh and Chen (1986) it has been considered as a variable and given certain rather low values. It was taken as 1 kg/m^2.h in the former and 0.86 kg/m^2.h in the latter paper. Such small a flow rate, which has to be uniform along the evaporator/absorber surface, is very difficult to maintain unless using high precision flow controllers.

Fig. 4.6.5 shows the predicted effect of the glass cover-absorber distance on the daily efficiency of the wick-type solar still This is for various input mass flow rate. The maximum efficiency can be seen when the separation is in the range of (20 - 25) mm.

Figs. 4.6.6 and 4.6.7 show the effect of the inclination angle of the still on its daily efficiency and the internal convective (h_c), evaporative (h_e) and radiative (h_r) heat transfer coefficients. It can be seen that the efficiency decreases as the inclination angle increases, but this is appreciable only when the angle is more than 50°. The same trend of behavior is seen for (h_e), but (h_r) and (h_c) are little affected by angle.

Figs. 4.6.8 and 4.6.9 show the effect of the cover transmittance on the daily and hourly efficiencies of the still. It is clear that the efficiencies are functions of the cover transmittance. Variations of the absorber and cover temperatures and their differences are shown in Figs. 4.6.10 and 4.6.11. They vary as the solar insolation varies through the hours of the day. The heat transfer

coefficients vary with time due to the variation in absorber and cover temperatures with time. These are shown in Fig. 4.6.12. From this figure it can be seen that the highest coefficient is the evaporative coefficient. The productivity and hence the hourly efficiency have the same trend of behavior as the evaporative coefficient as shown in Figs. 4.6.13 and 4.6.9. Fig. 4.6.14 shows that the productivity is a linear function of the absorber temperature. It varies with absorber temperature (T_{abs}) according to the following equation:

$$D = -0.95 + 0.026\, T_{abs} \qquad (4.6.5)$$

Table 4.6.1. Solar still material properties used for the numerical calculations.

$A_{(glass)}$	= 0.533 m^2	$A_{(masterclad)}$	= 0.475 m^2
$C_{p(glass)}$	= 750 J/kg.K	$C_{p(masterclad)}$	= 900 J/kg.K
$\alpha_{(glass)}$	= 0.05	$\rho_{(masterclad)}$	= 1500 kg/m^3
$\rho_{(glass)}$	= 2500 kg/m^3	$\alpha_{charcoal\ cloth}$	= 0.98
k_a	= 0.029 W/m.K	$C_{p.a}$	= 1006.9 J/kg.K
μ_a	= 1.998 x 10^{-5} kg/ms	ρ_a	= 1.0614 kg/m^3
ν_a	= 1.887 x 10^{-5} m^2/s	$C_{p.w}$	= 4186.8 J/kg.K
h_l	= 20.0 W/m^2.K	ρ_{water}	= 1000 kg/m^3
$k_{i1(masterclad)}$	= 0.29 W/m.K	$L_{i1(masterclad)}$	= 0.009 m
$k_{i2(polystyrene)}$	= 0.034 W/m.K	$L_{i2(polystyrene)}$	= 0.0125 m
$k_{i3(styrofoam)}$	= 0.039 W/m.K	$L_{i3(styrofoam)}$	= 0.035 m

Tabel 4.6.2. Predicted variation of the absorber and cover temperatures around noon (Tabs,Tcov) with input saline water flow rate of the wick-type solar still on 25/7/1990. Solar insolation = 3353.3 kJ/m^2.h, ambient temp. = 24.1°C.

Input Flow Rate kg/m^2.h	Cover Trans. 0.80		Cover Trans. 0.86	
	Tabs °C	Tcov °C	Tabs °C	Tcov °C
1	68.1	55.1	70.4	57.6
2	66	52.9	68.2	55.3
3	64.1	50.9	66.1	53.2
4	62.2	49.1	64.4	51.3
5	60.6	47.5	62.6	49.5
6	58.9	45.9	61	47.9
8	56.1	43.3	58.1	45.1
10	53.6	41.1	55.5	43.5
12	51.4	39.2	53.2	40.7

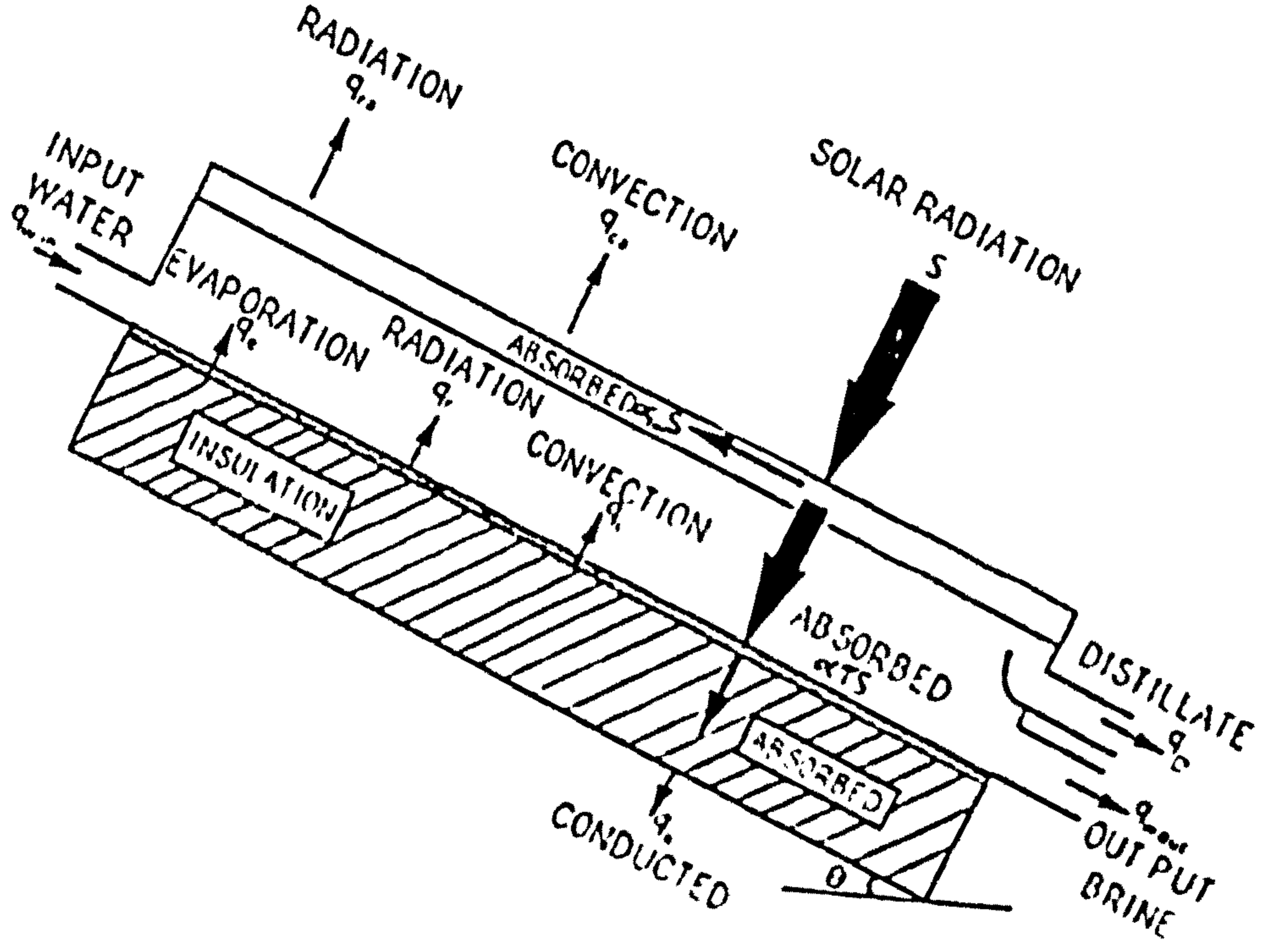

Fig. 4.2.1. Energy flow rates for a tilted wick-type solar still.

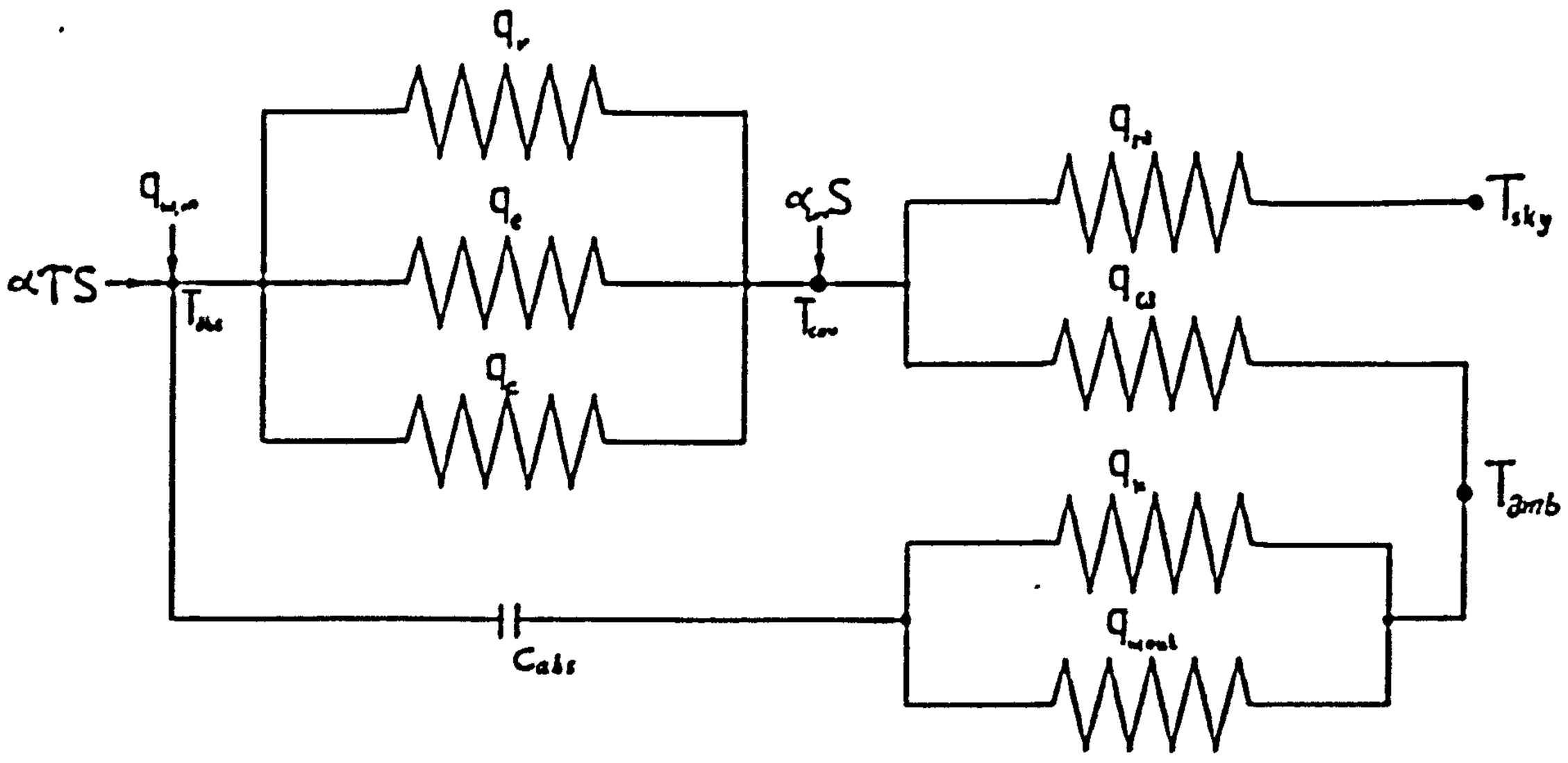

Fig. 4.2.2. Thermal network for the wick-type solar still.

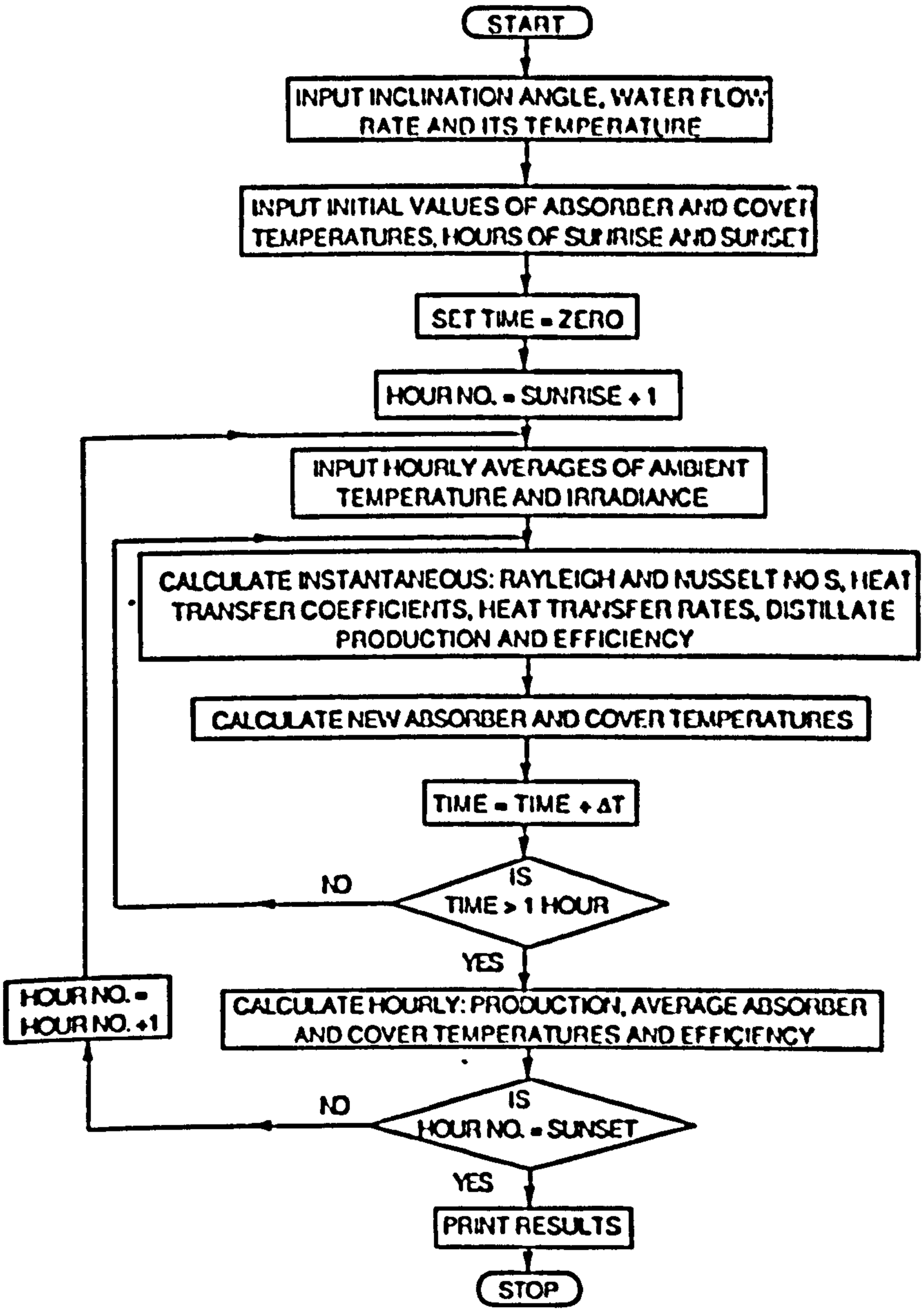

Fig. 4.6.1. The flowchart of the computation program.

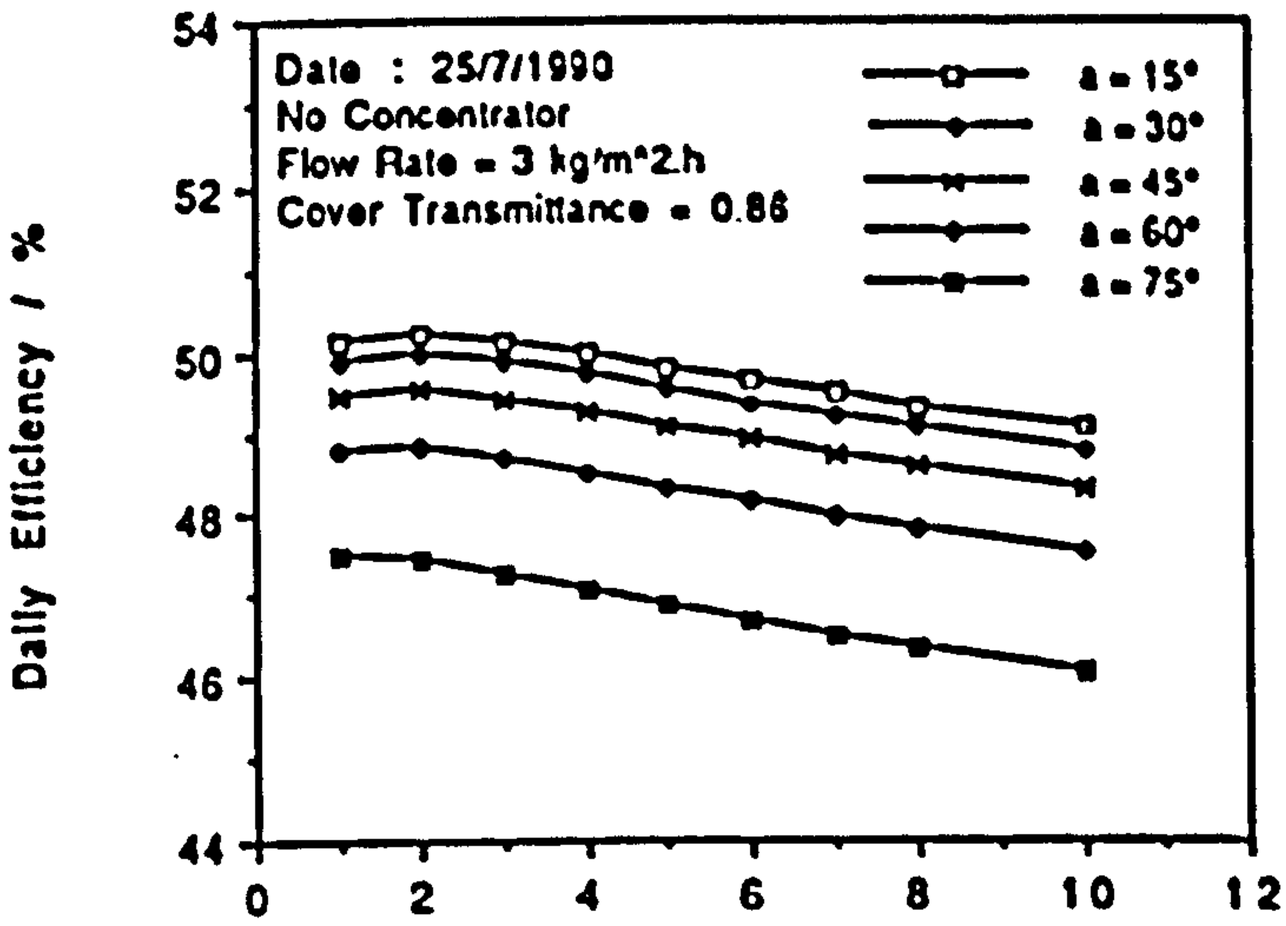

Fig. 4.6.2. Predicted variation of the daily still efficiency with wind speed for various inclination angles.

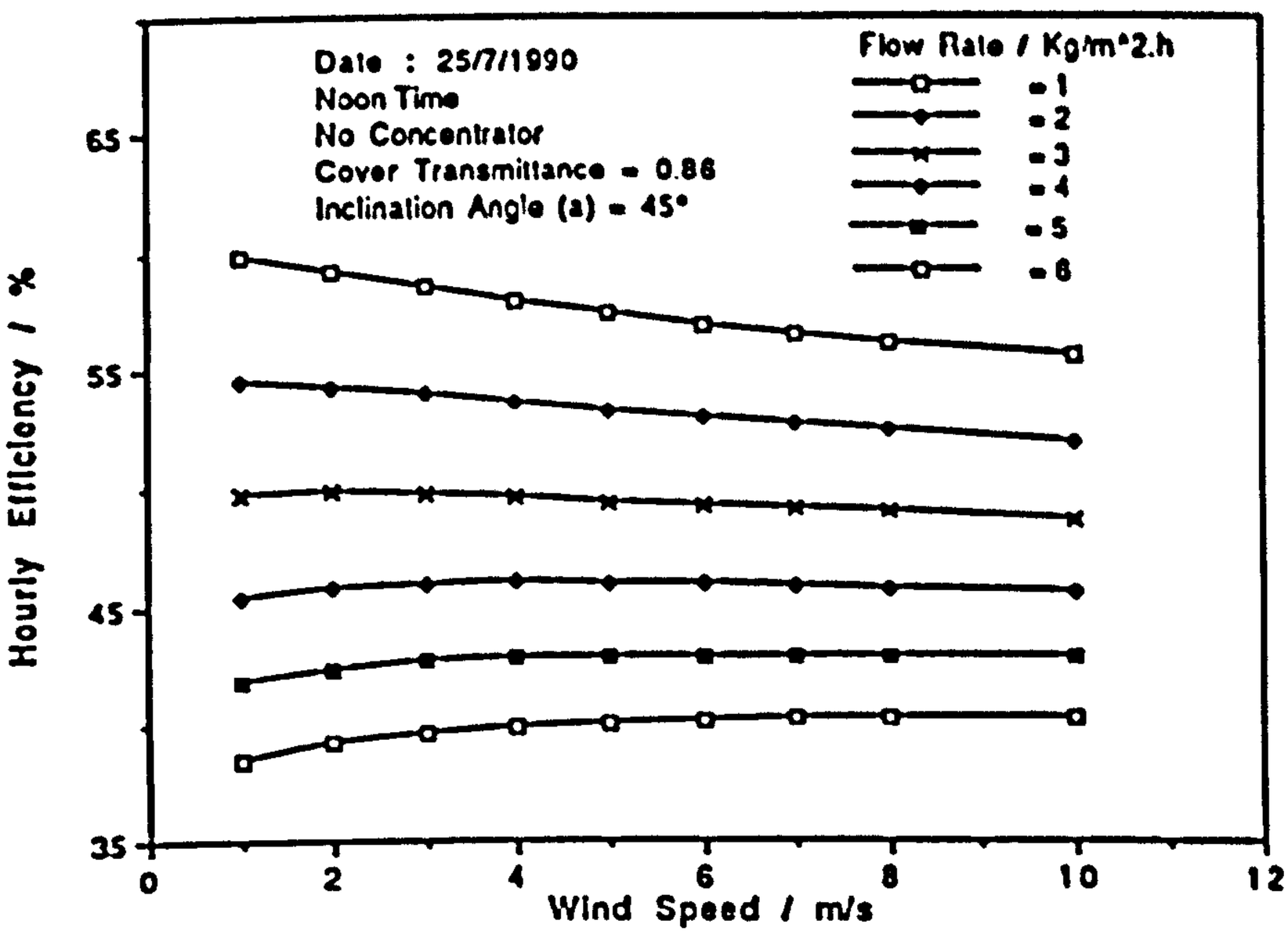

Fig. 4.6.3. Predicted variation of the still hourly efficiency at noon with wind speed at various input water flow rates and 45° inclination angle.

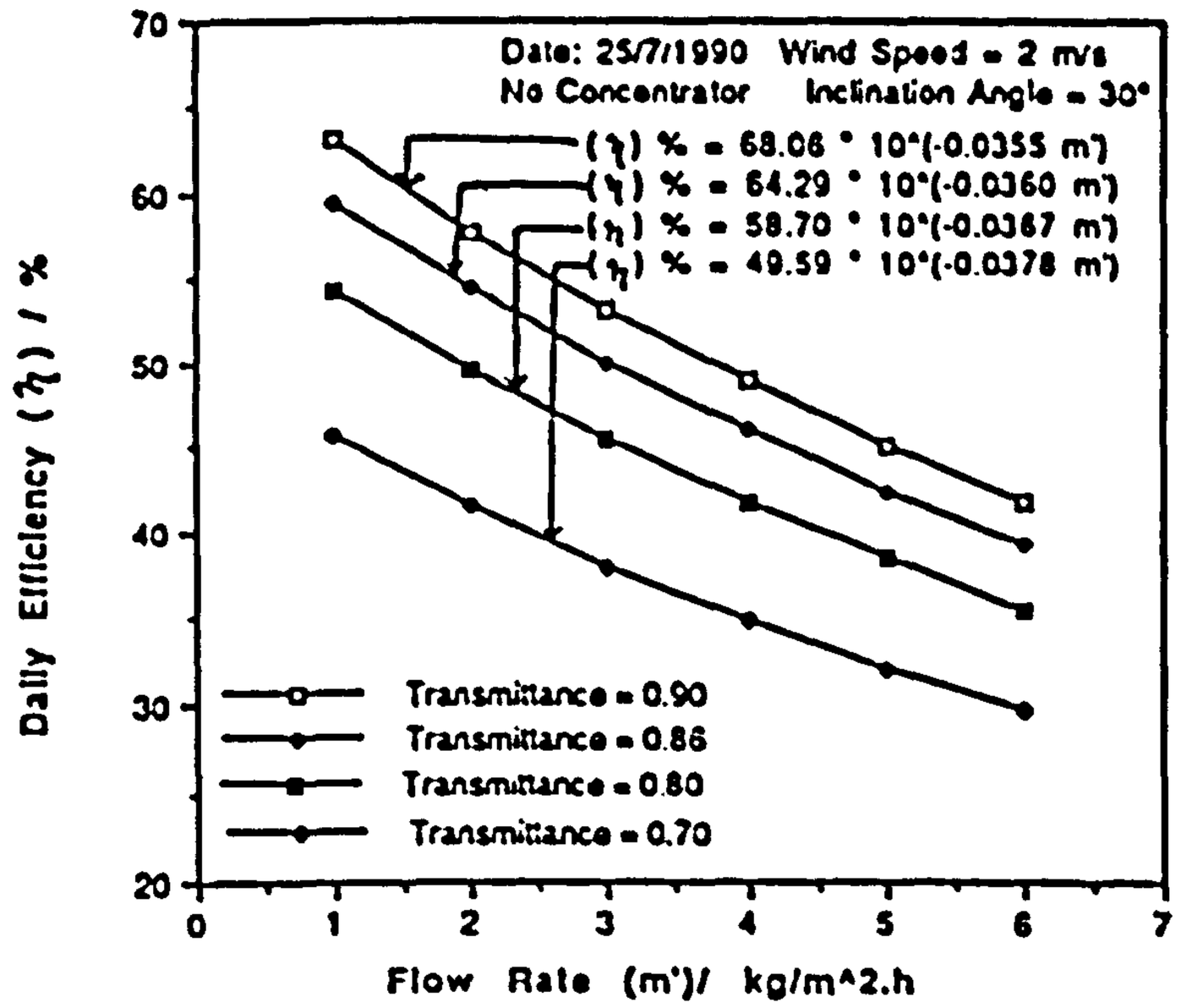

Fig.4.6.4. Predicted variation of daily efficiency of the wick-type solar still with input water flow rate, for various cover transmittances, on 25/7/1990.

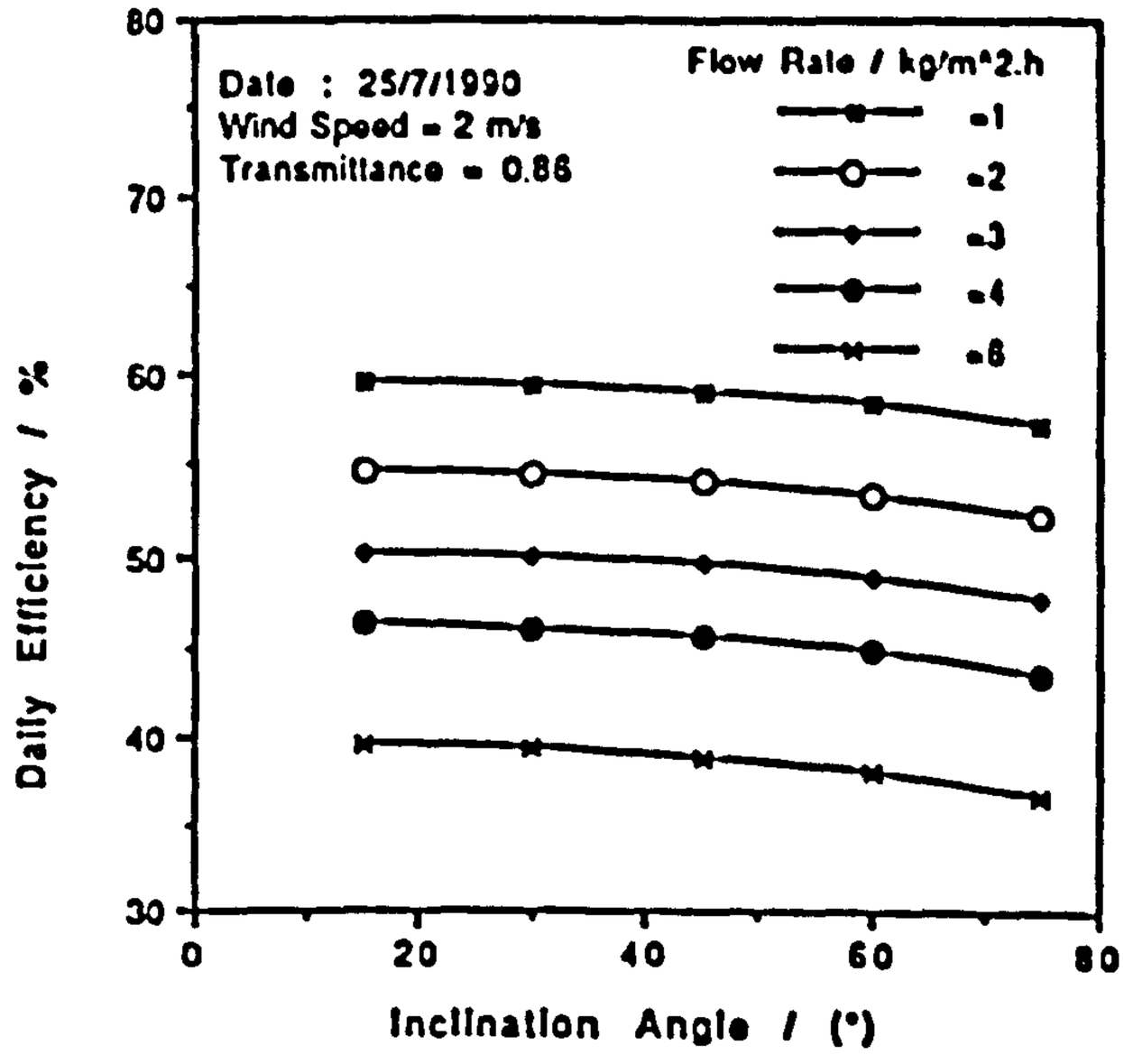

Fig. 4.6.6. Predicted variation of the still daily efficiency with inclination angle for various input water flow rates.

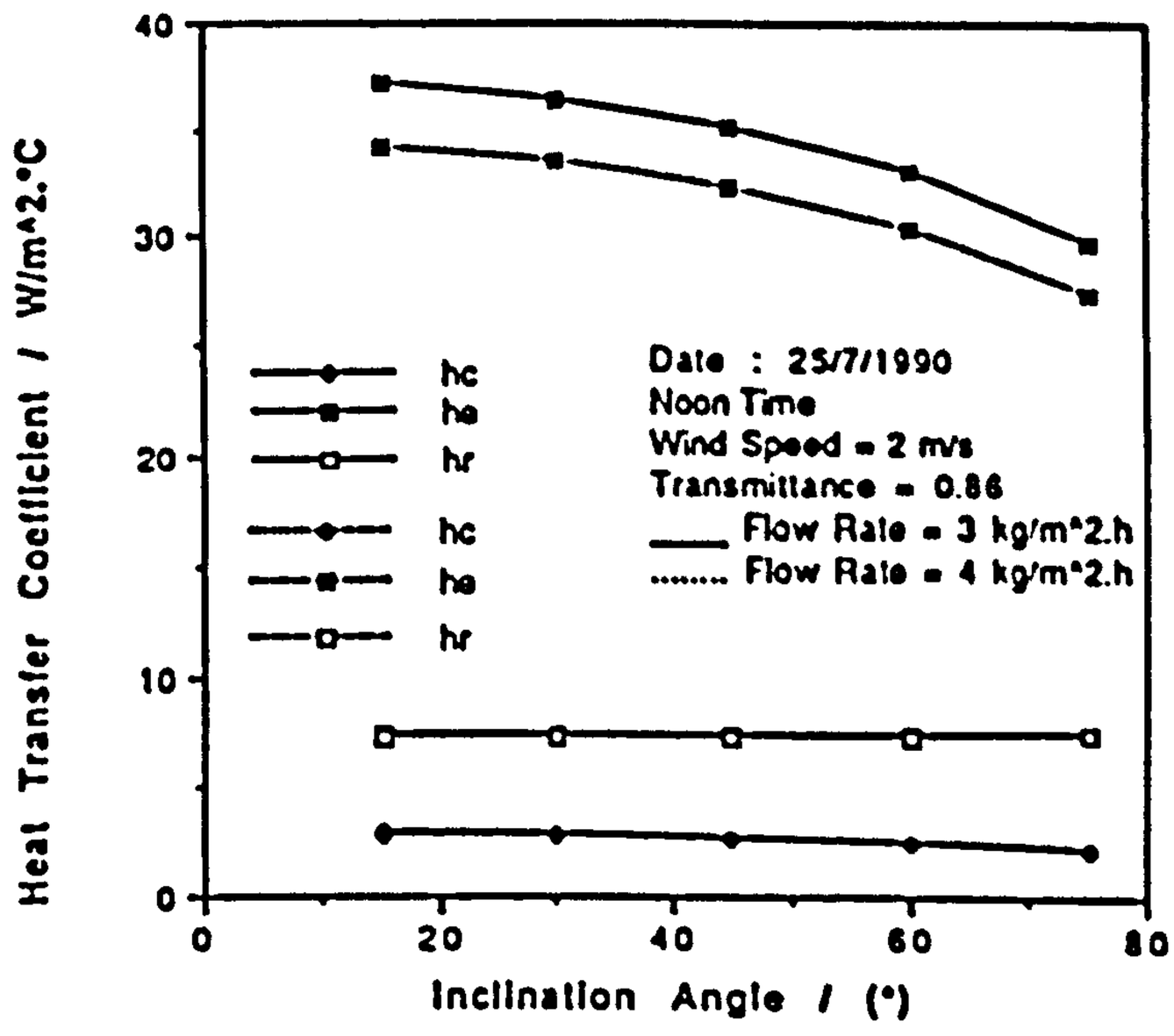

Fig. 4.6.7. Predicted variation of convective (hc), evaporative (he) and radiative (hr) internal heat tranfer coefficients with inclination angle of the wick type solar still on 25/7/1990.

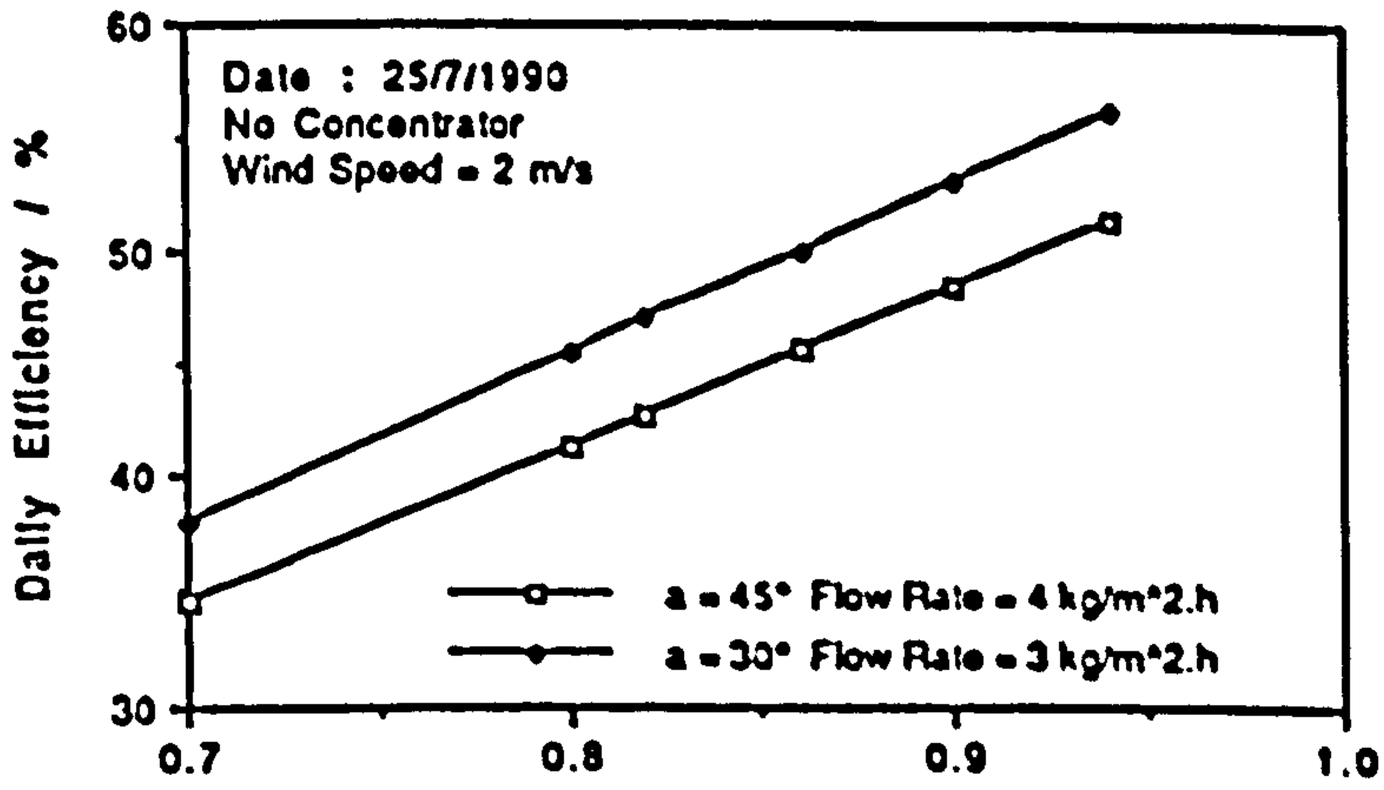

Fig. 4.6.8. Predicted variation of the still daily efficiency with cover transmittance for two inclination angles (a) and input water flow rates.

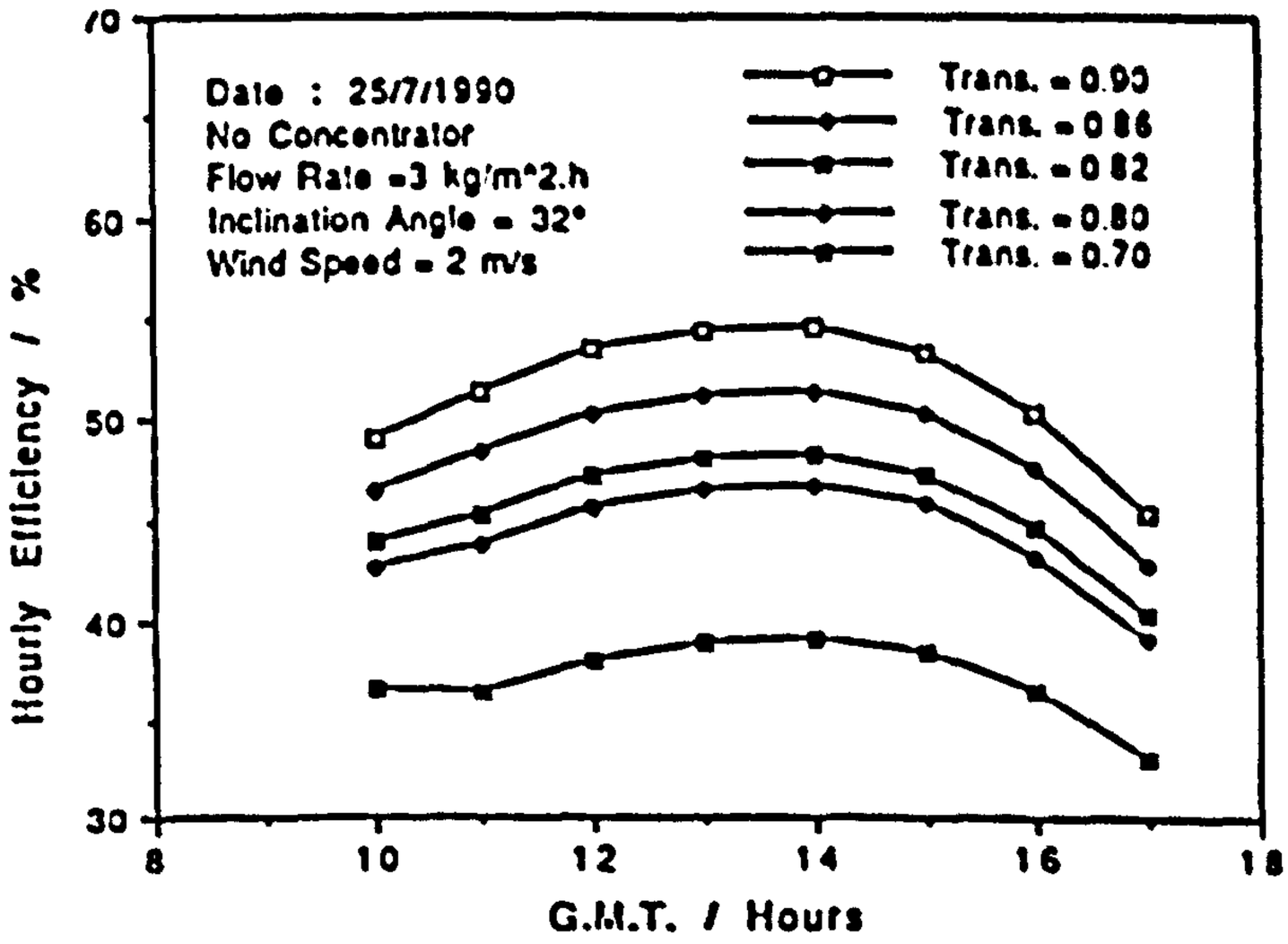

Fig. 4.6.9. Predicted variation of the still hourly efficiency with Greenwich Mean Time (G.M.T.) for various cover transmittances (Trans).

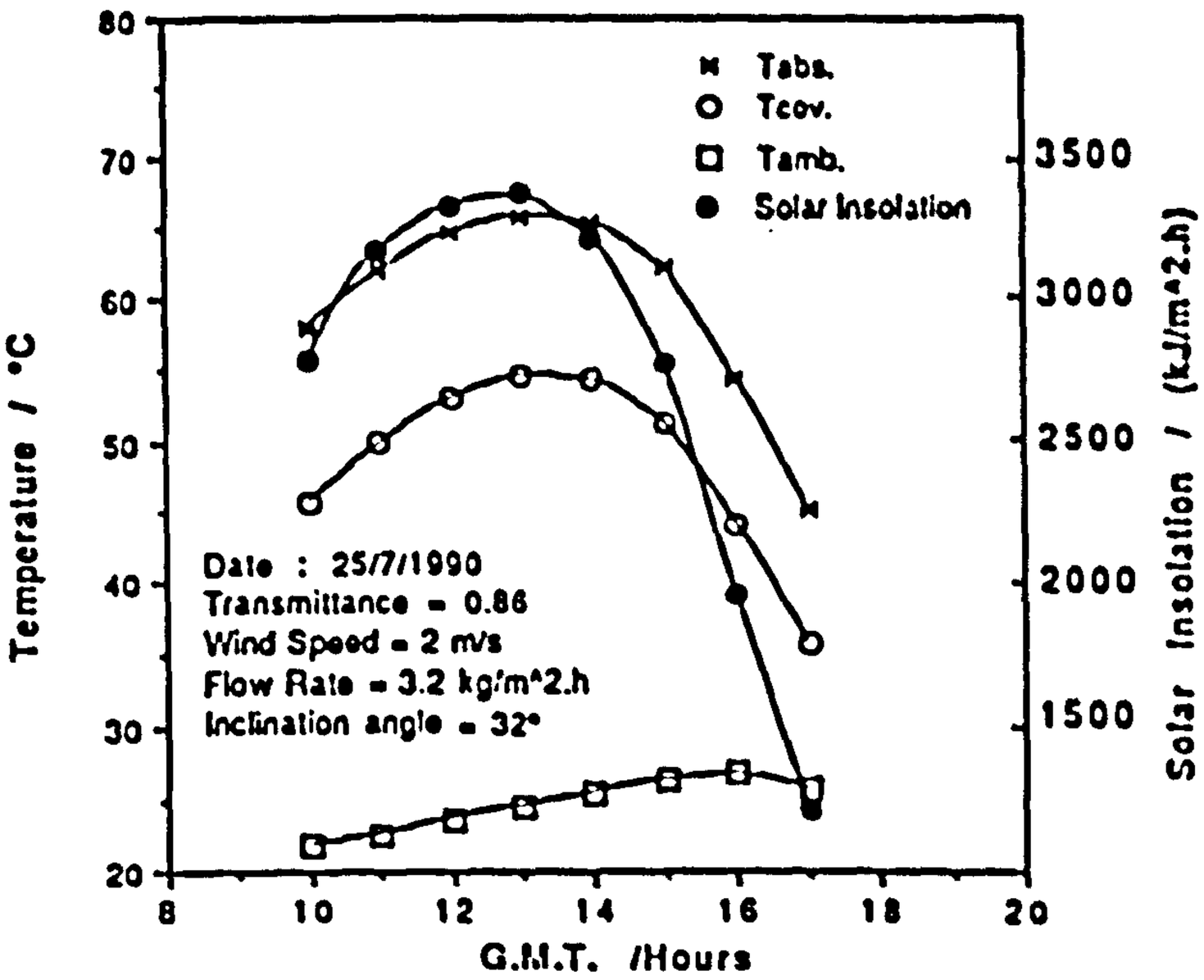

Fig. 4.6.10. Predicted variations of absorber and cover temperatures with time on 25/7/1990, for the measured solar insolation and ambient temperature.

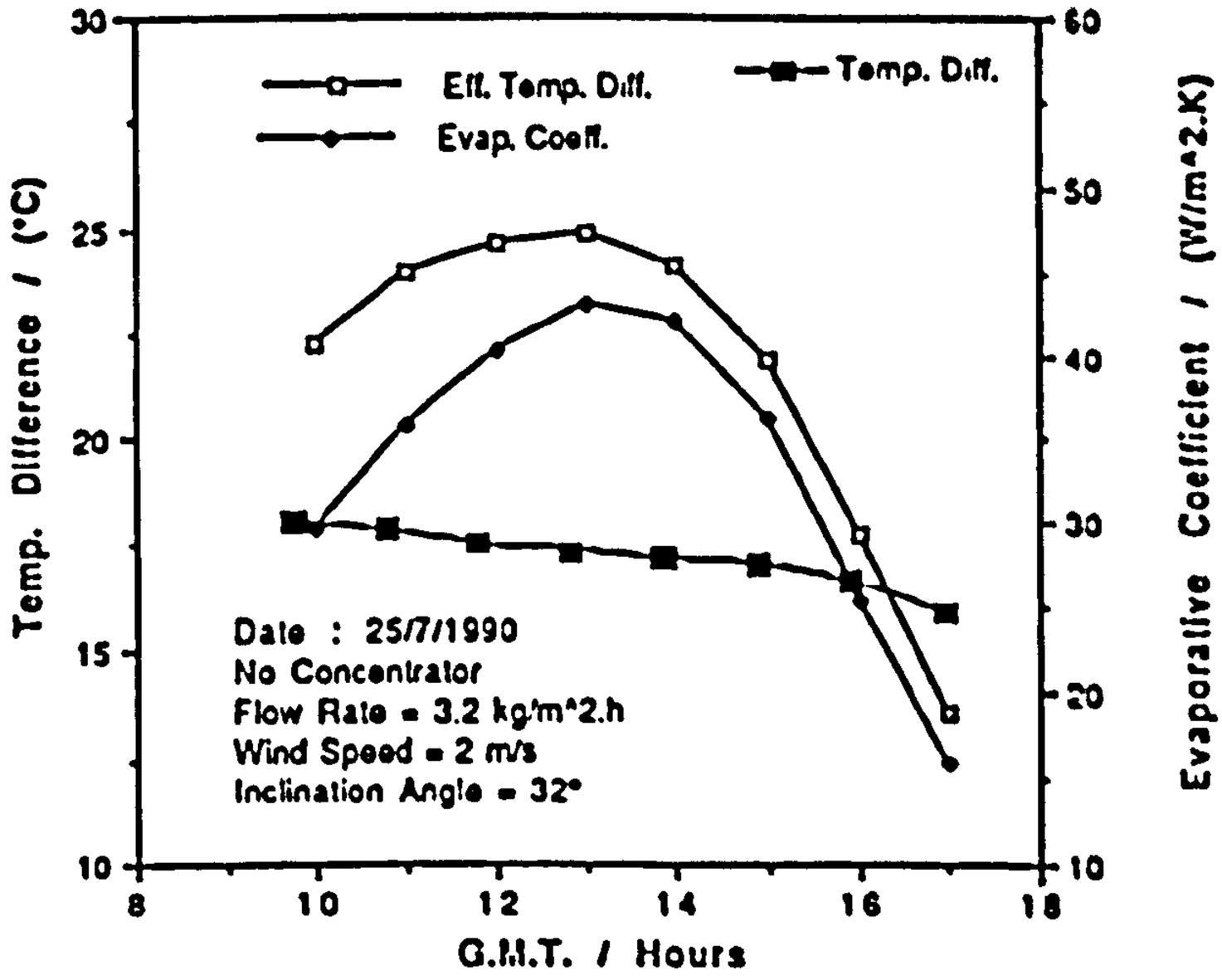

Fig. 4.6.11. Predicted variations of absorber-cover temperature difference, the effective temperature difference and the evaporative heat transfer coefficient with time on 25/7/1990.

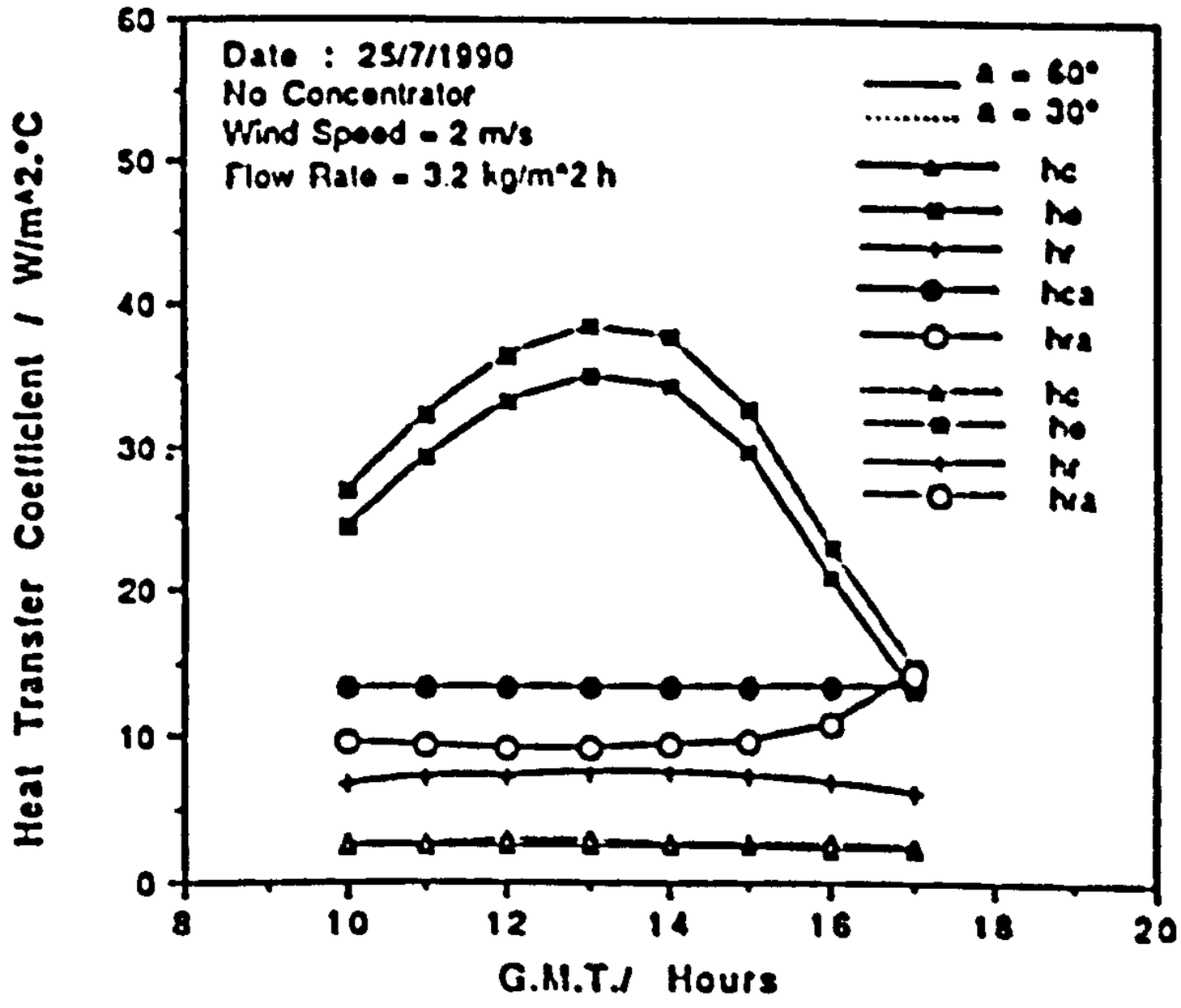

Fig. 4.6.12. Predicted variation of convective (h_c) and (h_{ca}), evaporative (h_e) and radiative (h_r) and (h_{ra}) heat transfer coefficients with time on 25/7/1990 for inclination angles (a) 30° and 60°.

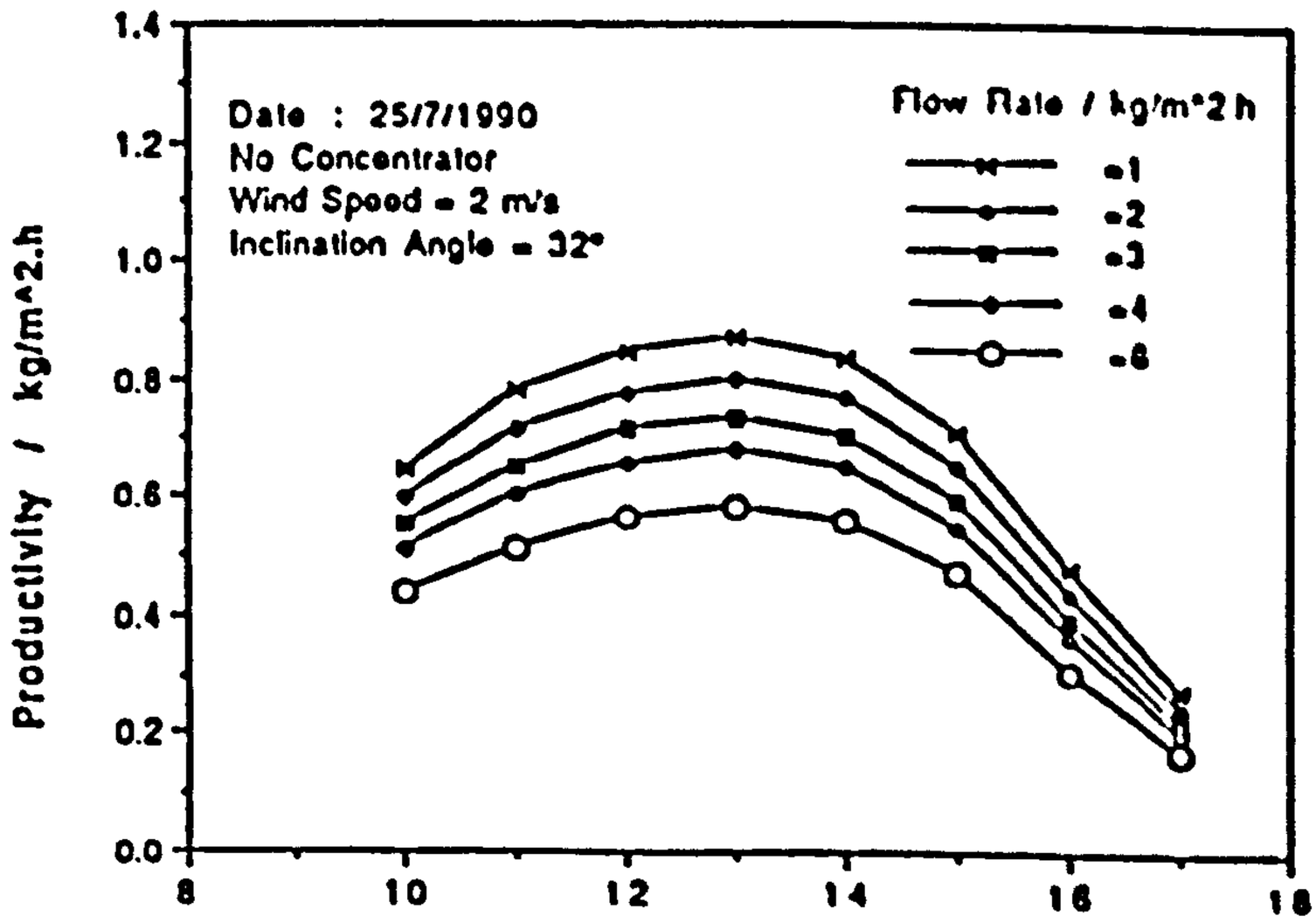

Fig. 4.6.13. Predicted variation of the still productivity with the time on 25/7/1990 for various input water flow rates.

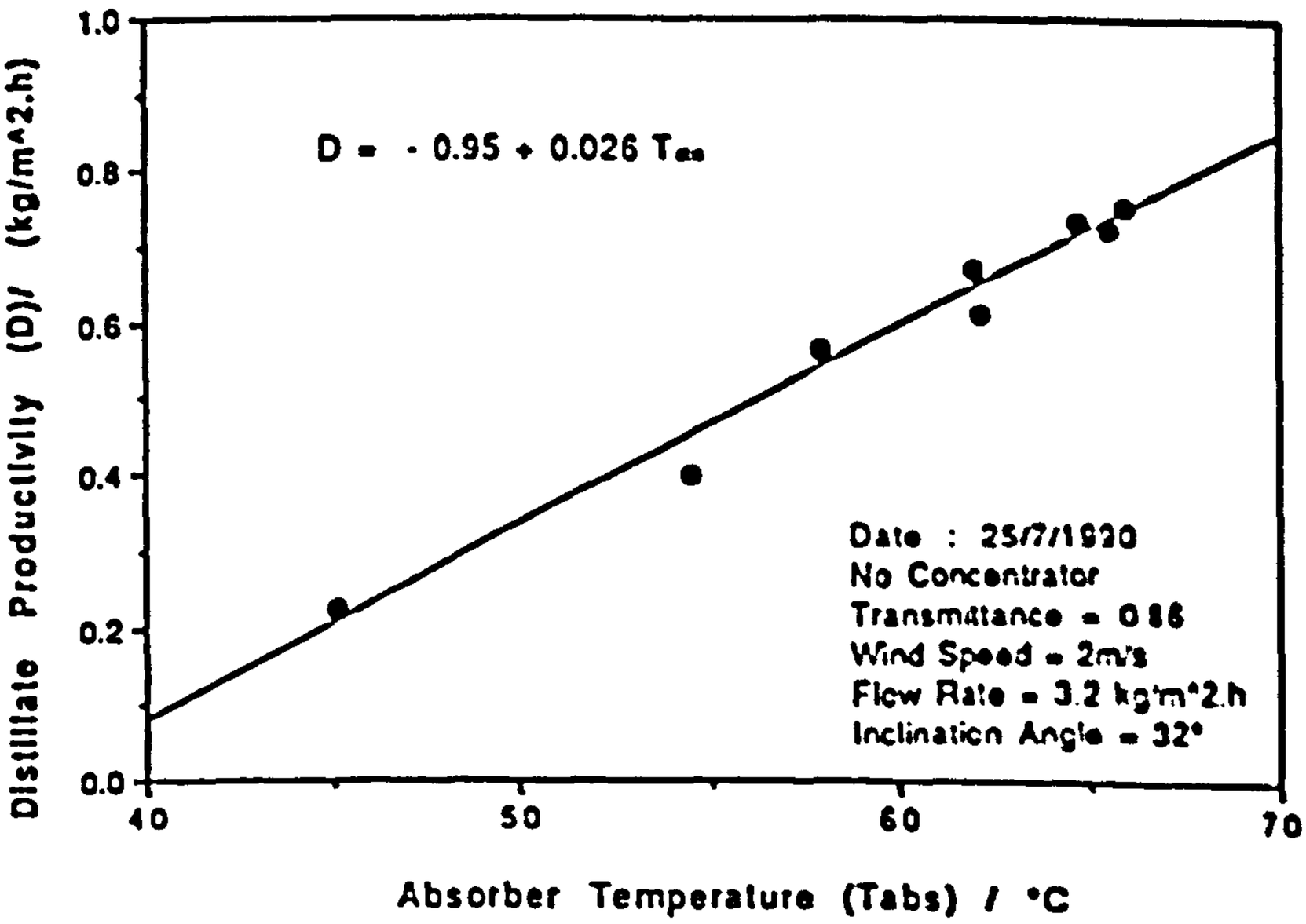

Fig. 4.6.14. Predicted variation of the still productivity (D) with the absorber temperature (Tabs).

CHAPTER FIVE

DISCUSSION

5.1 PERFORMANCE OF THE WICK-TYPE STILL

5.1.1 Comparison of theoretical and outdoor experimental results

In the numerical calculations and the graphs given in Ch.4, realistic solar insolation and ambient temperature data have been used. They were recorded experimentally during an outdoor test of the wick solar still on 25/7/1990. Based on these recorded data the predicted performance of the solar still has been determined. The other experimental variables are given ranges of variation from which can be seen the predicted behavior of the still performance. The day of 25/7/1990 was considered as one of the most clear summer days for running an experiment in solar distillation. It was almost calm. This test was followed by another experiment carried out using the solar concentrator. Therefore this day has been chosen to apply the numerical analysis and compare the predicted with the measured results.

Based on the initial predicted variation of the still efficiency with wind speed as shown in Fig. 4.6.3, no hourly variability was taken into account, but the daily average (wind speed = 2 m/s) was considered, i.e. the initial theoretical simulation had indicated only a small variation in still output with wind speed. This has been proved by indoor experiments by Yeh and Chen (1986).

Comparisons of some calculated and measured still parameters on the still performance are shown in Figs. 5.1.1-5.1.3. As can be seen from these figures the corresponding experimental curves are in fair agreement. They show the same trend of behavior relative to the Greenwich Mean Time (G.M.T.). The discrepancies are likely to be due to: (a) Various assumptions made to simplify the analysis (Ch.4). (b) The accuracy of the predicted determination of Nusselt number which is ± 5.0 % for $\theta < 60°$ and up to ±10% for $60° < \theta < 75°$ (subsection 4.3.1). (c) The uncertainty in the recorded data e.g. irradiance ±1.5%. This increases as the temperature increases above or decreases below 10 °C at a rate of 0.15% per °C (Appendix A2). (d) The non-uniform flow rate through and over the absorber cloth causes some variation (about ± 4 °C) in the absorber temperature (channels 16-19), hence the cover temperature (channels 8 and 11-14) at various points. This is shown in Appendix A4 (Table A4.1).

5.1.2 Input water flow rate

The effect of the flow rate on the performance of the solar still has been investigated experimentally and

theoretically. From Figs. (3.2.7) and (4.6.4) and Tables 3.2.1 and 4.6.2 it can be seen that the flow rate of the input saline water affects the efficiency of the solar still and absorber and cover temperatures. They decrease as the input water flow rate increases when other conditions are fixed e.g. under the effect of indoor conditions the still efficiency decreased from 38 percent to 11 percent (Fig. 3.2.7) and the absorber and cover temperatures decreased from 53 °C and 41.7 °C to 35.2 °C and 32.1 °C respectively (Table 3.2.1). These decreases occured when the input water mass flow rate increased from 2 $kg/m^2.h$ to 11.7 $kg/m^2.h$. This was because the heat loss associated with the output brine increased. The theoretical and experimental results have the same trend in behavior. Moustafa *et al.* (1979) estimated the input water flow rate should be as much as (3-4) times the production rate of the still. But in this work, a fixed flow rate was used for each experiment. It was estimated to be in the range of (4 - 8) times of the production rate. This is according to the incident energy/hour of the day and the salinity of the input brine. In theory, to get the highest efficiency, the input water flow rate should be proportional to the received solar energy and of the minimum required amount. It should be sufficient to keep the absorber surface wet during the time of the experiment. This is to avoid having parts of the evaporating cloth dry at times, as in Frick and Sommerfeld's still, Yeh and Chen (1986). This would help to suppress salt accumulation, pores blockage, colour fading and flow rate instability which might occur with highly concentrated brine. Hence the right choice of input water flow rate is essential.

Maintaining a constant flow rate in wick-type solar stills is a major problem Lof (1980). A constant flow rate is needed during settled conditions (specially the solar irradiance) to avoid energy loss or creation of dry spots in the absorber surface. The former occurs when a flow rate much higher than needed is supplied. The latter most likely occurs when the flow rate is insufficient or a non uniform distribution of water flow through the absorber cloth is present.

Theoretically, from Figs. 4.6.3 - 4.6.6 the flow rate should be just greater than the evaporation rate when other conditions are fixed. In outdoor experiments, where the irradiance varies with time, varying the flow rate accordingly, during clear weather, would decrease the heat loss and thus increase the still efficiency. It may be difficult to vary the flow rate according to the irradiance during semicloudy weather. These drawbacks are offset by many advantages of the tilted stills, such as: (a) Flowing saline water in a tray is an enhancing factor for evaporation, Narusawa and Springer (1975). (b) Having the liquid surface oriented at an optimal inclination with respect to the incident beam radiation. (c) The glass cover is parallel to the water surface. (d) Exposure of a relatively small amount of saline water to solar radiation leads to a high water temperature Malik *et al.* (1982).

5.1.3 Salinity of the input water

In wick-type solar stills the water flow is in the form of a film of salty water passing through and over a porous cloth. In

this work it has been shown experimentally (Fig. 3.2.9 and Table 3.3.2) that increasing the salinity of the input water to the wick-type solar still decreases the efficiency of the still. This may due to: (1) A decrease in the vapour pressure of the water as the salt concentration increases leading to a decrease in evaporation rate Spiegler and Laird (1980) (e.g. as the salinity increases from that of pure water to 10% of that of sea water at 60 °C the vapour pressure decreases from 149.4 mm Hg to 140.2 mm Hg. (2) Increase of density and viscosity of the salty water as the salt concentration increases leads to a decrease in evaporation rate. (3) Decrease of the absorptance of the porous cloth for incident radiation as the salt concentration increases. (4) Increase of the surface tension of the salty water during the evaporation process which decreases the evaporation rate and hence the still efficiency, Rai *et al.* (1990).

Study of this effect on the performance of wick-type solar stills has not been found in the literature. Rai *et al.* (1990) investigated the effect on the performance of a basin-type solar still and concluded that the daily distillate rate decreased from 1.10 kg to 0.50 kg as the salt concentration increased from 7% to 12%. In this work it has been found that in the wick solar still efficiency decreases from 38 percent to 20 percent as the salt concentration increases from 0.0% to 10%. This was under indoor conditions when the incident irradiance was 420 W/m^2, flow rate 2.5 $kg/m^2.h$, wind speed 0.7 m/s and the average ambient temperature 22.3 °C.

The outdoor testing results of the still with various salinities are shown in Table 3.3.2. They are for the still with and without the solar concentrator. It can be seen that the still efficiency decreases as the salinity increases due to the above mentioned reasons whether with or without the concentrator. But the daily efficiency decreases more markedly at 5% salinity when the concentrator was used i.e. to 35.3 percent. Without the concentrator the efficiency decreased to 33.7 percent. The reason for this is due to a required increase in the input water flow rate (in the case of the concentrator) by 30% in order to match the high insolation at the hours around noon i.e. to avoid creation of dry spots and salt clogging. However the hourly efficiency around noon (11.00-13.00) is still relatively high i.e. 48.9 percent.

5.1.4 Solar insolation and inclination angle

For maximum integrated solar insolation in a year a receiving surface should face south and be inclined to the horizontal at an angle equal to the latitude of the place Malik *et al.* (1982). Maximum solar insolation for a particular clear day with a stationary inclined still is possible by choosing an optimum inclination angle in which the incident radiation is perpendicular to the glass cover at noon. In this work the inclination angle was chosen to be equal to the solar altitude at noon (around which a major fraction of daily incident energy is received). It has been found that the inclination angle affects the productivity of the still in two ways: (i) affects the internal heat and mass transfer through the evaporative and convective

transfer coefficients i.e. h_e and h_c respectively as shown in Figs. 4.6.7 and 4.6.12 and (ii) affects the amount of radiation intercepted by and transmitted through the still cover and collected by the absorber. (Figs. 4.6.6 and 4.6.8). As the amount of radiation is a strong factor affecting the productivity of the still the still yield is affected strongly by the still inclination angle. (This is shown e.g. experimentally in Fig. 3.3.5 in the close correlation of increase and decrease of the productivity curve and the solar insolation curve.)

5.1.5 Use of the solar concentrator: advantages and disadvantages

The V-trough solar concentrator used with the solar still had an apex angle of 30° and aperture to base ratio 1.9 with depth to base ratio 1.75. An expected concentration factor for beam radiation of about 1.68 should be achieved according to Bannerot (1974) (see Appendix A8).

An approximate instantaneous concentration factor was determined during a very sunny day (20/7/1990) and a very cloudy day (27/7/1990) as shown in Fig. 3.3.2. Also the averaged local concentration factor on the base of the trough at different hours of the day has been determined as shown in Fig. 3.3.3. In both figures the effect of the shading of the absorber by the end walls of the trough is apparent and is more pronounced at the off-noon periods, during which time the ratio of the heat collected to the daily total insolation available is not significant. However, there was a considerable increase in the solar energy received on the solar still for the total operating period on a clear day. The

maximum averaged local concentration factor (ALCF) around noon was about 1.6 as shown in Fig. 3.3.3. The increase in the still efficiency was not in the same order for two reasons. First, the increase in the absorber temperature increases the heat losses from the back and sides of the still and also that of the outlet brine. Second, the presence of the trough decreases the absorber-cover temperature difference, i.e. the increase of the cover temperature is more than that of the absorber temperature as shown in Figs. 3.3.5 and 3.3.6. This is due to reduced convective heat transfer from the cover to the ambient air as the convective heat transfer coefficient varies linearly with wind speed (Eq. 4.3.17). The increase in the input water flow rate from 3.2 to 4.5 $kg/m^2.h$ when the solar concentrator was used would also tend to decrease the still efficiency (subsection 5.1.2). Nevertheless, the efficiency has been increased from 53.8 to 68.9 percent around noon and 53.4 to 63.6 percent daily (Tables 3.3.3 and 3.3.4 respectively) and a good response of the still performance to the incident energy displayed as shown in Figs. 3.3.5 - 3.3.11 for various weather conditions during different days. The comparison between the still performance with and without the solar concentrator can be seen in Figs. 3.3.10 and 3.3.11. These show a higher distillate production rate to solar insolation ratio in winter than in summer. This may be so in winter, because (i) the proportion of diffuse radiation was lower on clear winter days than on clear summer days, (ii) the high inclination angle may also have led to a lower water film thickness and density of dropwise of condensation and (iii) the high effectiveness of

retain the heat of the cover by the concentrator; i.e. concentration of the incident (beam) radiation may have been more effective on winter clear days and less heat loss from the cover with concentrator than without it.

The percentage efficiency difference (PED) of a solar still with and without the solar concentrator is expressed as:

$$PED = \frac{\text{Efficiency with concentrator} - \text{Efficiency without concentrator}}{\text{Efficiency without concentrator}} \times 100$$

Using this expression, it has been found that PED in selected winter days (23/11/1989 and 29/11/1989) is 43 percent, while in summer days (25/7/1990 and 1/8/1990) it is 19 percent. This illustrates that use of the concentrator on winter clear days appears to be more useful than use on clear days in summer.

5.1.6 Absorber and cover temperatures

Comparison of Figs. 3.2.8 and 4.6.14, shows similar behavior of the solar still; i.e. the productivity of the still varies linearly with absorber temperature. But they are applied for different conditions; i.e Fig. 3.2.8 is for the indoor conditions while Fig. 4.6.14 for the outdoor conditions. The productivity increases as the evaporation heat transfer coefficient increases which, in turn, increases as the effective absorber-cover temperature difference increases as shown in Figs. 4.6.11.

5.2 CONSTRUCTION OF THE WICK-TYPE SOLAR STILL

5.2.1 Absorber/evaporator surface

The solar still of this work was constructed with an absorber/evaporator made of charcoal cloth. This cloth has a high solar absorptance of about 98.0 ± 0.2 percent for VIS and NIR and 99.0 ± 0.2 percent for IR radiation. It is intrinsically black and no dye is required. It has not been used before for such a purpose. Many authors used jute cloth, e.g. Sodha *et al.* (1981), Yeh and Chen (1986), Tiwari and Yadav (1987) and others. Jute needs frequent replacement and/or black dye injections. Moustafa *et al.* (1979) used a synthetic wettable mat lined with black plastic on the underside. Charcoal pieces were used by Akinsete and Dura (1979) in a basin-type solar still so as to reduce the thermal inertia of the still due to following reasons:

(i) Charcoal exhibits capillary action.

(ii) Charcoal is reasonably 'black' to solar radiation.

(iii) The rough surface of a typical charcoal piece scatters rather than reflects incident radiation.

These characteristics are almost the same in the case of the charcoal cloth which has been used in this work. However, its cost is known to be well above that of blackened jute. So it is only convenient to use the charcoal cloth in a standard experimental solar still unless charcoal cloth will be produced from natural sources such as coir, Hitchcock *et al.* (1983). This might make it less expensive.

5.2.2 Evaporator support board

This is made of fire resistant flat hard board (Cape Insulation) to give a firm support to the charcoal cloth and a high durability to the high temperatures which might occur when using the solar concentrator and/or at high solar insolation. It has much lower heat conductivity ($k = 0.29$ W/m.°C) than that of the galvanized iron ($k = 51.2$ W/m.°C) which was used by Sodha *et al.* (1981), or the fibre resistance plastic, Dhiman and Tiwari (1990). It has a relatively high heat capacity so that it reduces the effect of sudden variation of solar insolation on the performance of the still.

5.2.3 Still cover

To separate the top of the still enclosure from the ambient air, a transparent cover either from plastic or glass is used in the conventional solar still. In this work, a four mm thickness of window glass is used as a condensation surface and a transparent cover. Its emissivity for IR radiation was estimated to be 0.94. However, solar still efficiency is not strongly dependent on cover glass emissivity, e.g. a value of 0.88 was recommended by Rabl (1985) and used by Kiatsiriroat *et al.* (1987). It affects only the radiative heat transfer between the glass cover and the absorber, eq. (4.3.14) (from the inner side) and the surroundings, eq. (4.3.20) (from the outer side of the cover). But both these radiative quantities are small compared with the evaporation rate inside the still and convection rate outside the still cover. This is shown in Fig. 4.6.12. Plastic covers for solar

stills offer some advantages over glass covers since they may be relatively inexpensive and not easy to fracture. However, they have operational problems such as low resistance to scratching, distortion and even drops of the condensation falling back to the absorber/evaporator surface Frick and Sommerfeld (1973).

In this work to avoid some drops of distillate falling back to the evaporator surface, the still cover is made of glass and a rectangular cross section aluminium channel is fixed firmly with the help of araldite, to its inner surface, so that the distillate can slide directly to the channel where it is conducted to the outer drainage tube.

The transmittance of the glass cover is an important factor in the predicted performance of the daily efficiency of the solar still due to its direct effect on the incident solar energy. It has been studied by many authors e.g. Norton *et al.* (1988). From the predicted numerical calculations which are shown in Fig. 4.6.8 it can be seen that the still efficiency is a strong function of the cover transmittance. It decreases from 53.6 to 38.4 when the transmittance decreases from 0.90 to 0.70. The real experimental value of the transmittance of the solar still cover with condensation on it, in the form of thin film or dropwise, is a variable quantity and depends on the distribution of the drops and their sizes or the thickness of the film of condensate on the cover. These vary with the instantaneous still operating and weather conditions. Cooper (1969 and 1969b) mentioned in his studies that the overall effect of condensate (as a thin film) is to increase the transmittance of the system by reducing reflectance.

Therefore, an attempt to prove this and to measure the transmittance in conditions like those faced during real operating time was carried out to get an estimated value of this factor (about 0.86). The method was similar to that published by Norton *et al.* (1988) who found experimentally that the unscattered beam transmittance was linearly dependent on the quantity of water sprayed on a cover; i.e. spraying water film continuously on the inner surface of the glass cover and fixing two solarimeters (in parallel planes facing the south at noon) one underneath the glass cover and the other nearby. The irradiance was therefore measured with and without the cover. Their ratio represents the cover transmittance and is given by 0.86.

5.2.4 Absorber-cover separation distance

It has been shown theoretically (Fig. 4.6.5) that the highest daily efficiency occurs when the absorber-cover separation distance (H) is in the range (20 - 25) mm. This is because it gives the highest evaporation coefficient. This is 41.0 $W/m^2.K$ when the separation distance is 20 mm, while in the separations of 10, 30 and 50 mm, it is 37.7, 38.9 and 34.5 $W/m^2.K$ respectively. Here the input mass flow rate is 3.2 $kg/m^2.h$, the inclination angle is 32°, the cover and condensation transmittance is 0.86 and the time is mid-day. However, the separation of the still of this work is designed to be 40 mm because of a practical reason.

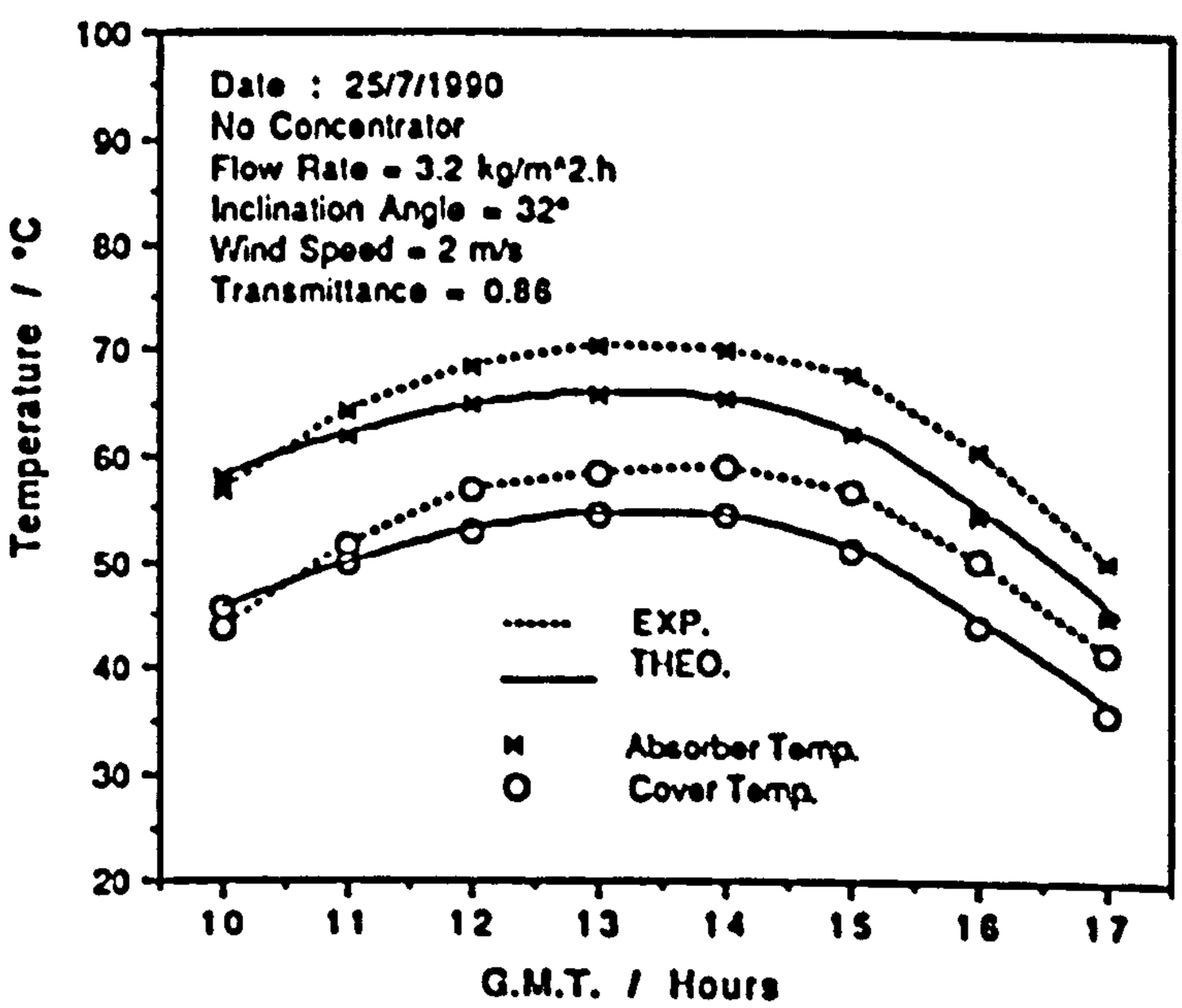

Fig. 5.1.1. Comparison of the experimental and theoretical absorber and cover temperatures of the wick solar still on 25/7/1990.

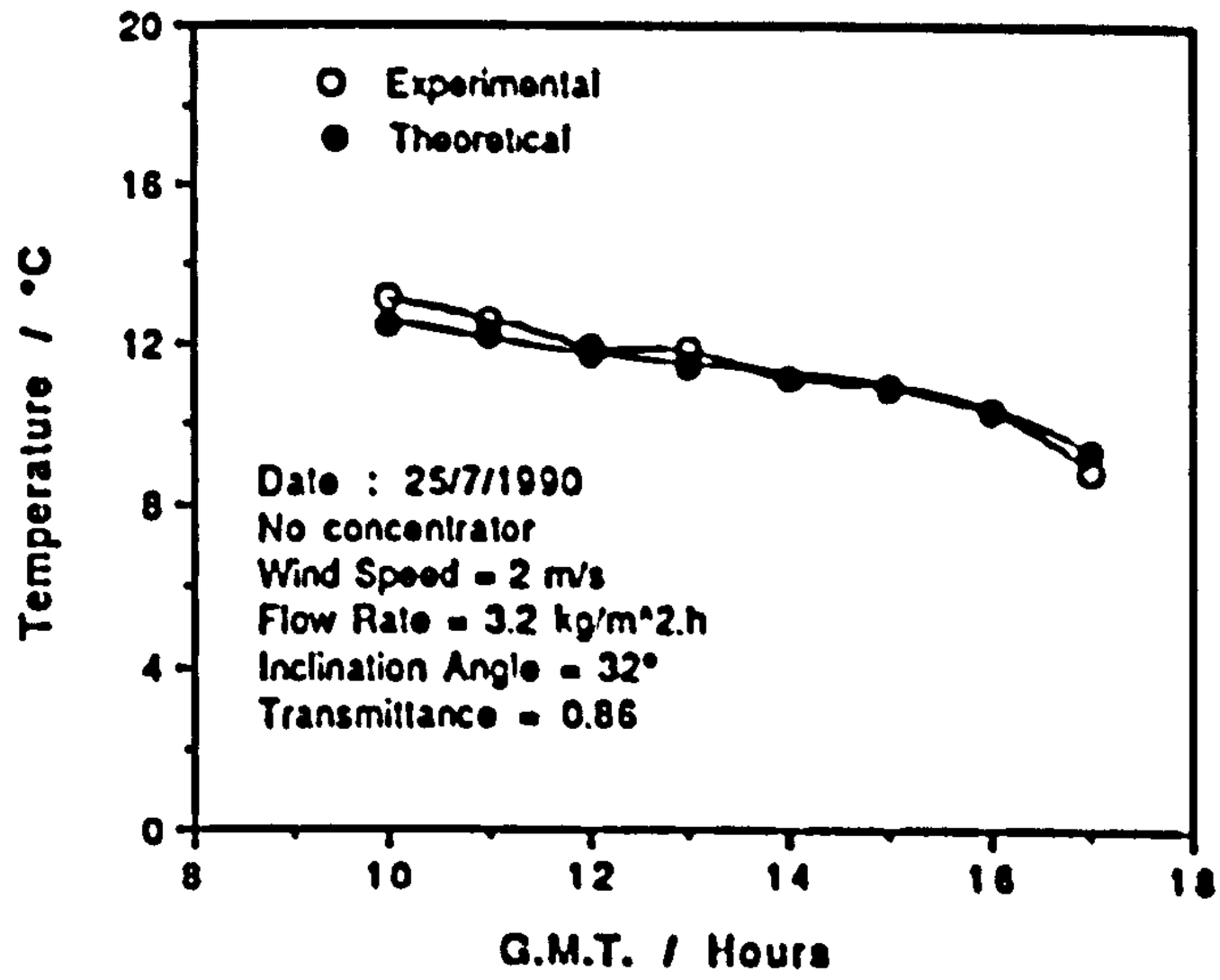

Fig. 5.1.2. Comparison of the experimental and theoretical absorber-cover temperature difference of the wick solar still on 25/7/1990.

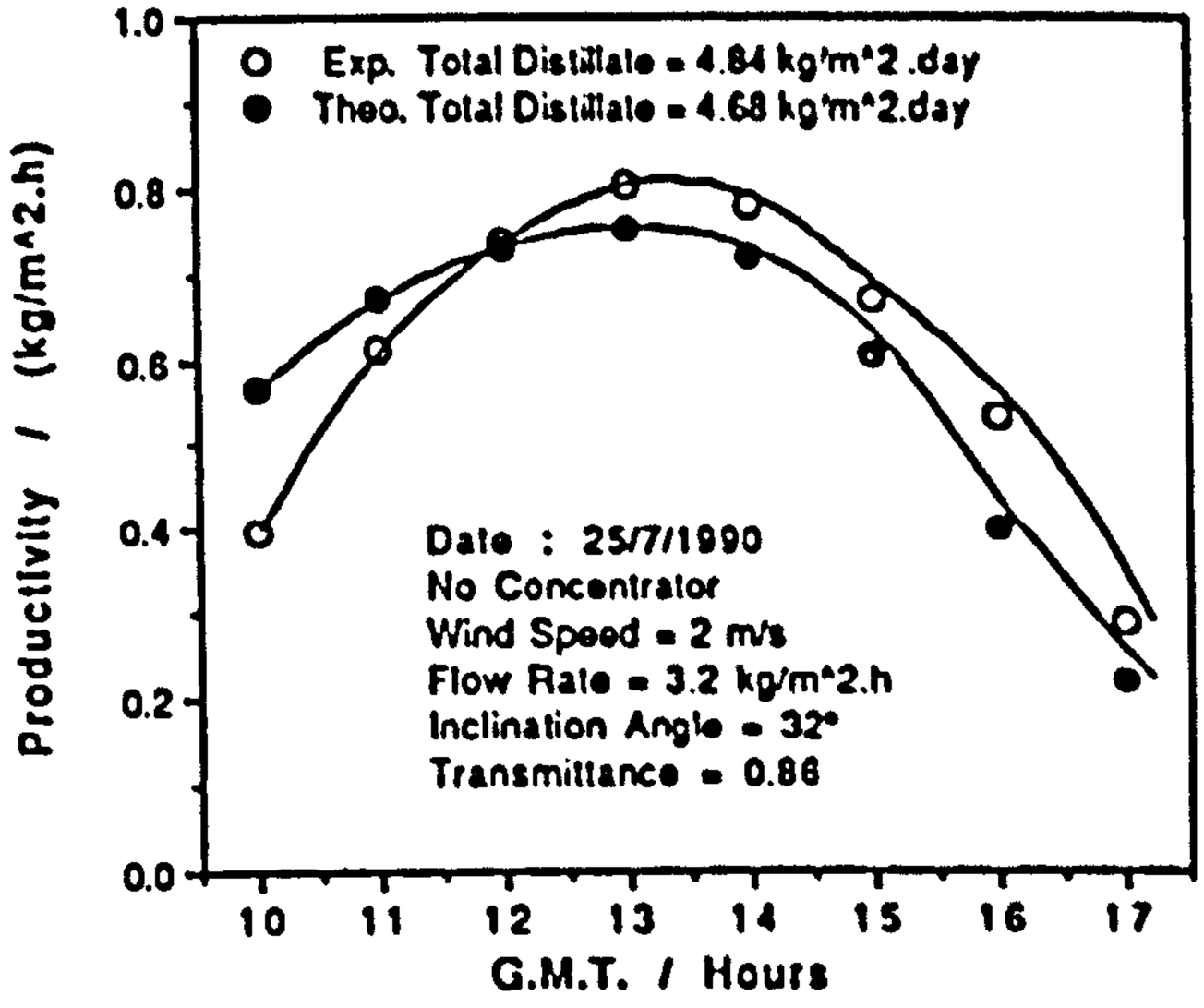

Fig. 5.1.3. Comparison of the experimental and theoretical productivity of the wick solar still on 25/7/1990.

CHAPTER SIX

CONCLUSIONS AND FUTURE WORK

6.1 CONCLUSIONS

Use of the charcoal cloth as a standard absorber material for a wick-type solar still is recommended (although it is comparatively expensive) as it has a very high absorptance for VIS and NIR radiation and for IR radiation (Figs. 3.4.1 and 3.4.2). Charcoal cloth showed only a slight change in its solar absorptance and no visual deterioration due to an outdoor exposure of about two years in a transparent plastic covered enclosure. The blackened hessian cloth faded completely within six months (Table 3.4.8).

The wick-type solar still efficiency varies with input water mass flow rate, i.e. increase of the input water mass flow rate leads to a reduction in the efficiency of the wick-type solar still (Fig. 3.2.7 and Table 3.3.1). This is in agreement with the

theoretical results (Fig. 4.6.4). Therefore, varying the input water mass flow rate in a wick-type solar still according to the incident energy is recommended, (Fig. 4.6.13).

Transmittance of the glass cover with condensation has an effective influence on the efficiency of the solar still. The higher the amount of the dropwise condensation on the still cover the less transmittance and consequently the less efficiency (Figs. 4.6.4, 4.6.8 and 4.6.9). The wick-type solar still productivity varies linearly with absorber temperature (Fig. 3.2.8). This shows the same trend in behavior as the theoretical results.

The ratios of productivity/insolation of the solar still show there is an observable effect due to use of the V-trough solar concentrator with the wick-type solar still (Figs. 3.3.10 and 3.3.11). The percentage efficiency difference due to use of the solar concentrator on certain clear winter days was more than double of that on certain clear summer days, (Table 3.3.4).

The still efficiency decreased linearly with increase of salinity of the input saline water (Fig. 3.2.9) as determined indoors. In outdoor experiments the daily efficiency decreased as in Table 3.3.2. The highest daily efficiency of the solar still is found to be when the absorber-cover separation is in the range (20 - 25) mm, (Fig. 4.6.5).

3M Scotchcal Film 530 had a good durability when exposed to elevated temperatures and relative humidity during various ageing time as compared with 3M Scotchcal films 3658 and 5400 and aluminised plastic (Tables 3.4.2 - 3.4.6 and Figs. 3.4.18 - 3.4.21).

6.2 FUTURE WORK

1) Application of the model using realistic data for a place in the Middle East e.g. southern Iraq.

2) Investigation of use of the latent heat of evaporation by using a double glazed cover for the wick solar still and letting the input water pass, firstly, through the cover and then to the evaporator cloth.

3) Investigation of connection of flat plate solar collector to the wick solar stills, with water flow over the glass cover and then input to the collector.

4) Investigation of the physical properties of the charcoal cloth, the still performance and their deterioration with various periods of time of running the still outdoors.

5) Investigation of the effect of input brine salinity on the input flow rate through the charcoal cloth.

6) Investigation of economics of the solar distillation plant with wick-type solar stills.

7) Investigate use a solar simulator with a more efficiency and uniformity incident flux.

8) Comparison of the performance of solar still by using different sources of charcoal cloth and hessian cloth.

9) Investigation of the performance of wick-type solar still with:

a) variation of the input water temperature in relation to efficiency and absorber temperature,

b) inclination angle of the still for various orientations relative to the incident flux,

c) variation of the cover-absorber separation.

REFERENCES

Abbas, M. A.; M. K. Einesr and Z. M. Magid, (1977)
Experimental studies on basin-type solar distillers in Iraq. Revue Int. Dheliotechnique, Vol.1, pp. (35-39).

Abdel-Aal, H. K., (1980)
Development plans and conceptual designs for multi-purpose solar desalination units (MSDU), Proceedings of the Int. Symp. Workshop on Solar Energy pt. III Cairo Egypt (16-22) June 1978, pp. (1587-1599).

Abdelrazek, I. D. and F. H. Hammad, (1980)
Direct solar distillation, Proceeding of the Int. Symp. Workshop on Solar Energy pt. III, Cairo Egypt (16-22) June 1978, pp. (1561-1569).

Akhtamov, R. A. ; B. M. Achilov; O. S. Kamilov and S. Kakharov, (1978)
Study of regenerative inclined-stepped solar still, Applied Solar Energy, Vol. 14, No. 4, pp. (41-44).

Akinsete, V. A. and C. V. Duru, (1979)
A cheap method of improving the performance of roof type solar stills, Solar Energy, Vol. 23, No.3, pp. (271-272).

Bannerot, R. B, (1974)
Moderately concentrating (not focusing) solar energy concentrators, in the annual progress report, The Evaluation of Surface Geometry Modification to Improve the Directional Selectivity of Solar Energy Collectors, edited by J R. Howell and R. B. Bannerot, New York, pp. (37-44).

Bannerot, R. B. and J. R. Howell, (1977)
The effect of non-direct insolation on the radiative performance of trapezoidal grooves used as solar energy collectors, Solar Energy, Vol. 19, No. 6, pp. (549-553).

Bapeswararao, V. S. V. ; V. Singh and G. N. Tiwari, (1983)
Transient analysis of double basin solar still, Energy Convers. Mgmt., Vol. 23, No. 2, pp. (83-90).

Broman, L., (1984)
Non-imaging solar concentrators with flat mirrors, Int. Conf. on Non-Imaging Concentrators, San Diego, Aug. (23-28)(1983), SPIE, Vol. 441, pp. (102-109).

Brown, B. (Holborn) Ltd., Felt and Display Textiles,
32 - 33 Greville Street, London, EC1N 8TD, U.K.

Burkhard, D. G. ; G. L. Strobel and D. R. Burkhard, (1978)
Flat-sided rectilinear trough as a solar concentrator: an analytical study, Applied Optics, Vol. 17, No. 12, pp.(1870-1883).

Charcoal Cloth Ltd., Eastwing, Bridge Water Lodge, 160 Bridge Road, Maidenhead, Berkshire, SL6 8DG, U.K.

Charters, W. W. S., (1977)
Solar energy utilization-liquid flat collector, Ch. 6 in Solar Energy Engineering, edited by A. A. M. Sayigh, Academic Press, New York, pp. (105-135).

Chiam, H. F., (1982)
Bi-yearly adjusted V-trough concentrators, Solar Energy, Vol. 28, No. 5, pp. (407-412).

Colley, J. P., (1975)
Vertical solar distillation, Solar Energy, Vol. 17, No. 4, pp. (375-378).

Cooper, P. I., (1969)
Digital simulation of transient solar still processes, Solar Energy, Vol. 12, No. 3, pp. (313-331).

Cooper, P. I., (1969b)
The absorption of radiation in solar stills, Solar Energy, Vol. 12, No. 3, pp. (333-346).

Cooper, P. I., (1972)
Some factors affecting the absorption of solar radiation in solar stills, Solar Energy, Vol. 13, No. 4, pp. (373-381).

Cooper, P. I., (1973)
Digital simulation of experimental solar still data, Solar Energy, Vol. 14, No. 4, pp. (451-468).

Dang, A; J. K. Sharma; A. Thakur and R. Chandra, (1983)
Optical and thermal analysis of trough-like concentrators, Applied Energy, Vol. 13, pp. (195-214).

Delta-T-Devices Manual, (1987)
Delta-T-Devices Ltd., 128 Low Road, Burwell, Cambridge, CB5 0EJ, U.K.

Delyannis, A. and E. Delyannis , (1983)
Recent solar distillation developments, Desalination, Vol. 45, pp. (361-369).

Delyannis, A. A. and E. Delyannis, (1984)
Solar desalination, Desalination, Vol. 50, pp. (71-81).

Dhiman, N. K. and G. N. Tiwari, (1990)
Effect of water flowing over the glass cover of a multi-wick solar still, Energy Convers. Mgmt., Vol. 30, No. 3, pp. (245-250).

Dorey, G., (1988)
Making the most of carbon fibres, Carbon 88 Conf. (18-23) Sept. 1988, U.K., pp. (613-616).

Duffie, J. A. and W. A. Beckman,(1980)
Solar Engineering of Thermal Processes, John Wiley, New York.

Dunkle, R. V., (1961)
Solar water distillation: the Roof type still and a multiple effect diffusion still, Int. Developments in Heat Transfer, ASME, Proc. Inter. Heat Transf. part V, pp. (895-902).

Dutt, D. K. ; S. N. Rai and G. N. Tiwari, (1988)
Thermal modeling of high temperature distillation, Energy Convers. Mgmt., Vol. 28, No. 2, pp. (151-159).

Eibling, J. A.; S. G. Talbert and G. O. G. Lof, (1971)
Solar stills for community use-digest of technology, Solar Energy, Vol. 13, No. 3, pp. (263-276).

Elsayed, M. M., (1983)
Comparison of transient performance predictions of a solar-operated diffusion-type still with a roof-type still, Journal of Solar Energy Engineering, Vol. 105, pp. (23-28).

Fabuss, B. M., (1980)
Properties of sea water, App. 2 in Principles of Desalination, part B, 2nd edition, edited by K. S. Spiegler and A. D. K. Laird, Academic Press, New York, pp. (765-799).

Freeman, J. J.; F. G. R. Gimblett; A. C. Gray; M. B. Kenny; R. A. Roberts and K. S. W. Sing, (1986)
Comparative studies of solute adsorption by charcoal cloths, Proc. of 4th Int. Carbon Conf., Baden-Baden, pp. (321-323).

Frick, G. and J. V. Sommerfeld, (1973)
Solar stills of inclined evaporating cloth, Solar Energy, Vol. 14, No. 4, pp. (427-431).

Gandhidasan, P., (1983)
Theoretical study of tilted solar still as a regenerator for liquid desiccants, Energy Convers. Mgmt., Vol. 23, No. 2, pp. (97-101).

Garg, H. P. (1991)
Solar desalination techniques, First Exposition and Symposium for New and Renewable Energy Equipment, Tripoli, Libya (4-6) May 1991, pp. (1-38).

Gomkale, S. D. and R. I. Datta, (1973)
Some aspects of solar distillation for water purification, Solar Energy, Vol. 14, No. 4, pp. (387-392).

Gupta, R. A.; S. N. Rai and G. N. Tiwari, (1988)
Transient analysis of double basin solar still with intermittent flow of waste hot water in night, Energy Convers. Mgmt., Vol. 28, No. 3, pp. (245-249).

Hirschmann, J. R., (1975)
Solar distillation in Chile, Desalination, Vol. 17, No. 1, pp. (17-30).

Hitchcock, S. J. ; B. McEnaney and S. J. Watling, (1983)
Fibrous active carbons from coir, J. Chem. Tech. Biotechnol, Vol. 33A, pp. (157-163).

Hollands, K. G. T., (1971)
A concentrator for thin film solar cells, Solar Energy, Vol. 13, No. 2, pp. (149-163).

Hollands, K. G. T., T. E. , Unny, G. D. Raithby and L. Konicek, (1976)
Free convective heat transfer across inclined air layers, J. Heat Transfer, Vol. 98 ,pp. (189-193).

Howe, E. D. and N. Dekker, (1974)
Fundamentals of Water Desalination, Academic Press, New York.

Howe, E. D. and B. W. Tleimat, (1977)
Fundamentals of water desalination, Chp. 20 in Soalr Energy Engineering, Edited by A. A. M. Sayigh, Academic Press, New York, pp. (431-464).

Howell, J. R. and R. B. Bannerot, (1975)
The evaluation of surface geometry modification to improve the directional selectivity of solar energy collectors. Report of National Science Foundation, NSF/RANN/SE/CI-41003/74/4.

Incropera, F. P. and D. P. De Witt, (1985)
Fundamentals of Heat and Mass Transfer, 2nd edition, John Wiley, New York.

Issa, M., (1989)
An investigation into the performance of a V-trough solar concentrator, Int. J. Solar Energy, Vol. 7, No. 3, pp. (181-189).

Jadecal Signs Limited, Denmark Street, Cordwallis Estate, Maidenhead, Berks.,
SL6 7BN, U. K.

Jundi, Z. M., (1982)
Portable tilted solar stills, Sunworld, Vol. 6, No. 1, pp. (7-9).

Kamaraj, G. ; K. N. Seetharamu; V. Ganesan and K. N. Rao, (1980)
A theoretical study of heat and mass transfer processes in horizontal-plane and inclined stepped solar stills, Alter. Energy Sources, Vol. 3, No. 3, pp. (13-17).

Kettani, M. A., (1979)
Review of solar desalination, Sunworld, Vol. 3, No. 3, pp. (76-85).

Khalifa, A. N., (1985)
Evaluation and energy balance study of a solar still with an internal condenser, J. Sol. Energy Res. (Iraq), Vol. 3, pp. (1-11).

Kiatsiriroat, T; S. C. Bhattacharya and P. Wibulswas, (1987)
Transient simulation of vertical solar still, Energy Convers. Mgmt., Vol. 27, No. 2, pp. (247-252).

Lawrence, S. A. ; S. P. Gupta and G. N. Tiwari, (1988)
Experimental validation of thermal analysis of solar still with dye, Int. J. Solar Energy, Vol. 6, No. 5, pp. (291-305).

Lawrence, S. A. and G. N. Tiwari, (1990)
Theoretical evaluation of solar distillation under natural circulation with heat exchanger, Energy Convers. Mgmt., Vol. 30, No. 3, pp. (205-213).

Lof, G. O. G., (1980)
Solar distillation, Chp. 11 in Principles of Desalination, 2nd ed. Part B, Edited by K. S. Spiegler and A. D. K. Laird, Academic Press, New York, pp. (679-723).

Madhuri and G. N. Tiwari, (1985)
Performance of solar still with intermittent flow of waste hot water in the basin, Desalination, Vol. 52, pp. (345-57).

Mahdi, J. T., (1987)
Solar Desalination, Internal report, Dept. of Mech. Eng., Brunel University.

Mahdi, J. T.; B. E. Smith and J. Freeman, (1990)
Investigation of materials for experimental wick-type solar stills, 1st World Renewable Energy Congress (23-28) Sep., Vol. 2, pp. (1329-1333).

Mahdi, J. T., (1992)
Transient performance analysis of a flat plate wick type solar still, Second Exposition and Symposium for New and Renewable Energy Equipment, Tripoli, Libya (25-27) May 1992, (accepted).

Malik, M. A.; G. N. Tiwari; A. Kumar and M. S. Sodha, (1982)
Solar Distillation, Pergamon Press, Oxford.

Mannan, K. D. and R. B. Bannerot, (1978)
Optimal geometries for one-and two-faced symmetric side-wall booster mirrors, Solar Energy, Vol. 21, No. 5, pp. (385-391).

Mazumder, R. K. and M. Hussain, (1991)
Optical and thermal performance testing of a discrete mirror, seasonally adjusted, linear solar concentrator with tubular absorber, Energy Convers. Mgmt, Vol. 31, No. 2, pp. (187-192).

Meyer, B. A. ; J. W. Mitchell and M. M. El-Wakil, (1982)
Convective heat transfer in Vee-trough linear concentrators, Solar Energy, Vol. 28, No. 1, pp. (33-40).

Morse, R. N. and W. R. W. Read, (1968)
A rational basis for the engineering development of a solar still, Solar Energy, Vol. 12, No. 1, pp. (5-17).

Mousa, M. M.; F. M. Abdelfattah and I. A. Saker, (1980)
Double exposure solar still, Proceeding of the Int. Symp. Workshop on Solar Energy pt. III, Cairo Egypt (16-22) June 1978, pp. (1546-1560).

Moustafa, S. M. ; G. H. Brusewitz and D.M.Farmer, (1979)
Direct use of solar energy for water desalination, Solar Energy, Vol. 22, No. 2, pp. (141-148).

Narusawa, U and G. S. Springer, (1975)
Measurement of evaporation rates of water, Journal of colloid and Interface Sciences, Vol. 50, No. 2, pp. (392-395).

Norton, B; S. A. M. Burek; C. J. B. Girod; D. E. Prapas and S. D. Probert, (1988)
Forward scattering of insolation through transparent and translucent materials, Proc. Solar Optical Materials, Oxford, U. K. (12-13) April 1988, edited by M. G. Hutchins, Pergamon Press, pp. (39-46).

Ordance Survey, (1988)
West London Area Map, Landranger 176.

Pandey, G. C., (1983)
Effect of dye on the performance of a double-basin solar sill, Int. J. Energy Res., vol. 7, No. 4, pp. (327-332).

Pandey, G. C., (1984)
Effect of dried and forced air bubbling on the partial pressure of water vapour and the performance of solar sill, Solar Energy, Vol. 33, No.1, pp. (13-18).

Proctor, D., (1973)
The use of waste heat in a solar still, Solar Energy, Vol. 14, No. 4, pp. (433- 449).

Rabl, A., (1976)
Comparison of solar concentrators, Solar Energy, Vol. 18, No. 2, pp. (93-111).

Rabl, A., (1985)
Active Solar Collectors and Their Applications, Oxford University Press, Oxford.

Rai, S. N.and G. N. Tiwari, (1983)
Single basin solar still coupled with flat plate collectors, Energy Convers. Mgmt, Vol. 23, No. 3, pp. (145-149).

Rai, S. N.; D. K. Dutt and G. N. Tiwari, (1990)
Some experimental studies of a single basin solar still, Energy Convers. Mgmt, Vol. 30, No. 2, pp. (149-153).

Rajvanshi, A. K., (1981)
Effects of various dyes on solar distillation, Solar Energy, Vol. 27, No. 1, pp. (51-65).

Rogers, G. F. C. and Y. R. Mayhew, (1980)
Thermodynamic and Transport Properties of Fluids, S.I. Units, 3rd edition, Basil Blackwell, Oxford.

Sakr, I. A. and M. A. Khalil, (1976)
Economical investigation of solar water distillation in Egypt, Proc. Int. Symp. on Water from the Sea, 5th, Event of the EurFed of Chem. Eng., 162 nd, Alghere, Italy, Vol. 2, pp. (477-482).

Sayigh, A. A. M., (1977)
Solar Energy Engineering, Published by Academic Press, New York.

Sayigh, A. A. M. and El-Salam, E. M. A. , (1977)
Optimum design of a single slope solar still in Riyadh, Saudi Arabia, Revue d' Heliotechnique, Vol.1, pp. (40-44).

Selcuk, M. K., (1979)
Analysis, development and testing of a fixed tilt solar collector employing reversible Vee-trough reflectors and vacuum tube receivers, Solar Energy, Vol. 22, No. 5, pp. (413-426).

Simonson, J. S., (1984)
Computing Methods in Solar Heating Design, Macmillan Press, London.

Singh, A. K. and G. N. Tiwari, (1992)
Performance study of double effect distillation in a multiwick solar still, Energy Convers. Mgmt, Vol. 33, No. 3, pp. (207-214).

Sodha, M. S.; J. K. Nayak; G. N. Tiwari and A. Kumar, (1980)
Double basin solar still, Energy Convers. Mgmt, Vol. 20, No. 1, pp. (23-32).

Sodha, M. S.; A. Kumar ; G. N. Tiwari and G. C. Pandey, (1980b)
Effect of dye on the still performance, Applied Energy, Vol. 7, pp. (147-162).

Sodha, M. S.; A. Kumar; G. N. Tiwari and R. C. Tyagi, (1981)
Simple multiple wick solar still: Analysis and performance, Solar Energy, Vol. 26, No. 2, pp. (127-131).

Sodha, M. S.; A. Kumar and G. N. Tiwari, (1981)
Utilization of waste hot water for distillation, Desalination, Vol. 37, No. 3, pp. (325-341).

Squires, G. L. , (1968)
Practical Physics, McGraw-Hill, London.

Szulmayer, W. (1973)
Solar stills with low thermal inertia, Solar Energy, Vol. 14, No. 4, pp. (415-421).

Tabor, H., (1975)
Solar ponds as heat source for low-teperature multi-effect distillation plants, Desalination, Vol. 17, No. 3, pp. (289-302).

Talbert, S. G.; J. A. Eibling and G. O. G. Lof, (1970)
Manual on Solar Distillation of Saline Water. Office of Saline Water , Research and Development Progress Report, 546.

Tamimi, A., (1987)
Performance of a solar still with reflectors and black dye, Solar and Wind Technology, Vol. 4, No. 4, pp. (443-446).

Tanaka, K.; A. Yamashita and K. Watanabe, (1981)
Experimental and analytical study of the tilted wick-type solar still, Solar World Forum, Proce. of the ISES congress, Brighton, England, (23-28) Aug. 1981, edited by D. O. Hall and J. Morton, Pergaman Press, Vol. 2 pp. (1087-1091).

Telkes, M., (1953)
Fresh water from sea water by solar distillation, Industrial and Engineering Chemistry, Vol. 45, No. 5, pp. (1108-1114).

Tiwari, G. N. and M. A. S. Malik, (1982)
Solar distillation, Chp. 5 in Reviews of Renewable Sources, Edited by M. S. Sodha *et al.*, Wiley Eastern, pp. (324-357).

Tiwari, G. N., (1984)
Demonstration plant of a multi-wick solar still, Energy Convers. Mgmt., Vol. 24, No. 4, pp. (313-316).

Tiwari, G. N. and V. S. V. Bapeshwararao, (1984)
Transient performance of a single basin solar still with water flowing over the glass cover, Desalination, Vol. 49, No. 3, pp. (231-241).

Tiwari, G. N.; S. B. Sharma and M. S. Sodha, (1984)
Performance of a double condensing multiple wick solar still, Energy Convers. Mgmt., Vol. 24, No. 2, pp. (155-159).

Tiwari, G. N., (1985)
Enhancement of daily yield in a double basin solar still, Energy Convers. Mgmt., Vol. 25, No.1, pp. (49-50).

Tiwari, G. N.; Madhuri and H. P. Garg, (1985)
Effect of water flow over the glass cover of a single basin solar still with an intermittent flow of waste hot water in the basin, Energy Convers. Mgmt., Vol. 25, No. 3, pp. (315-322).

Tiwari, G. N. and V. S. B. Rao, (1985)
A multi-wick solar distillation plant, Solar Engineering, Edited by R. B. Bannerot, The American Society of Mechanical Engineers, pp. (373-380).

Tiwari, G. N. and Y. P. Yadav, (1985)
Economic analysis of a G.I. sheet multi-wick solar distillation plant, Energy Convers. Mgmt., Vol. 25, No. 4, pp. (423-425).

Tiwari, G. N. and Y. P. Yadav, (1987)
Comparative designs and long term performance of various designs of solar distiller, Energy Convers. Mgmt., Vol. 27, No. 3, pp. (327-333).

Tiwari, G. N.; S. P. Gupta and A. Kumar, (1988)
Analytical model of inverted multiwick solar still, Int. J. Solar Energy, Vol. 6, No. 2, pp. (139-150).

Tiwari, G. N. and A. Kumar, (1988)
Nocturnal water production by tubular solar stills using waste heat to preheat brine, Desalination, Vol. 69, No. 3, pp.(308-318).

Tiwari, G. N.; S. A. Lawrence and S. P. Gupta, (1989)
Analytic study of multi-effect solar still, Energy Convers. Mgmt, Vol. 29, No. 4, pp. (259-263).

Tiwari, G. N. and N. K. Dhiman, (1991)
Performance study of a high temperature distillation system, Energy Convers. Mgmt, Vol. 32, No. 3, pp. (283-291).

Tiwari, G. N. and S. A. Lawrence, (1991)
New heat and mass transfer relations for a solar still, Energy Convers. Mgmt, Vol. 31, No. 2, pp. (201-203).

Tiwari, G. N.; C. Sumegha and Y. P. Yadav, (1991)
Effect of water depth on the transient performance of a double basin solar still, Energy Convers. Mgmt, Vol. 32, No. 3, pp. (293-301).

Tleimat, W. and E. D. Howe, (1966)
Nocturnal product of solar distillers, Solar Energy, Vol. 10, No. 2, pp. (61-66).

Tleimat, B. W., (1980)
Characteristics of saline water as related to freezing processes, in Chp. 7 in Principles of Desalination, part B, 2nd edition, edited by K. S. Spiegler and A. D. K. Laird, Academic Press, New York, pp. (367-374).

Walton, J. P. R. B. and N. Quirke, (1988)
Fluids in pores: amolecular simulation study, Carbon 88 Conf. (18-23) Sept. 1988, U.K., pp. (513-515).

Yadav, Y. P., (1990)
Indoor simulation of a basin-type solar still, Int. J. Solar Energy, Vol. 8, No. 1, pp. (31-40).

Yeh, H. M. and L. C. Chen, (1985)
Basin-type solar distillation with air flow through the still, Energy, Vol.10, No. 11, pp. (1237-1241).

Yeh, H. M. and L. C. Chen, (1986)
The effect of climatic design and operational parameter on the performance of wick-type solar distillers, Energy Convers. Mgmt., Vol. 26, No. 2, pp. (175-180).

Yeh, H. M. and L. C. Chen, (1987)
Experimental studies on double effect solar distillers, Energy, Vol. 12, No. 12, pp. (1251-1256).

APPENDIX A1

BASIN-TYPE SOLAR STILLS

In addition to what is mentioned in section 1.2 about basin type solar stills, a thorough review of the various designs of the basin-type still has given by Eibling *et al.* (1971), who also included a good discussion of the various factors which affect the productivity of such stills. That work was slightly modified by Morse and Read (1968) who considered the heat and mass transfer relationships which govern the operation of a solar still in the unsteady state and expressed the various heat fluxes as functions of the cover temperature. The analysis was then used to find the effects on output changes in various parameters such as wind speed, ambient temperature and heat loss from the base.

Several attempts have been made to improve the efficiency of basin type solar stills by using: (i) air flow through the still to carry the vapour to an external condenser Yeh and Chen (1985), (ii) forced bubbling of ambient air inside a solar still Pandey (1984), (iii) the latent heat of evaporation in either multieffect system Dunkle (1961) and Tiwari *et al.* (1989), double basin solar still Nayak (1980) and Sodha *et al.* (1980) or for preheating the brine Malik *et al.* (1982), Yeh and Chen (1987) and Tiwari *et al.* (1989), (iv) black and coloured dyes dissolved in

the brine Sodha *et al.* (1980b), Rajvanshi (1981), Pandey (1983), Tamimi (1987) and Lawrence *et al.* (1988), (v) waste hot water flowing through the still directly Madhuri and Tiwari (1985) and Yadav (1990), or through a heat exchanger Proctor (1973), (vi) heat provided to the stills by solar pond Tabor (1975) or by a flat plate solar collector either directly, by feeding the hot water Rai and Tiwari (1983) and Rai *et al.* (1990) and with and without water flowing on the cover Dutt *et al.* (1988), or through a heat exchanger Lawrence and Tiwari (1990) and Tiwari and Dhiman (1991), (vii) pieces of ordinary wood charcoal in the basin of a typical still Akinsete and Duru (1979) and blackened jute cloth floating over the water having wool knitted in it Rai *et al.* (1990) and (viii) an extended internal condenser Khalifa (1985).

Since solar stills are needed to work out of the sunny hours, so nocturnal production of distilled water has been studied by numerous investigators Tleimat and Howe (1966), Sodha *et al.* (1981), Tiwari and Dhiman (1985), Madhuri and Tiwari (1985) and Gupta *et al.* (1988). They used waste hot or warm water input from either power plants or chemical plants. In this process, stills can work even in the absence of sunlight. Tleimat and Howe (1966) compared experimentally the performance ofadeep basin solar still and that of the tilted-tray solar still. They studied also the nocturnal operation of a tubular glass solar still. They indicated a substantial increase of distillate production from the continuous addition of waste hot water to the still. This is a function of flow rate, feed-water temperature, evaporating and condensing areas and ambient temperature. Sodha *et al.* (1981)

presented an analysis of the performance of a solar still using the linearised Dunkle's relations for heat and mass transfer. Two modes of waste hot water utilisation have been considered:
(a) a flow of the waste hot water of constant rate through the solar still and (b) feeding the waste hot water once a day. A single basin solar still with intermittent flow of waste hot water has been analysed by Madhuri and Tiwari (1985). They discussed also the effect of various parameters on the performance of the still. Tiwari *et al.* (1985) also incorporated the analysis with the effect of water flow over the glass cover of the still. A transient analysis of a double basin solar still, incorporating the effect of intermittent flow of waste hot water into the lower basin, has been presented by Gupta *et al.* (1988). They found that the yield increases with flow rate in higher temperatures. Nocturnal production in tubular solar stills has been studied theoretically by Tiwari and Kumar (1988). Expressions for different parameters have been given.

Several investigators have also looked at the effect of floating porous pads on the surface of water so that the brine depth is effectively reduced such as life raft type solar distiller designed and tested in summer of 1943 by Telks (1953). Bloemer and Eibling (1966) reported an increase in productivity by 10 percent over the similar shallow basin stills. Later Szulmayer (1973) reported tests on flotation of a black liner with outputs of 2.934 l/m^2.day. Akinsete and Duru (1979) have studied the effect of charcoal pieces on performance of a basin still.

Charcoal is wettable and has a large absorption coefficient for solar radiation. It scatters rather than reflects the solar radiation. They concluded that the effect of charcoal pieces, floated on the water surface, is most pronounced in the morning and on cloudy days i.e. cases of low beam radiation.

A detailed study of digital simulation of the transient and experimental performance of solar stills have been published by Cooper (1969,1973). The factors affecting the absorption of solar radiation in solar stills by the reflecting layers of salt on the water surface and still liner have been discussed by Cooper (1972).

APPENDIX A2
INSTRUMENTS

A2.1 SOLARIMETERS

Two types of solarimeter were used 1) Kipp and Zonen solarimeter, 2) Delta-T-Devices tube solarimeter. The electrical output signal of both is produced by a copper constantan thermopile which lies under black and white areas. Signal magnitude is proportional to the difference in temperature, since the black areas absorb most short wave radiation and the white areas do not. A glass cover limits their response to within the range 0.35 to 2.5 microns, which involves visible to the near infrared wavelengths. The time constant stated by the manufacturer of the tube solarimeter is 5 seconds.

A2.1.1 Kipp and Zonen dome solarimeters

1) Dome solarimeter No. 1

Serial No. is CM5-774038

Calibration factor 12.677 mV/kWm^{-2} according to the certificate shown below.

Wavelength range 300 - 2500 nm.

Accuracy within 1.5 %.

Total response time approximately 10 s.

Screen diameter 30 cms.

Height 11 cms.

Weight 3.7 kg including base and screen.

Weight of solarimeter only 0.8 kg.

2) Dome solarimeter No. 2

Serial No. is CM5-752429.

Calibration factor 10.623 mV/kWm^{-2} according to the certificate shown below.

The other specifications are as the above one.

A2.1.2 Delta-T-Devices tube solarimeter

Serial No. is TSM-6640

Calibration factor 13.78 mV/kWm^{-2} measured as shown in Fig. 3.2.1.

Wavelength range 350 - 2500 nm.

Total response time approximately 5 s.

Length 380 mm.

Diameter 12 mm.

Detector area 320 mm x 8 mm

A2.2 THE OVEN

Medical Electronics Ltd., Industrial Division

Type M. P. C.

A2.3 HEAT AND HUMIDITY CHAMBER

Environmental Test Equipment Dept., Chiswick Flyover, Great West Road, London W4.

Model HCVH14.

Serial No. SO4145

72 cm x 72 cm x 68 cm = 0.3525 m^3 capacity

Test parameters:

Temperatures -65 to +150 ±5°C

Humidity range at temp. (30 - 85) °C is (30 - 95)%

Fully automatic through the range.

APPENDIX A3

CALCULATION OF SOLAR REFLECTANCE (ρ_s)

A3.1 WAVELENGTH OF ENERGY BANDS

Solar reflectance of the samples were calculated from total reflectance data in the solar region (0.3 - 2.5) µm using selected ordinates for air mass 2 and 23 km visibility in twenty equal increments of energy given by Weibelt and Henderson (1979) from Duffie and Beckman (1980), as shown in Table A3.1.

Table A3.1. Selected ordinates in solar region (0.3 - 2.5) µm.

Energy Band Number	Wavelength Range Micron	Midpoint Wavelength Micron
1	0.300 - 0.434	0.402
2	0.434 - 0.479	0.458
3	0.479 - 0.517	0.498
4	0.517 - 0.557	0.537
5	0.557 - 0.595	0.576
6	0.595 - 0.633	0.614
7	0.633 - 0.670	0.652
8	0.670 - 0.710	0.691
9	0.710 - 0.752	0.731
10	0.752 - 0.799	0.775
11	0.799 - 0.845	0.821
12	0.845 - 0.894	0.869
13	0.894 - 0.975	0.923
14	0.975 - 1.035	1.003
15	1.035 - 1.101	1.064
16	1.101 - 1.212	1.171
17	1.212 - 1.310	1.258
18	1.310 - 1.603	1.532
19	1.603 - 2.049	1.689
20	2.049 - 5.000	2.292

A3.2 COMPUTER PROGRAM

Printout of the computer program used to calculate solar reflectance of the samples measured by Lambda-9 Perkin Elmer spectrophotometer and traced by a cursor connected to a digitizer.

```
C•••••••••••••••••••••••••••••••••••••••••••••••••••••••••••••••
C      THIS PROGRAM CALCULATES SOLAR REFLECTANCE OF SAMPLES      •
C      MEASURED BY LAMBDA-9 PERKIN-ELMER SPECTROPHOTOMETER AND   •
C      TRACED BY A CURSOR CONNECTED TO A DIGITIZER               •
C•••••••••••••••••••••••••••••••••••••••••••••••••••••••••••••••
C
      dimension lambda(30),rou(30),x(30),y(30)
      write (6,10)
C
C
C
C     READ DATA RECORDED IN FILE NAMED 'iunit' FROM A DIGITIZER C AS 'X' AND
'Y' COORDINATES.
C
      read (5,*)iunit
    do 11 i = 1,20
          read (iunit,20) x(i),y(i)
11        continue
      write(iunit,30)
      write(iunit,40)

C
    do 22 i = 1,20
C
C     WRITE DOWN THE VALUES OF 'x' AND 'y' IN mm.
C
          write(iunit,50) x(i),y(i)
22    continue
      rout = 0.0
```

```
C       CALCULATE THE WAVELENGTH CORRESPONDING TO EACH 'x' AND
C       THE REFLECTANCEC CORRESPONDING TO EACH 'y'.
C
            do 33 i = 1,20
                lambda(i) = x(i)*10.0+300.0
                rou(i) = y(i)/2.0
                rout = rout+rou(i)
33          continue

C
C       CALCULATETHE SOLAR REFLECTANCE OF THE MEASURED SAMPLE
C       FROM THE AVERAGE OF REFLECTANCES OF THE TWENTY INCREMENTS OF
ENERGY.
C
            rouav = rout/20.0
            write(iunit,60)
            write(iunit,70)
             do 44 i = 1,20
C
C       WRITE DOWN THE WAVELENGTH 'LAMBDA' IN MICRONS
C       AND THE REFLECTANCE PERCENTAGE.
                    write(iunit,80) lambda(i),rou(i)
44           continue
            write(iunit,90)
            write(iunit,100)
C
C       WRITE DOWN THE SOLAR REFLECTANCE OF THE SPECTRUM
C       OF THE MEASURED SAMPLE.
            write(iunit,110) rouav
            write(iunit,120)

C
            STOP
C
10          format("iunit")
20      format(1x,f6.1,2x,f6.1)
30      format(' ',3x,'λ mm',3x,'ρ %')
```

```
 40   format(3x,"-----",3x,"-----")
 50   format(2x,f5.1,4x,f6.1)
 60   format(/1x,"LAMBDA/MICRON",2x,"ROU/ %")
 70   format(1x,"============",2x,"=======")
 80   format(3x,i6,7x,f5.1)
 90   format(//2x,"REFLECTIVITY")
 100  format(2x,"----------")
 110  format(4x,f5.1)
 120  format(12x,"**********")
C
      END
```

APPENDIX A4

SAMPLE OF CALCULATED EFFICIENCY OF THE STILL

The still efficiency (η) was calculated according to the relation:

$$\eta = \frac{\sum_{i=1}^{n} D_i h_{fg,i}}{\sum_{i=1}^{n} I_i} \qquad (A.4.1)$$

where:

D_i is the mass of distillate collected per 30 minutes ($kg/m^2.h$).

$h_{fg,i}$ is the latent heat of evaporation (J/kg).

I_i is the radiant energy incident on the glass cover ($J/m^2.h$).

n is number of the intervals, the distillate was collected in.

The data were collected by the data logger every five minutes as shown in Table A4.1 in addition to the manual measurement of the distilled water produced every thirty minutes. The arithmetic means of the recorded values over a larger period of time were used in calculating the efficiency of the solar still.

The manual working out the efficiency started by determination of the average absorber temperature of four thermocouples of channels 16, 17, 18 and 19 for five minutes interval and then the average of six intervals to get the average in thirty minutes, e.g. for the interval from 11.00 to 11.30 am the five minutes averages are 66.9, 67.1, 67.6, 68.0, 65.9 and 69.0. Hence, their average is 67.4 °C for which the latent heat of distilled water evaporation can be calculated as:

$$h_{fg} = 1000 \times (2501.67 - 2.389\ T_{abs}) \qquad (A.4.2)$$

where T_{abs} in °C and h_{fg} in (J/kg), Elsayed (1983)

i.e.

$$h_{fg} = 1000 \times (2501.67 - 2.389 \times 67.4)$$

$$h_{fg} = 2340600\ J/kg$$

The five minutes average of the measured solar irradiance is recorded by the data logger as it in channel No.2 in kW/m^2. The average of thirty minutes was determined by the arithmetic means of six intervals (5 mins. each) i.e.

$$\frac{0.898 + 0.906 + 0.921 + 0.922 + 0.913 + 0.921}{6} = 0.9135\ kW/m^2$$

This was converted to ($J/m^2.h$) by multiplying by 3600 sec/h to become 3288600 $J/m^2.h$.

The mass of distilled water produced from 11.00 to 11.30 am was 125.9 gm which is equivalent to 0.699 kg/m^2.h (using A = 0.36 m^2).

Hence, the efficiency is

$$\eta = \frac{0.699 \times 2340600}{3288600}$$

$$\eta = 0.4975$$

or

$$\eta = 0.498$$

and same for the other intervals. But when the still efficiency for n intervals is wanted Eq. A.4.1 can be applied i.e. for the test on 25/7/1990 which was seven hours long (fourteen intervals) the efficiency is

$$\eta = \frac{\sum_{i=1}^{n} D_i h_{fg,i}}{\sum_{i=1}^{n} I_i} = \frac{10876111}{20381600}$$

$$\eta = 0.534$$

Table A4.1. Print out of the data logger for the still test on 25/7/1990. It was carried out for the still without the solar concentrator, outdoors.

DELTA-LOGGER Data-Typing Utility
Typing Data File: JL7.DAT

| - over-run error
$ - noisy reading
\ - o/s limits reading
& - over-range reading

Serial Number: DL 6902
Experiment: CCT
Started Logging: 25/07 09:30:00
Data Collected: 25/07 17:21:43
Data Type: TIMED

Channel Number	1	2	3	4	5	6	7	8	9	10
Sensor Type	TMP	VLT	VLT	TSR	TCK	TCK	TCK	TCK	TCK	TCK
Label	COD	KIP1	KIP2	TSA	TC0	TC1	TC2	TC3	TC4	TC5
Unit	deg C	kWm-2	kWm-2	Wm-2	deg C	deg C	deg C	deg C	deg C	deg C
Minimum Value	22.5	0.116926	.557541E-2	.712331E-2	25	22.5	39	38.7	37.9	2111
Maximum Value	27.4	49.4	49	25.2	30.8	29.3	57.6	61.4	59.6	-2116
25/07 09:30:00	4.37E	.421711E-26	.236741E-36	2.32E-26	5.11E	4.51E	8.11E	7.75E	7.75E	409
25/07 09:35:00	22.7	0.723979	.422352E-2	0.872522	25	22.8	43.9	39.7	43.9	2281
25/07 09:40:00	22.9	0.750365	.424121E-2	0.9216	26.2	23.1	41.6	41.4	41.4	2291
25/07 09:45:00	21.9	0.77116	.522352E-2	0.9552	25.3	22.5	42	42.9	41.8	2201
25/07 09:50:00	22.8	0.732251	.724131E-2	1.05557	25.5	23.1	41.2	44.2	41.3	2291
25/07 09:55:00	21.7	0.757234	.492532E-2	1.11527	25.4	23.1	42.2	45.7	42.3	2224
25/07 10:00:00	22.3	0.827792	.651522E-2	1.25457	25.3	23.2	42.3	47.3	43.3	2281
25/07 10:05:00	22	0.82417	.730551E-2	[illegible]	25.4	22.6	42.5	48.5	45.2	2281
25/07 10:10:00	22	0.84127	.724152E-2	[illegible]	25	22.3	45.8	49.3	45	2271

Channel Number	11	12	13	14	15	16	17	18	19	20
Sensor Type	TCK	TCK	TCK	TCK	TCK	TCK	TCK	TCK	TCK	TCK
Label	TC6	TC7	TC8	TC9	TC10	TC11	TC12	TC13	TC14	TC15
Unit	deg C	deg C	deg C	deg C	deg C	deg C	deg C	deg C	deg C	deg C
Minimum Value	35.4	36.5	36.7	37.5	21.5	45.4	45.4	45.9	46.7	41.5
Maximum Value	59	63.3	53.2	52.9	30.2	73	69.4	69.4	72.1	62.4
25/07 09:30:00	7.95E	9.35E	7.82E	7.75E	4.39E	10.9E	10.6E	10.3E	10.6E	3.25E
25/07 09:35:00	42	43.7	39.7	42.6	22.5	55.7	53.4	51.9	51.1	42.4
25/07 09:40:00	41.9	45	43.4	43.9	23.1	57.4	54.6	53.1	56	43.9
25/07 09:45:00	42.2	45.2	43.3	44.5	22.3	53.6	55.7	54.3	57.5	45.2
25/07 09:50:00	42.6	45.6	42.5	44.6	22.5	53.5	55.3	55.4	58.6	45.4
25/07 09:55:00	43	47.5	42.2	45.2	22.5	56.5	57	55.6	53.3	47.4
25/07 10:00:00	46.5	50.2	42.6	47.5	23.2	61.8	57.7	57.5	60.4	49.3
25/07 10:05:00	46.3	52.7	45.2	50	24	62.5	59.6	59.4	62.4	49.4

Table A4.1. Print out of the data logger for the still test on 25/7/1990. It was carried out for the still without the solar concentrator, outdoors. (continued)

	46.8	49.4	45.8	33.8	23.2	52.6	63.2	59.7	62.4	53.2
25/07 10:15:00	21.9	0.831353	.623633-2	1.33507	26.2	23.4	47.4	58.4	41.1	2281
	48.7	51.4	47.8	53.5	23.9	63.1	61.3	60.7	63	51.1
25/07 10:20:00	22.3	0.841228	.630051-2	1.4324	26.8	24	48.6	58.9	49.8	2281
	49.8	53.2	49	52.3	25	64.6	62.2	61.8	63.9	52
25/07 10:25:00	22.5	0.854461	.573578-2	1.47893	27.1	24.1	49.6	51.5	49.9	2281
	50	53.5	48.9	52.7	25.3	65.4	62.9	62.1	64.9	52.8
25/07 10:30:00	22.6	0.856354	.855978-2	1.45667	27	24.1	50	52.1	49.1	2281
	49.8	54.1	48.1	52.4	25.3	65.8	63.1	62.2	65.3	53.6
25/07 10:35:00	22.9	0.856985	.912458-2	1.4464	27.1	24.2	58.7	52.7	50.5	2281
	53.8	55.4	49.1	54.2	24.8	66.6	63.8	63	66.2	54.4
25/07 10:40:00	22.9	0.8715	0.100725	1.43733	27.1	24.1	51.2	53.4	49.4	2281
	53.4	55.1	48.3	53	25.5	67.1	64.1	63.2	66.5	55.2
25/07 10:45:00	22.8	0.833159	.968548-2	1.4326	28.3	24.1	51.5	53.8	49.1	2281
	53.6	55.4	49	53.8	24.8	67.6	64.4	63.7	66.9	55.7
25/07 10:50:00	22.7	0.834218	.931208-2	2.4264	25.7	24	51.8	54.2	49.9	2281
	53.3	55.2	49.2	52.8	24.5	67.8	64.4	64	67.1	56.2
25/07 10:55:00	22.9	0.854849	.383048-2	1.4288	27.2	24.5	52	54.6	51.8	2281
	52.6	57.4	52.5	56.6	25.8	68.3	64.7	64.5	67.5	56.5
25/07 11:00:00	23.2	0.833587	.322458-2	2.4128	27.2	24.6	52.7	55.3	53.6	2281
	52	57.2	50.3	54.6	25.7	68.8	65.3	65	68.2	57
25/07 11:05:00	23.3	0.858204	.392632-2	1.4276	27.1	24.5	52.9	55.7	58.2	2281
	51.3	57.4	53	54.4	25.7	68.7	65.4	65.2	68.3	57.4
25/07 11:10:00	23.3	0.856208	.765358-2	1.44	27.4	24.6	53	55.9	51.3	2281
	52.8	58.4	51.5	55.9	26	69.1	65.6	65.4	68.4	57.7
25/07 11:15:00	23.4	0.820723	.648338-2	2.47347	27.3	24.6	53.3	56.2	52.6	2281
	53.1	58.6	51.6	56.9	25.8	69.5	66.1	65.9	69	57.9
25/07 11:20:00	23.5	0.821935	.658238-2	1.47573	27.8	24.9	53.8	55.6	53.1	2281
	56	59	52.2	56.6	25.8	69.9	66.4	66.2	69.3	58.3
25/07 11:25:00	23.7	0.812529	.724138-2	2.45547	28.2	25.3	54.2	57.2	56	2281
	55.1	60.5	52.6	58.7	27.6	67.7	64.2	64.2	67.4	58.1
25/07 11:30:00	23.9	0.820723	.572578-2	1.45667	28.4	25.5	54.9	57.7	56.5	2281
	55.6	60.5	52.9	59	28	70.9	67.4	67.3	70.4	59.2
25/07 11:35:00	23.3	0.832451	.633468-2	2.45547	23	24.6	55.1	58.2	51.5	2281
	53.6	59.8	52.5	56.1	25.8	71.1	67.4	67.4	70.2	59.7
25/07 11:40:00	23.7	0.844703	.582938-2	2.48207	28	25.3	58.8	59.2	58.2	2281
	55.2	60.4	53.8	58.3	26.7	71.2	67.5	67.5	72.4	59.9
25/07 11:45:00	24	0.831851	9.21948-2	1.4576	28.8	25.8	55.2	59.6	55.8	2281
	57.2	62.1	56.1	61.1	28.5	71.7	67.9	68.2	71	60.2
25/07 11:50:00	24	0.828289	.375338-2	1.4232	28.2	24.9	55.7	59.3	52.9	2281
	54.9	62.6	52.9	57.5	[illegible]	71.8	66.2	68.2	71.2	60.5
25/07 11:55:00	23.7	0.842441	.244838-2	2.43723	28	25.1	55.3	59.4	53	2281
	54.9	60.4	59.2	58.3	28	71.8	68	68	70.9	62.7
25/07 12:00:00	23.3	0.854159	.272228-2	1.44233	28.9	25.7	55.4	59.4	58.9	2281
	56.6	62.1	55.3	60.2	27.3	72	69.2	68.2	72	62.5
25/07 12:05:00	24.3	0.832244	.168788-2	1.46287	23	25.3	56.2	53.3	58.7	2281
	57.2	62.5	55.2	55.2	23	72.4	68.3	68.9	71.6	62
25/07 12:25:00	24.3	2.843402	.558748-2	1.4392	23.6	25.6	56.9	58.2	52.8	2281

Table A4.1. Print out of the data logger for the still test on 25/7/1990. It was carried out for the still without the solar concentrator, outdoors. (continued)

	55.3	61.2	53.2	55.2	26.9	72.2	61.7	61.6	71.1	61.4
25/07 12:15:00	24.4	0.937761	.573578-2	1.43247	28.5	25.4	56.5	60.2	52.2	[illegible]
	54.9	61	53	57	27	72	61.5	61.4	70.7	61.5
25/07 12:20:00	24.4	0.969215	.987758-2	1.51893	28.5	25.6	56.2	60.2	53.8	[illegible]
	55.4	61.2	53.8	59	26.5	72.2	61.5	61.4	71	61.5
25/07 12:25:00	24.5	0.953528	0.10176	1.5312	29.3	26.3	56.5	60.2	56.9	[illegible]
	57.8	62.9	56.5	61.3	28	72.6	69	69	71.6	61.6
25/07 12:30:00	24.7	0.93713	0.136279	1.52267	29.2	26.1	57	60.6	54.5	[illegible]
	57	62.4	55.4	59.4	27.9	72.9	69.2	69.3	71.8	61.8
25/07 12:35:00	24.7	0.888685	0.137126	1.456	29.2	26.4	56.9	69.9	54.8	[illegible]
	55.7	61.4	55.2	59.3	27.8	72.3	61.7	61.9	71.5	62
25/07 12:40:00	24.7	0.851663	0.103361	1.4432	28.9	26	57	61.1	55	[illegible]
	55.6	61.8	55.3	60.4	27.1	72.3	61.8	61.8	71.8	62.1
25/07 12:45:00	24.6	0.957355	0.103925	1.52707	28.7	25.6	56.8	61	53.8	[illegible]
	55.9	61.7	53.3	57.3	26.2	72.3	61.7	61.8	71.4	62.1
25/07 12:50:00	24.9	0.5548	.912458-2	1.512	28.5	25.7	56.8	60.8	55.9	[illegible]
	57.4	63	56.2	60.6	29.3	72.5	61.9	61.9	71.5	[illegible]
25/07 12:55:00	25.2	0.933975	.888328-2	1.45287	28.5	26.5	57	61.1	54.2	[illegible]
	56.7	62.3	54.8	59.4	27.8	72.6	69	69	71.6	[illegible]
25/07 13:00:00	25	0.928926	0.121655	1.42413	28.7	25.8	56.6	61.1	53	[illegible]
	55.4	61.3	52.8	57.7	26.1	72.2	61.6	61.6	71.1	[illegible]
25/07 13:05:00	24.9	0.963923	.978352-2	1.4615	28.4	26.2	55.1	60.7	53.1	[illegible]
	55.5	60.8	53.3	59.3	25.3	71.5	61.2	61.2	73.9	[illegible]
25/07 13:10:00	24.9	0.943441	.555528-2	1.436	28.7	25.4	55.8	60.5	55	[illegible]
	55.5	61.7	54.3	59.3	26.6	72	61.3	61.2	71	61.8
25/07 13:15:00	25.1	0.928925	.533468-2	1.52347	29.3	25.3	55.5	60.5	55.8	[illegible]
	57.8	62.5	56.5	62.4	27.6	72.4	61.9	61.9	71.5	[illegible]
25/07 13:20:00	25.1	0.920032	0.101161	1.53547	28.8	25.2	56.6	60.8	52.6	[illegible]
	55.4	60.6	53.8	57	26.7	72.2	61.6	61.7	71.4	61.9
25/07 13:25:00	25	0.918923	0.123681	1.53433	28.6	25.3	56.1	60.8	54.2	[illegible]
	55.8	62.4	53.3	58.6	26.2	72.3	61.3	61.2	72	[illegible]
25/07 13:30:00	25.3	0.925771	0.101572	1.5128	29.4	27.4	56.3	60.5	55.8	[illegible]
	57.9	62.5	56.8	61.3	28	72.2	61.6	61.6	72.2	[illegible]
25/07 13:35:00	25.7	0.958247	9.37482-2	1.46373	29.5	27.5	57	60.8	56.2	[illegible]
	58	62.7	55.8	61	29.2	72.2	61.9	61.8	72.5	[illegible]
25/07 13:40:00	25.7	0.992653	0.102478	1.43457	29.8	27.5	57.1	61	55	[illegible]
	57	62	55.8	60.5	28.4	72.2	61.9	61.9	71.4	[illegible]
25/07 13:45:00	25.8	0.882228	0.102812	1.37632	29.9	27.6	57	61	55.8	[illegible]
	58.9	62.2	58.2	63.7	28.2	72	61.6	61.6	71.1	[illegible]
25/07 13:50:00	25.8	0.964553	.988848-2	1.32693	30.4	28.2	57.2	61.2	59.2	[illegible]
	57.8	63.2	55.8	61.8	29.2	72.2	61.8	61.7	72.4	[illegible]
25/07 13:55:00	25.8	0.965283	0.12582	1.32827	28.8	27.1	57.4	61.3	[illegible]	[illegible]
	55.7	62.2	54.7	59	27.5	72	61.7	61.7	72.2	[illegible]
25/07 14:00:00	25.9	0.944781	0.122372	1.25227	29.3	27.3	57.1	[illegible]	57.2	[illegible]
	55.2	61.8	55.8	60.2	28.2	72.6	61.3	61.2	72.5	[illegible]
25/07 14:05:00	26.1	0.847520	[illegible]	1.22433	29	27.9	57	61	58	[illegible]
	56.5	62.4	56.2	62.2	28.2	[illegible]	61.2	61.4	[illegible]	[illegible]
25/07 14:10:00	26.2	0.922831	[illegible]	[illegible]	29.8	27.3	57.2	61	55.6	[illegible]

Table A4.1. Print out of the data logger for the still test on 25/7/1990. It was carried out for the still without the solar concentrator, outdoors. (continued)

	55.4	53.6	54.5	55	27.6	71.5	61.2	61.3	73.6	52.2
25/07 14:15:00	26	0.827325	0.224459	1.29333	23.5	27.1	56.7	60.3	55.9	2231
	55	62	53.4	58.2	26.7	71	57.8	57.8	70	62.2
25/07 14:20:00	25.9	0.829843	0.123515	1.2232	23.3	27.3	56.1	58.3	55.1	2231
	53.8	59.2	53.2	58.1	25.7	70.3	67.2	67.3	63.4	61.8
25/07 14:25:00	26.1	0.824704	0.227575	1.01353	23.4	27.8	55.7	59.9	55.7	2231
	54.5	53	53.8	58.4	27.2	73.2	67	67.1	69.2	61.3
25/07 14:30:00	26.2	0.772422	0.223733	0.356267	23.6	28.2	55.5	59.7	56.5	2231
	55	59.4	55.2	59.2	23.2	69.5	66.6	66.9	69	63.9
25/07 14:35:00	26.5	0.72951	0.224751	0.9254	23.6	27.8	55.8	59.7	55	2231
	54.1	58.7	53	56.9	27.9	69.3	66.3	66.4	68.4	63.6
25/07 14:40:00	26.2	0.738976	0.117659	0.349167	23.1	27.5	55	59.3	53.5	2281
	52.6	57.2	51.4	56	26.5	69.5	65.7	65.8	67.8	62.4
25/07 14:45:00	25.3	0.746543	0.122021	0.324533	23.5	28.4	54.5	59.6	54.6	2231
	53.8	58.2	53.4	56.5	27.4	69.2	65.4	65.5	67.4	59.9
25/07 14:50:00	26.6	0.722617	0.129157	0.332667	23.9	28.6	54.7	58.2	54.8	2231
	53.8	54.3	53.7	57	23.2	67.9	65.3	65.4	67.4	59.5
25/07 14:55:00	26.8	0.720675	0.110233	0.729567	23.8	28.8	54.6	58.1	53.3	2231
	53.1	57.2	52.9	55.8	28	67.5	65	65.2	67	59.4
25/07 15:00:00	26.9	0.63223	0.105325	0.548	23.8	28.7	54.4	57.8	53.8	2231
	53.1	56.9	52.6	56.2	27.8	66.8	64.7	64.7	66.6	59.2
25/07 15:05:00	27.2	0.6582	0.103152	0.6026	30.1	23.1	54.3	57.6	53.9	2231
	53	55.2	52.1	55.7	28.4	66.5	64.3	64.1	65.9	59
25/07 15:10:00	27.2	0.536356	0.111262	0.3256	23.5	27.9	53.4	57.4	52.2	2231
	53.3	53.4	50.2	52.5	27.5	65.2	63.2	63.4	61.8	58.6
25/07 15:15:00	25.6	0.555533	0.225524	0.4224	23.5	25.3	51.4	55.5	49	2231
	43.5	52.8	47.2	53	25.8	63.9	61.4	62.7	62	51
25/07 15:20:00	26.6	0.576733	0.228371	0.4022	23.2	23.3	43.4	55.7	50.1	2231
	49.2	52	48.3	52	26.7	63.5	62.4	61	62.6	57.2
25/07 15:25:00	27	0.631058	0.155633	0.4236	23.4	23.5	43.7	55.4	53.4	2231
	43.3	53.5	45.2	52.5	27.4	63.6	63.4	62	62.9	58.5
25/07 15:30:00	26.3	0.523557	0.125683	0.2253	23	23.2	47.7	55.3	48.8	2231
	47.9	52.5	47.5	50.6	26.8	63	53.5	62	61.9	55.5
25/07 15:35:00	25.6	0.512162	0.122733	0.232657	23.7	27.2	47.3	54.9	47.6	2231
	46.8	52.3	45.8	49.5	25.4	62	58.6	58	62.7	55.4
25/07 15:40:00	26.7	0.410353	0.115331	0.218	23.3	23.5	48.2	54.3	47.3	2231
	47	50.3	47	53.2	26.9	62	57.8	58.2	62.1	54.6
25/07 15:45:00	26.6	0.434537	0.112352	0.223533	23.3	23.2	43	53.6	46.7	2231
	45.9	45	45	48.7	26.5	59.8	57.2	57.9	59.5	58
25/07 15:50:00	26.4	0.512424	0.218023	0.245457	23.3	27.7	47.8	52.7	43.4	2231
	44.6	47.5	44.2	45.8	25.5	55	55.7	57.4	58.6	53.4
25/07 15:55:00	25.2	0.52757	0.127663	0.256332	23.3	27.7	47	52.3	43.6	2231
	44.5	47.3	44.2	45.5	25.3	58.2	58.4	57.2	55.2	52.7
25/07 16:00:00	25.2	0.426553	0.22374	0.2222	23.4	28.1	46.6	52	45.7	2231
	44.7	47.6	46.3	47	25.2	57.3	55.5	56.2	57.2	52.2
25/07 16:05:00	25.2	0.355328	0.114345	0.223567	23.2	27.7	46.3	52.3	44.7	2231
	43.7	45.6	42.7	45.7	25.2	55.4	51.8	55.4	55.2	52.4
25/07 16:10:00	25	0.425774	0.22325	0.2224	25	27.5	45.3	43.5	42.7	2231

Table A4.1. Print out of the data logger for the still test on 25/7/1990. It was carried out for the still without the solar concentrator, outdoors. (continued)

25/07 16:25:03	25.6	0.163754	.941498-2	.926678-2	27.1	26.9	43.8	46.1	48.4	2001
	38.6	40.9	39.7	40.8	25.5	50.2	50.1	50.2	50.6	48.4
25/07 16:30:00	25.3	0.209106	.965248-2	0.155733	26.6	26.2	42.8	45.6	38.5	2001
	37.6	38.9	37.6	39	24.8	49.2	49.1	49.4	49.8	47.1
25/07 16:35:00	25.2	0.319958	.818328-2	0.2328	27.1	26.5	42.2	44.4	38.9	2001
	38.2	39.3	38.4	39.2	25.2	48.6	48.6	49.3	49.4	45.9
25/07 16:40:03	25.4	0.407667	.888848-2	0.239667	27.4	27.4	42.1	43.8	39.7	2001
	38.9	38.2	39.5	40.4	26	47.9	48.6	49.3	49.4	45
25/07 16:45:00	25.4	0.342663	.859228-2	0.171133	27.5	27.4	41.8	43.3	39.2	2001
	38.3	38	39.3	40	26.3	47.3	48.1	48.7	48.7	44.5
25/07 16:50:03	25.4	0.376435	0.41578-2	0.1752	27.6	27.4	41.5	43	39.1	2001
	38.3	37.8	39.4	39.9	26	46.9	47.8	48.4	48.5	43.9
25/07 16:55:03	25.5	0.354027	.888548-2	0.153933	27.8	26.9	41.5	42.7	39.1	2001
	38.3	38.2	39.1	39.2	26.5	46.6	47.5	48	48.3	42.4
25/07 17:00:20	25.5	0.330947	.848428-2	0.137333	27.9	25.7	40.7	42.5	38.8	2001
	38.1	37.8	38.7	38.3	26.6	46.6	47	47.8	48.2	43.1
25/07 17:05:03	25.5	0.252128	.838318-2	0.108	27.7	27	39.5	42.4	37.9	2001
	37	37	37.4	38.3	26.4	46.2	46.1	46.6	47.5	42.8
25/07 17:10:03	25.3	35.24	33.34	16.24	2001	2001	2001	2001	2001	2001
	2001	2001	2001	2001	2001	2001	2001	2001	2001	2001
25/07 17:15:20	24.5	32.2	42.7	15.8	2001	2001	2001	2001	2001	2001

APPENDIX A5

WICK-TYPE SOLAR STILL WITH INTERNAL V-TROUGH SOLAR CONCENTRATOR

The experimental work originally started with the aim of using a truncated V-trough solar concentrator of 30° apex angle as an internal concentrator of a wick-type solar concentrator still. Its base represented the absorber surface of the still and its aperture was the glass cover of the still. In this design: (i) The concentrator mirrors act as reflectors for solar radiation as well as condenser surfaces. (ii) The cover on the concentrator prevents dust accumulation on the reflectors. (iii) The reflector angle is fixed. Therefore two wick-type solar distillation units with the same glass cover area were constructed for testing. One was a solar still with solar concentrator, its absorber area was a third of that of the cover to let the concentration factor be in order of 2. The other still was the conventional wick-type solar still.

After testing these stills outdoors with the same inclination angle facing the south, it was found that although the operating temperature of the solar concentrator still was higher than that of the other still, its yield was much less than that of

the conventional still. The high reflector temperatures (higher than of the cover) caused evaporation of the condensate occuring in some parts of the reflectors. So, these negative results discouraged further work on such a design. Other reasons why the performance of the solar concentrator still was low may have been the cover-absorber distance which was very large (D = 510 mm). This increased the convection heat losses. The absorber area was small due to the design.

Later the decision was made to fix a solar concentrator on the glass cover of the conventional wick-type solar still and compare its performance with that of the still without the concentrator.

APPENDIX A6

MEASURED DISTRIBUTION OF IRRADIANCE IN THE BASE OF THE CONCENTRATOR

The actual distribution of solar irradiance in the base of the V-trough solar concentrator has been measured at different times of a clear day 11/7/1990 using the digital irradiance meter. This was carried out by dividing the base of the concentrator to 108 squares 5 x 5 cm^2 each. Figs. A6.1-A6.5 show these distributions and the effect of the shadow created by the concentrator ends walls.

172	180	178	172	179	184	190	172	228	240	227	261	280	288	289	328	317	288
174	162	169	184	194	188	187	167	218	242	238	269	273	280	296	316	322	315
160	196	183	176	167	171	178	196	240	230	266	282	292	308	302	344	319	348
167	189	188	196	185	185	159	185	229	285	249	290	283	317	340	357	372	365
171	182	169	180	187	190	184	189	235	279	270	309	296	303	326	362	386	389
184	177	187	183	195	186	187	208	251	284	287	316	308	329	345	356	369	386

Fig. A6.1. Solar irradiance data obtained from outdoor measurements using the solar concentrator and the digital irradiance meter.
Inclination Angle = 29°. Date: 11/7/1990 at 8:00 am. Average Concentrated Irradiance = 246 W/m^2.
Aperture Irradiance = 604 W/m^2. C.F. = 0.408

1981	1976	1956	1893	1728	1750	1785	1650	1600	1512	1418	673	232	170	152	139	125	123
1965	1940	1882	1738	1630	1598	1578	1501	1472	1410	1280	475	199	168	150	136	126	121
1793	1803	1678	1642	1554	1517	1480	1325	1361	1317	1065	463	179	161	145	128	122	111
1695	1780	1643	1937	1530	1480	1406	1378	1308	1265	1007	418	162	154	140	126	119	117
1796	1756	1630	1619	1516	1502	1388	1406	1370	1220	1013	400	177	163	151	138	130	112
1701	1722	1698	1671	1620	1546	1499	1510	1451	1298	1152	386	180	168	142	125	127	100

Fig. A6.2. Solar irradiance data obtained from outdoor measurements using the solar concentrator and the digital irradiance meter.
Inclination Angle = 29°. Date: 11/7/1990 at 10:00 am. Average Concentrated Irradiance = 1028 W/m^2.
Aperture Irradiance = 978 W/m^2. C.F. = 1.051

1989	1961	1894	1915	1930	1922	1908	1953	1916	1892	1920	1809	1965	1880	1797	1782	1798	1976
1967	1917	1896	1862	1837	1831	1796	1738	1769	1747	1758	1781	1768	1693	1822	1753	1598	1753
1919	1936	1913	1813	1815	1689	1762	1769	1792	1861	1815	1901	1914	1951	1840	1865	1901	1720
1841	1778	1792	1699	1730	1679	1694	1743	1705	1669	1697	1739	1821	1656	1667	1646	1821	1648
1980	1949	1942	1977	1943	1879	1990	1969	1968	1938	1990	1943	1996	1790	1929	1900	1917	1920
1984	1958	1979	1938	1919	1968	1972	1882	1953	1910	1997	1972	1984	1957	1976	1982	1992	1995

Fig. A6.3. Solar irradiance data obtained from outdoor measurements using the solar concentrator and the digital irradiance meter.
Inclination Angle = 29°. Date: 11/7/1990 at 12:00 Noon. Average Concentrated Irradiance = 1860 W/m^2.
Aperture Irradiance = 1151 W/m^2. C.F. = 1.616

102	108	117	129	137	154	175	412	1606	1746	1806	1745	1758	1788	1749	1889	1958	1970
98	107	117	128	138	156	179	348	1404	1560	1636	1755	1749	1780	1799	1789	1975	1929
112	117	122	136	146	159	181	237	1022	1215	1465	1482	1526	1512	1481	1497	1610	1731
111	117	124	132	153	159	177	208	997	1606	1708	1833	1668	1574	1682	1895	1828	1702
103	110	115	126	139	153	172	210	977	1390	1472	1631	1670	1444	1554	1594	1524	1684
97	113	118	127	135	148	170	192	1062	1500	1634	1649	1573	1621	1654	1672	1563	1612

Fig. A6.4. Solar irradiance data obtained from outdoor measurements using the solar concentrator and the digital irradiance meter.
Inclination Angle = 29°. Date: 11/7/1990 at 15:00 pm. Average Concentrated Irradiance = 963 W/m^2.
Aperture Irradiance = 929 W/m^2. C.F. = 1.037

106	99	92	94	95	96	98	102	108	110	109	112	115	117	116	110	102	84
92	93	93	95	95	96	97	102	106	111	108	113	118	121	120	115	106	93
85	87	87	89	91	93	96	100	105	110	115	121	122	126	126	121	114	94
88	89	89	90	102	97	99	104	107	113	116	119	123	127	125	122	113	92
88	89	89	89	90	93	96	103	107	113	118	123	128	130	130	128	117	91
83	90	87	88	91	93	96	99	104	109	115	125	129	131	130	124	112	83

Fig. A6.5. Solar irradiance data obtained from outdoor measurements using the solar concentrator and the digital irradiance meter.
Inclination Angle = 29°. Date: 11/7/1990 at 18:00 pm. Average Concentrated Irradiance = 104 W/m^2.
Aperture Irradiance = 430 W/m^2. C.F. = 0.242

APPENDIX A7

COMPUTER PROGRAM TO MODELTHE PERFORMANCE OF THE WICK-TYPE SOLAR STILL

```
C*************************************************************************
C THIS PROGRAM SOLVES THE DAILY TRANSIENT EQUATIONS OF THE WICK-TYPE    *
C SOLAR STILL USING FINITE DIFFERENCE METHOD BASED ON REAL DATA FOR     *
C AMBIENT TEMPERATURE AND SOLAR INSOLATION.                            *
C*************************************************************************
C       PROGRAM WICK-TYPE
        IMPLICIT REAL*8(A-H,O-Z)
C
        DO 999 XX=0.80,0.90,0.02
C
        WRITE(6,111) XX
        WRITE(331,111) XX
        WRITE(382,111) XX
        TAO = XX
        CALL WICK(TAO)
C
 999    CONTINUE
 111    FORMAT(///,10X,'TRANSMITTANCE =',F5.3)
C
        STOP
        END
C*************************************************************************
        SUBROUTINE  WICK(TAO)
C
        IMPLICIT REAL*8(A-H,O-Z)
        PI = 4.0D0*ATAN(1.0D0)
C
      DO 250 FLO = 3.20, 3.40, 0.10
          DO 260 A = 30.0, 40.0, 2.0
              DO 270 H = 0.025, 0.040, 0.005
                  RAD = PI/180.0
                  SN = SIN(RAD*A)
                  CN = COS(RAD*A)
```

```
C       PRINT*,'INPUT TABS TCOV DT SUNRISE SUNSET'
C
C       READ*, TABS, TCOV, DT, SUNRIS, SUNSET
                        TABS = 56.8
                        TCOV = 43.7
                        DT = 0.01
                        SUNRIS = 9.0
                        SUNSET = 17.0
C
C------ START COUNTING HOURS OF THE DAY
                        SUNRIS = SUNRIS + 1
C
C------ START UP SPECIFICATIONS
                        TOINSO = 0
                        THPRM = 0
C
                        CALL CONSTRUCTION_SPECIFICATIONS(RMAS1,RMAS2)
C
                        G = 9.8
                        CPW = 4186.8
                        CPA = 1006.9
                        HMEU = 1.998E-5
                        ROU = 1.0614
                        ENEW = HMEU/ROU
                        THK = 2.90E-2
                        ALFA = THK/(ROU*CPA)
C
C       FOR TEMPERATURE = 60 C=333K
                        ALFACH = 0.93
                        ABSW = 0.9
                        ABSG = 0.88
                        SIGMA = 5.67E-8
                        HI = 20.0
```

```
C------READ THE REALISTIC DATA OF HOURLY SOLAR INSOLATION AND AMBIENT
C       TEMPERATURE. THE DATA IS BASED ON A SET OF MEASUREMENTS TAKEN
C                    ON  25/7/1990
C
                                    DO 200 HD = SUNRIS, SUNSET

                                    READ(266,*) HINSOL, TAMB
C------HINSOL IN (KJ/M^2.H) AND TAMB IN ( C)
                                    GAMA = 0.0

C       TAKE THE NORMAL (VERTICAL) COMPONENT OF THE INSOLATION I.E. AS AT -
C       NOON TIME.
                                    OINSO = HINSOL*COS(RAD*GAMA)
                                    OINSO = OINSO*1000
C
                                    HS = OINSO/3600
C------THE INSOLATION (HS) IS CONVERTED TO (W/M^2)
C------SET INITIAL CONDITIONS
                                    N = 0
                                    T = 0.0
                                    TTABS = 0.0
                                    TTCOV = 0.0
                                    TTEMPD = 0.0
                                    TPAB = 0.0
                                    TPC = 0.0
                                    TRA = 0.0
                                    TCNU = 0.0
                                    THE = 0.0
                                    THC = 0.0
                                    THR = 0.0
                                    THRA = 0.0
                                    THCA = 0.0
                                    TPRM = 0.0
```

```
C----------
                      TWIN = TAMB
                      TAB = TABS + 273.15
                      TC = TCOV + 273.15
                      TA = TAMB + 273.15
                      TWO = TWIN + 273.15
 99   CONTINUE

                      CALL MAIN_EQUATIONS (TSKY,TA,TAB,TC,PAB,PC,
     &                CLAT,HS,TAO,TEMPD,RA,CNU,G,H,ALFA,ENEW,HC,
     &                HE,HR,H1,HCA,HRA,H2,QE,QB,QWIN,QWOUT,QABIN,
     &                QABOUT,ALFA1,ALFA2,SIGMA,ALFACH,ABSW,CPW,
     &                FLO,TWO,PRM,RMAS1,RMAS2,SN,CN,EFF,RAD,III,
     &                A,THK,ABSG,DT,HD)
                      T = T + DT
C------- COUNT (N) WITHIN AN HOUR ACCORDING TO THE TIME INTERVAL (DT)
                      N = N + 1
C------ ACCUMULATING THE INSTANTANEOUS DATA ACCORDING TO (N AND DT).
                      TPAB = TPAB + PAB
                      TTPC = TPC + PC
                      TTEMPD = TTEMPD + TEMPD
                      TRA = TRA + RA
                      TCNU = TCNU + CNU
                      TPRM = TPRM + PRM
                      THE = THE + HE
                      THC = THC + HC
                      THR = THR + HR
                      THRA = THRA + HRA
                      THCA = THCA + HCA
                      TABS = TAB - 273.15
                      TTABS = TTABS + TABS
                      TCOV = TC - 273.15
                      TTCOV = TTCOV + TCOV
```

```
                    TAMB = TA - 273.15
                    IF( T.LT.1.D0 ) GO TO 99
C       AVERAGING THE DATA TO THE HOURLY
                    HPAB = TPAB/N
                    HPC = TPC/N
                    HTEMPD = TTEMPD/N
                    ORA = TRA/N
                    HCNU = TCNU/N
                    HPRM = TPRM/N
                    OHE = THE/N
                    OHC = THC/N
                    OHR = THR/N
                    OHRA = THRA/N
                    OHCA = THCA/N
                    OTABS = TTABS/N
                    OTCOV = TTCOV/N
                    HEFF = HPRM*CLAT*100.0/OINSO
                    OTEMPD = OTABS - OTCOV
C   ACCUMULATING THE HOURLY DISTILLATE PRODUCTION AND THE INSOLATION
                    THPRM = THPRM + HPRM
                    TOINSO = TOINSO + OINSO
200                 CONTINUE
                  TEFF = THPRM*CLAT*100.0/TOINSO
                  WRITE(382,*) 'DAILY EFFICIENCY (%) = ', TEFF
                  WRITE(381,*) 'DAILY EFFICIENCY (%) = ', TEFF
                  WRITE(381,*)
270               CONTINUE
260           CONTINUE
250   CONTINUE
C
      RETURN
      END
C     ******************************************************************
```

```
      SUBROUTINE OUTPUT_HOURLY_RESULTS(HD,OTABS,OTCOV,OTEMPD,
     &  ORA,OCNU,OHE,OHC,OHR,OHRA,OINSO,
     &  HEFF,HS,HPRM,FLO,A,HTEMPD,HPAB,HPC,HCNU,CPAB,H)
C
      IMPLICIT REAL*8(A-H,O-Z)
C
C     WRITE(382,82) HD, OTABS, OTCOV, HEFF, HS, HPRM, FLO, A
      WRITE(382,82) HD, OTABS, OTCOV, OTEMPD, HTEMPD, HPAB, HPC, ORA,
     &  HCNU, FLO, A
      WRITE(381,81) HD, OHE, OHC, OHR, OHRA, H, FLO, A, HPRM,
     &  HEFF, OINSO

   80 FORMAT(//'TABS(C)',2X,'TCOV(C)',2X,'IRR(W/M2)',1X,'TAMB(C)',
     &  1X,'PRM(KG/H)',3X,'EFF %',4X,'HE',4X,'FLO',2X,'TWIN')
   81 FORMAT(2X,F5.1,6F8.3,F7.1,2F8.3,F12.1)
   82 FORMAT(2X,F5.1,4F8.2,3F12.1,F8.3,2F5.1)
C
      RETURN
      END
C*****************************************************************
      SUBROUTINE MAIN_EQUATIONS (TSKY, TA, TAB, TC, PAB, PC,
     &  CLAT, HS, TAO, TEMPD, RA, CNU, G, H, ALFA, ENEW, HC, HE, HR, H1,
     &  HCA, HRA, H2, QE, QB, QWIN, QWOUT, QABIN, QABOUT, ALFA1, ALFA2,
     &  SIGMA, ALFACH, ABSW, CPW, FLO, TWO, PRM, RMAS1, RMAS2, SN, CN,
     &  EFF, RAD, HI, A, THK, ABSG, DT, HD)
C
      IMPLICIT REAL*8(A-H,O-Z)
C
      TSKY = 0.055*TA**1.5
      BETA = 2.0/(TAB+TC)
C     VAPOUR PRESSURE AT ABSORBER TEMP. (MMHG CONVERTED TO N/M^2)
      PAB = 10.0**(0.622 + 7.5*(TAB - 273.15)/(TAB - 35.0))
      PAB = PAB*1.0E+5/750.0
```

```
C       VAPOUR PRESSURE AT COVER TEMP. (MMHG CONVERTED TO N/M^2)
        PC = 10.0**(0.622+7.5*(TC-273.15)/(TC-35.0))
        PC = PC*1.0E+5/750.0

C          EFFECTIVE TEMPERATURE DIFFERENCE
        TEMPD = (TAB-TC)+(PAB-PC)*TAB/(268900.0-PAB)
C
        RA = G*BETA*TEMPD*H**3/(ALFA*ENEW)
        CNNU = 1.0-1708.0*(SIN(RAD*1.8*A))**1.6/(RA*CN)
C
        BRAC1 =1.0-1708.0/(RA*CN)
        IF ( BRAC1 .LT. 0.0 ) BRAC1 =0.0
        BRAC2 = ((RA*CN/5830.0)**(0.3333))-1.0
        IF ( BRAC2 .LT. 0.0 ) BRAC2 =0.0
        CNU = 1.0+1.44*BRAC1*CNNU+BRAC2
        HC = THK*CNU/H
        HE = 0.016*HC*(PAB-PC)/(TAB-TC)
        QE = HE*(TAB-TC)
C       QE : EVAPORATION ENERGY RATE (W/M^2)
        CLAT = (2501.67-2.389*(TAB-273.15))*1000.0
C       CLAT : LATENT HEAT OF EVAPORATION (J/KG)
        PRM = QE*3600.0/CLAT
C       PRM : PRODUCTION MASS RATE OF DISTILLATE (KG/M^2.H)
        EFF = QE*100.0/HS
        HR = ABSG*SIGMA*(TAB**4-TC**4)/(TAB-TC)
        H1 = HE+HR+HC
        V = 2.0
        HCA = 5.7+3.8*V
        HRA = ABSG*SIGMA*(TC**4-TSKY**4)/(TC-TA)
        H2 = HCA+HRA
        DLI1 = 0.009
        THKI1 = 0.29
        DL1 = DLI1/THKI1
```

```
      DLI2 = 0.0125
      THKI2 = 0.034
      DL2 = DLI2/THKI2
      DLI3 = 0.035
      THKI3 = 0.039
      DL = DLI3/THKI3
      HBB = (1/HI)+DL1+DL2+DL3
      HB = 1/HBB
      QK = HB*(TAB-TA)
      ALFA1 = 0.05
C     ALFA2 = CHARCOAL ABSORPTIVITY * GLASS TRANSMISSIVITY
      ALFA2 = ALFACH*TAO
      QWIN = FLO*CPW*(TWO-TC)/3600
C     FLO: INPUT WATER FLOW RATE IN KG/(M2.H)
      QWOUT = (FLO-PRM)*CPW*(TAB-TC)/3600
      QCIN = ALFA1*HS+H1*(TAB-TC)
      QCOUT = H2*(TC-TA)
C     QABIN = ALFA2*HS+QWIN
      QABIN = ALFA2*HS
      QABOUT = H1*(TAB-TC)+QK+QWOUT
C     QABOUT = H1*(TAB-TC)+QK
      TC = TC+3600.0*DT*RMAS2*(QCIN-QCOUT)
      TAB = TAB+3600.0*DT*RMAS1*(QABIN-QABOUT)
      RETURN
      END
C     ******************************************************************
      SUBROUTINE CONSTRUCTION_SPECIFICATIONS(RMAS1,RMAS2)
C
      IMPLICIT REAL*8(A-H,O-Z)

C----ABSORBER SUPPORT CHARACTERS
      W1 = 0.95
      Y1 = 0.50
```

```
      A1 = W1*Y1
      THICK1 = 0.003
      ROW1 = 1500
      MASS1 = ROW1*THICK1*A1
      CPAB = 900.D0
      RMAS1 = A1/(MASS1*CPAB)

C-----GLASS COVER CHARACTERS
      W2 = 0.97
      Y2 = 0.55
      A2 = W2*Y2
      THICK2 = 0.004
      ROW2 = 2500
      MASS2 = ROW2*THICK2*A2
      CPC = 750.D0
      RMAS2 = A2/(MASS2*CPC)
C
      RETURN
      END
```

APPENDIX A8
V-TROUGH SOLAR CONCENTRATOR

In the literature this sort of concentrator was studied to be used with flat plate solar collectors for providing higher water temperatures than can be achieved without the concentrator, e.g. Issa (1989). In this work the concentrator was combined with a flat plate tilted wick-type solar still. The concentrator longitudinal axis was oriented along the east-west direction and receiver/aperture planes tilted according to the solar altitude at noon facing the south.

The V-trough solar concentrator is a flat sided rectilinear concentrator as shown in Fig. A8.1. It has two side mirrors of reflectance (ρ) having the cone apex angle (2α), length (L), aperture width (A) and truncated somewhere to form the base of width (B) and aperture-base depth (D). The solar radiation incident upon the aperture with solar insolation (I) forming an angle (γ) with the normal to the base and aperture. The concentration factor (C.F.) of the V-trough solar concentrator is defined as the ratio of the energy incident on the aperture that reaches the base, in this case $A\cos\gamma$, to the energy that would

appear over the base if exposed to the sunlight directly, that is, without the presence of the reflecting sides Burkhard *et al.* (1978). The latter energy is Bicosγ.

Thus

$$C.F. = \frac{A}{B} \qquad (A8.1)$$

Under the assumption of direct beam, noon-time solar incidence optimal groove designs are possible based on a one-reflection, maximum concentration criterion. This criterion, accounting for seasonal variations in noon-time incident solar angles resulted in a near-optimum geometry of an opening angle near 30 degrees, and with the depth to base ratio (D/B) of 1.75 Howell and Bannerot (1975). Therefore, the geometry which has been adopted for the concentrator (Fig. A8.1) has: A = 0.600 m, B = 0.310 m, L = 0.561 m and $2\alpha = 30°$.

Since

$$D = L\cos\alpha = L\cos 15$$

hence

$$D = 0.542 \text{ m}$$

Then the ideal C.F. is:

$$C.F. = A/B = 1.935$$

and the expected C.F. for beam radiation = 1.68. (Bannerot (1974)).

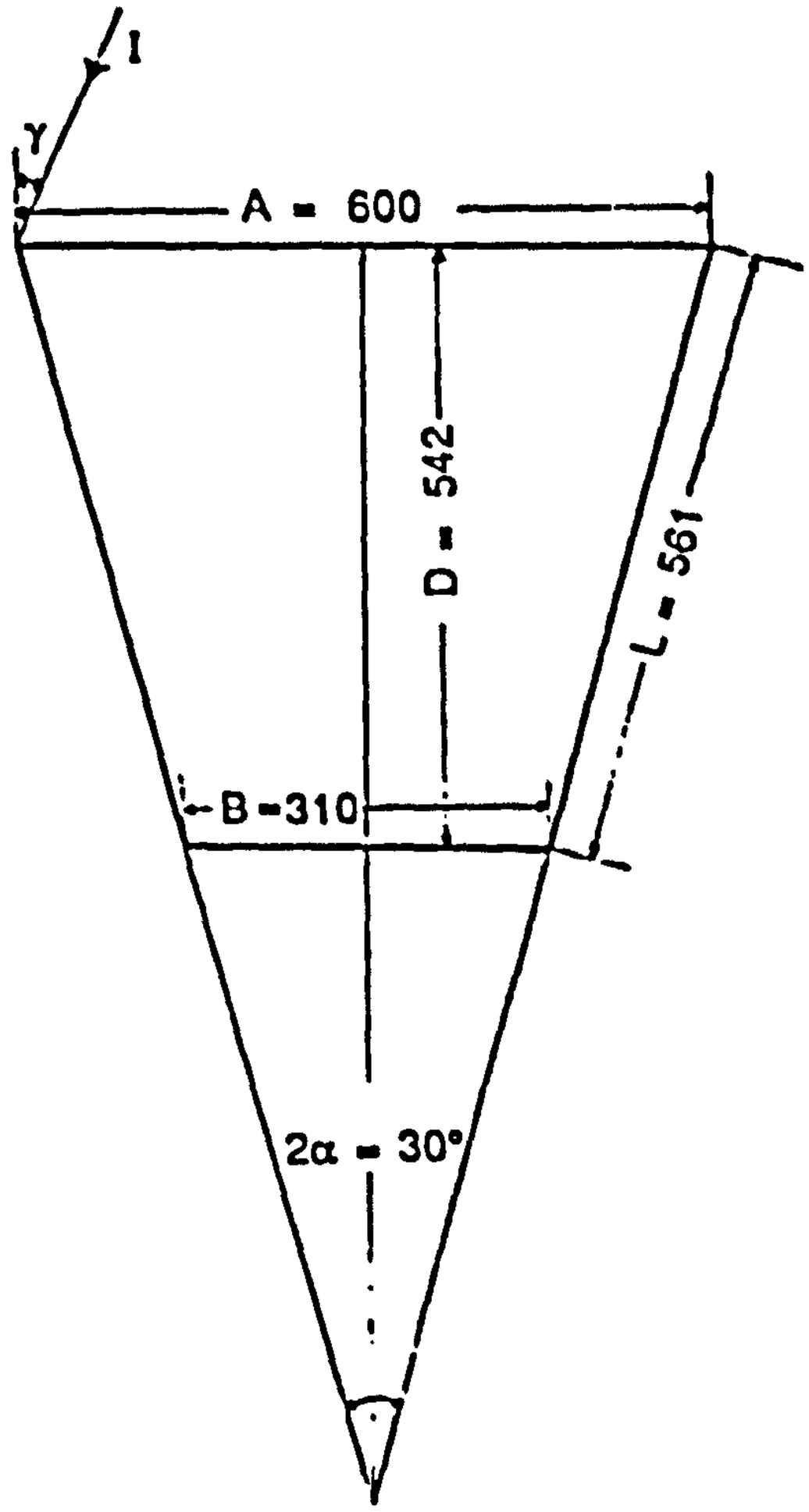

Fig. A8.1. Geometry of the V-trough solar concentrator. Dimensions in mm.

APPENDIX A9
ERRORS CALCULATION

A9.1 ERRORS CALCULATION OF THE SOLAR REFLECTANCE

Solar reflectance of different materials was measured using Lambda-9 Perkin-Elmer spectrometer. The random error in this measurement was calculated by successive measurements of the solar reflectance and calculation of their values then the standard error in the mean (σ_m) Squires (1968) as in the following example using the relations:

$$\sigma_m = \frac{s}{(n-1)^{\frac{1}{2}}} \qquad \text{(A9.1)}$$

where

$$s = \left(\frac{1}{n}\sum_{1}^{n} d_i^2\right)^{\frac{1}{2}} \qquad \text{(A9.2)}$$

$$d_i = x_i - \bar{x} \qquad \text{(A9.3)}$$

where

d_i is the standard deviation

n is the number of successive measurements

s is the standard deviation

x_i is a measured variable

$\bar{x}$ is the arithematic mean value of n measurements

and

$$\bar{x} = \frac{1}{n}\sum_{1}^{n} x_i \qquad \text{(A9.4)}$$

Example of typical error calculations:

Five successive measurements of total reflectance of an as received sample of 3M Scotchcal Film 530 were carried out. The solar reflectance was calculated using each spectrum and the values are:

86.3, 86.6, 86.1, 86.4, 86.1

Their average is :

$\bar{x} = 86.3$

The deviations of each from the average respectively are:

0.0, +0.3, -0.2, +0.1, -0.2 .

so the standard deviation (s) of the sample according to Eq. A9.2 is:

$s = 0.1897$

Hence the standard error in the mean (σ_m) according to Eq. A9.1 is:

$\sigma_m = 0.095$

Thus the measured value of the reflectance is:

$\rho = 86.3 \pm 0.095$

A9.2 ERROR CALCULATION OF THE SOLAR STILL EFFICIENCY

Solar still efficiency has been calculated according to the expression:

$$\eta = \frac{D h_{fg}}{I} \qquad \text{(A9.5)}$$

So the error induced in its value is dependent on the accuracy of measuring the rate of distillate mass (D), rate of solar energy (I) and the absorber temperature (T_{abs}) on which h_{fg} is dependent.

After calculating the errors in these parameters by using the equations below Squires (1968) the error in the efficiency can be estimated.

If Z is a function of A, B, C, ... then

$$\frac{\Delta Z}{Z} = \sqrt{\left(\frac{\Delta A}{A}\right)^2 + \left(\frac{\Delta B}{B}\right)^2 + \left(\frac{\Delta C}{C}\right)^2 + \dots} \qquad \text{(A9.6)}$$

Hence

$$\frac{\Delta \eta}{\eta} = \sqrt{\left(\frac{\Delta D}{D}\right)^2 + \left(\frac{\Delta I}{I}\right)^2 + \left(\frac{\Delta h_{fg}}{h_{fg}}\right)^2} \qquad \text{(A9.7)}$$

As a typical example the error in the still efficiency at the interval 11.00 to 11.30 am on 25/7/1990 has been chosen . That was when:

T_{abs} = 67.4 °C, m_d = 125.9 gm, h_{fg} = 2340600 J/kg, t = 1800 sec, S = 0.9135 kW/m² (as in Appendix A4).

According to Eq A9.6 the following expressions can be written:

$$\frac{\Delta D}{D}=\sqrt{\left(\frac{\Delta L}{L}\right)^2+\left(\frac{\Delta W}{W}\right)^2+\left(\frac{\Delta m_d}{m_d}\right)^2+\left(\frac{\Delta t}{t}\right)^2} \qquad \text{(A9.8)}$$

and

$$\frac{\Delta I}{I}=\sqrt{\left(\frac{\Delta L}{L}\right)^2+\left(\frac{\Delta W}{W}\right)^2+\left(\frac{\Delta S}{S}\right)^2+\left(\frac{\Delta t}{t}\right)^2} \qquad \text{(A9.9)}$$

Where L, W are the length and width of the still absorber, m_d is the mass of distillate produced in an interval time, S is the solar irradiance and t is the interval time.

Since when Z = Z (A)

$$\Delta Z=\frac{dZ}{dA}\Delta A \qquad \text{(A9.10)}$$

and h_{fg} = 1000 x (2501.67- 2.389 T_{abs}) Elsayed (1983)

Hence $\Delta h_{fg} = \pm 2400\ \Delta T_{abs}$

$= \pm 2400 \times 0.1 = \pm 240$ J/kg

where $\Delta T_{abs} = \pm 0.1$ °C

Therefore by applying Eqs. A9.7 - A9.10 for the above interval and according to the calibration certificate $\Delta S = \pm 1.5\%$ (Appendix A2) the followings can be obtained:

$\Delta D = \pm 0.004$ kg/m².h

$\Delta h_{fg} = \pm 240$ J/kg

$\Delta I = \pm 50200\ J/m^2.h$

Thus :

$\Delta\eta = \pm 8.2 \times 10^{-3}$

i.e. $\eta = 0.498 \pm 0.008$